

The Role of the AdeRS Two Component System and the  
AdeABC RND Efflux Pump in Antibiotic Resistance, Biofilm  
Formation and Virulence in *Acinetobacter baumannii*

by

Grace Emma Richmond

A thesis submitted to the University of Birmingham for the degree of  
DOCTOR OF PHILOSOPHY

Antimicrobials Research Group

Institute of Microbiology and Infection

College of Medical and Dental Sciences

University of Birmingham

July 2016

UNIVERSITY OF  
BIRMINGHAM

**University of Birmingham Research Archive**

**e-theses repository**

This unpublished thesis/dissertation is copyright of the author and/or third parties. The intellectual property rights of the author or third parties in respect of this work are as defined by The Copyright Designs and Patents Act 1988 or as modified by any successor legislation.

Any use made of information contained in this thesis/dissertation must be in accordance with that legislation and must be properly acknowledged. Further distribution or reproduction in any format is prohibited without the permission of the copyright holder.

## **Abstract**

*Acinetobacter baumannii* is a nosocomial pathogen and causes infections in hospitals worldwide. This organism is often multi-drug resistant (MDR), can persist in the environment and forms a biofilm on environmental surfaces and wounds.

This thesis describes research that investigates the role of the two component system AdeRS, which regulates production of the AdeABC MDR efflux pump. Its role in MDR, biofilm formation and virulence of *A. baumannii* was determined in mutants constructed for this study. Deletion of AdeRS or AdeABC resulted in increased susceptibility to antibiotics, decreased biofilm formation on biotic and abiotic surfaces and decreased virulence in a strain dependent manner. RNA-Seq revealed that loss of AdeRS or AdeB significantly altered the transcriptome, resulting in changed expression of many genes, notably those associated with antimicrobial resistance and virulence interactions.

This study demonstrated the scope of AdeRS mediated regulation and suggests that inhibition of AdeABC could prevent biofilm formation or colonisation in patients by *A. baumannii* and so provides a good target for drug discovery. This study also highlighted the differences between *A. baumannii* strains and shows that conclusions for the species should not be drawn from the study of single strains.

## **Acknowledgements**

I would like to thank my supervisor Professor Laura Piddock for all her help and advice over the last few years. I would also like to thank my second supervisor Dr Mark Webber for his guidance and for answering all my questions.

I am extremely grateful to Professor Marnie Peterson for hosting me at the University of Minnesota and her constant support despite some major setbacks! I would also like to thank Dr Mark Sutton for hosting my visit to Public Health England and for his ongoing input on the project. Thank you also to Al Ivens for sharing his bioinformatics expertise, Michele Anderson for her help with the PVM model and Matthew Wand and Laura Bonney for their assistance with making genetic modifications and the *Galleria* work.

Thank you to all members of ARG, past and present. In particular those who made me so welcome at the beginning and those who got me through the final months. And finally thank you to my friends and family, who always believed in me.

## Contents

<b>1. Introduction</b> .....	<b>1</b>
1.1. <i>Acinetobacter</i> species .....	1
1.1.1. Natural habitat .....	2
1.1.2. Epidemiology .....	2
1.2. <i>Acinetobacter baumannii</i> complex .....	6
1.3. <i>Acinetobacter baumannii</i> infection .....	8
1.3.1. Hospital acquired infections .....	8
1.3.2. Community acquired infections .....	10
1.3.3. Infection in military and disaster zone casualties .....	10
1.4. Persistence in the hospital environment.....	11
1.5. Treatment of <i>Acinetobacter</i> infections.....	12
1.5.1. Antibiotics .....	12
1.5.2. Novel therapeutics .....	18
1.6. Mechanisms of antibiotic resistance.....	19
1.6.1. Target site modification.....	24
1.6.2. Drug inactivation .....	24
1.6.3. Reduced drug accumulation .....	26
1.7. Regulation of antibiotic resistance .....	32
1.8. Pathogenesis and virulence of <i>Acinetobacter</i> .....	36
1.8.1. Biofilm formation .....	40
1.9. Biofilm models for <i>Acinetobacter</i> .....	41
1.10. The role of efflux pumps in biofilm formation and virulence .....	44
1.11. Background to this research .....	45
1.12. Hypotheses .....	47
1.13. Aims .....	47

<b>2. Materials and Methods</b> .....	<b>48</b>
2.1. Bacterial strains, growth, storage and identification .....	48
2.1.1. Bacterial strains .....	48
2.1.2. Growth and storage .....	51
2.1.3. Phenotypic and genotypic identification.....	51
2.2. Primer design and PCR .....	51
2.3. Construction of gene deletion mutants.....	56
2.3.1. Construction of pMo130-TelR-adeBUPDOWN .....	59
2.3.2. Integration of pMo130-TelR-adeBUPDOWN into <i>A. baumannii</i> AYE chromosome .....	59
2.3.3. Gene deletion .....	61
2.4. Bacterial growth kinetics .....	62
2.5. Susceptibility testing.....	62
2.6. Measurement of efflux activity.....	65
2.6.1. Accumulation of Hoechst 33342 .....	65
2.6.2. Efflux of ethidium bromide .....	66
2.7. Measurement of biofilm formation .....	67
2.7.1. Biofilm formation on porcine vaginal mucosal tissue .....	67
2.7.2. Biofilm formation in a microfluidic flow cell.....	70
2.7.3. Biofilm formation on polypropylene pegs .....	72
2.7.4. Pellicle formation .....	72
2.7.5. Biofilm formation on glass cover slips.....	73
2.8. Measurement of twitching and swarming motility .....	73
2.9. Measurement of virulence in <i>Galleria mellonella</i> .....	74
2.10. Statistical analysis.....	74
2.11. RNA-Seq.....	75

2.11.1.	RNA extraction .....	75
2.11.2.	DNase treatment of RNA samples .....	76
2.11.3.	Quantification of RNA .....	76
2.11.4.	Preparation of RNA-Seq libraries .....	77
2.11.5.	Sequencing of RNA-Seq libraries .....	78
2.11.6.	Analysis of RNA-Seq data .....	78
<b>3.</b>	<b>The Role of the Two Component System AdeRS in Antibiotic Resistance, Biofilm Formation and Virulence .....</b>	<b>80</b>
3.1.	Summary of background to this research.....	80
3.2.	Hypothesis .....	80
3.3.	Aims .....	80
3.4.	Choice of strains and verification of strains.....	81
3.5.	Determining the phenotype of an <i>A. baumannii</i> AYE mutant lacking the TCS AdeRS .....	87
3.5.1.	Bacterial growth kinetics of AYE $\Delta$ adeRS.....	87
3.5.2.	Antimicrobial susceptibility of AYE $\Delta$ adeRS .....	87
3.5.3.	Hoechst 33342 (bis-benzimide) accumulation by AYE $\Delta$ adeRS.....	89
3.5.4.	Ethidium bromide efflux by AYE $\Delta$ adeRS .....	93
3.5.5.	Biofilm formation by AYE $\Delta$ adeRS in an <i>ex vivo</i> model .....	93
3.5.6.	Biofilm formation <i>in vitro</i> by AYE $\Delta$ adeRS .....	97
3.5.7.	Motility of AYE $\Delta$ adeRS .....	106
3.5.8.	Virulence of AYE $\Delta$ adeRS in the <i>G. mellonella</i> model of infection.....	106
3.6.	Determining the transcriptome of AYE $\Delta$ adeRS.....	108
3.7.	Discussion.....	119
3.8.	Further work .....	125
3.9.	Key findings .....	127

<b>4. The Role of the RND Efflux Pump AdeB in Antibiotic Resistance, Biofilm Formation and Virulence .....</b>	<b>128</b>
4.1. Background.....	128
4.2. Hypothesis .....	128
4.3. Aims.....	129
4.4. Choice of strains and verification of strains.....	129
4.5. Optimisation of the gene deletion method and deletion of <i>adeB</i> in AYE ...	132
4.5.1. Verification of <i>adeB</i> deletion in AYE .....	136
4.6. Determining the phenotype of an <i>A. baumannii</i> AYE mutant lacking AdeB and an S1 mutant lacking AdeAB .....	140
4.6.1. Bacterial growth kinetics of AYE $\Delta$ <i>adeB</i> and S1 $\Delta$ <i>adeAB</i> .....	140
4.6.2. Antimicrobial susceptibility of AYE $\Delta$ <i>adeB</i> and S1 $\Delta$ <i>adeAB</i> .....	140
4.6.3. Hoechst 33342 (bis-benzimide) accumulation by AYE $\Delta$ <i>adeB</i> and S1 $\Delta$ <i>adeAB</i> .....	145
4.6.4. Ethidium bromide efflux by AYE $\Delta$ <i>adeB</i> and S1 $\Delta$ <i>adeAB</i> .....	145
4.6.5. Biofilm formation by AYE $\Delta$ <i>adeB</i> and S1 $\Delta$ <i>adeAB</i> in an <i>ex vivo</i> model .	148
4.6.6. Biofilm formation by AYE $\Delta$ <i>adeB</i> and S1 $\Delta$ <i>adeAB</i> <i>in vitro</i> .....	150
4.6.7. Motility of AYE $\Delta$ <i>adeB</i> and S1 $\Delta$ <i>adeAB</i> .....	158
4.6.8. Virulence of AYE $\Delta$ <i>adeB</i> and S1 $\Delta$ <i>adeAB</i> in the <i>Galleria mellonella</i> model of infection.....	158
4.7. Determining the transcriptome of AYE $\Delta$ <i>adeB</i> and S1 $\Delta$ <i>adeAB</i> .....	161
4.8. Discussion.....	177
4.9. Further work.....	183
4.10. Key findings .....	184
<b>5. The Role of AdeRS and AdeAB in Antibiotic Resistance, Biofilm Formation and Motility in Military Isolate AB5075 .....</b>	<b>185</b>
5.1. Background.....	185



5.2.	Hypothesis .....	185
5.3.	Aims .....	185
5.4.	Choice of strains and verification of strains .....	186
5.5.	Determining the phenotype of <i>adeR</i> , <i>adeS</i> , <i>adeA</i> and <i>adeB</i> transposon mutants in AB5075 .....	198
5.5.1.	Bacterial growth kinetics of AB5075 transposon mutants .....	198
5.5.2.	Antimicrobial susceptibility of AB5075 transposon mutants .....	198
5.5.3.	Hoechst 33342 (bis-benzimide) accumulation by AB5075 transposon mutants .....	201
5.5.4.	Ethidium bromide efflux by AB5075 transposon mutants .....	204
5.5.5.	Biofilm formation by AB5075 transposon mutants <i>in vitro</i> .....	204
5.5.6.	Motility of AB5075 transposon mutants .....	213
5.6.	Protein modelling of AB5075 transposon mutants .....	216
5.7.	Discussion .....	219
5.8.	Further work .....	223
5.9.	Key findings .....	224
<b>6.</b>	<b>Overall Discussion and Conclusions .....</b>	<b>225</b>
6.1.	Future work arising from this study .....	231

## List of Figures

Figure 1.6.1 Schematic diagram of the AdeABC tripartite RND system .....	28
Figure 1.7.1 A schematic of a two component signal transduction system .....	34
Figure 1.8.1 Summary of the genes shown to be directly or indirectly involved in antibiotic resistance, virulence, biofilm formation, motility and adherence in <i>A. baumannii</i> .....	37
Figure 2.3.1 A schematic diagram of the markerless deletion method used to create gene deletions in <i>A. baumannii</i> .....	57
Figure 2.7.1 Experimental setup of the porcine vaginal mucosal model.....	68
Figure 2.7.2 Cartoon representation of a Bioflux 200 microfluidic channel.....	71
Figure 3.4.1 Relationships between 615 <i>A. baumannii</i> isolates based on MLST data (Pasteur scheme) as calculated by the BURST algorithm.....	82
Figure 3.4.2 Verification of <i>adeRS</i> gene deletion in AYE by PCR and DNA sequencing .....	83
Figure 3.4.3 Predicted protein structure of AdeR and AdeS in AYE $\Delta$ <i>adeRS</i> .....	86
Figure 3.5.1 Growth kinetics of AYE and AYE $\Delta$ <i>adeRS</i> in LB broth at 37°C .....	88
Figure 3.5.2 Accumulation of H33342 by AYE and AYE $\Delta$ <i>adeRS</i> .....	92
Figure 3.5.3 Efflux of ethidium bromide by AYE and AYE $\Delta$ <i>adeRS</i> .....	94
Figure 3.5.4 Confocal laser scanning microscopy of AYE and ATCC19606 biofilms using LIVE/DEAD <sup>®</sup> staining and visualised at 1-6 days .....	95
Figure 3.5.5 Adherent and planktonic bacterial cells counts of AYE and AYE $\Delta$ <i>adeRS</i> grown at 37°C on PVM.....	98
Figure 3.5.6 Confocal laser scanning microscopy of AYE and AYE $\Delta$ <i>adeRS</i> biofilms using LIVE/DEAD <sup>©</sup> staining and visualised at 1-6 days.....	99

Figure 3.5.7 Phase contrast microscopy images of AYE and AYE $\Delta$ <i>adeRS</i> biofilms formed under flow conditions of 0.3 dynes up to 48 hrs .....	101
Figure 3.5.8 Biofilm formation by AYE and AYE $\Delta$ <i>adeRS</i> on polypropylene pegs as determined by crystal violet staining.....	102
Figure 3.5.9 Pellicle formation by AYE and AYE $\Delta$ <i>adeRS</i> incubated statically at 37°C .....	104
Figure 3.5.10 Scanning electron microscopy of AYE and AYE $\Delta$ <i>adeRS</i> biofilms grown for 24 hrs on glass cover slips .....	105
Figure 3.5.11 Twitching and swarming motility of AYE and AYE $\Delta$ <i>adeRS</i> grown on 1% and 0.3% agar for 24 hrs at 37°C .....	107
Figure 3.6.1 Kaplan Meir survival curve to show virulence of AYE and AYE $\Delta$ <i>adeRS</i> in <i>G. mellonella</i> .....	109
Figure 3.6.2 Heat map plot of gene expression changes in 6 biological replicates (3 x AYE and 3 x AYE $\Delta$ <i>adeRS</i> ) prepared and sequenced on different days.....	111
Figure 3.6.3 Number of reads aligned to each base across the <i>adeRS adeABC</i> region in each AYE and AYE $\Delta$ <i>adeRS</i> sample.....	112
Figure 3.6.4 Log <sub>2</sub> fold change in expression of all genes of the AYE genome in AYE $\Delta$ <i>adeRS</i> compared with AYE .....	116
Figure 3.6.5 Clusters of orthologous groups (COG) and the percentage of genes with increased expression (red) and decreased expression (blue) in AYE $\Delta$ <i>adeRS</i> compared with AYE within each group as determined by RNA-Seq .....	118
Figure 4.4.1 Relationships between 615 <i>A. baumannii</i> isolates based on MLST data (Pasteur scheme) as calculated by the BURST algorithm.....	130
Figure 4.4.2 Verification of <i>adeAB</i> gene deletion in S1 by PCR.....	131

Figure 4.5.1 Predicted protein structure of AdeA and AdeB in <i>S1ΔadeAB</i> .....	133
Figure 4.5.2 pMo130-TeIR suicide vector containing a <i>groES</i> promoter driving a modified <i>sacB</i> gene with AYE <i>relA</i> up and down fragments.....	134
Figure 4.5.3 Verification of <i>adeB</i> gene deletion in AYE by PCR and DNA sequencing .....	137
Figure 4.5.4 Predicted protein structure of AdeB in <i>AYEΔadeB</i> .....	139
Figure 4.6.1 Growth kinetics of AYE, <i>AYEΔadeB</i> , S1 and <i>S1ΔadeAB</i> in LB broth at 37°C .....	141
Figure 4.6.2 Accumulation of H33342 by AYE, <i>AYEΔadeB</i> , S1 and <i>S1ΔadeAB</i> .....	146
Figure 4.6.3 Efflux of ethidium bromide by AYE, <i>AYEΔadeB</i> , S1 and <i>S1ΔadeAB</i> ..	147
Figure 4.6.4 Adherent and planktonic bacterial cells counts of AYE, <i>AYEΔadeB</i> , S1 and <i>S1ΔadeAB</i> grown at 37°C on PVM .....	149
Figure 4.6.5 Confocal laser scanning microscopy of AYE, <i>AYEΔadeB</i> , S1 and <i>S1ΔadeAB</i> biofilms using LIVE/DEAD® staining and visualised at 1-6 days .....	151
Figure 4.6.6 Phase contrast microscopy images of AYE, <i>AYEΔadeB</i> , S1 and <i>S1ΔadeAB</i> biofilms formed under flow conditions of 0.3 dynes up to 48 hrs.....	153
Figure 4.6.7 Biofilm formation by AYE, <i>AYEΔadeB</i> , S1 and <i>S1ΔadeAB</i> on polypropylene pegs as determined by crystal violet staining.....	154
Figure 4.6.8 Pellicle formation by AYE, <i>AYEΔadeB</i> , S1 and <i>S1ΔadeAB</i> incubated statically at 37°C.....	156
Figure 4.6.9 Scanning electron microscopy of AYE, <i>AYEΔadeB</i> , S1 and <i>S1ΔadeAB</i> biofilms on glass cover slips .....	157
Figure 4.6.10 Twitching and swarming motility of AYE, <i>AYEΔadeB</i> , S1 and <i>S1ΔadeAB</i> grown on 1% and 0.3% agar for 24 hrs at 37°C.....	159

Figure 4.6.11 Kaplan Meir survival curves to show virulence of AYE, AYE $\Delta$ <i>adeB</i> , S1 and S1 $\Delta$ <i>adeAB</i> in <i>G. mellonella</i> .....	160
Figure 4.7.1 Number of reads aligned to each base across the <i>adeRS adeABC</i> region in each sample .....	162
Figure 4.7.2 Log2 fold change in expression of all genes of the AYE genome in AYE $\Delta$ <i>adeB</i> compared with AYE .....	167
Figure 4.7.3 Log2 fold change in expression of all genes of the AYE genome in S1 $\Delta$ <i>adeAB</i> compared with S1 .....	168
Figure 4.7.4 Clusters of orthologous groups (COG) and the percentage of genes with increased expression (red) and decreased expression (blue) in AYE $\Delta$ <i>adeB</i> compared with AYE within each group as determined by RNA-Seq .....	174
Figure 4.7.5 Clusters of orthologous groups (COG) and the percentage of genes with increased expression (red) and decreased expression (blue) in S1 $\Delta$ <i>adeAB</i> compared with S1 within each group as determined by RNA-Seq .....	175
Figure 5.4.1 BRIG output image of BLAST comparison of the AB5075 genome (purple) against an AYE reference genome .....	187
Figure 5.4.2 Snapshot of a BLASTN comparison of the <i>adeRS</i> and <i>adeABC</i> regions of AYE and AB5075 using ACT.....	188
Figure 5.4.1 Schematic showing the location of transposon insertion in each AB5075 transposon mutant.....	192
Figure 5.4.2 Verification of transposon insertion in AB5075 transposon mutants by PCR.....	194
Figure 5.5.1 Growth kinetics of AB5075 transposon mutants in LB broth at 37°C ..	199
Figure 5.5.2 Accumulation of H333342 by AB5075 transposon mutants .....	205

Figure 5.5.3 Efflux of ethidium bromide by AB5075 transposon mutants .....	207
Figure 5.5.4 Phase contrast microscopy images of AB5075 transposon mutant biofilms formed under flow conditions of 0.3 dynes at 48 hrs .....	210
Figure 5.5.5 Biofilm formation by AB5075 transposon mutants on polypropylene pegs as determined by crystal violet staining.....	211
Figure 5.5.6 Pellicle formation by AB5075 transposon mutants incubated statically at 37°C and visualised under white light.....	214
Figure 5.5.7 Swarming motility of AB5075 Tn mutants grown on 0.3% agar for 24 hrs at 37°C .....	215
Figure 5.6.1 Predicted protein structures of AdeR, AdeS, AdeA and AdeB generated by I-TASSER.....	217

## List of Tables

Table 1.1.1 <i>Acinetobacter</i> spp. with formal species names.....	3
Table 1.6.1 Resistance mechanisms in <i>Acinetobacter</i> spp. ....	21
Table 2.1.1 Bacterial strains used in this study .....	49
Table 2.2.1 Primers .....	52
Table 2.2.2 Generic PCR reaction volumes .....	55
Table 2.3.1 Generic PCR parameters .....	58
Table 2.3.2 Restriction enzymes used in this study.....	60
Table 2.5.1 Antibiotics and dyes used in this study .....	63
Table 3.5.1 MICs of antibiotics and dyes against AYE and AYE $\Delta$ <i>adeRS</i> .....	90
Table 3.6.1 The top 10 genes with the most significantly changed expression in AYE $\Delta$ <i>adeRS</i> compared with AYE .....	114
Table 3.6.2 The top 10 genes with the largest fold change in expression in AYE $\Delta$ <i>adeRS</i> compared with AYE .....	115
Table 4.6.1 MICs of antibiotics and dyes against AYE, AYE $\Delta$ <i>adeB</i> , S1 and S1 $\Delta$ <i>adeAB</i> .....	142
Table 4.7.1 The top 10 genes with the most significantly changed expression in AYE $\Delta$ <i>adeB</i> compared with AYE .....	170
Table 4.7.2 The top 10 genes with the largest fold change in expression in AYE $\Delta$ <i>adeB</i> compared with AYE .....	171
Table 4.7.3 The top 10 genes with the most significantly changed expression in S1 $\Delta$ <i>adeAB</i> compared with S1 .....	172
Table 4.7.4 The top 10 genes with the largest fold change in expression in S1 $\Delta$ <i>adeAB</i> compared with S1 .....	173

Table 4.8.1 Protocols used for RNA-Seq experiments .....	179
Table 5.4.1 Transposon mutants obtained from the University of Washington Transposon Mutant Library.....	190
Table 5.5.1 Generation times and optical density at stationary phase of AB5075 transposon mutants in LB broth at 37°C.....	200
Table 5.5.2 MICs of antibiotics and dyes against AB5075 transposon mutants .....	202
Table 5.9.1 Summary of mutant phenotypes compared with their respective parental strains.....	226



## List of Abbreviations

<b>Abbreviation</b>	<b>Definition</b>
µg	Microgram
µl	Microlitre
µM	Micromolar
Acb	<i>Acinetobacter calcoaceticus – baumannii</i>
AFLP	Amplified fragment length polymorphism
AHL	acyl-homoserine lactone
AME	Aminoglycoside-modifying enzyme
ATCC	American Type Culture Collection
ATP	Adenosine triphosphate
Bp	Base pair
BSAC	British Society for Antimicrobial Chemotherapy
CCCP	carbonyl cyanide-m-chlorophenyl hydrazone
cDNA	complimentary DNA
CEM	Centre for Electron Microscopy
CFU	Colony forming units
CLSI	Clinical and Laboratory Standards Institute
DNA	Deoxyribonucleic acid
eDNA	Extracellular DNA
ECM	Extracellular matrix
ESBL	Extended spectrum β-lactamase
EU	European
EUCAST	European Committee on Antimicrobial Susceptibility Testing
G	Grams
G	Gravity
H33342	Hoechst 33342
Hr	Hour
ICU	Intensive care unit
IS	Insertion sequence
Kb	Kilobase
LB	Luria-Bertani

LPS	Lipopolysaccharide
MATE	Multi-drug and toxic compound extrusion
MBL	Metallo- $\beta$ -lactamase
MDR	Multi-drug resistant
MFP	Membrane fusion protein
MFS	Major facilitator superfamily
mg	Milligrams
MIC	Minimum inhibitory concentration
min	Minute
ml	Millilitre
mRNA	Messenger RNA
nm	Nanometres
OD	Optical density
OD600	Optical density at 600 nm
OMP	Outer membrane protein
OXA	Oxacillinase
PA $\beta$ N	Phenylalanine-arginine $\beta$ -naphthylamide
PBP	Penicillin binding protein
PCR	Polymerase chain reaction
PDR	Pan-drug resistant
PFGE	Pulsed field gel electrophoresis
PHE	Public Health England
PNAG	Poly- $\beta$ -1-6-N-acetylglucosamine
PVM	Porcine vaginal mucosa
QEH	Queen Elizabeth Hospital
RNA	Ribonucleic acid
RND	Resistance nodulation division
RPMI	Roswell Park Memorial Institute
rRNA	Ribosomal RNA
sec	Second
SMR	Small multi-drug resistance
TCS	Two component system

Tn	Transposon
tRNA	Transfer RNA
TSA	Tryptic soy agar
UV	Ultraviolet
VNTR	Variable number tandem repeats
WGS	Whole genome sequencing
XDR	Extensively-drug resistant

# 1. Introduction

## 1.1. *Acinetobacter* species

*Acinetobacter* are Gram-negative coccobacilli responsible for an increasing number of nosocomial infections in the UK and worldwide. *Acinetobacter* are currently defined as aerobic, non-fermenting, non-fastidious, non-motile, catalase-positive and oxidase-negative bacteria, with a DNA G+C content of ~40% (Rossau, Van Landschoot et al. 1991). They are opportunistic pathogens and are a serious problem in immunocompromised patients within the hospital setting (Antunes, Visca et al. 2014). The clinical success of this organism is due to a number of factors including its propensity to acquire antibiotic resistance determinants and to over-express existing intrinsic resistance genes, allowing it to avoid eradication by antibiotics and biocides. Its ability to survive desiccation means it is also able to persist in the hospital environment for extended periods of time (Wendt, Dietze et al. 1997, Jawad, Seifert et al. 1998, Jawad, Snelling et al. 1998).

The taxonomy of *Acinetobacter* has a long and complicated background and there are still difficulties with species identification. The bacterium was first identified in 1911 by the Dutch microbiologist, Beijerinck, who isolated a bacterium he named *Micrococcus calcoaceticus* from soil samples (Beijerinck 1911). Since then, bacteria now known as *Acinetobacter* have been isolated many times and assigned to various genera. In 1971, the genus *Acinetobacter* was officially acknowledged by the Subcommittee on Nomenclature of Moraxella and Allied Bacteria (Lessele 1971). In 1986, the genera was divided into 12 DNA groups with formal species names

(Bouvet and Grimont 1987) and has since been further categorised to give at least 38 genomic groups with formal species names (Table 1.1.1) (Towner 2009, Visca, Seifert et al. 2011) (<http://www.bacterio.net/acinetobacter.html>).

### **1.1.1. Natural habitat**

Not all *Acinetobacter* species pose a threat to human health. Many species are non-pathogenic and can be isolated from the soil; they also often form part of the normal human skin flora (Baumann 1968, Seifert, Dijkshoorn et al. 1997). This has led to the common misconception that all *Acinetobacter* species are ubiquitous and that pathogenic species such as *A. baumannii* can be isolated from environmental sources. However, it is now generally accepted that this is not the case. Although *Acinetobacter* can be isolated from human skin, highly pathogenic species such as *A. baumannii* are rarely found colonising the skin of healthy humans (Berlau, Aucken et al. 1999). Clinically relevant strains of *Acinetobacter* are often found colonising hospital surfaces, hospital staff and medical instrumentation (Lewis, Loman et al. 2010, Kirkgoz and Zer 2014, Duszynska, Rosenthal et al. 2015, Ye, Shan et al. 2015), although the natural habitat of these strains remains unknown.

### **1.1.2. Epidemiology**

*Acinetobacter* is well-recognised for its ability to cause nosocomial outbreaks, and particular strains are able to cause epidemics in multiple hospitals within a city, in various regions in a country and can even spread worldwide (van Dessel, Dijkshoorn et al. 2004, Coelho, Woodford et al. 2006, Coelho, Turton et al. 2006). *A. baumannii* European (EU) clones I and II were first identified as outbreak strains in North-western Europe in 1996 (Dijkshoorn, Aucken et al. 1996). A third clone was later

**Table 1.1.1 *Acinetobacter* spp. with formal species names**

Species name	Representative strain	Reference
<i>A. apis</i>	HYN 18	(Kim, Shin et al. 2014)
<i>A. baumannii</i>	ATCC 19606	(Bouvet and Grimont 1986)
<i>A. baylyi</i>	DSM 14961	(Carr, Kämpfer et al. 2003)
<i>A. beijerinckii</i>	NIPH 838	(Nemec, Musílek et al. 2009)
<i>A. bereziniae</i>	ATCC 17924	(Nemec, Musílek et al. 2010)
<i>A. bohemicus</i>	ANC 3994	(Krizova, McGinnis et al. 2015)
<i>A. boissieri</i>	SAP 284.1	(Álvarez-Pérez, Lievens et al. 2013)
<i>A. bouvetii</i>	DSM 14964	(Carr, Kämpfer et al. 2003)
<i>A. brissouii</i>	5YN5-8	(Anandham, Weon et al. 2010)
<i>A. calcoaceticus</i>	ATCC 23055	(Baumann 1968)
<i>A. gandensis</i>	UG 60467T	(Smet, Cools et al. 2014)
<i>A. gernerii</i>	DSM 14967	(Carr, Kämpfer et al. 2003)

Species name	Representative strain	Reference
<i>A. grimontii</i>	DSM 14968	(Carr, Kämpfer et al. 2003)
<i>A. guangdongensis</i>	1NM-4	(Feng, Yang et al. 2014)
<i>A. guillouiae</i>	ATCC 11171	(Nemec, Musílek et al. 2010)
<i>A. gyllenbergii</i>	NIPH 2150	(Nemec, Musílek et al. 2009)
<i>A. haemolyticus</i>	ATCC 17906	(Bouvet and Grimont 1986)
<i>A. harbinensis</i>	HLTLi-7	(Li, Zhang et al. 2014)
<i>A. indicus</i>	A648	(Malhotra, Anand et al. 2012)
<i>A. johnsonii</i>	ATCC 17909	(Bouvet and Grimont 1986)
<i>A. junii</i>	ATCC 17908	(Bouvet and Grimont 1986)
<i>A. kookii</i>	11-0202	(Choi, Ko et al. 2013)
<i>A. lwoffii</i>	ATCC 15309	(Brisou and Prevot 1954)
<i>A. nectaris</i>	SAP 763.2	(Álvarez-Pérez, Lievens et al. 2013)
<i>A. nosocomialis</i>	RUH 2376	(Nemec, Krizova et al. 2011)

Species name	Representative strain	Reference
<i>A. parvus</i>	NIPH384	(Nemec, Dijkshoorn et al. 2003)
<i>A. pittii</i>	RUH 2206	(Nemec, Krizova et al. 2011)
<i>A. puyangensis</i>	BQ4-1	(Li, Piao et al. 2013)
<i>A. quingfengensis</i>	2BJ1	(Li, He et al. 2014)
<i>A. radioresistens</i>	IAM 13186	(Nishimura, Kanzaki et al. 1988)
<i>A. rudis</i>	G30	(Vaz-Moreira, Novo et al. 2011)
<i>A. schindleri</i>	NIPH1034	(Nemec, De Baere et al. 2001)
<i>A. soli</i>	KCTC 22184	(Kim, Baik et al. 2008)
<i>A. tandoii</i>	DSM 14970	(Carr, Kämpfer et al. 2003)
<i>A. tjernbergiae</i>	DSM 14971	(Carr, Kämpfer et al. 2003)
<i>A. towneri</i>	DSM 14962	(Carr, Kämpfer et al. 2003)
<i>A. ursingii</i>	NIPH137	(Nemec, De Baere et al. 2001)
<i>A. venetianus</i>	ATCC 31012	(Vanechoutte, Nemec et al. 2009)

Adapted from <http://www.bacterio.net/acinetobacter.html>



identified as a European outbreak strain and named EU clone III (van Dessel, Dijkshoorn et al. 2004). These clones are widespread throughout Europe and contribute significantly to the spread of carbapenem-resistant *Acinetobacter* (Towner, Levi et al. 2008). Other individual lineages are more prevalent in certain areas of Europe, such as the AYE-VEB-1 clone found in France and Belgium (Naas, Bogaerts et al. 2006) and the OXA-40 (OXA-24) carbapenem-resistant clone found in Spain and Portugal (Da Silva, Quinteira et al. 2004). The EU clones are in fact international lineages and not limited to Europe. Outbreaks have been identified in the USA and South Africa (van Dessel, Dijkshoorn et al. 2004, Petersen, Cannegieter et al. 2011). In Asia, carbapenem resistant European clones have been described in hospitals in China (Fu, Zhou et al. 2010) and Korea (Park, Lee et al. 2010). In Singapore, carbapenem resistance is also observed in clinical isolates, with outbreak isolates related to EU clones I and II identified in the hospital setting, and the majority of carbapenem resistance due to OXA-23 carrying clones (Park, Lee et al. 2010). In a study of UK hospitals between 2003 and 2006, sub-lineages of EU clone II dominated, with the South-east (SE) and OXA-23 clones being the most prevalent (Coelho, Turton et al. 2006).

## **1.2. *Acinetobacter baumannii* complex**

Four of the identified *Acinetobacter* species are often grouped into the *Acinetobacter calcoaceticus* – *baumannii* (Acb) complex. This group comprises of *A. baumannii*, *A. calcoaceticus*, *A. pittii* and *A. nosocomialis* (Gerner-Smidt 1992, Nemeč, Krizova et al. 2011). *A. baumannii*, *A. pittii* and *A. nosocomialis* are clinically relevant species, often implicated in infection, whereas *A. calcoaceticus* is largely non-pathogenic and is rarely identified in the hospital setting (Peleg, Seifert et al. 2008, Koh, Tan et al.

2012). Therefore, from a clinical perspective, identification of different species of *Acinetobacter*, especially those within the Acb complex, is extremely important. Species also has implications for treatment and infection control as many of the non-*A. baumannii* complex species are drug susceptible and strict infection control is not necessary (Chuang, Sheng et al. 2011). However, discrimination between species is difficult, particularly between members of the *A. baumannii* complex, which cannot be differentiated phenotypically and are often misidentified (Gerner-Smidt, Tjernberg et al. 1991, Gerner-Smidt 1992). Semi-automated systems such as the API 20NE system are often unreliable and also cannot distinguish between closely related species (Bernards, van der Toorn et al. 1996). There are a number of methods currently used for the routine identification of *Acinetobacter* species in clinical laboratories; DNA-DNA hybridisation was first used to describe a total of 12 genomic species of *Acinetobacter* (Bouvet and Grimont 1986). However this process is lengthy and is impractical for a routine diagnostic laboratory. For this reason various methods have been adopted and verified for species identification. These include 16S rRNA gene restriction (ARDRA) (Vaneechoutte, Dijkshoorn et al. 1995), high resolution fingerprint analysis by amplified fragment length polymorphism (AFLP) (Janssen, Maquelin et al. 1997), ribotyping (Gerner-Smidt 1992), tRNA spacer analysis (Ehrenstein, Bernards et al. 1996), restriction analysis of 16S-23S rRNA intergenic spacer regions (Dolzani, Tonin et al. 1995, Chang, Wei et al. 2005) and sequence analysis of the *rpoB* gene (La Scola, Gundi et al. 2006). Nonetheless, apart from a small number of *Acinetobacter* reference laboratories, species identification is not always possible in most clinical laboratories.

### **1.3. *Acinetobacter baumannii* infection**

#### **1.3.1. Hospital acquired infections**

*A. baumannii* most commonly causes nosocomial infections, including ventilator-associated pneumonia, skin and soft-tissue infections, wound infections, surgical site infections, catheter-related and urinary tract infections, secondary meningitis and bloodstream infections (Forster and Daschner 1998). Studies have found that up to 18% of patients infected with *A. baumannii* develop bacteraemia, most often acquired in the intensive care unit (ICU) (Cisneros, Reyes et al. 1996). The assessment of the outcome of *Acinetobacter* infection is difficult and reported mortality rates range from 5% in general wards to 54% in the ICU (Poutanen, Louie et al. 1997, Siau, Yuen et al. 1999). Seifert et al. showed the crude mortality rate of *A. baumannii* bacteraemia to be as high as 44%. However, it is difficult to determine morbidity and mortality directly attributable to *A. baumannii* as opposed to co-morbidity, which is very common in these patients. Death attributable to *A. baumannii* bacteraemia, at 19%, was assessed to be much lower than the crude mortality rate (Seifert, Strate et al. 1995). Several predisposing factors to infections with *A. baumannii* have been identified. These include immunosuppression, unscheduled hospital admission, respiratory failure at admission, previous antimicrobial therapy, previous sepsis in the ICU and invasive procedures; all of which have been recognised as risk factors for *A. baumannii* infection (Garcia-Garmendia, Ortiz-Leyba et al. 2001). *A. baumannii* can be cultured from different environmental sites within hospitals and it is thought that cross contamination between sites is a major mode of transmission in hospital outbreaks (van den Broek, Arends et al. 2006). Carriage of *A. baumannii* on the hands of hospital staff and on medical instrumentation can contribute to the spread of

the organism (Ye, Shan et al. 2015, Al-Mousa, Omar et al. 2016). The ability of *A. baumannii* to survive on dry surfaces for extended periods of time may also increase transmissibility. It has been suggested that desiccation tolerance, along with multi-drug resistance (MDR) demonstrated by some strains, may explain why *A. baumannii* is able to establish itself in the hospital environment and cause recurring nosocomial outbreaks (Jawad, Heritage et al. 1996, Jawad, Seifert et al. 1998, Jawad, Snelling et al. 1998).

Hospital outbreaks often occur within the intensive care unit, where immunocompromised patients provide a niche for opportunistic pathogens such as *A. baumannii* (Dijkshoorn, Nemec et al. 2007). Whole genome sequencing to investigate genome dynamics of clinical isolates of *A. baumannii* within the hospital have indicated that an endemic and interacting population can exist in the hospital environment or in colonised patients. Movement of patients and staff may contribute to transmission and diversification of this population (Halachev, Chan et al. 2014, Wright, Haft et al. 2014). *A. baumannii* wound infections in military casualties are also a concern and can spread to civilian patients in the hospital (Davis, Moran et al. 2005, Hujer, Hujer et al. 2006, Sebeny, Riddle et al. 2008, O'Shea 2012). Military casualties repatriated to Selly Oak Hospital, Birmingham or the Queen Elizabeth Hospital (QEH), Birmingham were often treated alongside civilian patients. Investigation of a MDR *A. baumannii* outbreak in the Selly Oak Hospital showed two civilian and four military patients to be colonised with isolates identical by variable number tandem repeats (VNTR) and pulsed field gel electrophoresis (PFGE) analyses. Subsequent whole genome sequencing (WGS) provided insight into transmission events and supported transmission from the wound of a military patient

to the respiratory tract of a civilian patient (Lewis, Loman et al. 2010). Similarly, WGS of 114 isolates from a second protracted hospital outbreak of *A. baumannii* at the QEH, Birmingham, between July 2011 and February 2013 linked military patient derived isolates directly to civilian patient and environmental isolates (Halachev, Chan et al. 2014).

### **1.3.2. Community acquired infections**

Although most common in the hospital environment, community acquired *Acinetobacter* infection has been observed. In Portugal, necrotising community acquired pneumonia due to *Acinetobacter lwoffii* contamination of a nebuliser in a previously healthy child was identified (Moreira Silva, Morais et al. 2011). This type of infection is usually associated with underlying conditions such as alcoholism, smoking, chronic obstructive pulmonary disease and diabetes mellitus and is a particular problem in tropical climates such as Southeast Asia and Australia, where skin carriage is more common due to environmental conditions (Anstey, Currie et al. 1992, Chu, Leung et al. 1999). In these areas *A. baumannii* can be a cause of severe community-acquired pneumonia, especially in young alcoholic patients (Chen, Hsueh et al. 2001) and mortality rates as high as 64% have been reported (Dexter, Murray et al. 2015).

### **1.3.3. Infection in military and disaster zone casualties**

*Acinetobacter* species are also commonly isolated from deep wound and burn infections, and osteomyelitis in military and disaster zones. Reports from the Marmara earthquake in Turkey in 1999 described a high incidence of *Acinetobacter* strains as responsible for healthcare associated infection in trauma patients (Oncul,

Keskin et al. 2002). *Acinetobacter* wound infections have been reported in military casualties returning from Iraq and Afghanistan, many of them exhibiting MDR (Murray, Roop et al. 2006, Johnson, Burns et al. 2007, Petersen, Riddle et al. 2007, Scott, Deye et al. 2007). Due to the misconception that *A. baumannii* is ubiquitous and can be isolated from environmental sources it was initially considered that the organism was being introduced at the site of injury, or was due to skin colonisation at the time of injury. However, there is now evidence of the role of environmental contamination and transmission of organisms within health care facilities and it is likely that patients with a prolonged stay in US field hospitals provide a reservoir for this organism (Davis, Moran et al. 2005, Scott, Deye et al. 2007).

#### **1.4. Persistence in the hospital environment**

*A. baumannii* is found almost exclusively in the hospital environment and environmental contamination is often responsible for the high incidence of infections in military and civilian patients (Catalano, Quelle et al. 1999, Scott, Deye et al. 2007, Chaladchalam, Diraphat et al. 2008, O'Shea 2012). *A. baumannii* has a high level of desiccation tolerance and in addition can form biofilms (Tomaras, Dorsey et al. 2003, Gaddy and Actis 2009, Gaddy, Tomaras et al. 2009, de Breij, Haisma et al. 2012, Greene, Vadlamudi et al. 2016), in which cells are enclosed in an extracellular matrix composed of polysaccharides, extracellular DNA and protein (Hobley, Harkins et al. 2015). Biofilms are significantly more resistant to biocide and antimicrobial treatment, host immune responses, desiccation and UV light, which enables them to persist in harsh environments, including the hospital setting (Hall-Stoodley, Costerton et al. 2004, Rajamohan, Srinivasan et al. 2009). In a biofilm, a gradient of nutrients and oxygen from the top to the bottom is associated with decreased bacterial metabolic

activity and increased doubling times of bacterial cells, which is in part responsible for tolerance to antibiotics. Furthermore, biofilm growth can be associated with an increased level of mutations, leading to antibiotic resistance (Høiby, Bjarnsholt et al. 2010). Growth on medical devices and tissue surfaces can lead to biofilm formation and increase the risk of bloodstream and respiratory infections (Dijkshoorn, Nemec et al. 2007). *In vitro* studies have shown that biofilms can survive antibiotic concentrations of up to 1000 x the minimum inhibitory concentration (MIC) of a planktonic culture and *in vivo* bacteria that survive antibiotic exposure in a biofilm state can cause recurrence of infection once antibiotic treatment is stopped (Mah and O'Toole 2001, Stewart and William Costerton 2001)

## **1.5. Treatment of *Acinetobacter* infections**

### **1.5.1. Antibiotics**

Due to the wide spectrum of intrinsic and acquired antibiotic resistance mechanisms present in *A. baumannii*, treatment of infections poses a major challenge. Clinical isolates displaying resistance to several classes of antibiotics are commonly observed and treatment of MDR isolates is now limited to very few antibiotics.

#### **1.5.1.1. Sulbactam**

Sulbactam is a  $\beta$ -lactamase inhibitor that binds penicillin binding protein (PBP) 2 in *A. baumannii* (Urban, Go et al. 1995). Whilst its primary purpose is to limit the degradation of active  $\beta$ -lactams by  $\beta$ -lactamases, it also demonstrates some intrinsic activity against *Acinetobacter* species when used alone (Levin 2002, Higgins, Wisplinghoff et al. 2004). Sulbactam is most commonly used in combination with other antibiotics and an ampicillin-sulbactam combination provides an effective

therapeutic option for the treatment of MDR *Acinetobacter* infections (Levin, Levy et al. 2003). Oliveira et al. showed that ampicillin-sulbactam may be more efficacious in treating carbapenem-resistant *Acinetobacter* spp. than polymyxins (Oliveira, Prado et al. 2008). However, one clinical study has shown that the *in vitro* activity of an ampicillin-sulbactam combination was a result of the antimicrobial activity of sulbactam alone and no synergy was observed between ampicillin and sulbactam (Corbella, Ariza et al. 1998). It has been suggested that sulbactam should be the preferred treatment for infections with this pathogen (Levin 2002, Peleg 2007). Unfortunately, increasing clinical use has led to a rise in sulbactam resistance and minimum inhibitory concentrations (MICs) of >32 µg/ml have been observed in clinical isolates (Henwood, Gatward et al. 2002, Higgins, Wisplinghoff et al. 2004). However, spontaneous resistance is rare, with high-level resistance due to mutations in *pbp3* resulting in a fitness cost in *A. baumannii* (Penwell, Shapiro et al. 2015). Low-level resistance is associated with mutations in genes involved in cell wall biosynthesis, such as *galE* and *mraY* or stress responses such as *rpoC* (Penwell, Shapiro et al. 2015). Resistance to an ampicillin-sulbactam combination has also been seen; in a study conducted in Taiwan, 70% of clinical isolates were ampicillin-sulbactam resistant (Yang, Chang et al. 2010).

#### **1.5.1.2. Polymyxins**

Polymyxins are polycationic lipopeptide antimicrobials that show bactericidal activity against *Acinetobacter* spp. They include polymyxin B, polymyxin E and colistin. The polymyxins were discovered as chemotherapeutic agents in 1947 (Stansly, Shepherd et al. 1947), but use has been minimal due to concerns over neurotoxicity and nephrotoxicity (Falagas, Fragoulis et al. 2005, Falagas, Rafailidis et al. 2006).



However, with MDR bacteria becoming more prevalent, the use of polymyxins has increased and in some cases is recommended for the treatment of carbapenem-resistant *Acinetobacter* (Kim, Peleg et al. 2009). Polymyxins show high success rates in the clinical setting. Kallel *et al.* showed successful treatment of 76% of patients with MDR *A. baumannii* or *Pseudomonas aeruginosa* treated with colistin in the ICU (Kallel, Bahloul et al. 2006) and others have also shown success with polymyxin treatment against MDR *Acinetobacter* (Holloway, Roupheal et al. 2006, Falagas, Rafailidis et al. 2010). Resistance to these drugs has been rare, however increasing use means that the isolation of resistant strains is on the rise (Matthaiou, Michalopoulos et al. 2008) with reported polymyxin resistance levels of up to 18% in *A. baumannii* isolates in South Korea (Ko, Suh et al. 2007). Colistin and other polymyxins target the lipid A component of lipopolysaccharide (LPS) of Gram negative bacteria during initial binding of the outer membrane. Mutations in the lipid A biosynthesis genes *lpxA*, *lpxC*, and *lpxD* can result in loss of ability to produce lipid A and therefore LPS. This prevents the interaction of colistin with LPS in colistin resistant *A. baumannii* isolates (Moffatt, Harper et al. 2010). An alternative mechanism of resistance was identified by Beceiro *et al.* who observed mutations in *pmrB* and upregulation of *pmrAB* leading to modification of lipid A and consequently colistin resistance (Beceiro, Llobet et al. 2011). Modifications in *pmrAB* resulting in upregulation of the phosphethanolamine gene *pmrC*, and lipid A modification have been also identified in clinical isolates displaying resistance to colistin (Arroyo, Herrera et al. 2011, Lesho, Yoon et al. 2013). Resistance to colistin has been shown to have a virulence and fitness cost in *A. baumannii* (López-Rojas, Jiménez-Mejías et al. 2011, Hraiech, Roch et al. 2013, Pournaras, Poulou et al. 2014). However, studies

have identified *pmrB* mutants with resistance to colistin and retention of virulence (Durante-Mangoni, Del Franco et al. , Wand, Bock et al. 2015). Recent studies have shown the emergence of the first plasmid-mediated polymyxin resistance mechanism, MCR-1, in *Enterobacteriaceae*, posing the threat of dissemination of *mcr-1* among other Gram-negative bacteria such as *A. baumannii* (Liu, Wang et al. 2016).

### **1.5.1.3. Carbapenems**

Carbapenems are one of the most valuable treatment options against MDR *A. baumannii*. This class of  $\beta$ -lactams shows good bactericidal activity against  $\beta$ -lactamase producing MDR *Acinetobacter* isolates (Fishbain and Peleg 2010). However, increasing resistance to imipenem and meropenem has been observed in the last decade (Karageorgopoulos and Falagas 2008). Resistance to carbapenems is most commonly due to production of class D  $\beta$ -lactamases e.g. OXA-51-like, and OXA-23-like enzymes (Turton, Ward et al. 2006, Corvec, Poirel et al. 2007), increased production of multi-drug efflux pumps, such as AdeABC (Magnet, Courvalin et al. 2001, Huang, Sun et al. 2008), and decreased permeability due to reduced expression of porins such as CarO (Ravasi, Limansky et al. 2011). Carbapenem resistant isolates are often resistant to other classes of antibiotics, leaving polymyxins and tigecycline as the only remaining treatment options. A 2007 study of antimicrobial susceptibility in isolates collected from around the world identified susceptibility to imipenem ranging from 60.6% in Latin America to 88.6% in North America. Susceptibility was also high in Europe (85.9%), whereas susceptibility rates in Asia were moderate to low (69.2%) (Reinert, Low et al. 2007). Since then, various studies have highlighted the emergence of carbapenem-resistant isolates in

the clinical setting (Scott, Deye et al. 2007, Enoch, Summers et al. 2008, Lee, Fung et al. 2011, Kempf and Rolain 2012). However, susceptibility data based on a particular carbapenem antibiotic cannot be generalised to all drugs in this class. Differing imipenem and meropenem resistance levels have been observed in clinical isolates (Ikonomidis, Pournaras et al. 2006). Misinterpreted susceptibility results can also give rise to dire consequences; based on susceptibility to imipenem, a case of *A. baumannii* pneumonia by a meropenem resistant isolate was treated with meropenem, leading to patient death (Lesho, Wortmann et al. 2005).

#### **1.5.1.4. Tigecycline**

Tigecycline is a glycycline antibiotic and is a semi-synthetic modified minocycline (Neonakis, Spandidos et al. 2011). *In vitro* activity has been demonstrated against 595 clinical isolates of *Acinetobacter* spp. isolated throughout the UK (Henwood, Gatward et al. 2002) and global studies have shown MIC<sub>90</sub> values of 1-2 µg/ml (Reinert, Low et al. 2007, Garrison, Mutters et al. 2009), although breakpoint concentrations to define resistance have not yet been established by The Clinical and Laboratory Standards Institute (CLSI), The European Committee on Antimicrobial Susceptibility Testing (EUCAST) or The British Society for Antimicrobial Chemotherapy (BSAC) for this antibiotic class. A good clinical and microbiological response to tigecycline treatment of MDR *A. baumannii* has been observed in some cases (Poulakou, Kontopidou et al. 2009). Vasilev *et al.* identified a cure rate of 82.4% for resistant *A. baumannii* infections in a multicentre study (Vasilev, Reshedko et al. 2008). However, Gordon *et al.* observed microbiological clearance of the infection in only 68% of cases in a retrospective study of tigecycline treated *A. baumannii* infections in a UK hospital and of 30 patients with pneumonia caused by

MDR *A. baumannii* treated with tigecycline in Korea, only 47% showed clinical success (Kim, Moon et al. 2016). This result suggests that tigecycline monotherapy may not always be appropriate (Gordon and Wareham 2009). Treatment failure has also been observed with tigecycline therapy. In one case of a MDR *A. baumannii* infection of the urinary tract, tigecycline resistance developed during therapy, after only three weeks exposure to the drug (Reid, Grim et al. 2007). Evaluation of tigecycline treatment in unrelated studies of patients with MDR *A. baumannii* infections has also identified single isolates that developed resistance during treatment (Schafer, Goff et al. 2007, Anthony, Fishman et al. 2008). In a study of 70 *A. baumannii* isolates from patients in ICU and surgical wards in Poland, 90% exhibited tigecycline MICs of  $> 2 \mu\text{g/ml}$  (Talaga, Krzysciak et al. 2016). Tigecycline diffuses rapidly into tissues resulting in low mean peak serum concentrations at recommended doses. As a consequence, therapeutic failure is possible, even with susceptible isolates, and so tigecycline is not recommended for bloodstream infections (Fishbain and Peleg 2010).

#### **1.5.1.5. Synergistic combinations**

Due to the increase in the occurrence of MDR *Acinetobacter* infections and the increasingly limited choice of antibiotics available for treatment, there have been numerous attempts to identify synergistic combinations of antibiotics to use to treat patients. However, many of these studies have been conducted *in vitro* or in animal models and there are few clinical studies to confirm their findings. Most work focuses on combinations that increase the efficacy of last line drugs such as carbapenems, tigecycline and colistin. Sheng *et al.* used time kill studies to identify synergism between imipenem and colistin, tigecycline, amikacin and ampicillin-sulbactam

against carbapenem-resistant *Acinetobacter* species (Sheng, Wang et al. 2011). Synergy was also observed with a combination of colistin and the glycopeptide antibiotics vancomycin and teicoplanin, which are usually associated with the treatment of Gram-positive infections (Gordon, Png et al. 2010, Wareham, Gordon et al. 2011). Clinical data comes from a limited number of studies and these do not always support the findings of *in vitro* studies. In a cohort study, Falagas *et al.* found that cure of infection was not improved with colistin-meropenem combination therapy compared with colistin monotherapy (Falagas, Rafailidis et al. 2006). Nonetheless, there are some clinical studies that identify a synergistic effect with antibiotic combinations; a carbapenem and ampicillin-sulbactam combination was shown to give a lower mortality rate than carbapenem monotherapy in a retrospective study of 55 MDR *A. baumannii* bacteraemia infections in Taiwan (Kuo, Lai et al. 2007). A combination of rifampicin with both colistin and imipenem has shown activity against carbapenem resistant *A. baumannii* infections in critically ill patients (Motaouakkil, Charra et al. 2006, Saballs, Pujol et al. 2006). The use of minocycline in combination with other antimicrobials has also been suggested as a valid, alternative therapy for MDR *A. baumannii* (Neonakis, Spandidos et al. 2014).

### **1.5.2. Novel therapeutics**

With the rapid emergence of MDR, extremely-drug resistant (XDR) and even pan-drug resistant (PDR) isolates of *A. baumannii*, it is becoming necessary to develop alternative therapies for the treatment of this pathogen. Anti-virulence drugs, anti-biofilm drugs and phage therapy are thought promising in the treatment of resistant infections. For example, Lood *et al.* identified a highly active therapeutic lysin capable of killing *A. baumannii* clinical isolates, representing a potential novel treatment for *A.*

*baumannii* infection (Lood, Winer et al. 2015). The development of an effective vaccine for *A. baumannii* could also provide a solution for reducing morbidity and mortality in certain patient populations. OmpA (Luo, Lin et al. 2012), Bap (Fattahian, Rasooli et al. 2011), Ata (Bentancor, Routray et al. 2012) and Poly- $\beta$ -1-6-N-acetylglucosamine (PNAG) (Bentancor, O'Malley et al. 2012) have all been shown to be good candidates and multicomponent vaccines have also shown potential as therapeutics (Garcia-Quintanilla, Pulido et al. 2014).

## **1.6. Mechanisms of antibiotic resistance**

*Acinetobacter* spp. possess a wide range of antibiotic resistance mechanisms, both intrinsic and acquired, chromosomal and plasmid borne, allowing this bacterium to survive challenge by many classes of antibiotics (Peleg, Seifert et al. 2008, Roca, Espinal et al. 2012). The plasticity of the *Acinetobacter* genome also allows it to adapt to antibiotic pressure by capturing antibiotic resistance genes. An 86 kb genomic resistance island (AbaR1) was identified in clinical isolates of MDR *A. baumannii*, harbouring 45 genes conferring resistance to various classes of antibiotics including  $\beta$ -lactams, aminoglycosides, tetracycline and chloramphenicol (Fournier, Vallenet et al. 2006). This highlights the remarkable ability of this organism to acquire large mobile genetic elements, allowing it to rapidly adapt to its surroundings. Recent studies have also shown that *A. baumannii* can act as a source of emerging antibiotic resistance genes. Bonnin *et al.* suggested that the genetic structure responsible for the dissemination of the *bla* NDM-1 gene most probably originates from *Acinetobacter* and that the *bla* NDM-1 gene itself may be constructed through a recombination event in *Acinetobacter* (Bonnin, Poirel et al. 2014). The most widespread mechanisms of resistance in *A. baumannii* are modification of the

target, degradation or inactivation of the antibiotic and reduced permeability and active efflux of the agent. These mechanisms often work in combination to produce high levels of antibiotic resistance. For example, production of  $\beta$ -lactamases, overexpression of outer membrane proteins such as CarO and PBP modifications may all contribute towards carbapenem resistance in *A. baumannii* (Poirel and Nordmann 2006). A summary of the mechanisms of resistance to commonly used classes of antibiotics is shown in Table 1.6.1.

**Table 1.6.1 Resistance mechanisms in *Acinetobacter* spp.**

Antimicrobial	Resistance mechanism	Protein
β-Lactams	1. Target site modification	
	Modified penicillin-binding proteins	PBP
	2. Drug Inactivation	
	Chromosomal cephalosporinase	AmpC
	Carbapenem-hydrolysing class D β-lactamases	OXA-51-like, OXA-23-like, OXA-24/40-like, OXA-58-like, OXA-143-like
	Metallo-β-lactamases	IMP, VIM, SIM-1, NDM
	Other β-lactamases	TEM, SHV, SCO-1, CARB, PER, VEB, CTX-M, GES, KPC, OXA-2, 10, 20, 37
	3. Reduced drug accumulation	
	Decreased permeability	CarO, 47 kDa OMP, 44 kDa OMP, 37 kDa OMP, 33–36 kDa OMP, 22–33 kDa OMP, HMP-AB, 43 kDa OMP
	Efflux pump	AdeABC, AdeIJK, AdeFGH, AdeDE,



Antimicrobial	Resistance mechanism	Protein
		AdeXYZ
Aminoglycosides	1. Target site modification	16S rRNA methylases
	2. Drug Inactivation	
	Aminoglycoside-modifying enzymes	Acetyltransferases, Nucleotidyltransferases, Phosphotransferases
	3. Reduced drug accumulation	
	Efflux pump	AdeABC, AbeM, AdeDE
Quinolones	1.Target site modification	GyrA/ParC
	3. Reduced drug accumulation	
	Efflux pump	AdeABC, AdeIJK, AdeFGH, AdeDE, AbeM, AbeS
Chloramphenicol	3. Reduced drug accumulation	
	Efflux pump	AdeABC, AdeIJK, AdeFGH, AdeDE, AdeXYZ, CmlA, CraA, AbeM, AbeS
Tetracyclines	1. Target site modification	
	Ribosomal protection	TetM
	3. Reduced drug accumulation	
	Efflux pump	TetA, TetB, AdeDE, AdeXYZ

---

Antimicrobial	Resistance mechanism	Protein
Tigecycline	3. Reduced drug accumulation	
	Efflux pump	AdeABC, AdeIJK
Polymyxins	1. Target site modification	
	Lipid A modification	PmrCAB
	Loss of lipopolysaccharide	LpxABC
	3. Reduced drug accumulation	
	Decreased permeability	CarO, OmpA38, OmpA32, OmpW

---

Adapted from (Roca, Espinal et al. 2012).

### **1.6.1. Target site modification**

Target modification occurs in various systems in *A. baumannii*. Mutations in *gyrA* and *parC* are common, resulting in modified DNA gyrase or topoisomerase and preventing fluoroquinolones from interacting with the DNA-gyrase complex (Hamouda and Amyes 2004). Changes in PBPs and ribosomal protection by the TetM protein have also been observed (Lambert 2005). Phosphoethanolamine modification of lipid A was shown to lead to resistance to colistin in *Acinetobacter* by reducing the affinity of LPS for the antibiotic (Beceiro, Llobet et al. 2011). Modification of LPS may occur via two pathways; complete loss of LPS due to mutations in the lipid biosynthesis genes *lpxA*, *lpxC* and *lpxD* (Moffatt, Harper et al. 2010), or mutations in the two component system (TCS) genes *pmrAB* that lead to upregulation of *pmrC*, which encodes a phosphoethanolamine responsible for modification of LPS (Durante-Mangoni, Del Franco et al. , Arroyo, Herrera et al. 2011, Lesho, Yoon et al. 2013, Wand, Bock et al. 2015).

### **1.6.2. Drug inactivation**

$\beta$ -lactamases confer resistance to various  $\beta$ -lactam antibiotics in *Acinetobacter* spp. by inactivation of the drug. Chromosomally encoded AmpC cephalosporinases can be found in all strains of *A. baumannii* and increased expression due to an upstream insertion sequence (IS) element, ISAbA1, provides resistance to cephalosporins (Bou and Martinez-Beltran 2000, Hujer, Hujer et al. 2006, Ruiz, Marti et al. 2007). Extended spectrum  $\beta$ -lactamases (ESBLs) including VEB (Carbonne, Naas et al. 2005), PER (Naas, Bogaerts et al. 2006), TEM (Endimiani, Luzzaro et al. 2007), SHV (Huang, Mao et al. 2004) and CTX-M (Nagano, Nagano et al. 2004) have all been described in *A. baumannii*, and can be found both plasmid and chromosomally

encoded. Carbapenem hydrolysing enzymes are the most clinically relevant  $\beta$ -lactamases in *Acinetobacter* and both metallo- $\beta$ -lactamases (MBLs) and serine oxacillinases (OXA) have been identified in *Acinetobacter* (Poirel and Nordmann 2006). The most widespread of these are the OXA-type enzymes, which can be encoded chromosomally or on a plasmid. *bla*OXA-51-like enzymes are naturally occurring in *A. baumannii* and encoded chromosomally. In the presence of an upstream promoter found associated with ISAbal, *bla*OXA-51-like genes provide intrinsic resistance to carbapenems (Turton, Ward et al. 2006, Turton, Woodford et al. 2006). *bla*OXA-51-like genes have a high prevalence worldwide and have been described in several studies (Héritier, Poirel et al. 2005, Coelho, Woodford et al. 2006, Hujer, Hujer et al. 2006, Turton, Woodford et al. 2006, Evans, Brown et al. 2007). *bla*OXA-23-like, *bla*OXA-24-like and *bla*OXA-58 like gene clusters have also been described as conferring carbapenem resistance in *Acinetobacter* (Donald, Scaife et al. 2000, Afzal-Shah, Woodford et al. 2001, Da Silva, Quinteira et al. 2004, Boo, Walsh et al. 2006, Coelho, Woodford et al. 2006, Corvec, Poirel et al. 2007).

Aminoglycoside-modifying enzymes (AMEs) are the primary mechanism of resistance to aminoglycosides in *A. baumannii*. AME genes are typically found on transposable elements and isolates of *A. baumannii* may carry a number of different ones (Gallego and Towner 2001, Zhu, Wang et al. 2009). AME genes *ant*(3'')-Ia, *aac*(6')-Ib, *aph*(3')-1a, *aac*(3)-Ia, *aph*(3')-VI, *ant*(3'')-Ia, *aac*(6')-Ib and 16S ribosomal RNA (rRNA) methylase *armA* have all been previously identified in *A. baumannii* (Cho, Moon et al. 2009).

### **1.6.3. Reduced drug accumulation**

#### **1.6.3.1. OMP expression**

Loss of outer membrane proteins (OMPs) has also been implicated in *A. baumannii* resistance to antibiotics. *A. baumannii* possess few outer membrane porins, and intrinsic low level resistance can be partly attributed to low permeability of the outer membrane (Sato and Nakae 1991). Altered expression of OMPs in response to antibiotic challenge can further reduce permeability to antimicrobials and lead to MDR. Expression of OmpA38, OmpA32, CarO and OmpW is reduced in the presence of sub-MIC levels of tetracycline, suggesting a role for OMPs in tetracycline resistance (Yun, Choi et al. 2008) and disruption of the OmpA gene in *A. baumannii* leads to decreased MICs of chloramphenicol, aztreonam and nalidixic acid (Smani, Dominguez-Herrera et al. 2013). Furthermore, loss of OMPs has been implicated in carbapenem resistance and is seen in clinical isolates worldwide (Bou, Cerveró et al. 2000, Tomás, Beceiro et al. 2005, Hwa, Subramaniam et al. 2010).

#### **1.6.3.2. Efflux**

Intrinsic expression of efflux pumps in *A. baumannii* allows a broad range of substrates to be removed from the cell, conferring resistance to various antibiotic classes. Increased expression of chromosomal efflux pumps and acquisition of additional efflux systems can then lead to MDR (Coyne, Courvalin et al. 2011).

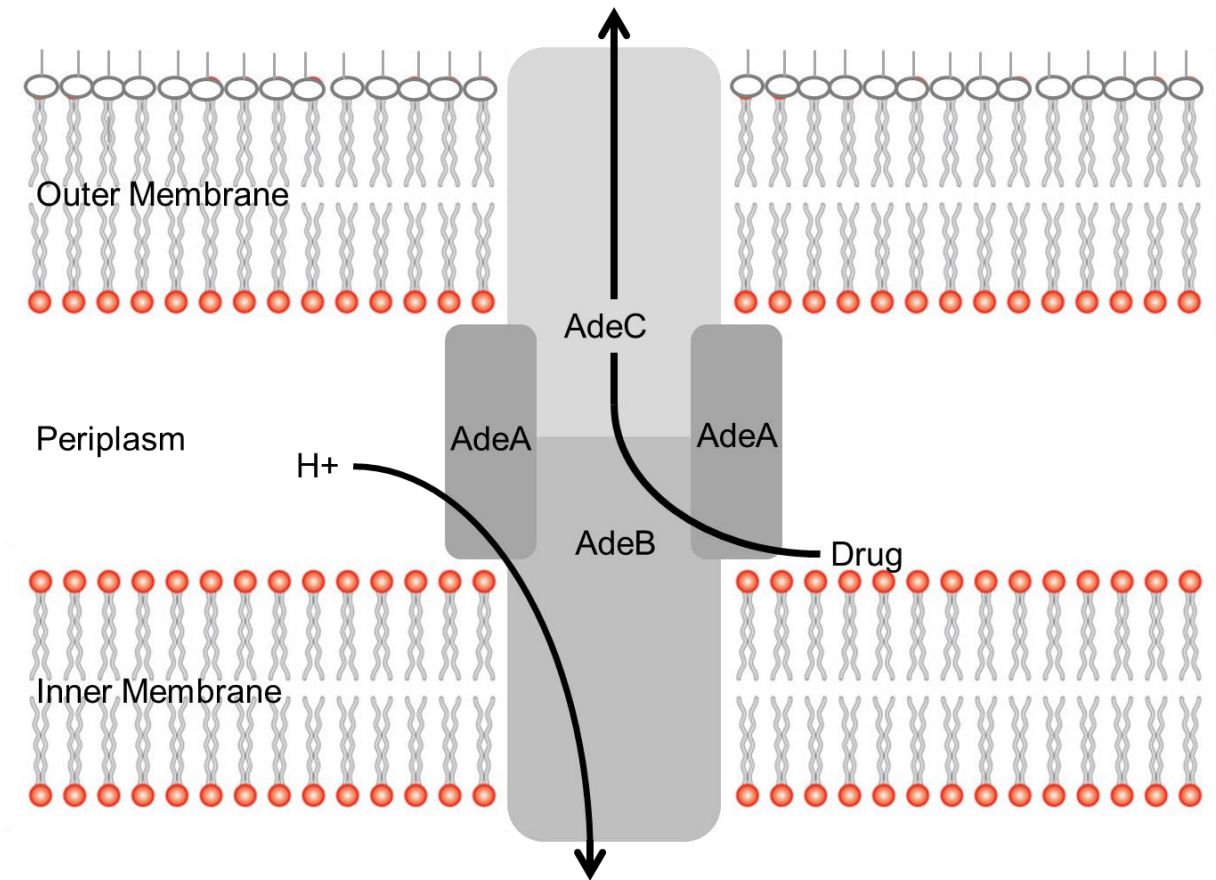
##### **1.6.3.2.1. RND efflux pumps**

The resistance nodulation division (RND) family are the most common efflux systems causing MDR in *Acinetobacter* and six pumps of this type have been identified and characterised in species belonging to the Acb complex. RND pumps in Gram

negative bacteria comprise of three components, forming a tripartite pump. The efflux protein is located in the inner membrane, the OMP channel spans the outer membrane and a membrane fusion protein (MFP) links the two (Figure 1.6.1) (Pidcock 2006). There is often a high level of homology between proteins in this family and RND pump proteins identified in *A. baumannii* show similarity to the MexXY-OprM and MexD previously characterised in *P. aeruginosa* and MtrC from *Neisseria gonorrhoeae* (Magnet, Courvalin et al. 2001, Coyne, Courvalin et al. 2011). Much of the work to characterise the *Acinetobacter* RND family efflux pumps comes from the Courvalin team and is based on analysis of a single strain of *A. baumannii*, BM4454. This may not necessarily represent all strains or species and further work is required to confirm these findings in other strains.

AdeABC is the most well characterised tripartite RND MDR efflux system in *Acinetobacter*. AdeA is a MFP, AdeB is a RND protein and AdeC is an OMP (Magnet, Courvalin et al. 2001). Found in both *A. baumannii* and other clinically relevant species (Magnet, Courvalin et al. 2001, Roca, Espinal et al. 2011), AdeABC is chromosomally encoded but has only been identified in clinical isolates, is tightly regulated and only confers MDR when overexpressed (Magnet, Courvalin et al. 2001, Yoon, Courvalin et al. 2013, Yoon, Nait Chabane et al. 2015). MIC studies with mutants that lack or overexpress specific efflux pump genes revealed that substrates for this pump include aminoglycosides,  $\beta$ -lactams, fluoroquinolones, tetracyclines, tigecycline, macrolides, chloramphenicol and trimethoprim (Magnet, Courvalin et al. 2001, Marchand, Damier-Piolle et al. 2004, Yoon, Nait Chabane et al. 2015). A role for AdeABC in efflux of carbapenems has also been shown. Studies of clinical MDR isolates showed a correlation between carbapenem resistance and overexpression

Figure 1.6.1 Schematic diagram of the AdeABC tripartite RND system



The RND pump (e.g. AdeB) is situated in the inner membrane in complex with the outer membrane channel (e.g. AdeC) and a periplasmic adaptor protein (e.g. AdeA)

of AdeABC (Héritier, Poirel et al. 2005, Huang, Sun et al. 2008, Hou, Chen et al. 2012) and AdeABC has been shown to work synergistically with enzymatic mechanisms to contribute towards carbapenem resistance. However, addition of efflux inhibitors carbonyl cyanide-m-chlorophenyl hydrazone (CCCP) did not affect carbapenem MICs in imipenem-resistant clinical isolates from Greece (Pournaras, Markogiannakis et al. 2006). Inactivation of *adeB* causes loss of intrinsic resistance to multiple antibiotics (Magnet, Courvalin et al. 2001), whereas inactivation of *adeC* does not have the same effect. This suggests that AdeC is not essential for MDR and that other OMPs may be recruited by AdeAB (Marchand, Damier-Piolle et al. 2004). AdeABC is encoded as an operon, *adeABC*, and is regulated by the two-component system AdeRS (Marchand, Damier-Piolle et al. 2004). However, MDR due to AdeABC overexpression has been seen in the absence of AdeRS mutations, suggesting another mechanism causing increased pump activity is also possible (Peleg, Adams et al. 2007, Sun, Chan et al. 2010). It has been proposed that the two component system BaeSR may also influence transcription of *adeAB* by functioning as a global regulator (Lin, Lin et al. 2014).

AdelJK is found only in *A. baumannii* and has not been observed in any of the other members of the Acb complex. AdeJ shows 57% identity with AcrB from *Escherichia coli* and 97% identity with the AdeY RND protein from *Acinetobacter pittii* (Chu, Chau et al. 2006) and confers intrinsic MDR (Damier-Piolle, Magnet et al. 2008, Lin, Ling et al. 2009). AdelJK is constitutively expressed and is responsible for intrinsic resistance to multiple classes of antibiotics in *A. baumannii* (Yoon, Nait Chabane et al. 2015). Evidence from MIC studies with mutants that lack specific efflux pump genes suggest that AdelJK exports  $\beta$ -lactams, fluoroquinolones, tetracyclines,



tigecycline, lincosamides, rifampicin, chloramphenicol, co-trimoxazole, novobiocin and fusidic acid, but not aminoglycosides (Damier-Piolle, Magnet et al. 2008, Coyne, Guigon et al. 2010, Amin, Richmond et al. 2013). AdeIJK is only expressed at low levels in *A. baumannii* BM4454 and once expression reaches threshold levels in *E. coli* AG100A the pump becomes toxic to the host (Damier-Piolle, Magnet et al. 2008, Coyne, Guigon et al. 2010). AdeIJK is encoded by the *adeIJK* operon and regulated by the TetR transcriptional regulator *adeN* (Rosenfeld, Bouchier et al. 2012).

AdeFGH is encoded by the *adeFGH* operon but is not expressed constitutively and so does not appear to contribute to intrinsic resistance (Coyne, Rosenfeld et al. 2010, Yoon, Nait Chabane et al. 2015). MIC data for mutants overexpressing *adeFGH* indicate that the substrates of this pump include fluoroquinolones, chloramphenicol, trimethoprim, clindamycin, tetracyclines, tigecycline and sulfamethoxazole (Coyne, Rosenfeld et al. 2010, Yoon, Nait Chabane et al. 2015). Spontaneous MDR mutants selected from BM4652 (*BM4454ΔadeABCΔadeIJK*) on norfloxacin and chloramphenicol contain mutations in a putative LysR-type transcriptional regulator gene, *adeL*, located upstream of *adeFGH*. It is proposed that these mutations cause a constitutive phenotype, leading to increased expression of the AdeFGH efflux system (Coyne, Rosenfeld et al. 2010).

AdeDE was identified as a novel RND efflux system in *A. pittii* by Chau *et al.* (Chau, Chu et al. 2004) but no OMP gene was found encoded alongside *adeDE*. It is suggested that AdeDE recruits an OMP encoded elsewhere on the chromosome. Inactivation of *adeE* in a clinical isolate reduced susceptibility to aminoglycosides, carbapenems, ceftazidime, fluoroquinolones, erythromycin, tetracycline, rifampicin and chloramphenicol (Chau, Chu et al. 2004). Although initially described in *A. pittii*,

AdeDE has also been observed in *A. nosocomialis* and *Acinetobacter* gsp 17. However, prevalence is highest in *A. pittii*, with 70% of 83 clinical isolates studied containing the *adeDE* operon (Chu, Chau et al. 2006). AdeE was also found to coexist with AdeB in six out of 50 *A. baumannii* isolates studied (Hou, Chen et al. 2012).

AdeXYZ is a RND pump found in *Acinetobacter* spp. other than *A. baumannii*. It was identified in 90% of 83 *A. pittii* isolates tested in a study of blood culture isolates in China and was also been observed in *A. nosocomialis* and *A. gsp. 17* (Chu, Chau et al. 2006). Although AdeXYZ has not been well characterised, the pump proteins show high homology with AdeIJK, suggesting a similar function and possibly substrate range (Chu, Chau et al. 2006, Damier-Piolle, Magnet et al. 2008, Coyne, Courvalin et al. 2011).

#### **1.6.3.2.2. Non-RND efflux pumps**

*Acinetobacter* spp. also possess other chromosomally encoded non-RND efflux systems: CraA contributes to intrinsic resistance to chloramphenicol (Roca, Marti et al. 2009), AmvA is a major facilitator superfamily (MFS) pump that exports erythromycin (Rajamohan, Srinivasan et al. 2010), AbeM is a member of the multi-drug and toxic compound extrusion (MATE) family and has a suggested role in resistance to a range of antibiotics and dyes (Su, Chen et al. 2005), and AbeS is a small multi-drug resistance (SMR) efflux pump involved in chloramphenicol, fluoroquinolone, erythromycin, novobiocin and dye and detergent resistance (Srinivasan, Rajamohan et al. 2009). Acel is a member of the new family of

antibacterial efflux pumps discovered in *A. baumannii* that confers resistance to biocides (Hassan, Jackson et al. 2013, Hassan, Liu et al. 2015).

Various acquired efflux systems have also been identified in *Acinetobacter* spp., carried either on plasmids, transposons or resistance islands (Vila, Martí et al. 2007). Most common are pumps of the MFS type that give resistance to tetracycline. The TetA pump, has been observed in 13.6% of 59 tetracycline resistant strains of *A. baumannii* and the TetB pump, conferring tetracycline and minocycline resistance, in 66% of the 59 isolates (Martí, Fernandez-Cuenca et al. 2006)(Martí, Fernandez-Cuenca et al. 2006). In a study of 32 clinical isolates of *A. baumannii* conducted by Mak *et al.*, 28 contained the *tetB* gene whilst *tetA* was not present in any isolate (Mak, Kim et al. 2009)(Mak, Kim et al. 2009). The *tetG* and *tetR* MFS pump genes have also been observed in *Acinetobacter* spp., as part of the acquired ISAbA1 resistance island (Fournier, Vallenet et al. 2006). The MFS pumps CmlA and FloR, and the SMR pump QacE are also acquired on the ISAbA1 resistance island identified in *A. baumannii* AYE (Fournier, Vallenet et al. 2006).

## **1.7. Regulation of antibiotic resistance**

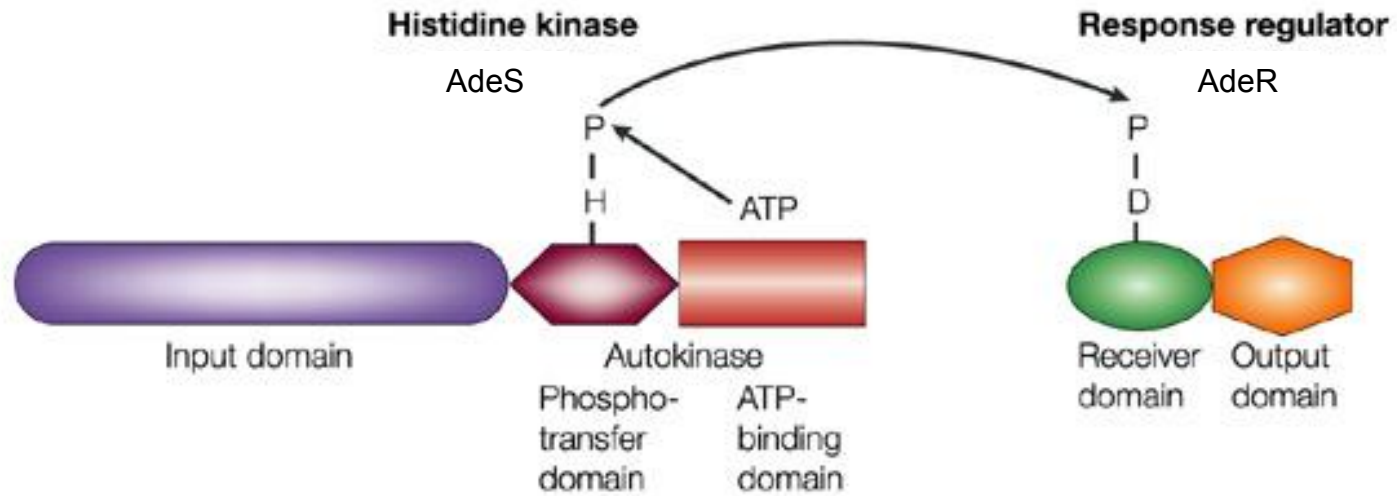
Very little is known about the regulatory networks of *A. baumannii*. A number of two component systems (TCSs) are encoded in the genome of this pathogen and of these, AdeRS and PmrAB have been most well characterised with regards to antimicrobial resistance. TCSs allow bacteria to regulate their internal environment in response to extracellular signals. A signal recognition domain on a sensor kinase recognises an external cue and activates an autokinase domain, resulting in ATP hydrolysis and phosphorylation of a histidine located on the phosphotransferase sub-

domain of the autokinase. The phosphoryl group is then transferred to the receiver domain of a response regulator (Figure 1.7.1). This relieves inhibition of the output domain of the response regulator and results in changes in DNA binding and transcription, enzymatic activity, binding of RNA or protein–protein interactions (Hoch 2000, Mitrophanov and Groisman 2008).

#### **1.7.1.1. AdeRS**

AdeRS is a two component system responsible for the regulation of the RND efflux pump AdeABC (Marchand, Damier-Piolle et al. 2004). The system is encoded by *adeRS*, which is upstream and in the opposite direction to *adeABC* (Marchand, Damier-Piolle et al. 2004). AdeS is a sensor kinase and AdeR is its associated response regulator. Whole genome analysis of longitudinal clinical isolates has revealed that genes involved in antibiotic resistance and host interaction, such as *adeRS*, are significantly enriched for novel genetic variants (Wright, Iovleva et al. 2016). In an analysis of 40 patients, 16 independent mutations and insertion events were observed in 12 patients. Sequence variation in *adeRS* has been previously associated with tigecycline resistance, however only three patients were confirmed to have received tigecycline therapy, suggesting that the regulation of *adeABC* is under selection for more than just tigecycline efflux. The amino acid sequence of AdeRS is widely variable in clinical isolates and mutations in the *adeRS* regulatory system genes are associated with constitutive expression of AdeABC and MDR (Marchand, Damier-Piolle et al. 2004, Peleg, Adams et al. 2007, Hornsey, Loman et al. 2011, Yoon, Courvalin et al. 2013). The Gly186Val amino acid substitution in AdeS is crucial for reducing tigecycline susceptibility and results in increased expression

Figure 1.7.1 A schematic of a two component signal transduction system



Nature Reviews | Molecular Cell Biology

(Jensen, Wang et al. 2002)

*adeA* and *adeB* (Sun, Jeng et al. 2016). The Asp20Asn amino acid substitution in AdeR is associated with reduced susceptibility to meropenem, amikacin, fluoroquinolones, erythromycin and tetracycline due to increased expression of *adeB* and enhanced efflux activity (Nowak, Schneiders et al. 2016). Overexpression of AdeABC has also been seen in a clinical isolate due to the insertion of ISAbal into *adeS* (Ruzin, Keeney et al. 2007). A truncated AdeS generated by the *P<sub>out</sub>* promoter within the ISAbal insertion of the *adeS* gene that is able to activate AdeR and increase expression of *adeABC* has been proposed by Sun *et al.* (Sun, Perng et al. 2012). Furthermore, it has been suggested that genetic variability in AdeRS may account for differing levels of tigecycline resistance in clinical isolates of *A. baumannii* (Montaña, Vilacoba et al. 2015).

#### **1.7.1.2. PmrAB**

PmrAB is a TCS that has been linked to colistin resistance in several species including *Klebsiella pneumoniae* and *P. aeruginosa* (Moskowitz, Ernst et al. 2004, Cheng, Chen et al. 2010) as well as *A. baumannii* (Adams, Nickel et al. 2009). The system is encoded by *pmrAB* where *pmrA* encodes the response regulator and *pmrB* encodes the sensor kinase (Adams 2009). In *Salmonella enterica*, PmrAB controls the modification of lipid A with aminoarabinose and phosphoethanolamine (Zhou, Ribeiro et al. 2001). Phosphorylation of PmrA by PmrB activates the *pmrC* gene, which is an inner membrane protein that is required for the incorporation of phosphoethanolamine into lipid A. This modification of lipid A reduces the binding affinity for polymyxins and results in resistance (Lee, Hsu et al. 2004). Mutations in, or increased expression of, *pmrA* or *pmrB* in *A. baumannii* has been associated with resistance to colistin (Adams, Nickel et al. 2009, Beceiro, Llobet et al. 2011, Park,

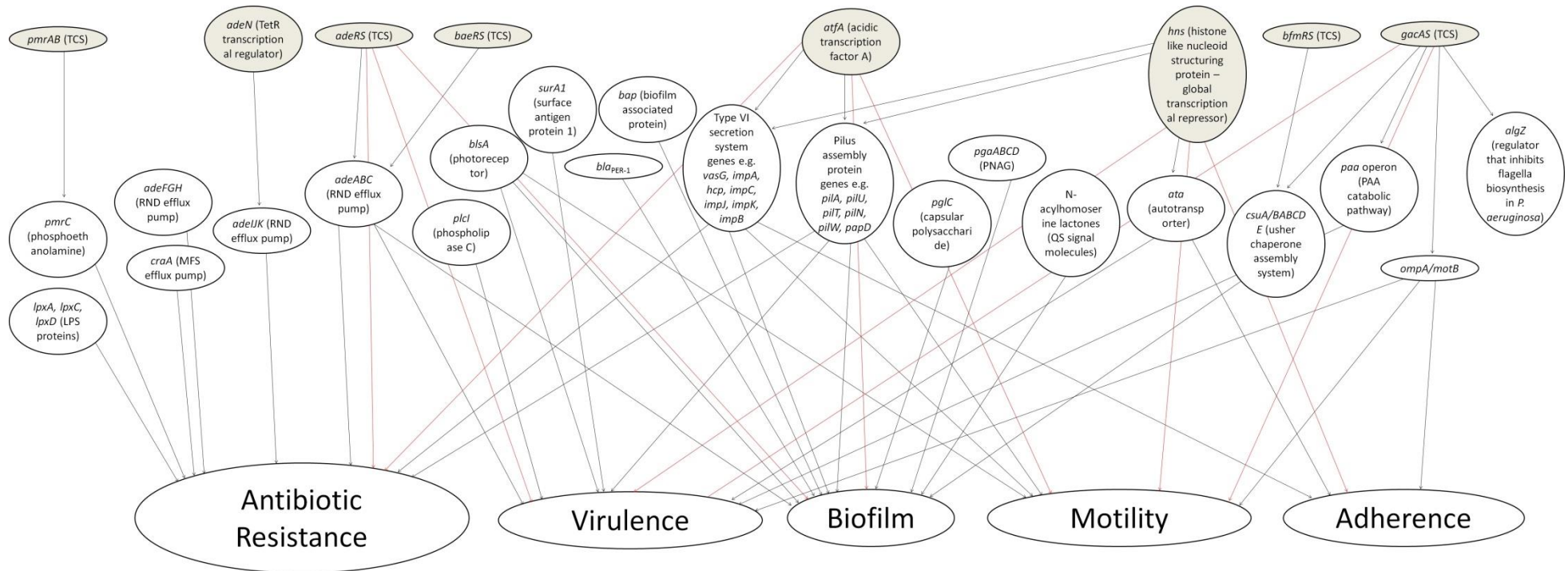
Choi et al. 2011, Kim, Bae et al. 2014, Wand, Bock et al. 2015). Arroyo *et al.* showed that deletion of the *pmrB* gene led to a decrease in susceptibility to polymyxins in *A. baumannii* clinical isolates and demonstrated a correlation between increased expression of *pmrC* and polymyxin resistance. Addition of phosphethanolamine to lipid A also correlated with resistance, in line with results previously seen in *S. enterica* (Zhou, Ribeiro et al. 2001, Arroyo, Herrera et al. 2011).

### **1.8. Pathogenesis and virulence of *Acinetobacter***

As well as the concern of rising antibiotic resistance, investigation into the pathogenicity of *Acinetobacter* is also an important area of research. Relatively little is known about pathogenicity and virulence factors in *Acinetobacter* as most studies have focused on epidemiology and risk factors for infection. Key to the success of pathogenic species of *Acinetobacter* is their metabolic adaptability. Their ability to persist on abiotic surfaces allows them to survive in the hospital environment and cause nosocomial outbreaks (Wendt, Dietze et al. 1997, Jawad, Seifert et al. 1998). Outbreak strains of *A. baumannii* have been isolated from bed rails up to nine days after the infected patient was discharged, allowing transmission of the organism throughout the hospital (Catalano, Quelle et al. 1999). Pathogenic species, such as *A. baumannii*, are able to adhere to, colonise and invade human epithelial cells (Choi, Lee et al. 2008) and are often able to survive antibiotic treatment due to upregulation of existing antibiotic resistance genes and acquisition of foreign genetic material (Peleg, Seifert et al. 2008).

Various approaches have been taken to identify genes that are associated with pathogenicity in this organism. Figure 1.8.1 shows the genes known to be involved in

**Figure 1.8.1 Summary of the genes shown to be directly or indirectly involved in antibiotic resistance, virulence, biofilm formation, motility and adherence in *A. baumannii***



Shaded circles indicate regulatory genes. Red arrows indicate a direct association between regulator and phenotype.



antibiotic resistance, virulence, biofilm, motility and adherence in *Acinetobacter*. Sahl *et al.* conducted a global comparison of genomic features between species of *Acinetobacter* in order to identify genes that had been acquired and lost in different species in the genus (Sahl, Gillece *et al.* 2013). Pathogenic species, such as *A. baumannii*, and other species included in the Acb complex, had acquired various genes when compared to the *Acinetobacter* root species, *A. radioresistens*. They proposed that these acquired genes may be associated with the increased ability of these species to persist and cause infection in the hospital environment. Amongst those genes unique to the Acb complex were several genes that have been previously linked to *Acinetobacter* pathogenicity including iron acquisition systems and the *csuE* gene.

The *csuA/BABCDE* operon encodes a chaperone-usher pilus assembly system and is involved in attachment to, and biofilm formation on, abiotic surfaces in *A. baumannii* (Tomaras, Dorsey *et al.* 2003, de Breij, Gaddy *et al.* 2009). Disruption of *csuE* in strain ATCC 19606 eliminated pilus formation and cells were no longer able to attach or form a biofilm (Tomaras, Dorsey *et al.* 2003). The *csuE* gene is highly conserved in *A. baumannii* and its absence from non-Acb complex species may explain why these species are not able to persist in the hospital environment (Sahl, Gillece *et al.* 2013). However, de Breij *et al.* have shown that deletion of *csuE* has no effect on adherence to bronchial epithelial cells and suggest that an alternative mechanism is responsible for attachment to host cells (de Breij, Gaddy *et al.* 2009).

Unique to the Acb complex were also a number of regulatory genes with unknown function, which may contribute to persistence and virulence in pathogenic *Acinetobacter*. The importance of the two component system BfmRS in regulating

expression of the CsuA/BABCDE system has been shown in *A. baumannii* ATCC 19606, suggesting a role for BfmRS in attachment to, and biofilm formation on, abiotic surfaces (Tomaras, Flagler et al. 2008). The role of BfmRS in the regulation of Csu dependent attachment could suggest that this regulatory system has no involvement in attachment to biotic surfaces. However, deletion of *bfmS* in *A. baumannii* strain ATCC 17978 resulted in a reduction in biofilm formation, loss of adherence to A549 human alveolar epithelial cells and greater sensitivity to serum killing, indicating that it may regulate virulence genes other than *csu* (Liou, Soo et al. 2013).

Siderophore mediated iron acquisition systems are also known virulence factors in *Acinetobacter*. The acinetobactin iron acquisition cluster is highly conserved in *A. baumannii* and is required for persistence and killing of A549 human alveolar epithelial cells in ATCC 19606 (Gaddy, Arivett et al. 2012, Sahl, Gillece et al. 2013). BasD and BauA, two proteins required for acinetobactin biosynthesis and transport, are not required for initial interaction with human alveolar epithelial cells. However, these proteins are necessary for persistence and cell death in epithelial cells and for effective killing of *Galleria mellonella* larvae (Gaddy, Arivett et al. 2012).

The most well studied virulence factor in *Acinetobacter* is OmpA, previously called Omp38. This outer membrane protein (OMP) binds to human laryngeal epithelial HEp-2 cells, localises to the mitochondria and leads to apoptosis. A mutant of *A. baumannii* ATCC 19606 lacking OmpA showed a decrease in invasion and death of human laryngeal epithelial HEp-2 cells, and less lung and tissue destruction in a murine pneumonia model (Choi, Lee et al. 2005, Choi, Lee et al. 2008). OmpA is also involved in a number of other functions including biofilm formation (Gaddy, Tomaras

et al. 2009) and serum resistance (Kim, Choi et al. 2009). Another porin associated with virulence in *A. baumannii* is the Omp33-36 porin. Omp33-36 plays an important role in fitness and virulence in *A. baumannii* and is a virulence factor in a systemic mouse model of infection (Smani, Dominguez-Herrera et al. 2013, Rumbo, Tomás et al. 2014).

Other virulence factors identified in *Acinetobacter* species include surface antigen protein 1 (SurA1) (Liu, Liu et al. 2016), the type VI secretion system (Repizo, Gagne et al. 2015), penicillin binding protein (PBP) 7/8 (Russo, MacDonald et al. 2009), capsule formation (Russo, Luke et al. 2010), and phospholipase C and D (Camarena, Bruno et al. 2010, Jacobs, Hood et al. 2010). However, little is known about how these factors affect pathogenicity and virulence.

### **1.8.1. Biofilm formation**

Formation of a biofilm is commonly a feature of *A. baumannii* clinical isolates and the ability to form a biofilm has been linked to pathogenesis in this organism (Hall-Stoodley, Costerton et al. 2004, Sanchez, Mende et al. 2013, Badave and Kulkarni 2015, He, Lu et al. 2015). Biofilms are an important virulence factor in wound infection (Percival, Hill et al. 2012) and infection with *A. baumannii* is often associated with indwelling medical devices, which can provide a surface for biofilm development (Rodríguez-Baño, Martí et al. 2008, Jung, Park et al. 2010). Biofilm formation has also been correlated with MDR in clinical *A. baumannii* isolates (Badave and Kulkarni 2015). Furthermore, high biofilm phenotype is important for both clinical and environmental isolates to tolerate desiccation (Hu, Johani et al. 2015, Greene, Vadlamudi et al. 2016). A homologue of the staphylococcal biofilm-

associated protein (Bap) has been identified as a virulence factor in *A. baumannii* (Loehfelm, Luke et al. 2008). A transposon mutant lacking Bap was unable to sustain biofilm thickness and volume on a glass coverslip. Lack of Bap did not affect primary attachment, suggesting a role in maintaining the mature biofilm architecture. Bap is also important for adherence to normal human bronchial epithelial cells and normal human neonatal keratinocytes, although it has no involvement in invasion of these cells (Brossard and Campagnari 2012). Poly- $\beta$ -1-6-N-acetylglucosamine (PNAG) is a key virulence factor in the formation of biofilms (Choi, Slamti et al. 2009). Deletion of *pgaABCD*, which encodes proteins that synthesise cell-associated PNAG resulted in the loss of a strong biofilm phenotype under dynamic conditions, simulated by vigorous shaking of cultures, but had no effect under static conditions (Choi, Slamti et al. 2009). The *abal* autoinducer synthase gene is also important in biofilm formation in *A. baumannii* and encodes a distinct acyl-homoserine lactone (AHL) signal. The Abal autoinducer synthase was required for the later stages of biofilm development, suggesting that quorum sensing influences expression of genes involved in maturation of the biofilm (Niu, Clemmer et al. 2008). Extracellular DNA (eDNA) is a component of microbial biofilms and is able to augment *A. baumannii* biofilms on an abiotic surface, suggesting a role in biofilm formation in this organism (Sahu, Iyer et al. 2012). Furthermore, pre-formed *A. baumannii* biofilms were destroyed by DNase I, supporting the role of eDNA in biofilms (Sahu, Iyer et al. 2012).

## **1.9. Biofilm models for *Acinetobacter***

Expression of virulence factors involved in bacterial biofilm formation can vary widely depending on the model system used (Anderson, Moreau-Marquis et al. 2008, Otto 2008, Anderson, Lin et al. 2012). Previous studies have shown that genes involved in

biofilm formation on abiotic surfaces are not necessarily required for attachment to, and biofilm formation on, biological surfaces (Anderson, Moreau-Marquis et al. 2008, Otto 2008, Anderson, Lin et al. 2012). For example, production of the *A. baumannii* CsuA/BABCDE-mediated pilus is essential for biofilm formation on abiotic surfaces but is not required for attachment to bronchial epithelial cells *in vitro* (de Breij, Gaddy et al. 2009). This highlights the need to measure biofilm formation in multiple models to determine the specific roles of individual virulence factors.

There are several models used to study biofilm formation on biotic and abiotic surfaces. Formation of biofilms on hospital surfaces and indwelling medical devices is a particular problem with *A. baumannii* and it is therefore necessary to investigate the mechanisms of biofilm formation on abiotic surfaces. The most common method of measuring biofilm formation on solid surfaces, such as plastics, is by staining with crystal violet, a dye that stains bacterial cells but not the surface they are bound to (Tomaras, Dorsey et al. 2003, Tomaras, Flagler et al. 2008, de Breij, Gaddy et al. 2009, Gaddy, Tomaras et al. 2009). Liou *et al.* demonstrated the involvement of *bfmS* in formation of biofilms by *A. baumannii* by growing cultures in polyvinylchloride (PVC) microtitre dishes and staining the biofilm that formed in each well with crystal violet (Liou, Soo et al. 2013). This method has also been used by King *et al.* to study biofilm formation on polystyrene by serum resistant isolates of *A. baumannii* (King, Pangburn et al. 2013). The Calgary biofilm device (Ceri, Olson et al. 1999) uses a similar principle and measures formation of a biofilm on plastic pegs suspended in a bacterial culture, by crystal violet staining. This method has been successfully used to measure biofilm formation by clinical isolates of *A. baumannii* (Wand, Bock et al. 2012).

Study of *A. baumannii* biofilm formation on biotic surfaces is also a key area of research. Infection of wounds by *A. baumannii* has been a significant problem in military casualties (Murray, Yun et al. 2006, Scott, Deye et al. 2007, Sebeny, Riddle et al. 2008, Johnson, Marconi et al. 2009) and it is possible that the ability of this organism to form a biofilm is a major virulence factor in this environment (Beachey 1981, Costerton, Stewart et al. 1999). However, research in this area is limited. Although mouse models have been used to investigate *A. baumannii* infections in partial-thickness skin abrasions and full-thickness burns, biofilm formation was not studied (Dai, Murray et al. 2012). Most work in this area has focussed on attachment to and invasion of respiratory surfaces such as human bronchial epithelial H<sub>292</sub> cell lines (de Breij, Gaddy et al. 2009), human epithelial HeLa cells (Lee, Oh et al. 2001) and human laryngeal Hep-2 cells (Choi, Lee et al. 2005).

Anderson *et al.* have developed a novel *ex vivo* model of biofilm formation on a mucosal surface that allows the contribution of microbial virulence factors to biofilm formation to be studied (Anderson, Parks et al. 2013). This model measures growth of bacterial cells on porcine vaginal mucosal (PVM) tissue by measuring the number of planktonic and adherent cells on tissue explants over time. Previous work has shown uninfected PVM explants to remain viable for up to six days (Anderson, Parks et al. 2013). Confocal laser scanning microscopy can also be used to visualise biofilm formation. The model was developed using *Staphylococcus aureus*, as this is an important mucosal pathogen that colonises the human vaginal mucosa. Porcine vaginal mucosa is made up of stratified squamous epithelium, similar in structure to human vaginal and other mucosal surfaces (Squier, Mantz et al. 2008, Anderson, Parks et al. 2013) and so provides a surface to study *S. aureus* in an environment

that mimics a natural infection. Specimens are relatively large so many small biopsies can be produced from a single animal, allowing many variables to be tested without inter-animal variation. In addition, tissue is inexpensive, easy to procure from abattoirs and the model is semi-high throughput (Anderson, Parks et al. 2013). *A. baumannii* infections often initiate at wound or mucosal surfaces and the PVM model allows this organism to be studied in a more clinically relevant environment.

### **1.10. The role of efflux pumps in biofilm formation and virulence**

Efflux pumps have several roles in the bacterial cell and are required for virulence in several species and their hosts (Piddock 2006). For instance, lack of efflux pumps in Gram-negative bacteria has previously been shown to affect the organism's ability to infect the host (Buckley, Webber et al. 2006, Nishino, Latifi et al. 2006, Padilla, Llobet et al. 2010, Unemo and Shafer 2011, Perez, Poza et al. 2012) and Yoon *et al.* recently showed that overproduction of the AdeABC efflux pump in *A. baumannii* BM4587 resulted in increased virulence in a mouse model of pneumonia (Yoon, Balloy et al. 2016). Inactivation of efflux pumps in *S. enterica*, *E. coli* and *P. aeruginosa* reduces biofilm formation on abiotic surfaces (Kvist, Hancock et al. 2008, Matsumura, Furukawa et al. 2011, Baugh, Ekanayaka et al. 2012, Liao, Schurr et al. 2013). The role of efflux pumps in biofilm formation of *A. baumannii* on plastic has implications for biofilm formation on hospital surfaces and on intravenous medical devices, such as catheters, which can result in UTIs and other device related infections (Dijkshoorn, Nemec et al. 2007). Yoon *et al.* showed a 39% decrease in biofilm formation in 24-well plates by an *adeB* deletion mutant of clinical strain BM4587 when measured using a crystal violet colorimetric assay (Yoon, Nait Chabane et al. 2015). A 63% and 82% decrease in biofilm formation was also

observed with overexpression of either of the RND efflux systems AdeABC or AdeFGH, respectively (Yoon, Nait Chabane et al. 2015). Upregulation of *adeG* was also correlated with biofilm formation in 48 clinical isolates and a potential role of AdeFGH in the synthesis and transport of autoinducer molecules, such as acylated homoserine lactones (AHLs), during biofilm formation has been suggested (He, Lu et al. 2015).

### **1.11. Background to this research**

AdeRS is a two component system that regulates expression of the multi-drug efflux pump AdeABC. Mutations in *adeRS* can cause overexpression of AdeABC and lead to MDR (Marchand, Damier-Piolle et al. 2004, Peleg, Adams et al. 2007). Deletion of either *adeR* or *adeS* in clinical isolates overexpressing AdeABC results in susceptibility to substrates of this pump (Marchand, Damier-Piolle et al. 2004). Strain AYE is a well-characterised clinical isolate that is MDR (Fournier, Vallenet et al. 2006, Hornsey, Loman et al. 2011) and represents a clinically successful clone. AYE contains an Ala94Val mutation in AdeS that has been previously associated with upregulation of the AdeABC efflux system and increased resistance to antibiotics (Hornsey, Loman et al. 2011). Increased expression of MDR efflux pump genes such as *adeABC* leads to MDR and is commonly seen in clinical isolates of *A. baumannii* (Marchand, Damier-Piolle et al. 2004, Yoon, Courvalin et al. 2013). Deletion of *adeB* in clinical isolate BM4587 resulted in decreased MICs of multiple classes of antibiotics and a reduction in biofilm formation (Yoon, Nait Chabane et al. 2015). Multi-drug efflux systems have previously been associated with biofilm formation and virulence in a number of organisms using various models (Buckley, Webber et al. 2006, Nishino, Latifi et al. 2006, Kvist, Hancock et al. 2008, Padilla, Llobet et al.



2010, Matsumura, Furukawa et al. 2011, Baugh, Ekanayaka et al. 2012, Perez, Poza et al. 2012, Liao, Schurr et al. 2013, Baugh, Phillips et al. 2014, Yoon, Nait Chabane et al. 2015).

## 1.12. Hypotheses

- Disruption of MDR efflux pumps in *A. baumannii* will alter the expression of many genes in related regulatory networks.
- Deletion of *adeRS*, *adeAB* or *adeB* alone will affect the *A. baumannii* transcriptome and hence antibiotic resistance, biofilm formation and virulence.
- Inactivation of *adeR*, *adeS*, *adeA* or *adeB* by transposon mutagenesis will affect antibiotic resistance, biofilm formation and motility in *A. baumannii*.

## 1.13. Aims

- To determine the effect of deletion of the TCS AdeRS on antibiotic resistance, biofilm formation and virulence in *A. baumannii* strain AYE.
- To use RNA-Seq to identify transcriptomic changes in *A. baumannii* strain AYE with the deletion of AdeRS.
- To determine the effect of lack of AdeB on antibiotic resistance, biofilm formation and virulence in *A. baumannii* strain AYE and clinical isolate S1.
- To identify transcriptomic changes in *A. baumannii* strain AYE and clinical isolate S1 with the deletion of the RND efflux pump gene *adeB* by RNA sequencing and compare these with changes in *AYEΔadeRS*.
- To optimise the porcine vaginal model mucosal model to measure *A. baumannii* biofilm formation on a mucosal surface.
- To determine the effect of inactivation of *adeR*, *adeS*, *adeA* or *adeB* by transposon mutagenesis on antibiotic resistance, biofilm formation and motility in *A. baumannii* strain AB5075.

## 2. Materials and Methods

### 2.1. Bacterial strains, growth, storage and identification

#### 2.1.1. Bacterial strains

*Acinetobacter baumannii* strain AYE (Table 2.1.1) was selected as a reference MDR strain for use in this study. A fully annotated genome sequence is available for AYE and shows this epidemic strain to contain 52 antibiotic resistance genes, including all of the previously described efflux pumps (Fournier, Vallenet et al. 2006, Evans 2012). Clinical isolate, S1 (Table 2.1.1), was cultured from a hospital infection in Singapore and was provided by collaborator Kim Lee Chua (National University of Singapore, Singapore). Deletion of *adeRS* in AYE and *adeAB* in S1 to give AYE $\Delta$ *adeRS* and S1 $\Delta$ *adeAB* was carried out by Laura Evans (University of Birmingham, UK), and Kim Lee Chua, respectively, using a markerless deletion method (Amin, Richmond et al. 2013). Deletion of *adeB* in AYE was carried in this project in collaboration with Matthew Wand (Public Health England (PHE), UK) using a modification to the markerless deletion method (Amin, Richmond et al. 2013) (see Chapter 4.5). Due to the difficulties with making genetic modifications in *A. baumannii*, clinical isolate AB5075 and transposon mutants Tn-*adeR1*, Tn-*adeR2*, Tn-*adeS1*, Tn-*adeS2*, Tn-*adeA1*, Tn-*adeA2*, Tn-*adeB1* and Tn-*adeB2* of this strain (Table 2.1.1) were purchased from The University of Washington Transposon Mutant Library (Gallagher, Ramage et al. 2015) (<http://www.gs.washington.edu/labs/manoil/baumannii.htm>). Strain ATCC 19606 (obtained from American Type Culture Collection, USA) was used as a reference strain as it has been previously characterised for biofilm formation (Gaddy, Tomaras et al. 2009).

**Table 2.1.1 Bacterial strains used in this study**

Code	Source	Supplier
AYE	MDR bloodstream isolate, France	Laurent Poirel (Poirel, Menuteau et al. 2003)
AYE $\Delta$ <i>adeRS</i>	<i>adeRS</i> deletion mutant in AYE	L. P. Evans & L. J. V. Piddock, unpublished
AYE $\Delta$ <i>adeB</i>	<i>adeB</i> deletion mutant in AYE	This study
S1	Clinical isolate (Singapore)	K. L. Chua, unpublished
S1 $\Delta$ <i>adeAB</i>	<i>adeAB</i> deletion mutant in S1	K. L. Chua, unpublished
ATCC 19606	Clinical isolate, type strain	American Type Culture Collection
AB5075	Osteomyelitis isolate, USA military	University of Washington, USA
AB5075 Tn- <i>adeR1</i>	Transposon inserted in nucleotide (nt) 671 in <i>adeR</i>	University of Washington, USA
AB5075 Tn- <i>adeR2</i>	Transposon inserted in nucleotide (nt) 121 in <i>adeR</i>	University of Washington, USA
AB5075 Tn- <i>adeS1</i>	Transposon inserted in nucleotide (nt) 593 in <i>adeS</i>	University of Washington, USA
AB5075 Tn- <i>adeS2</i>	Transposon inserted in nucleotide (nt) 133 in <i>adeS</i>	University of Washington, USA

AB5075 Tn- <i>adeA1</i>	Transposon inserted in nucleotide (nt) 558 in <i>adeA</i>	University of Washington, USA
AB5075 Tn- <i>adeA2</i>	Transposon inserted in nucleotide (nt) 782 in <i>adeA</i>	University of Washington, USA
AB5075 Tn- <i>adeB1</i>	Transposon inserted in nucleotide (nt) 1030 in <i>adeB</i>	University of Washington, USA
AB5075 Tn- <i>adeB2</i>	Transposon inserted in nucleotide (nt) 2185 in <i>adeB</i>	University of Washington, USA

---

### **2.1.2. Growth and storage**

All strains and isolates were routinely cultured on Luria-Bertani (LB) (Sigma-Aldrich Ltd., UK, cat. no. L2897) or tryptic soy agar (TSA) II (Sigma-Aldrich Ltd., UK, cat. no. 22091) containing 5% sheep's blood and in LB (Sigma-Aldrich Ltd., UK, cat. no. L3022) or Todd Hewitt (TH) broth (Sigma-Aldrich Ltd., UK, cat. no. T1438), overnight, statically at 37°C. Agar plates were stored at 4°C for two weeks. All strains were kept at -20°C on Protect™ beads (Technical Service Consultants Ltd., U.K., cat. no. Tn/80-GN) for long-term storage.

### **2.1.3. Phenotypic and genotypic identification**

Colonies were confirmed as Gram-negative coccobacilli by Gram staining and microscopic observation. Isolates were confirmed as *A. baumannii* using a *gyrB* specific polymerase chain reaction (PCR) (Higgins, Wisplinghoff et al. 2007, Higgins, Lehmann et al. 2010). Details of the primers used can be found in Table 2.2.1.

## **2.2. Primer design and PCR**

All primers were designed using Genius software (Biomatters, New Zealand) and made by ThermoFisher Scientific (UK). For use in PCRs, primers were diluted in sterile distilled water to a concentration of 25 µM. Primers were stored at -20°C. Unless otherwise specified, PCRs were carried out using ReddyMix™ PCR buffer (ThermoFisher Scientific, cat. no. AB0575DCLDA). Reaction volumes for a typical PCR are shown in Table 2.2.2.

A negative water contamination control was used for each PCR experiment.

**Table 2.2.1 Primers**

Primer	5' to 3' sequence	PCR
Sp2F	G TTCCTGATCCGAAATTCTCG	<i>gyrB</i> species check
Sp4F	CACGCCGTAAGAGTGCATTA	
Sp4R	AACGGAGCTTGTCAGGGTA	
D14	GACAACAGTTATAAGGTTTCAGGTG	
D19	CCGCTATCTGTATCCGCAGTA	
D16	GATAACAGCTATAAAGTTTCAGGTGGT	
D8	CAAAAACGTACAGTTGTACCACTGC	
AYE UP FW <i>adeS</i>	GGGGCGGCCGCCCTCCGACTTGCGGACGGAT	Check for deletion of
AYE DOWN RV <i>adeS</i>	GGGGCATGCAGGTGAGCAAGTCGGCCCTT	<i>adeRS</i> in AYE
AYE <i>adeB</i> UP F (NotI)	GCGGCGGCCGCTGTAGCCCCGCCACAGGTGA	Amplify <i>adeB</i> UP
AYE <i>adeB</i> UP R (BamHI)	GCGGGATCCAACGGCGCGGTGTCGTAAGG	fragment

AYE <i>adeB</i> DOWN F (BamHI)	GCGGGATCCTGAAGGGTTGCCACAAGGTGAC	Amplify <i>adeB</i> DOWN fragment
AYE <i>adeB</i> DOWN R (SphI)	GCGGCATGCGCCACCAAAAACCCCTGTGCC	
pMO130 insert flanking F	TTTACCACGACCGCATTCTC	Check for UP or DOWN fragment integration in pMO130- Tel <sup>R</sup>
pMO130 insert flanking R	AAATAGGCGTATCACGAGGC	
AYE <i>adeB</i> external F	TCGATGGGTTGGCTAGCGTGC	Check for deletion of <i>adeB</i> in AYE
AYE <i>adeB</i> external R	TGCCGCACTGCATTTCCCGT	
<i>gyrB</i> RT F	AGGGTGACTCTGCGGGTGGT	Primers for quantification of RNA
<i>gyrB</i> RT R	TCAAAGCGCGCACGCTCAAC	
Tn26 check F	TGAGCTTTTTAGCTCGACTAATCCAT	Check for Tn26 insertion in Tn- <i>adeR1</i> and Tn- <i>adeS1</i>
<i>adeS</i> gene R	GAATGCAGCTATCGCACATG	



<i>adeR</i> RT-PCR upstream F	AGGCATCATCTTTTACAGCTAGGGGA	Check for Tn101
<i>adeR</i> RT-PCR downstream R	GTGGTAGAAGATGAC	insertion in Tn- <i>adeR2</i>
<i>adeS</i> gene F	TGCGTGGCGTGGGATATAGACTA	Check for Tn26
<i>adeS</i> gene R	GAATGCAGCTATCGCACATG	insertion in Tn- <i>adeS2</i>
Tn26 check F	TGAGCTTTTTAGCTCGACTAATCCAT	Check for Tn26
<i>adeAB</i> DOWN R	ATCTATTGGGCTGATATTAC	insertion in Tn- <i>adeA1</i> , Tn- <i>adeA2</i> and Tn- <i>adeB1</i>
AYE <i>adeB</i> F	TGTAGCCCCGCCACAGGTGA	Check for Tn26
Tn26 check F	TGAGCTTTTTAGCTCGACTAATCCAT	insertion in Tn- <i>adeB2</i>

**Table 2.2.2 Generic PCR reaction volumes**

Reagent	Volume ( $\mu$ l) in a 25 $\mu$ l PCR
2x ReddyMix™ buffer (ThermoFisher Scientific)	12.5
10 $\mu$ M Forward primer	1
10 $\mu$ M Reverse primer	1
Sterile distilled water	9.5
Cell lysate	1

PCR parameters varied upon size of expected amplicon and annealing temperature of the primers but a typical PCR cycle for an amplicon of around 1 kilobase (kb) is shown in Table 2.3.1. Full details of all primers and PCRs are shown in Table 2.2.1.

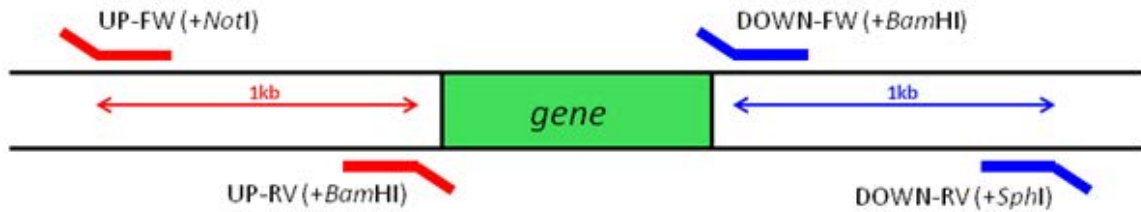
PCR amplicons were electrophoresed on a 1% agarose gel supplemented with 5  $\mu$ l Midori green (Nippon Genetics, Germany, cat. no. MG04) per 100 ml agarose alongside Hyperladder 1kb (Bioline, UK, cat.no. BIO33053), at 100 V for one hour. Agarose gels were visualised using a G:Box (Syngene, UK) PCR products were purified using a QIAQuick PCR Purification Kit (Qiagen, UK, cat. no. 28106).

### **2.3. Construction of gene deletion mutants**

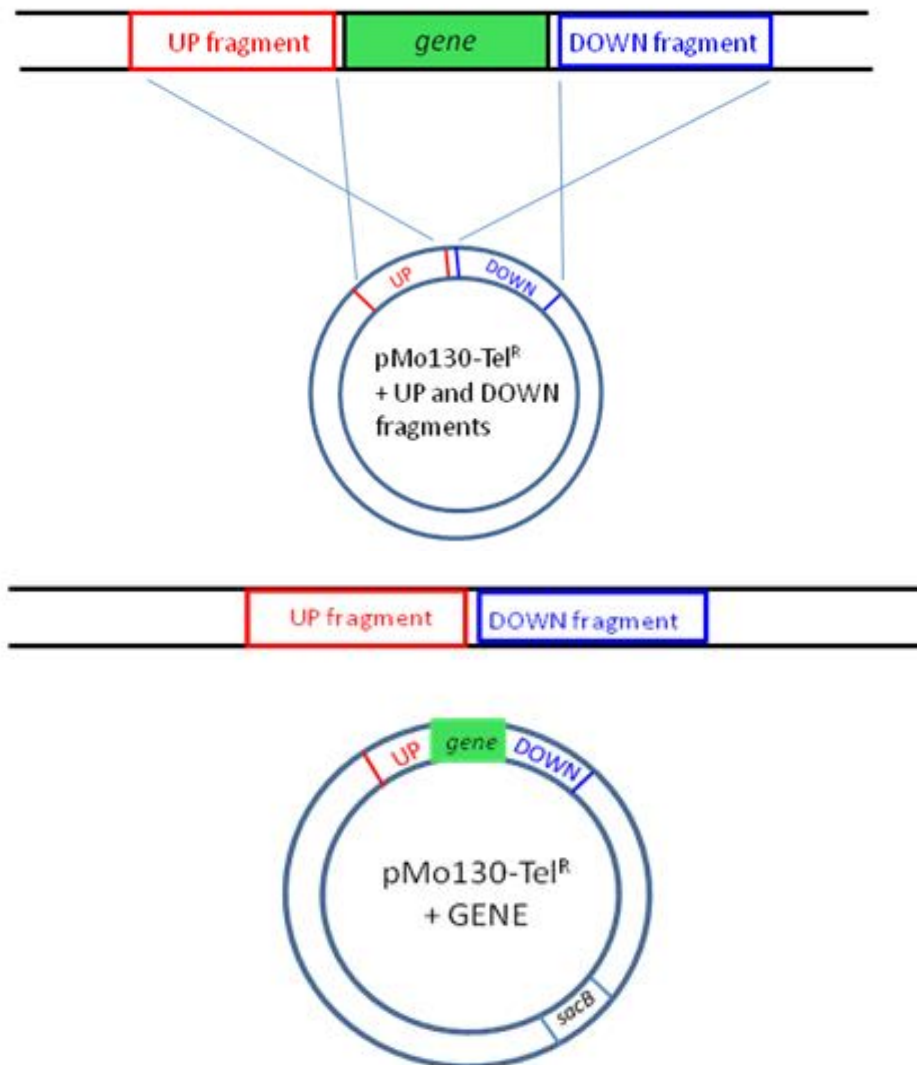
Deletion of *adeB* in AYE was carried out in collaboration with Matthew Wand and Laura Bonney (PHE, UK) using a modified version of the markerless deletion method used previously to delete *adeRS* in AYE and *adeAB* in S1 (Amin, Richmond et al. 2013) (Figure 2.3.1). Briefly, *E. coli* S17-1 containing a modified version of the pMo130-TelR suicide vector was created by Matthew Wand (PHE) and sent to the University of Birmingham, UK. Fragments upstream (UP) and downstream (DWN) of the region of *adeB* to be deleted were amplified and the UP fragment was ligated into the digested pMo130-TelR vector at the University of Birmingham by Grace Richmond. The DWN fragment was ligated into the digested pMo130-TelR vector at PHE, UK by Grace Richmond and Laura Bonney. The vector was then conjugated into AYE and candidate colonies containing an *adeB* deletion were verified by Matthew Wand and Laura Bonney at PHE, UK. Candidates were sent to the University of Birmingham for verification by PCR and sequencing by Grace Richmond.

Figure 2.3.1 A schematic diagram of the markerless deletion method used to create gene deletions in *A. baumannii*

A. Fragments upstream and downstream of the gene of interest were amplified by PCR and ligated into pMo130-TelR.



B. Plasmid was transformed into *A. baumannii* AYE and double recombination events selected for.



**Table 2.3.1 Generic PCR parameters**

Step	Temperature °C	Time	No. of cycles
Initial denaturation	95	2 min	1
Denaturation	95	25 sec	30-40
Annealing	53*	35 sec	30-40
Extension	72	1 min*	30-40
Final extension	72	5 min	1

\*Variable parameters – annealing temperature was dependent on GC content of primers and extension time was typically 1 min per kb.

### **2.3.1. Construction of pMo130-TeIR-adeBUPDOWN**

Isolation of the pMo130-TeIR plasmid created by Matthew Wand (PHE, UK) from *E. coli* S17-1 was carried out using the QIAprep® Spin Cell Mini Kit (Qiagen, UK, cat. no. 27106). To construct the plasmid used in this method, an 885 base pair (bp) and an 874 bp fragment upstream (UP) and downstream (DWN), respectively, of the region of *adeB* to be deleted were amplified by PCR using primers containing restriction enzyme sites (Table 2.2.1, Table 2.3.2). Amplification of the correct sized amplicons was confirmed by electrophoresis. Amplicons were purified using a QIAquick Purification Kit (Qiagen, UK, cat. no. 28104) and ligated sequentially into pMO130-TeIR digested with NotI and BamHI for ligation of the UP fragment and BamHI and SphI for ligation of the DWN fragment using Quick Stick Ligase (Bioline, UK, cat. no. BIO27027). All restriction enzymes were from New England Biolabs, UK, (cat. no. R0189S, R0136S, R0182S) and were used according to manufacturer's instructions. The modified construct was then transformed into  $\alpha$ -Select Electrocompetent Cells (Bioline, UK, cat. no. BIO-85028) by electroporation (4.5 kV, 200  $\Omega$ , 25  $\mu$ F) and transformants were selected on LB supplemented with 50  $\mu$ g/ml kanamycin (Sigma-Aldrich Ltd., UK, cat. no. B5264). Presence of the UP or DWN fragments was confirmed by PCR (Table 2.2.1).

### **2.3.2. Integration of pMo130-TeIR-adeBUPDOWN into *A. baumannii* AYE chromosome**

The pMO130-TeIR-adeBUPDOWN construct was introduced into *Escherichia coli* electrocompetent S17-1 by electroporation. Cells were made competent by harvesting cells from a 100 ml mid-logarithmic S17-1 culture by centrifugation in a

**Table 2.3.2 Restriction enzymes used in this study**

Restriction Enzyme	Cut site	Reaction conditions
BamHI HF®	5'...G↓GATCC...3' 3'...CCTAG↑G...5'	37°C for 2 hr in CutSmart® buffer
NotI HF®	5'...G↓CGGCCGC...3' 3'...CGCCGG↑CG...5'	37°C for 2 hr in CutSmart® buffer
SphI HF®	5'...GCATG↓C...3' 3'...C↑GTACG...5'	37°C for 2 hr in CutSmart® buffer

Hereaus Megafuge 40R (ThermoFisher Scientific, UK) at 2200 x *g* for 15 min at 4°C. Cells were washed five times in ice-cold 15% glycerol and resuspended in 1 ml glycerol. For transformation, 50 µl of competent cells and 1 ng of plasmid DNA was added to a microcentrifuge tube and incubated on ice for 20 minutes. Suspensions were transferred to a 2 mm electrocuvette and electroporated immediately (4.5 kV, 200 Ω, 25 µF). Cells were recovered by adding 950 µl of LB broth and incubated at 37°C with shaking (200 rpm) for 1.5 hours. Transformants were selected on LB supplemented with 50 µg/ml kanamycin and confirmed by PCR (Table 2.2.1). The pMO130-TelR-*adeBUPDOWN* construct was introduced into *A. baumannii* AYE by patch-mating at PHE, UK. Transformants with the plasmid integrated into the chromosome were selected for by growth on LB supplemented with 50 µg/ml ampicillin (Sigma-Aldrich Ltd., UK, cat. no. A9393) and 30 µg/ml tellurite (Sigma-Aldrich Ltd., UK, cat. no. 60539). Yellow colonies with a green-yellow haze, indicating XylE gene expression due to presence of the plasmid were PCR screened to confirmed plasmid integration into the chromosome.

### **2.3.3. Gene deletion**

Colonies that grew with a green-yellow haze on LB agar and were confirmed by PCR to have pMo-TelR-*adeBUPDOWN* integrated onto the chromosome were cultured on LB agar supplemented with 10% sucrose (Sigma-Aldrich Ltd., UK, cat. no. S0389) and incubated overnight at 37°C. Colonies were examined for loss of plasmid encoded XylE gene activity by loss of the yellow colour. White colonies were selected and streaked onto LB agar before PCR testing for gene deletion.



## **2.4. Bacterial growth kinetics**

Bacterial strains were grown with aeration in LB broth at 37°C overnight. Bacterial cultures were diluted 1:1000 in sterile LB broth and 100 µl of this suspension was added to each well of a clear, sterile 96 well microtitre tray. Optical density (OD) at an absorbance of 600 nm (OD<sub>600</sub>) was measured over 16 hours in a BMG FLUOstar Optima (BMG labtech, UK) at 37°C. The FLUOstar is sensitive to an OD<sub>600</sub> of between 0.0 and 4.0 and reproducibility is ±0.010 for the OD range of 0.0-2.0 ([www.BMG-labtech.com](http://www.BMG-labtech.com)).

## **2.5. Susceptibility testing**

The MICs of antibiotics (Table 2.5.1) were determined by the agar doubling dilution method according to the British Society for Antimicrobial Chemotherapy (BSAC) standard methodology (Andrews 2001). Stock solutions of 10,000, 1000 and 100 µg/ml of antibiotics were made up and appropriate amounts added to 20 ml of cooled, molten Iso sensitest agar (ThermoFisher Scientific, UK, cat. no. CM0471) in sterile universals. This was dispensed aseptically into petri dishes and allowed to set. Overnight cultures of each bacterial strain to be tested were diluted 1:100 to give a final inoculation in 1 µl of approximately 10<sup>7</sup> CFU/ml. Each agar plate was inoculated with 1 µl of diluted culture giving approximately 10<sup>4</sup> CFU per spot. Plates were incubated overnight at 37°C and read according to BSAC guidelines (Andrews 2001). The MIC of each agent was determined as the lowest concentration of antibiotic that inhibited visible growth (Andrews 2001) The MICs of imipenem and meropenem were determined by E-test (Biomérieux, UK). Colonies grown overnight on LB agar were emulsified in sterile water to a concentration of approximately 10<sup>8</sup> CFU/ml. A sterile swab was soaked in the suspension and the surface of an Isosensitest agar

**Table 2.5.1 Antibiotics and dyes used in this study**

Agent	Solvent	Supplier
Ciprofloxacin	Distilled water and acetic acid	Sigma-Aldrich, UK, cat no. 17850
Kanamycin	Distilled water	Sigma-Aldrich, UK, cat. no. B5264
Gentamicin	Distilled water	Sigma-Aldrich, UK, cat. no. G3632
Ceftazidime	0.1 M sodium hydroxide	Sigma-Aldrich, UK, cat. no. A6987
Imipenem	n/a	Biomerieux, UK, cat. no. IP0,002-32
Meropenem	n/a	Biomerieux, UK, cat. no. 513858
Ampicillin	1 M sodium bicarbonate	Sigma-Aldrich, UK, cat. no. A1593
Chloramphenicol	70% methanol	Sigma-Aldrich, UK, cat. no. C0378
Tigecycline	Distilled water	Pfizer, UK
Tetracycline	Distilled water	Sigma-Aldrich, UK, cat. no. 87128

Colistin	Distilled water	Sigma-Aldrich, UK, cat. no. C4461
Ethidium Bromide	Distilled water	Sigma-Aldrich, UK, cat. no. E7637
Carbonyl cyanide m-chlorophenyl hydrazine	Dimethyl sulphoxide	Sigma-Aldrich, UK, cat. no. C2759
Phenylalanine-arginine $\beta$ - naphthylamide	Distilled water	Sigma-Aldrich, UK, cat. no. P4157
Hoechst 33342	Distilled water	Sigma-Aldrich, UK, cat. no. B2261

---

(ThermoFisher Scientific, UK, cat. no. CM0471) plate streaked in three directions. The plate was allowed to dry for approximately 15 minutes before E-test gradient strips were positioned on the surface. Plates were incubated overnight at 37°C and read according to the manufacturer's instructions. Resistance was determined using EUCAST recommended breakpoint concentrations for *A. baumannii* ([http://www.eucast.org/clinical\\_breakpoints/](http://www.eucast.org/clinical_breakpoints/)).

## **2.6. Measurement of efflux activity**

Two methods were used to determine the permeability and efflux activity of *A. baumannii* strains. A Hoechst 33342 (H33342) (Table 2.5.1) accumulation assay and an ethidium bromide (Table 2.5.1) efflux assay. The use of two different dyes allowed the efflux of different substrates of the AdeABC efflux pump to be measured. Furthermore, the ethidium bromide efflux assay directly measured the rate of efflux from the cell, whereas the H33342 accumulation assay measured the total accumulation of dye within the cell and may also be affected by the rate of influx.

### **2.6.1. Accumulation of Hoechst 33342**

A H33342 accumulation assay developed by (Coldham, Webber et al. 2010) and modified for use with *A. baumannii* (Richmond, Chua et al. 2013) was used to measure differences in accumulation between strains. Higher concentrations of H33342 within the cell indicate reduced efflux or increased permeability when compared with an isogenic control. Bacterial strains were grown with aeration in LB broth at 37°C overnight. A 4% inoculum (120 µl in 3 ml) of bacterial culture was added to fresh LB broth. This suspension was incubated with aeration at 37°C until the cells reached mid-logarithmic phase (OD600 of 0.6-0.7). Cells were harvested by

centrifugation at 2200 x *g* in a Hereaus Megafuge 40R (ThermoFisher Scientific) for ten minutes at room temperature and resuspended in phosphate buffered saline (PBS) (Sigma-Aldrich, UK, cat. no. D8537) at room temperature. The OD600 was adjusted to 0.3 and 180  $\mu$ l of the cell suspension was dispensed into the wells of a black, 96 well microtitre tray (Corning, Amsterdam, cat. no. 3792). A 25  $\mu$ M H33342 stock solution was prepared to give a final concentration of 2.5  $\mu$ M and loaded into the FLUOstar OPTIMA for injection after an initial fluorescence reading. Fluorescence was measured over 117 minutes at excitation and emission wavelengths of 350 nm and 461 nm, respectively, in a FLUOstar OPTIMA. The time and fluorescence values at which maximum fluorescence was reached and remained unchanged within the time period of the assay was taken to indicate the steady state of accumulation. As fluorescence is measured in arbitrary units which can vary between assays, fold change in fluorescence of mutants compared to the parental strain was calculated to enable comparison between experiments.

### **2.6.2. Efflux of ethidium bromide**

To measure efflux of ethidium bromide, bacterial strains were grown with aeration in LB broth at 37°C overnight. A 4% inoculum (120  $\mu$ l in 3 ml) of bacterial culture was added to fresh LB broth. This suspension was incubated with aeration at 37°C until the cells reached mid-logarithmic phase (OD600 of 0.6-0.7). Cells were harvested by centrifugation at 2200 x *g* in a Hereaus Megafuge 40R (ThermoFisher Scientific) for ten minutes at room temperature and resuspended to an OD600 of 0.2 in ice cold 50 mM phosphate buffer. Cells were exposed to 20  $\mu$ g/ml ethidium bromide for 20 min and, washed and resuspended in phosphate buffer. The wells of a black, 96 well microtitre tray were inoculated with 180  $\mu$ l of the cell suspension and fluorescence

was measured over 1 hour at an excitation of 530 nm and an emission of 600 nm in a FLUOstar OPTIMA. The time and fluorescence at which minimum fluorescence was reached and remained unchanged within the time period of the assay was taken to indicate the steady state of efflux. As fluorescence is an arbitrary number and can vary between assays, fold change in fluorescence of mutants compared to the parental strain was calculated to enable comparison between individual experiments.

## **2.7. Measurement of biofilm formation**

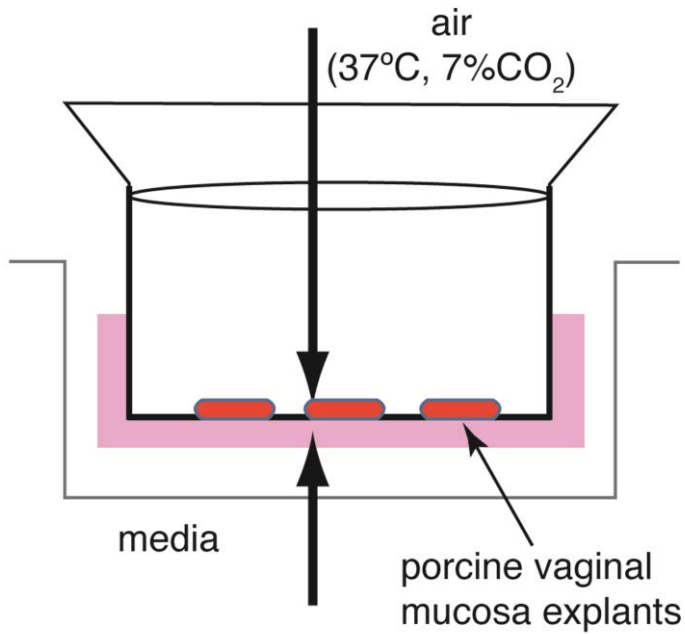
To measure the formation of a biofilm on different abiotic and abiotic surfaces, four different *in vitro* models and an *ex vivo* model was used.

### **2.7.1. Biofilm formation on porcine vaginal mucosal tissue**

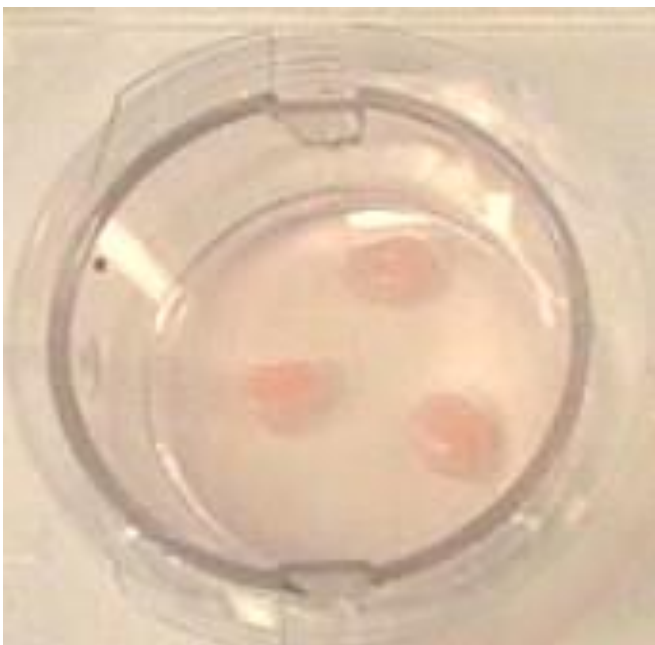
Biofilm formation on mucosal tissue was measured as described by Anderson *et al.* (Anderson, Parks et al. 2013). Specimens of normal porcine vaginal mucosa (PVM) were excised from animals at slaughter and washed in Roswell Park Memorial Institute 1640 medium (RPMI) (ThermoFisher Scientific, USA, cat. no. 21875-034) supplemented with 10% fetal bovine serum (ThermoFisher Scientific, USA, cat. no. 26400044), penicillin (50 IU/ml, MP Biomedicals, USA, cat. no. 029194537), streptomycin (50 µg/ml, MP Biomedicals, cat. no. 02194797) and amphotericin B (2.5 µg/ml, Hyclone, USA, cat. no. SV30078-01) to remove any bacteria and fungi colonising the mucosa. Tissue explants of 5 mm were cut and excess muscle was trimmed away. Tissue explants were washed in serum- and antibiotic-free media three times. Explants were placed mucosal side up on a 0.4 µm cell culture insert (BD Bioscience, USA, cat. no. 353090) in 6-well plates (BD Bioscience, USA, cat. no. 353502) containing fresh serum- and antibiotic-free RPMI 1640 (Figure 2.7.1). 1 ml

**Figure 2.7.1 Experimental setup of the porcine vaginal mucosal model**

**A. A cartoon depiction of explants resting on a transwell membrane inside a well of a cell culture plate (Anderson, Parks et al. 2013).**



**B. A mucosal explant placed on the membrane of a transwell seated in a 6-well tissue culture plate (Anderson, Parks et al. 2013).**



overnight culture of bacterial cells was pelleted by centrifugation, washed twice in 1 ml RPMI 1640 medium and resuspended in 1 ml RPMI 1640 medium. 300  $\mu$ l of this suspension was diluted in 5 ml RPMI 1640 medium to give  $5 \times 10^6$  CFU/ml. Explants were inoculated with 2  $\mu$ l of this suspension and incubated at 37°C. Bacterial cell counts of adherent and planktonic cells were carried out at 24, 48, 72, 96, 120 and 144 h. To enumerate planktonic cells, explants were washed in 3 ml sterile PBS at room temperature and the wash medium collected. The wash was sub-cultured onto TSA II agar plates containing 5% sheep's blood using a Wasp II spiral plater (Microbiology International, USA) and incubated at 37°C overnight. Colonies were counted using a Protocol plate reader (Microbiology International, USA) and the CFU/ml was calculated. To enumerate cells adhering to the mucosa, washed explants were placed in a 1.5 ml tube containing 250  $\mu$ l sterile PBS at room temperature and mixed by vortexing for 4 min. The wash was then sub-cultured onto TSA II agar plates containing 5% sheep's blood using a Wasp II spiral plater (Microbiology International, USA) and incubated at 37°C overnight. Colonies were counted using a Protocol plate reader (Microbiology International) and CFU/ml was calculated. The difference in the number of adherent cells between parental strain and mutant or clinical isolates versus index isolate was calculated. For imaging, explants were stained using FilmTracer™ LIVE/DEAD® Biofilm Viability kit (ThermoFisher Scientific, cat. no. L10316). Three microliters of propidium iodide and 3  $\mu$ l of SYTO9 were added to 1 ml sterile water and 200  $\mu$ l was distributed over three explants by pipetting. Explants were incubated at room temperature, without light, for 20 minutes and excess liquid was removed by pipetting. Explants were then gently washed three times with 1 ml Hanks Balanced Salt Solution (HBSS) (ThermoFisher

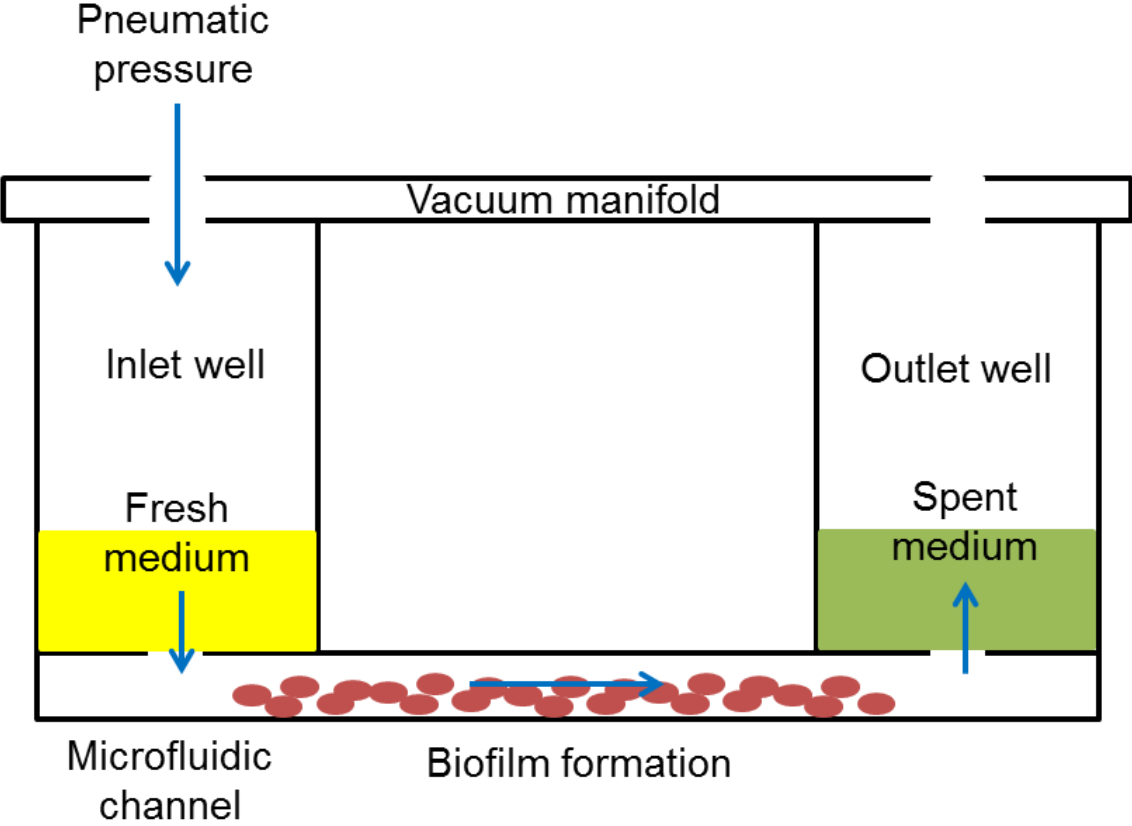


Scientific, cat. no. 14170070) and the final wash solution was left in the well. Explants were placed mucosal side up on glass slides and covered with a 20 mm coverwell imaging chamber (VWR, USA, cat. no. 100490-802). After staining, specimens were gently washed 3 x with HBSS and transferred to glass slides. A coverslip with 1 mm spacer (Electron Microscopy Sciences) was then applied and specimens were imaged on an Olympus Fluoview 1000 BX2 (Olympus America Corporation, USA) using a 60 x oil immersion objective. Images were captured and processed using Fluoview software (Olympus America Corporation, USA, <http://www.olympus-lifescience.com/en/support/downloads>).

### **2.7.2. Biofilm formation in a microfluidic flow cell**

A Bioflux 200 (Fluxion, USA) was used to visualise biofilm formation under microfluidic flow conditions. To prime the flow cells with media, 200 µl of LB broth was added to the inner circle of the output wells of a 48 well Bioflux flow cell plate (Fluxion, USA, cat. no. 910-004) (Figure 2.7.2) and the Bioflux 200 manifold was attached. Medium was flowed through the wells at 5 dyne and any residual medium was removed. Flow channels were inoculated by transferring 50 µl of overnight culture diluted to an OD600 of 0.1 to the output wells. To ensure that there was no flow from output to the inlet well, 50 µl of fresh LB broth was added to the inlet well also. Bacteria were introduced into the flow channel at 3 dynes for approximately 3 seconds. Even coverage of the bacterial cells in the flow channel was ensured by microscopic visualisation before the bacteria were left to attach at 30°C for 1 hour. Fresh LB broth was then added to the inlet well and flowed through the channel at 0.3 dynes for 16 hours. Biofilm formation was imaged at various time points using a LTSi-1000 inverted microscope (Labtech, USA).

Figure 2.7.2 Cartoon representation of a Bioflux 200 microfluidic channel



### **2.7.3. Biofilm formation on polypropylene pegs**

Crystal violet staining was used to measure biofilm formation on plastic pegs (Ceri, Olson et al. 1999, Baugh, Ekanayaka et al. 2012). Bacterial strains were grown with aeration overnight at 37°C and cultures were diluted in LB broth to an OD at 600 nm of 0.1. The wells of a 96 well microtitre tray were inoculated with 100 µl of diluted culture and a sterile, 96 well PCR plate (Starlabs, UK, cat. no. E1403-0209) was placed into the microtitre tray. Plates were sealed and incubated with gentle agitation for 8 hrs at either 30°C or 37°C. After incubation, the liquid culture was removed and pegs were washed with sterile distilled water to remove planktonic cells. PCR plates were placed in fresh microtitre trays containing 100 µl 1% crystal violet, in order to stain the biofilm, and left at room temperature for 15 min. The crystal violet was removed and pegs were washed with sterile distilled water. PCR plates were placed in fresh microtitre trays containing 100 µl 70% ethanol, to solubilise the dye and left at room temperature for 2 hrs. OD at an absorbance of 600 nm was measured a BMG FLUOstar Optima. As final OD can vary between individual experiments, OD<sub>600</sub> was converted to fold change compared to the parental strain in order to compare results between experiments.

### **2.7.4. Pellicle formation**

In order to measure the ability of the strains to form a biofilm at the air-liquid interface, pellicle formation was measured as described previously (Nait Chabane, Marti et al. 2014). Bacterial strains were grown with aeration in LB broth at 37°C overnight. Cultures were diluted in LB broth to an OD at 600 nm of 0.1 and 2 ml was added to polystyrene test tubes (13 mm x 75 mm). Cultures were incubated statically

at 37°C for 72 hrs and pellicle formation was identified visually. Isolates were considered positive when the surface was covered with an opaque layer of biomass.

### **2.7.5. Biofilm formation on glass cover slips**

In order to visualise biofilm formation on an abiotic surface, biofilms were grown on glass cover slips and imaged at the Centre for Electron Microscopy (CEM), University of Birmingham, by scanning electron microscopy. A 4% inoculum (200 µl in 5 ml) of bacterial culture grown overnight was added to fresh LB broth containing a 10 mm glass coverslip (ThermoFisher Scientific, UK, cat. no. 12658116) and incubated at 37°C for 24 hrs. The cover slip was removed and placed in a primary fixative of 2.5% glutaraldehyde in phosphate buffer. Subsequent dehydration and mounting steps were carried out by Paul Stanley at the CEM. Scanning electron microscopy images were viewed at various magnifications on a Philips XL30 FEG ESEM (FEI, USA.)

### **2.8. Measurement of twitching and swarming motility**

To investigate motility of strains the ability to migrate in the medium-plastic interface of solid media (twitching) and migration on semi-solid agar (swarming) was measured as described previously for *A. baumannii* (Eijkelkamp, Stroehler et al. 2011). To investigate twitching motility, 1 µl of a liquid culture grown overnight at 37°C was stabbed through Mueller-Hinton medium (Sigma-Aldrich, UK, cat. no. 70192) containing 1% agar (Sigma-Aldrich, UK, cat. no. A5306) to the bottom of the petri dish. To investigate swarming motility, 1 µl of a liquid culture grown overnight at 37°C was inoculated onto the surface of LB medium containing 0.3% agar. Plates were incubated for 24 hrs at 37°C after which the motility phenotype was assessed visually and using ImageJ software (Schneider, Rasband et al. 2012).

## **2.9. Measurement of virulence in *Galleria mellonella***

Survival assays in *G. mellonella* were carried out by Matthew Wand (PHE), as previously described (Wand, Bock et al. 2012). Bacteria were injected into *G. mellonella* larvae at an inoculum of  $10^6$  CFU. Larvae were incubated statically at 37°C inside petri dishes and the number of dead larvae scored at 24, 48, 72, 96 and 120 hr. Data were sent to Birmingham for statistical analysis and interpretation.

## **2.10. Statistical analysis**

All data was analysed using Prism version 6.00 for Windows (GraphPad Software, USA). Growth kinetics, H33342 accumulation, ethidium bromide accumulation, biofilm formation on plastic and PVM cell counts were analysed using an unpaired Student's t-test to calculate significant differences between parental and mutant strains. A Student's t-test allows comparison of the means of a normally distributed variable for two independent groups. Tests returning a P value of  $< 0.05$  were considered significant. All analyses included at least nine biological replicates, each of which were replicated at least twice and data inputted into Microsoft Excel and entered into the appropriate table format in Prism. Virulence in *G. mellonella* was displayed as a Kaplan Meier survival curve. This method allows you to measure the fraction of subjects living for a certain amount of time after infection (Goel, Khanna et al. 2010). Statistical significance was calculated using a Log-rank (Mantel-Cox) test and a Gehan-Breslow-Wilcoxon test. Differences between parental and mutant strains were considered significant when both tests returned a P value of  $< 0.05$ .

## **2.11. RNA-Seq**

### **2.11.1. RNA extraction**

RNA was extracted from 4 bacterial cultures (= 4 biological replicates) using a RNAprotect™ Bacteria Reagent (Qiagen, UK, cat. no. 76506) and RNeasy Mini kit (Qiagen, UK, cat. no. 74104) for stabilisation and isolation of total RNA from bacterial cultures, using the enzymatic lysis protocol. Bacterial strains were grown with aeration overnight at 37°C and 1 ml of culture was added to 2 ml of RNAprotect Bacteria Reagent. The suspension was mixed by vortexing for 5 s and incubated at room temperature for 5 min. The suspension was centrifuged at 5000 x *g* for 10 min in a Hereaus Megafuge 40R (ThermoFisher Scientific, UK) and the supernatant removed.

To enzymatically lyse the cells, 200 µl TE buffer containing 1 mg/ml lysozyme was added and mixed by using a vortex for 10 s. The suspension was incubated at room temperature for 5 min with 10 s mixing every 2 min. After incubation, 700 µl of RLT buffer was added and the suspension was vortexed vigorously. Finally, 500 µl of ethanol was added to the lysate and mixed by pipetting.

To extract the RNA from the sample, the lysate was applied to an RNeasy Mini Column placed in a 2 ml collection tube and centrifuged for 15 s at 8000 x *g* in an Eppendorf MiniSpin Centrifuge. 700 µl Buffer RW1 was added to the RNeasy column and centrifuged for 15 s at 8000 x *g* to wash the column. Flow through was discarded after each step. The RNeasy column was transferred to a new 2 ml collection tube and 500 µl of Buffer RPA added to the column. The tube was centrifuged for 15 s at 8000 x *g* in an Eppendorf MiniSpin Centrifuge and the flow through discarded. To

elute, the RNeasy column was transferred to a 1.5 ml collection tube and 30  $\mu$ l RNase-free water was applied directly to the silica-gel membrane. The tube was centrifuged at 8000 x *g* for 1 min and the RNeasy column removed from the collection tube. RNA was stored at -80°C.

### **2.11.2. DNase treatment of RNA samples**

DNA was removed from the RNA samples using an Ambion TURBO DNA-free™ kit (ThermoFisher Scientific, UK, cat. no. AM1907). After RNA extraction, 0.1 volume 10 X TURBO DNase Buffer and 2  $\mu$ l TURBO DNase was added to each RNA sample and incubated at 37°C for 1 hr. After incubation, 0.2 volume DNase Inactivation Reagent was added and mixed by pipetting. The suspension was incubated at room temperature for 5 min with occasional mixing and then centrifuged at 10,000 x *g* for 1.5 min before transferring the supernatant to a fresh tube. RNA samples were confirmed as DNA by quantification of DNA and RNA concentrations using a Qubit® Fluorometer (Sigma-Aldrich Ltd., UK). Samples were prepared using the Qubit® dsDNA HS Assay Kit (Sigma-Aldrich Ltd., UK, cat. no. Q32851) and Qubit® RNA HS Assay Kit (Sigma-Aldrich Ltd., UK, cat. no. Q32852) as per the manufacturer's instructions. Samples with a DNA concentration < 5% of the total nucleic acid concentration were considered DNA negative.

### **2.11.3. Quantification of RNA**

The quality of the RNA samples was assessed using an Agilent 2100 Bioanalyzer (Agilent Technologies, USA) and Nanodrop 2100 (ThermoFisher Scientific, UK). Samples with total RNA > 1  $\mu$ g, RNA concentration > 40 ng/ $\mu$ l, RNA integrity number

(RIN) > 7.0, 23S/16S > 1.0, OD260/280 > 1.8 and OD260/230 > 1.8 were considered acceptable for sequencing.

#### **2.11.4. Preparation of RNA-Seq libraries**

RNA-Seq experiments were carried out at different stages of the study and therefore different companies and protocols were used for library preparation and sequencing as protocols were improved over time. AYE and AYE $\Delta$ *adeRS* libraries were prepared and sequenced by ARK genomics (Edinburgh, UK) in August 2012, AYE and AYE $\Delta$ *adeB* libraries were prepared and sequenced by Grace Richmond at the University of Birmingham in March 2015 and S1 and S1 $\Delta$ *adeAB* libraries were prepared and sequenced by BGI genomics (Hong Kong) in September 2015. For preparation of RNA-Seq libraries at the University of Birmingham, a Zymo RNA Clean and Concentrator™-5 (Zymo Research, USA, cat. no. R1015) was used to recover 5 µg high quality, concentrated RNA from DNase treated samples. Diluted samples were added to a Zymo-Spin™ IC column and centrifuged for 30 seconds at 8000 x *g*. Columns were washed and the RNA was eluted in 26 µl RNase-free water by centrifugation for 1 min at 8000 x *g*. Ribosomal RNA was removed using a Ribo-Zero™ Magnetic Kit (Illumina, USA, cat. no. MRZB12424). Treatment of the total RNA samples with Ribo-Zero rRNA removal solution was carried out according to the kit protocol and rRNA was removed using a magnetic bead reaction. rRNA-depleted samples were then purified using a Zymo RNA Clean and Concentrator™-5 as described above. Samples were eluted in 20 µl RNase-free water. Samples were prepared for sequencing using a Tru-Seq® Stranded mRNA Sample Preparation Kit (Illumina, USA, cat. No. 122-2101). PolyA containing mRNA molecules were purified using polyT oligo attached magnetic beads and the RNA was fragmented and primed



for cDNA synthesis. Following this, first strand and second strand cDNA was synthesised and a single 'A' nucleotide was added to the 3' ends of the blunt fragments to prevent them from ligating to one another. Multiple indexing adapters were then ligated to the ends of the double stranded cDNA, preparing them for hybridisation onto a flow cell. DNA fragments with an adaptor molecule on both ends were selectively enriched by PCR and the libraries were validated using the Agilent D1000 ScreenTape System (Agilent Technologies, UK) and a KAPA library Quantification Kit for Illumina Sequencing Platforms (KAPA Biosystems, UK, cat. no. KK4824). Finally, libraries were normalised and pooled in preparation for sequencing using a MiSeq sequencing platform.

#### **2.11.5. Sequencing of RNA-Seq libraries**

AYE and AYE $\Delta$ *adeB* libraries were sequenced at Birmingham using an Illumina MiSeq. AYE and AYE $\Delta$ *adeRS* libraries were sequenced by ARK genomics using an Illumina HiSeq. S1 and S1 $\Delta$ *adeAB* libraries were sequenced by BGI genomics using an Illumina MiSeq.

#### **2.11.6. Analysis of RNA-Seq data**

All RNA-Seq datasets were analysed together by Al Ivens (University of Edinburgh). Raw sequences were quality assessed using FASTQC, which performs quality control checks on raw sequence data, and processed. Alignments to an AYE reference genome (Kersey, Allen et al. 2014) were performed using bowtie2. A bed file of the gene loci was generated from the gff annotation and bedtools used to count tags overlapping the regions of interest. Raw tag counts per sample were scale normalised to the sample with the lowest number of tags within each data set.

Counts were converted to log<sub>2</sub> and quantile normalised within each series for comparisons within each data set. Pairwise comparisons were performed on the normalised tag counts using linear modelling (Bioconductor limma package). A raw P cut-off value of 0.05 was used to produce a list of changed genes that could be examined by phenotypic testing. No fold-change cut off was used. RNA-Seq data were submitted to ArrayExpress (accession E-MTAB-4047, E-MTAB-4049, E-MTAB-4071).

### **3. The Role of the Two Component System AdeRS in Antibiotic Resistance, Biofilm Formation and Virulence**

#### **3.1. Summary of background to this research**

AdeRS is a two component system that regulates expression of the multi-drug efflux pump AdeABC. Mutations in *adeRS* can cause overexpression of AdeABC and lead to MDR (Marchand, Damier-Piolle et al. 2004, Peleg, Adams et al. 2007). Deletion of either *adeR* or *adeS* in clinical isolates overexpressing AdeABC results in susceptibility to substrates of this pump (Marchand, Damier-Piolle et al. 2004). Strain AYE contains an Ala94Val mutation in AdeS that has been previously associated with upregulation of the AdeABC efflux system and increased resistance to antibiotics (Hornsey, Loman et al. 2011). Furthermore, two component systems have been shown previously to be involved in the regulation of other bacterial functions, such as growth, competence, metabolism, adaptation to starvation, osmoregulation and expression of toxins (West and Stock 2001, Mitrophanov and Groisman 2008).

#### **3.2. Hypothesis**

Deletion of *adeRS* will affect expression of genes and their products encoding antibiotic resistance, biofilm formation and virulence.

#### **3.3. Aims**

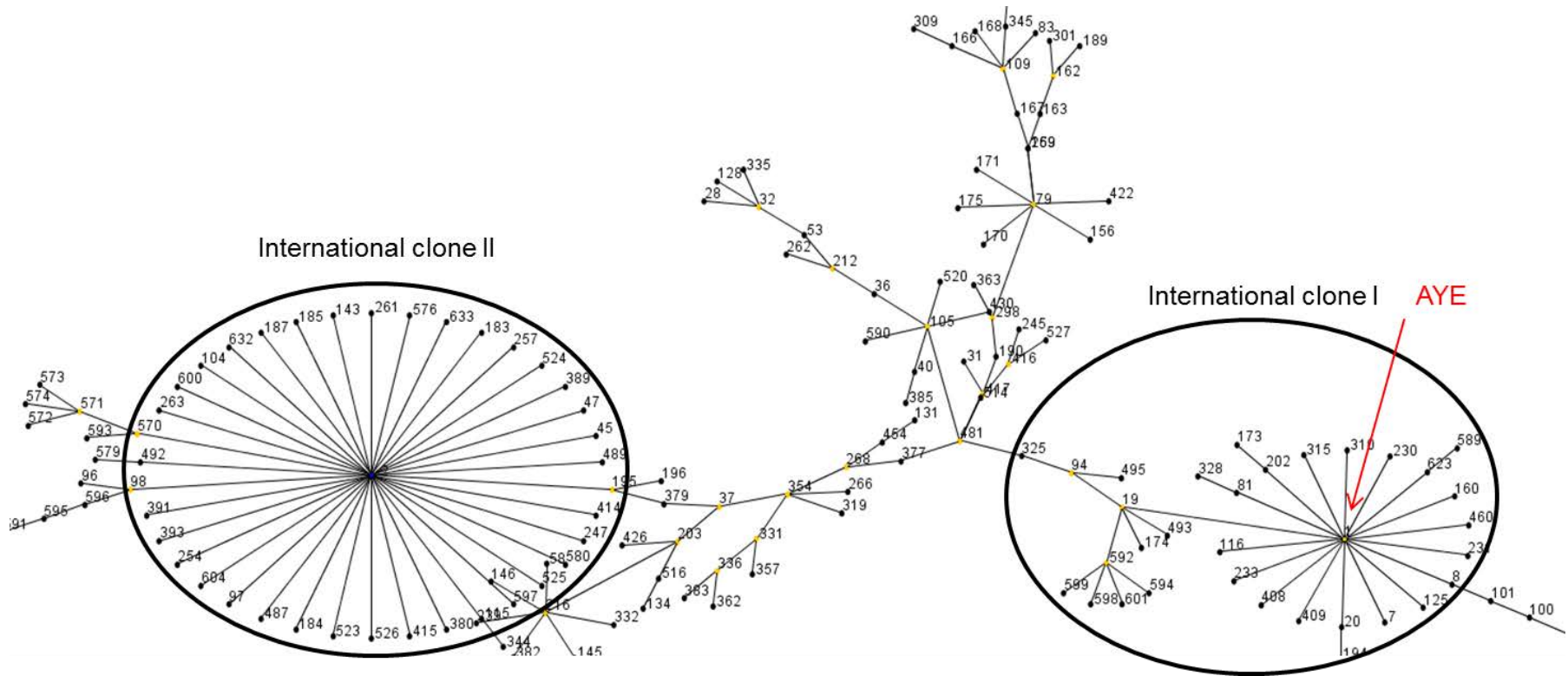
The aim of this study was to identify the consequences of deletion of *adeRS* in *A. baumannii* AYE. The objectives were to optimise the porcine vaginal mucosal model to measure *A. baumannii* biofilm formation on a mucosal surface, to use this and other methods to characterise the antibiotic resistance, biofilm formation and

virulence phenotype of deletion mutant *AYEΔadeRS* and to use RNA-Seq to identify transcriptomic changes in this strain.

### **3.4. Choice of strains and verification of strains**

*A. baumannii* AYE was selected for this work as it is a well-characterised clinical isolate that is MDR (Fournier, Vallenet et al. 2006, Hornsey, Loman et al. 2011). AYE is sequence type (ST) 1 of International clone I and represents a clinically successful clone (Figure 3.4.1). Type strain ATCC 19606 (ST52) was included as a control in the *ex vivo* biofilm experiments as a strain that has a well-characterised biofilm phenotype (de Breij, Gaddy et al. 2009, de Breij, Haisma et al. 2012). Deletion of *adeRS* in AYE was carried out by Laura Evans (University of Birmingham) using a markerless deletion method (Amin, Richmond et al. 2013). Deletion was verified by amplification of the deleted region by PCR (Figure 3.4.2A). Amplification of the region in AYE produced a 3377 bp amplicon, whereas amplification in *AYEΔadeRS* produced a 2011 bp amplicon, confirming deletion of a 1366 bp fragment spanning the whole of the *adeS* gene and 126 bp of the *adeR* gene. This was subsequently confirmed by Sanger sequencing (Figure 3.4.2B). To predict how much of the AdeR protein was removed by deletion of 126 bp of the *adeR* gene and to illustrate which part of the protein remained and may still be functional, I-TASSER protein modelling software was used to generate a predicted protein model based on sequence homology to known protein structures (Yang, Yan et al. 2015). The protein structure was viewed in PyMOL (<http://www.pymol.org>) and the 42 amino acids for which the coding bases were deleted were highlighted in red (Figure 3.4.3). Deletion of 126 bp of *adeR* removed 27 amino acids of the signal receiver domain predicted by the NCBI domain predictor (<http://www.ncbi.nlm.nih.gov/Structure/cdd/wrpsb.cgi>).

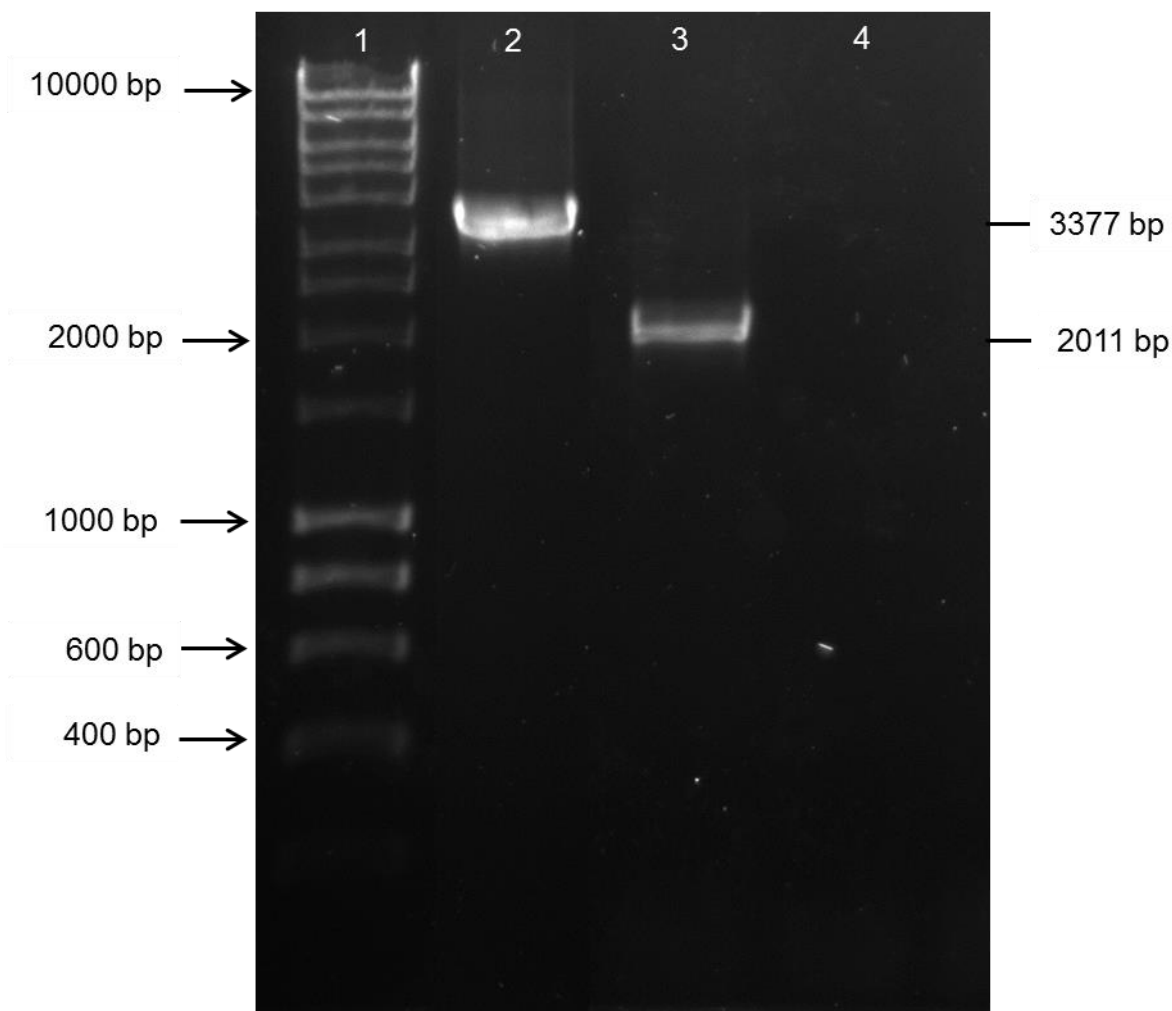
Figure 3.4.1 Relationships between 615 *A. baumannii* isolates based on MLST data (Pasteur scheme) as calculated by the BURST algorithm



Circles indicate major international groups and AYE is marked in red

**Figure 3.4.2 Verification of *adeRS* gene deletion in AYE by PCR and DNA sequencing**

**A. PCR to assess the size of the *adeRS* region**



Lane	Template	Predicted fragment size (bp)	Actual fragment size (bp)
1	Hyperladder 1kb	-	-
2	AYE	3377	3377
3	AYE $\Delta$ <i>adeRS</i>	2011	2011
4	Negative control	0	0

## B. Alignment of AYE *adeRS* sequence with upstream sequencing data for *AYEΔadeRS*

AYE	TCATAGCGTTTATATACACTCTGAGAATAAGAAGATCTTGCTTAATCTGACGCTGACTGA
AYEΔ <i>adeRS</i>	TCATAGCSTTTATATACACTCTGAGAATAAGAAGATCTTGCTTAATCTGACGCTGACTGA *****
AYE	ATATAAAATTTATTCATTCATGATTGATCAGCCTCATAAAGTTTTACGCGCGGAGAGCT
AYEΔ <i>adeRS</i>	ATATAAAATTTATTCATTCATGATTGATCAGCCTCATAAAGTTTTACGCGCGGAGAGCT *****
AYE	TATGAATCACTGCATGAATGATAGCGATGCAC TAGAGCGAACCGTAGATAGCCATGTGAG
AYEΔ <i>adeRS</i>	TATGAATCA----- *****
AYE	TAAAGCTGAGAAAAAACTAGAAGAACAAGGCATATTTCAAATGTTAATTAATGTGCGTGG
AYEΔ <i>adeRS</i>	-----
AYE	CGTGGGATATAGACTAGATAATCCCCTAGCTGTAAAAGATGATGCCTAA
AYEΔ <i>adeRS</i>	-----ataatattaa
AYE	aaatagctagggaaatattttATGAAAAGTAAGTTAGGAATTAGTAAGCAACTTTTTATTG
AYEΔ <i>adeRS</i>	-----
AYE	CCTTAACTATTGTGAATTTAAGCGTTACGCTATTTTCTATAGTATTGGGTTATATCATT
AYEΔ <i>adeRS</i>	-----
AYE	ATAACTATGCGATTGAAAAAGGCTGGATTAGCTTAAGCTCATTCAACAAGAAGATTGGA
AYEΔ <i>adeRS</i>	-----
AYE	CCAGTTTTCATTTTTGTAGACTGGATCTGGTTAGCCACTGTATCTTCTGTGGCTGTATTA
AYEΔ <i>adeRS</i>	-----
AYE	TTTCATTAGTGATTGGCATGCGCCTCGCAAAGCGTTTTATTGTGCCAATTAACCTCCTAG
AYEΔ <i>adeRS</i>	-----
AYE	TCGAAGCAGCAAAAAAATTAGTCACGGCGACCTCTCTGCTAGAGCTTACGATAATAGAA
AYEΔ <i>adeRS</i>	-----
AYE	TTCACTCCGCCGAAATGTCGGAGCTTTTATATAATTTAATGATATGGCTCAAAAGCTAG
AYEΔ <i>adeRS</i>	-----
AYE	AGGTTTCCGTCAAAAATGCGCAGGTTTGAATGCAGCTATCGCACATGAGTTAAGAACGG
AYEΔ <i>adeRS</i>	-----
AYE	CTATAACGATATTACAAGTCGTTTACAGGAATTATTGATGGCGTTTTTAAACCTGATG
AYEΔ <i>adeRS</i>	-----
AYE	AAGTCTATTTAAAAGCCTTTTAAATCAAGTTGAAGGTTATCTCACTTAGTCGAAGACT
AYEΔ <i>adeRS</i>	-----
AYE	TACGGACTTTAAGCTTAGTAGAGAACCAGCAACTCCGGTTAAATTAATGAATTGTTTGACT
AYEΔ <i>adeRS</i>	-----
AYE	TGAAGGCGGTAGTTGAAAAAGTTCTTAAAGCATTGAAGATCGTTTGGATCAAGCTAAGC
AYEΔ <i>adeRS</i>	-----
AYE	TAGTACCAGAACTTGACCTAACGTCCACTCCTGTATATTGCGACCGCCGTCGTATTGAGC

```

AYEΔadeRS -----
AYE AAGTTTTAATTGCTTTAATTGATAATGCGATTGCTATTCAAATGCAGGCAAACCTAAAA
AYEΔadeRS -----

AYE TCTCTTCAGAAGTGGTTGCAGACAACCTGGATATAAAAATTGAGGATGAAGCCCCGGCA
AYEΔadeRS -----

AYE TTGCAACCGAGTTTCGGGACGATTATTAAAGCCTTTCTTTAGATTAGAAGAATCAAGGA
AYEΔadeRS -----

AYE ATAAAGAATTGGCGGCACAGGTTAGGTCTTGCTGTTGTACATGCAATTATTGTGGCA
AYEΔadeRS -----

AYE TGAAAGGCACTATTCAATATAGCAATCAAGGCTCGAAAAGTGTTCACCATAAAAATTT
AYEΔadeRS -----

AYE CTATGGGTCATGAAGAGATGGGGTAAttcgctaaattaaataatccttagagttaagtgc
AYEΔadeRS -----

AYE cccctcactctcttttattcttctacgaatttcttctcgccattttgtggcattttcctg
AYEΔadeRS -----CTGCATGAATG
* **

AYE ttgtttgtttaataggacacctaacaataaagctgtaaccgcagcgccaattaaggctat
AYEΔadeRS ATAGCGATGCACTAGAGCGAACCGGATCCAAGCTGTAACCGCAGCSCCAATTAAGGCTAT
* * * * * ** *****

AYE accggtttcataaataatctataacaaattcgagcactccctccgacaaaaaatctaa
AYEΔadeRS ACCGGTTTCATAAATAATATCTATAACAAATTCGAGCACTCCCTCCGACAAAAATCTAA
*****

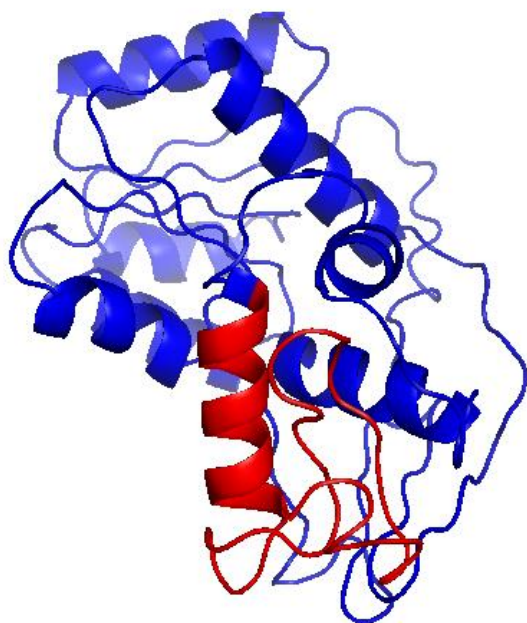
```

Sequences were aligned using Clustal Omega. \* indicates a position with a single, fully conserved residue. The *adeR* gene is highlighted in yellow and the *adeS* gene is highlighted in blue.

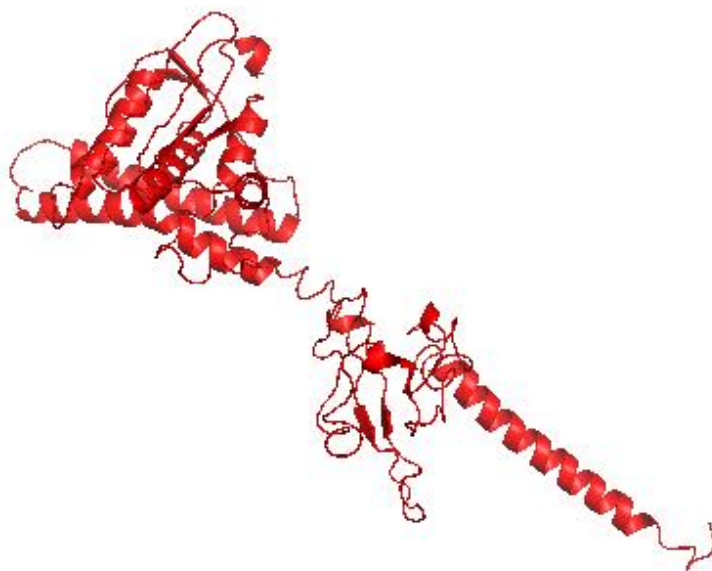


Figure 3.4.3 Predicted protein structure of AdeR and AdeS in *AYEΔadeRS*

AdeR



AdeS



Amino acids for which the coding sequence was deleted are highlighted in red.

All strains used in this study were confirmed as *A. baumannii* using a *gyrB* PCR (Higgins, Wisplinghoff et al. 2007, Higgins, Lehmann et al. 2010). This protocol uses seven primers in a multiplex PCR to produce different sized amplicons, allowing differentiation between *A. baumannii*, *A. calcoaceticus*, *A. pittii* and *A. nosocomialis*. Each strain produced a 294 bp amplicon and a 490 bp amplicon, characteristic of this species.

### **3.5. Determining the phenotype of an *A. baumannii* AYE mutant lacking the TCS AdeRS**

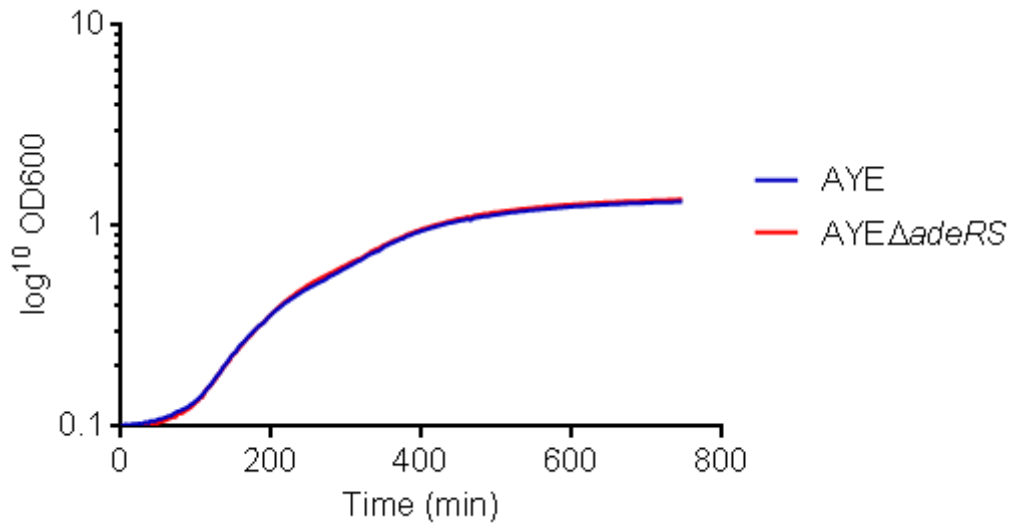
#### **3.5.1. Bacterial growth kinetics of AYE $\Delta$ adeRS**

To determine whether there was a growth defect in the AdeRS deletion mutant that may affect the results of subsequent experiments, the growth kinetics of AYE and AYE $\Delta$ adeRS were determined by measuring optical density of cell cultures grown in LB broth at 37°C over time. There was no significant difference between the lag phase, generation time or the final optical density at stationary phase of AYE and deletion mutant AYE $\Delta$ adeRS (Figure 3.5.1). To verify that there was no change in cell morphology, which can affect optical density measurements, cells were Gram-stained and visualised by microscopy during lag phase, exponential phase and stationary phase. All cells appeared as Gram-negative rods, characteristic of this species, and no filamentation was observed at any growth stage.

#### **3.5.2. Antimicrobial susceptibility of AYE $\Delta$ adeRS**

To determine whether there was a change in the drug resistance profile of AYE with deletion of AdeRS, the minimum inhibitory concentration (MICs) of commonly used antibiotics and dyes and those previously shown to be substrates of the AdeABC

**Figure 3.5.1 Growth kinetics of AYE and AYE $\Delta$ adeRS in LB broth at 37°C**



Data are shown as the mean of 3 biological replicates and are representative of a single independent experiment carried out at least 3 times.

Generation times and optical density at stationary phase ( $\pm$ standard deviation)				
Strain	Mean generation time (min)	<i>P</i> value	OD600 at stationary phase	<i>P</i> value
AYE	121 $\pm$ 3.295	-	1.323 $\pm$ 0.030	-
AYE $\Delta$ adeRS	115 $\pm$ 2.695	0.084	1.357 $\pm$ 0.007	0.129

RND efflux pump (Yoon, Nait Chabane et al. 2015) were determined (Table 3.5.1). Parental strain AYE was resistant to gentamicin and ciprofloxacin according to EUCAST breakpoint concentrations ([http://www.eucast.org/clinical\\_breakpoints/](http://www.eucast.org/clinical_breakpoints/)). There were no EUCAST breakpoint concentrations available for *Acinetobacter* spp. and seven drugs: ampicillin, ceftazidime, kanamycin, norfloxacin, tetracycline, tigecycline or chloramphenicol. There was a decrease in the MIC of kanamycin, gentamicin, ciprofloxacin, tetracycline, tigecycline, chloramphenicol and the dye ethidium bromide with deletion of *adeRS* in AYE. Although some of these changes were only 2-fold, which is considered to be the margin of error for this method, these changes were consistent in multiple experiments (n = 3).

### **3.5.3. Hoechst 33342 (bis-benzimide) accumulation by AYE $\Delta$ adeRS**

Hoechst (H) 33342 is a dye that can be used to measure relative levels of efflux in bacterial cells (Coldham, Webber et al. 2010, Richmond, Chua et al. 2013). It fluoresces when bound to DNA and therefore its accumulation can be measured (Coldham, Webber et al. 2010). It has been previously shown that accumulation of H33342 is a good indication of efflux activity in *A. baumannii* (Richmond, Chua et al. 2013). Accumulation of H33342 in AYE was compared with AYE $\Delta$ adeRS to investigate whether there was a relative difference in the intracellular levels of this substrate. When compared with strain AYE, accumulation of H33342 in strain AYE $\Delta$ adeRS was 40% higher ( $P < 0.0001$ ), indicating reduced levels of efflux of this dye in the mutant (Figure 3.5.2).

**Table 3.5.1 MICs of antibiotics and dyes against AYE and AYE $\Delta$ adeRS**

		MIC ( $\mu$ g/ml)	
		AYE	AYE $\Delta$ adeRS
Ampicillin	experiment 1	>1024	>1024
	experiment 2	>1024	>1024
	experiment 3	>1024	>1024
Ceftazidime	experiment 1	1024	1024
	experiment 2	1024	1024
	experiment 3	1024	1024
Imipenem	experiment 1	1.5	0.75
	experiment 2	1.5	0.75
	experiment 3	1.5	0.75
Meropenem	experiment 1	0.25	0.25
	experiment 2	0.25	0.25
	experiment 3	0.25	0.25
Kanamycin	experiment 1	1024	512
	experiment 2	512	256
	experiment 3	1024	512
Gentamicin	experiment 1	128	8
	experiment 2	64	8
	experiment 3	128	8
Norfloxacin	experiment 1	128	128
	experiment 2	128	128
	experiment 3	128	128
Ciprofloxacin	experiment 1	128	32
	experiment 2	128	32
	experiment 3	64	32
Colistin	experiment 1	1	1

	experiment 2	1	1
	experiment 3	1	1
Tetracycline	experiment 1	256	128
	experiment 2	256	128
	experiment 3	256	64
Tigecycline	experiment 1	1	0.25
	experiment 2	1	0.25
	experiment 3	1	0.25
Chloramphenicol	experiment 1	512	256
	experiment 2	512	256
	experiment 3	512	256
	experiment 1	32	32
	experiment 2	32	32
Carbonyl cyanide 3-chlorophenylhydrazone	experiment 3	32	32
	experiment 1	1024	1024
Phenylalanine-arginine beta-naphthylamide	experiment 2	1024	1024
	experiment 3	1024	1024
Ethidium bromide	experiment 1	512	256
	experiment 2	512	512
	experiment 3	512	256

---

Data are shown as the results of three individual experiments carried out on different days. Blue text indicates a decrease in MIC value compared with AYE.



### **3.5.4. Ethidium bromide efflux by AYE $\Delta$ adeRS**

Ethidium bromide is a DNA intercalating dye and exhibits weak fluorescence when external to the cell and becomes strongly fluorescent when bound to DNA or in the periplasm due to binding to cellular components (Jernaes and Steen 1994). Ethidium bromide was allowed to accumulate in bacterial cells and fluorescence was used to monitor subsequent efflux of the dye. Fluorescence relative to the starting fluorescence in each strain was calculated to account for differing dye accumulation levels in the parent and mutant. AYE was compared with AYE $\Delta$ adeRS to investigate whether there was a difference in efflux levels of this substrate. The rate of efflux of ethidium bromide was lower and the final level of accumulation was 92% higher ( $P < 0.0001$ ) in the AdeRS mutant than in parental strain AYE (Figure 3.5.3). These data suggest less efflux activity in AYE $\Delta$ adeRS when compared with AYE.

### **3.5.5. Biofilm formation by AYE $\Delta$ adeRS in an *ex vivo* model**

To study biofilm formation in a clinically relevant model, an *ex vivo* porcine vaginal mucosal (PVM) model was used. This *ex vivo* model mimics a biofilm infection of the epithelium (Anderson, Parks et al. 2013).

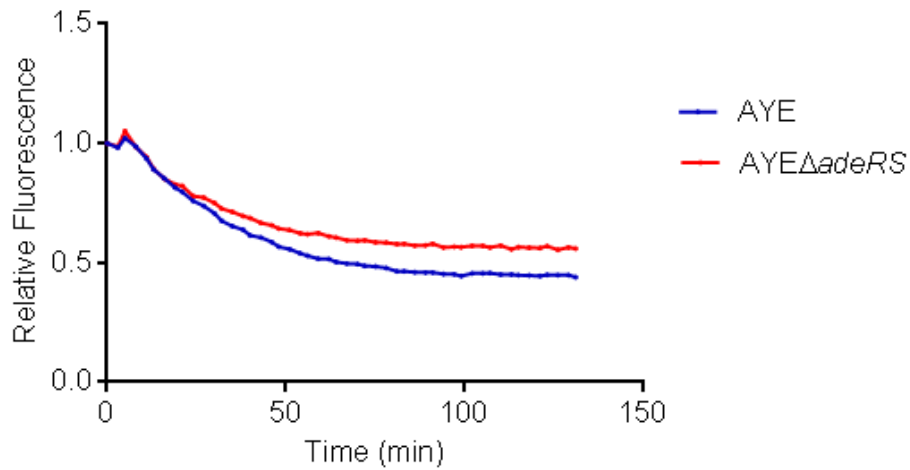
#### **3.5.5.1. Validation of a porcine vaginal mucosal (PVM) biofilm model**

*A. baumannii* ATCC 19606 has been shown to form a robust biofilm on both plastic and human skin equivalents (de Breij, Gaddy et al. 2009, Gaddy, Tomaras et al. 2009, de Breij, Haisma et al. 2012). Therefore, attachment of AYE and ATCC19606 cells to PVM was imaged over six days using LIVE/DEAD<sup>®</sup> staining and confocal laser scanning microscopy (Figure 3.5.4). The LIVE/DEAD<sup>®</sup> stain consists of SYTO9



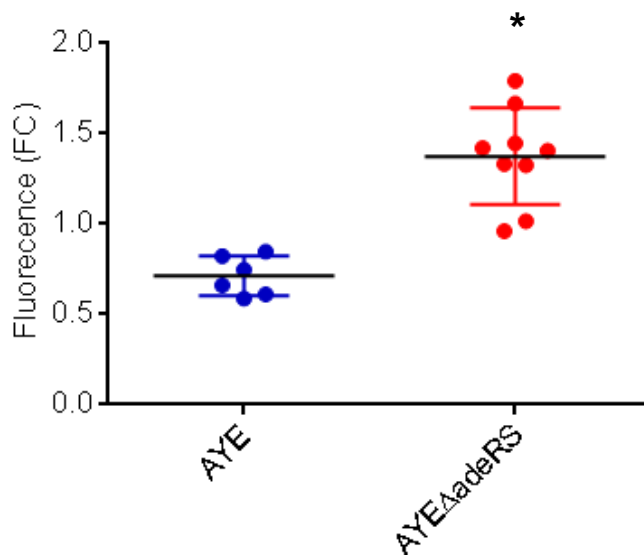
**Figure 3.5.3 Efflux of ethidium bromide by AYE and AYE $\Delta$ adeRS**

**A. Efflux of ethidium bromide by AYE and AYE $\Delta$ adeRS over time**



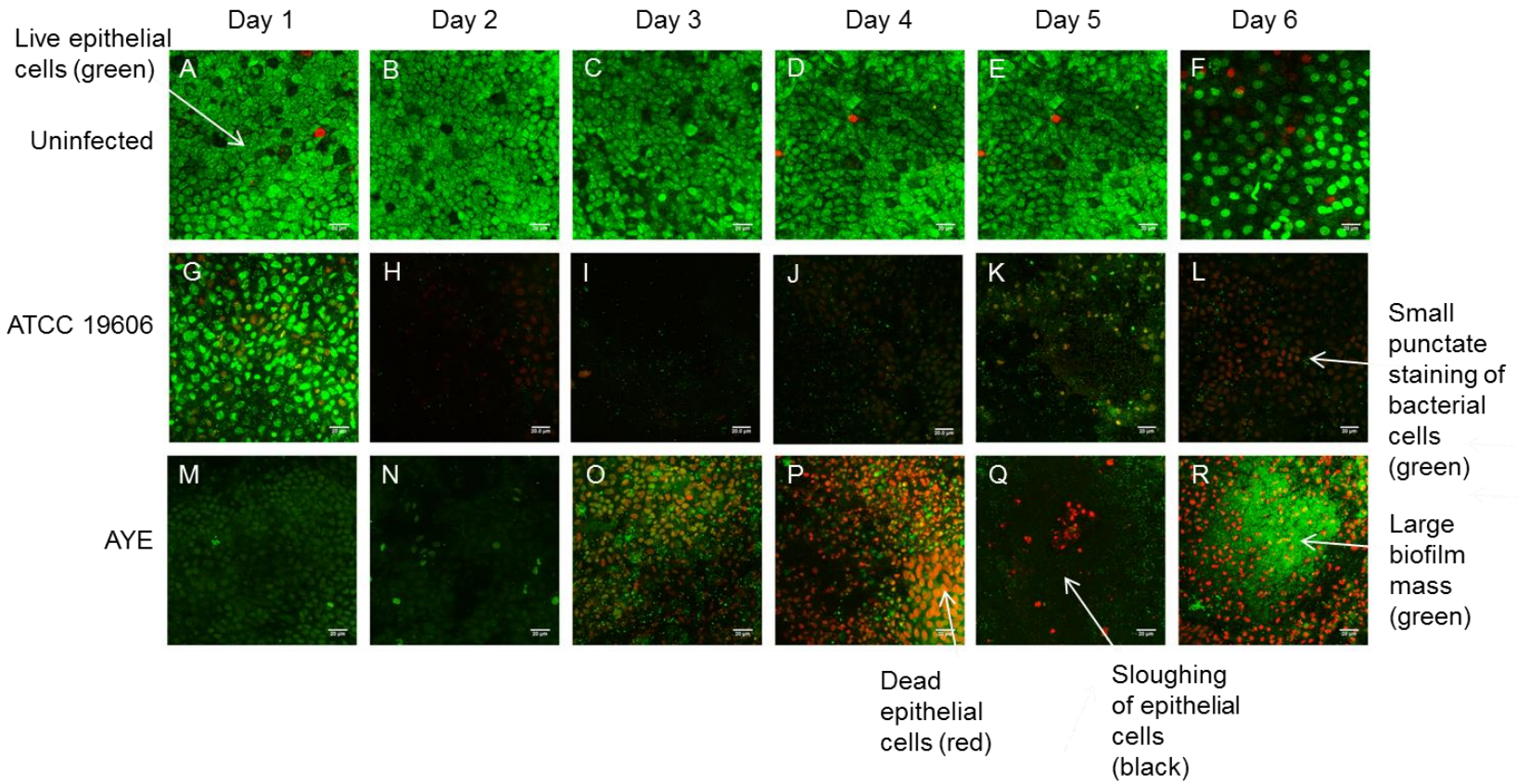
Data are shown as fluorescence relative to the starting fluorescence levels for each strain and represent the mean of three biological replicates. Data are a representative example of a single independent experiment carried out at least three times.

**B. Fold change in intracellular levels of ethidium bromide in AYE and AYE $\Delta$ adeRS**



Data are plotted as independent biological replicates to show variation within each strain. Data are presented as fold change in final fluorescence value compared to AYE +/- standard deviation. Student's t-tests were performed and those returning P values of less than 0.05 are indicated by \*.

**Figure 3.5.4 Confocal laser scanning microscopy of AYE and ATCC19606 biofilms using LIVE/DEAD® staining and visualised at 1-6 days**



Uninfected epithelia are live (green) and intact. Red, rounded epithelial cells indicate cell death. Small, punctate, green staining indicates bacterial cells and large, green staining masses indicate bacterial biofilm. Black areas depict exposed extracellular matrix. Arrows indicate examples of live and dead epithelial cells, bacterial cells, epithelial cell sloughing and biofilm masses.

which stains live cells green, and propidium iodide (PI), which stains dead cells red. PI only penetrates cells with damaged membranes and once in close proximity to the SYTO9 it quenches the green signal, so only the red is visible (<https://tools.thermofisher.com/content/sfs/manuals/mp10316.pdf>). This allows live versus dead cells to be detected. These dyes are non-specific nucleic acid dyes, which do not discern between prokaryotic and eukaryotic cells (Haimovich and Tanaka 1995, Anderson, Parks et al. 2013, Tsai, Lin et al. 2013, Li, Gorle et al. 2015). Epithelial and bacterial cells were distinguished from each other based on the size of the punctate staining, which could be clearly viewed by confocal microscopy, and the fact that the uninfected tissue, which had no bacteria present, stained green. Viability of the tissue at six days was confirmed by imaging of uninfected tissue over the same time course. Uninfected tissue stained green, indicating live, intact cells with tight cell junctions (Figure 3.5.4A-F). Over the six day time course, AYE and ATCC19606 showed a similar biofilm phenotype. At one day post infection, loss of mucosal integrity was evidenced by rounding of epithelial cells and adherent bacteria (small, bright green punctate staining) were visible on the tissue (Figure 3.5.4G&M). By three days post infection, epithelial cell death (red) was observed and the number of bacteria visualised was greater (Figure 3.5.4I&O). Black areas indicated sloughing of cells as the extra cellular matrix does not stain and some biofilm formation was visible with ATCC19606. By six days post infection, a large biofilm mass was visible for AYE and most of the tissue was covered by the biofilm (Figure 3.5.4R).

### **3.5.5.2. Biofilm formation by *AYEΔadeRS* on mucosal tissue**

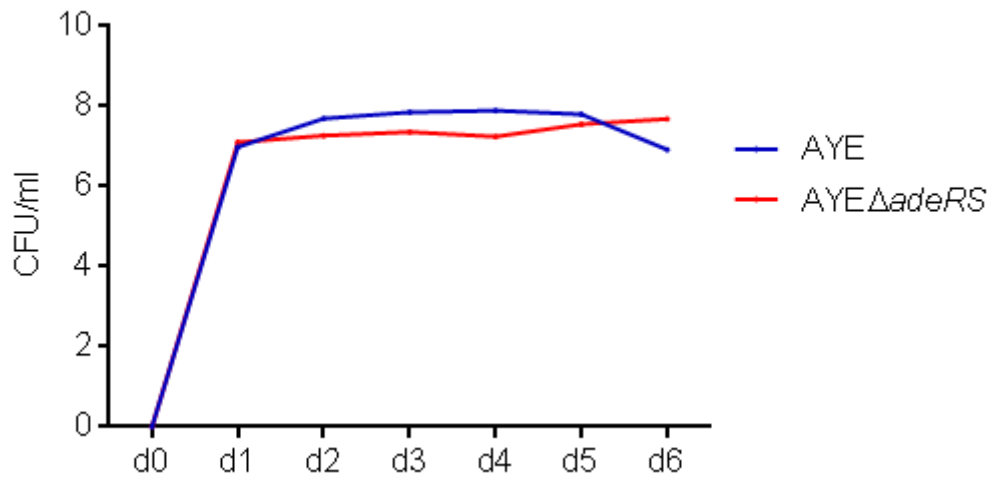
To investigate whether AdeRS is important for biofilm formation on biotic surfaces, growth of AYE and *AYEΔadeRS* on PVM was measured. Initial experiments were

carried out during a research visit to the University of Minnesota. Later experiments to confirm the phenotype were carried out by Michele Anderson (University of Minnesota). Counts of adherent and planktonic cells were taken at 24 hr time points up to 144 hours. There was a rapid increase in the number of adherent cells on PVM up to the one day time point, followed by a slow but steady increase between one and six days (Figure 3.5.5). There was no significant difference between numbers of adherent cells for AYE and AYE $\Delta$ *adeRS* at any time point (Figure 3.5.5). However, LIVE/DEAD<sup>®</sup> staining and confocal laser scanning microscopy showed a difference between the infection phenotype of AYE and AYE $\Delta$ *adeRS* (Figure 3.5.6). At three days post-infection, AYE infected tissue displayed epithelial cell death (Figure 3.5.6C) and by six days post-infection large biofilm masses and epithelial cell sloughing was visible, as described above (Figure 3.5.6F). However, for AYE $\Delta$ *adeRS*, although epithelial cell death was evident and the tissue exhibited some epithelial cell sloughing, in contrast to AYE infection, many dead epithelial cells remained visible. AYE $\Delta$ *adeRS* cells appeared as single attached cells with no biofilm observed (Figure 3.5.6L). These data suggest a critical role for AdeRS in mucosal biofilm infections and host cell cytotoxicity.

### **3.5.6. Biofilm formation *in vitro* by AYE $\Delta$ *adeRS***

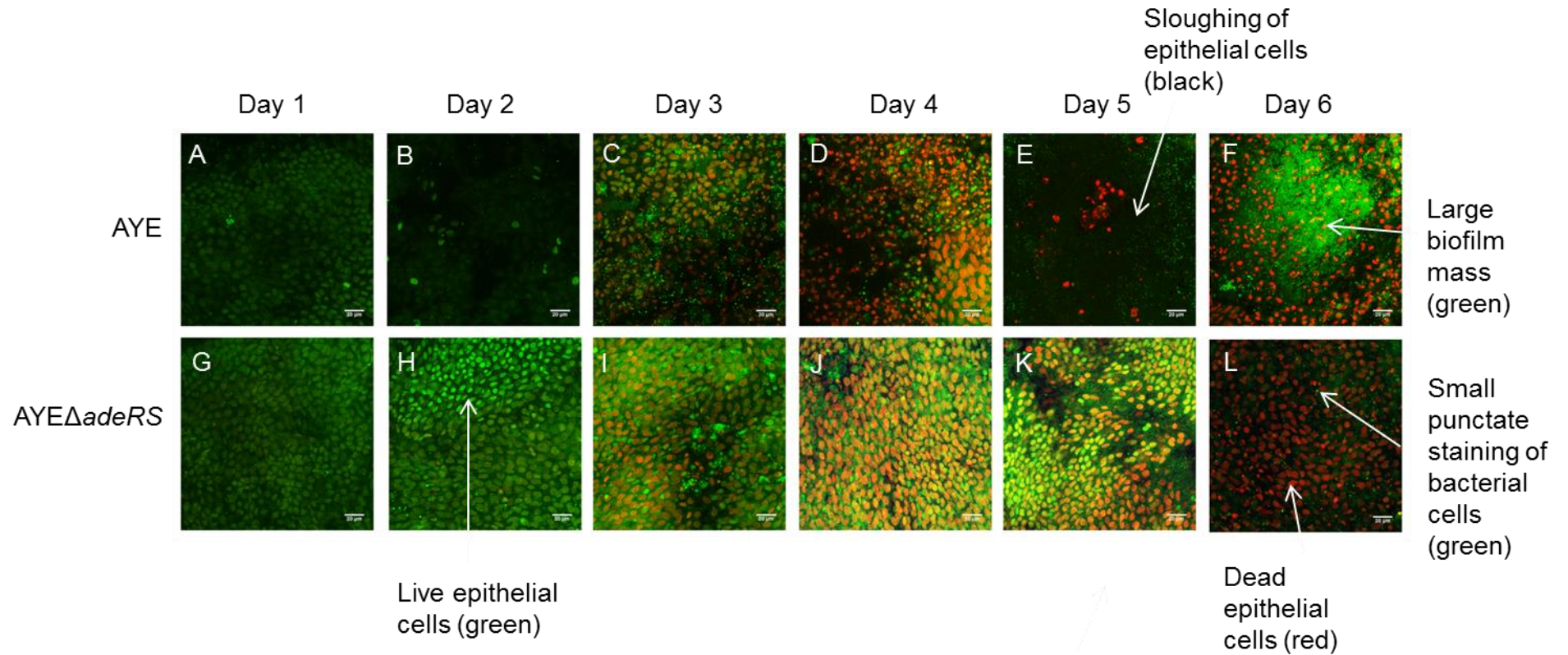
To determine whether lack of AdeRS conferred a change in biofilm formation on an abiotic surface, the parental strain AYE and *adeRS* deletion mutant were grown in four different *in vitro* models to measure biofilm; a microfluidic cell, polypropylene pegs, polystyrene test tubes and glass cover slips.

**Figure 3.5.5 Adherent and planktonic bacterial cells counts of AYE and AYE $\Delta$ adeRS grown at 37°C on PVM**



Data are shown as mean CFU/ml of three biological replicates and are representative of a single independent experiment carried out at least three times.

**Figure 3.5.6 Confocal laser scanning microscopy of AYE and AYE $\Delta$ adeRS biofilms using LIVE/DEAD<sup>®</sup> staining and visualised at 1-6 days**



Uninfected epithelia are live (green) and intact. Red, rounded epithelial cells indicate cell death. Small, punctate, green staining indicates bacterial cells and large, green staining masses indicate bacterial biofilm. Black areas depict exposed extracellular matrix. Arrows indicate examples of live and dead epithelial cells, bacterial cells, epithelial cell sloughing and biofilm masses.

### **3.5.6.1. Biofilm formation by AYE $\Delta$ adeRS in a microfluidic cell**

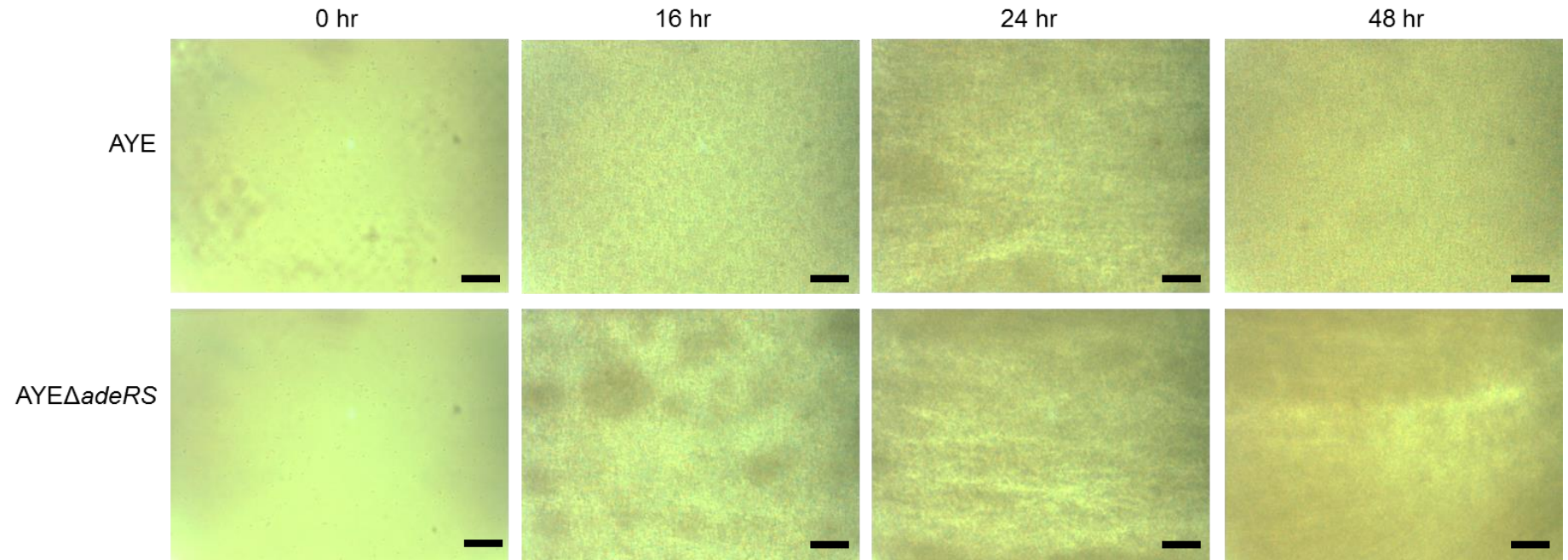
Biofilm formation by AYE and AYE $\Delta$ adeRS was studied under flow conditions in order to more closely mimic biofilm formation on a medical device implanted in the body. Infection with *A. baumannii* is often associated with indwelling medical devices, which can provide a surface for biofilm development (Rodríguez-Baño, Martí et al. 2008, Jung, Park et al. 2010). At 0 hrs, attachment of individual bacterial cells to the walls of the flow cell could be seen by phase microscopy (Figure 3.5.7). There was no difference in initial attachment of AYE and AYE $\Delta$ adeRS. Both AYE and the deletion mutant formed a robust biofilm after 16 hrs and rapid growth could be seen in this time period. Thick biofilm coverage of the surface of the microfluidic cell was observed at 16, 24 and 48 hrs. When compared visually, there was no difference in the biofilm formed by either strain at any time point.

### **3.5.6.2. Biofilm formation by AYE $\Delta$ adeRS on polypropylene pegs**

To quantify the amount of biofilm formed by AYE and AYE $\Delta$ adeRS after 8 hrs incubation, cells were grown in microtitre trays with polypropylene pegs submerged in the wells. This allows a biofilm to form on the peg at the air/liquid interface and previous experiments showed that at this time point AYE formed a similar biofilm to the previously characterised biofilm forming strain ATCC 19606. Plates were incubated at 30°C and 37°C to replicate wound and body temperature, respectively. Burns wards and operating theatres, where many patients become infected with *A. baumannii*, are also maintained at 37°C. Biofilms were quantified by crystal violet staining in order to compare biofilm mass between AYE and AYE $\Delta$ adeRS. In this *in vitro* model, when compared with the parental strain there was no change in biofilm mass produced by the *adeRS* deletion mutant at either 30°C or 37°C (Figure 3.5.8).



**Figure 3.5.7 Phase contrast microscopy images of AYE and AYE $\Delta$ adeRS biofilms formed under flow conditions of 0.3 dynes up to 48 hrs**

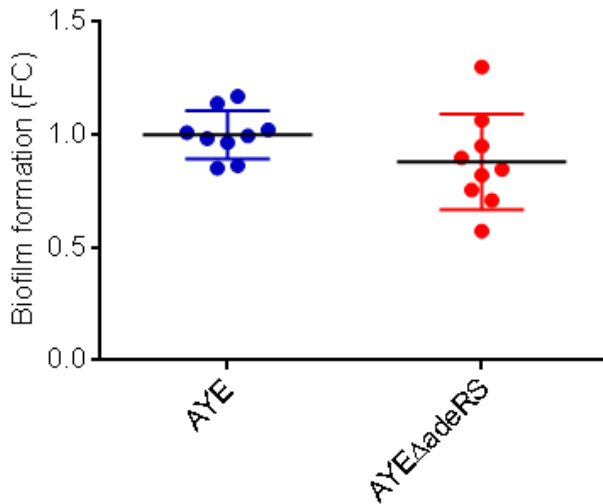


Images show attachment of bacterial cells to the inner surface of a microfluidic channel. Grey dots show adherence of individual cells to the surfaces whereas solid grey areas indicate bacterial growth and biofilm production. Black bar depicts a 10  $\mu$ m scale.



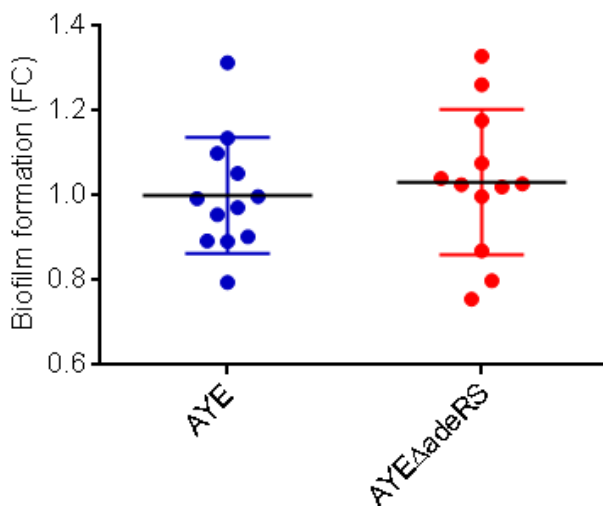
**Figure 3.5.8 Biofilm formation by AYE and AYE $\Delta$ adeRS on polypropylene pegs as determined by crystal violet staining**

**A. 30°C**



Data are plotted as independent biological replicates to show variation within each strain. Data are presented as fold change compared to AYE +/- standard deviation. Student's t-tests were performed and those returning P values of less than 0.05 are indicated by \*.

**B. 37°C**



Data are plotted as independent biological replicates to show variation within each strain. Data are presented as fold change compared to the parental strain +/- standard deviation. Student's t-tests were performed and those returning P values of less than 0.05 are indicated by \*.

### **3.5.6.3. Pellicle formation by *AYEΔadeRS***

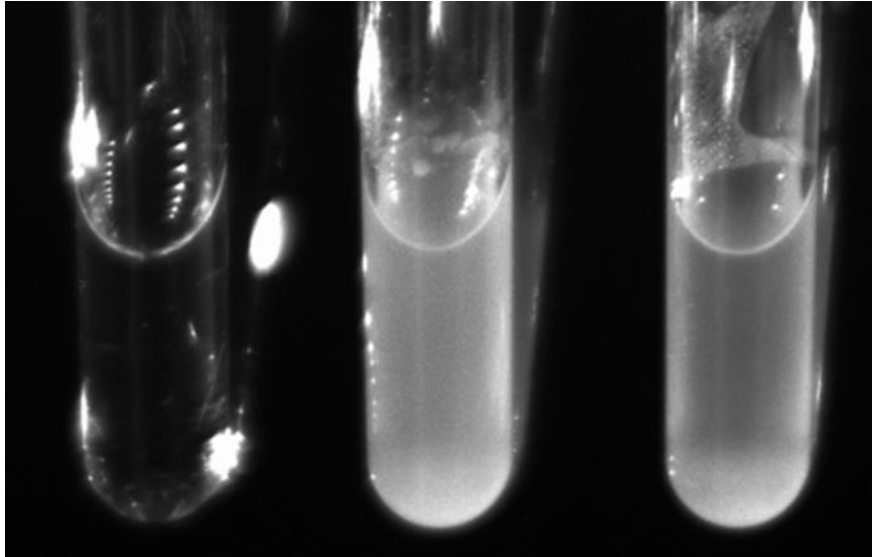
To assess the ability of *AYE* and *AYEΔadeRS* to form a pellicle at the air/liquid interface, cultures were incubated statically in polystyrene test tubes for 48 hours at 37°C. A thick biofilm mat could be seen at the surface with both strains. However, there was no difference in the amount of pellicle formed by *AYE* or *AYEΔadeRS* (Figure 3.5.9).

### **3.5.6.4. Biofilm formation by *AYEΔadeRS* on glass cover slips**

In order to visualise biofilms formed by *AYE* and *AYEΔadeRS* and to determine whether the two-component system (TCS) mutant was unable to adhere to abiotic surfaces or was adherent but unable to form a biofilm (as seen in the mucosal model) bacterial cultures were incubated on glass slides for 24 hrs before being fixed for scanning electron microscopy (SEM). Images obtained from the SEM showed an early biofilm formed by *AYE* with areas of complex three dimensional biofilm visible (Figure 3.5.10). Furthermore, an extracellular matrix (ECM) could clearly be seen in-between cells. *AYEΔadeRS* showed an altered biofilm phenotype compared with the parental strain *AYE*. Individual cells appeared attached to the glass cover slip but there was no clear biofilm formation (Figure 3.5.10). The coverage of the surface of the cover slip was more sparse after incubation with the mutant strain and no extracellular matrix was produced. This is in agreement with the phenotype observed in the mucosal biofilm model, in which the *adeRS* deletion mutant did not appear to form a mature biofilm. However, this difference was not seen in the other *in vitro* biofilm models used.

**Figure 3.5.9 Pellicle formation by AYE and AYE*adeRS* incubated statically at 37°C**

**A. Visualised under white light**



Negative

AYE

AYEΔ*adeRS*

**B. Visualised under natural light**

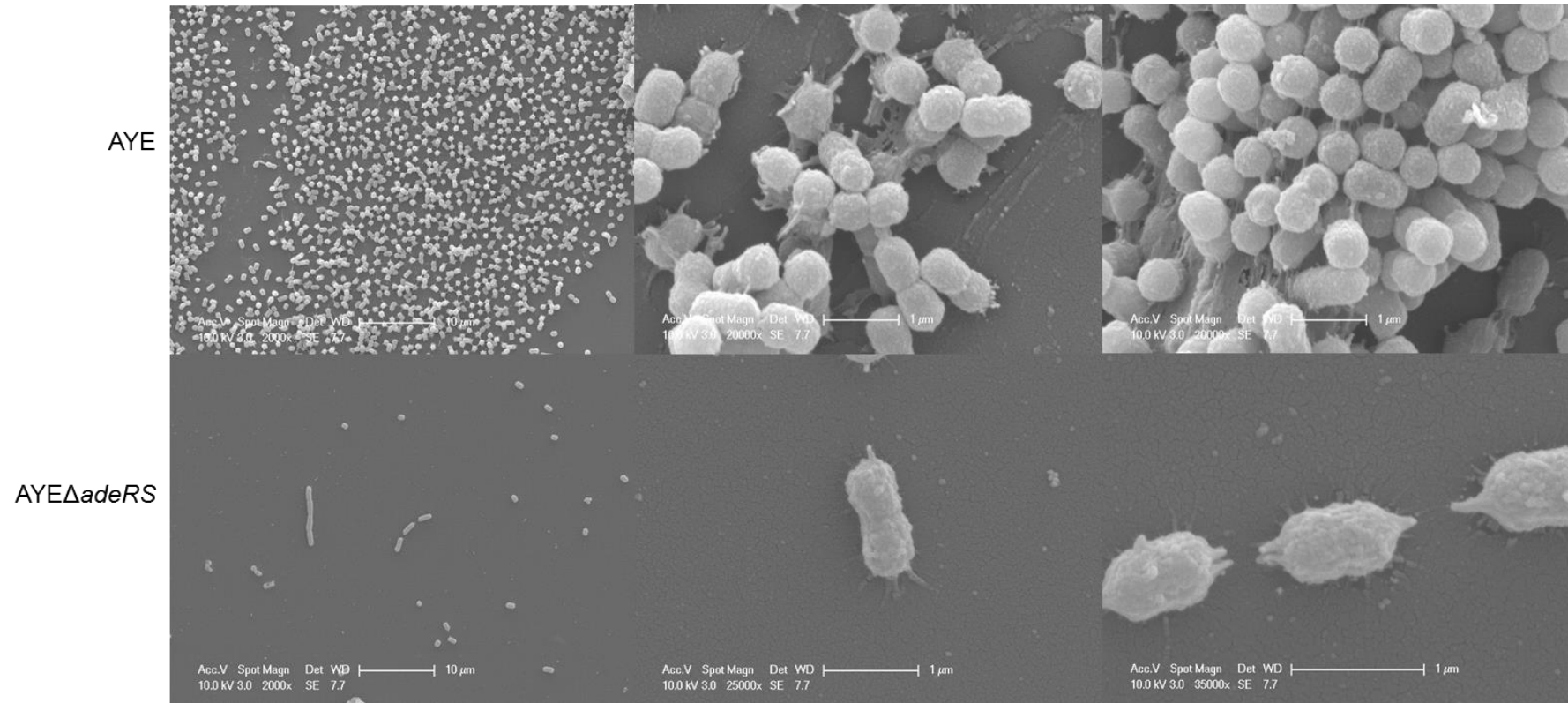


Negative

AYE

AYEΔ*adeRS*

Figure 3.5.10 Scanning electron microscopy of AYE and AYE $\Delta$ adeRS biofilms grown for 24 hrs on glass cover slips



Images show attachment of bacterial cells, production of ECM and formation of a biofilm on the surface of a glass cover slip.

### **3.5.7. Motility of *AYEΔadeRS***

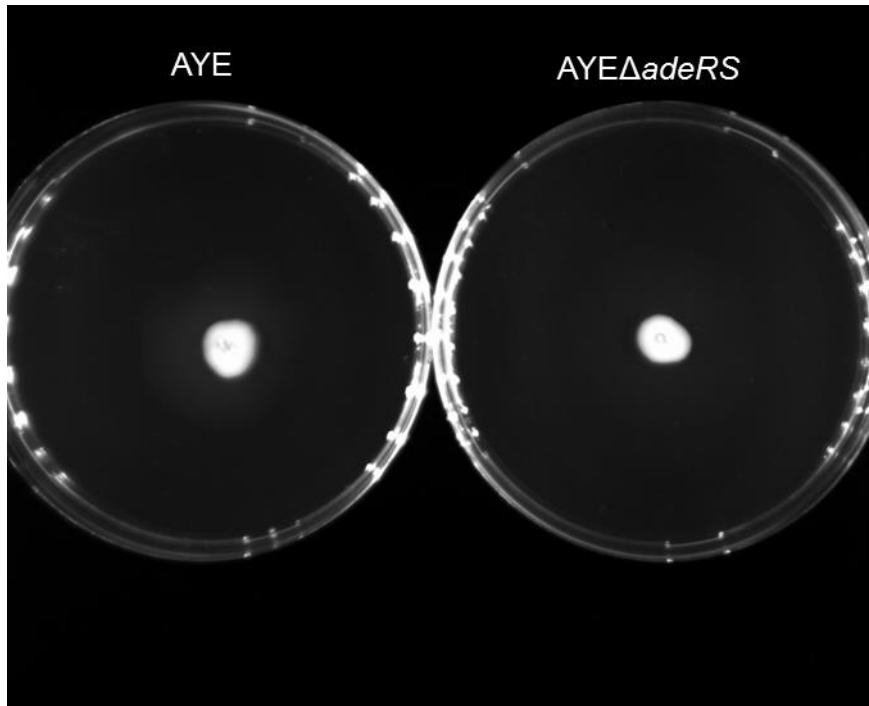
*A. baumannii* is generally considered to be non-motile due to its lack of flagella, but swarming and twitching motility have both been shown (Henrichsen 1975, Eijkelkamp, Stroehler et al. 2011, Skiebe, de Berardinis et al. 2012). AYE has been shown previously to display twitching motility but not swarming motility, typical of International Clone I (Eijkelkamp, Stroehler et al. 2011). To determine whether the AdeRS TCS is involved in the regulation of genes required for motility in AYE, twitching motility and swarming experiments were carried out with 1% Mueller Hinton agar and 0.3% Luria-Bertani agar, respectively (Figure 3.5.11). Strain AYE displayed twitching motility, but did not display swarming motility, as with the majority of *A. baumannii* strains. *AYEΔadeRS* did not display an altered twitching motility or swarming phenotype.

### **3.5.8. Virulence of *AYEΔadeRS* in the *G. mellonella* model of infection**

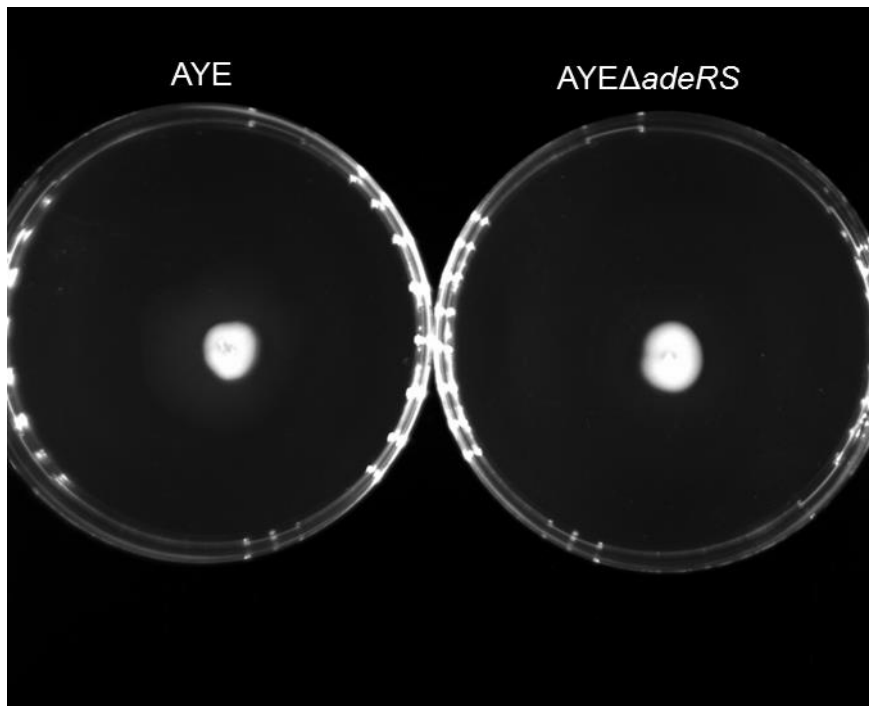
It was hypothesised that AdeRS regulates the expression of genes responsible for virulence in *A. baumannii* AYE. For example, it has been shown that MDR efflux pumps are required for infection by several other Gram negative bacterial species (Buckley, Webber et al. 2006, Nishino, Latifi et al. 2006, Kvist, Hancock et al. 2008, Padilla, Llobet et al. 2010, Matsumura, Furukawa et al. 2011, Baugh, Ekanayaka et al. 2012, Perez, Poza et al. 2012, Liao, Schurr et al. 2013, Baugh, Phillips et al. 2014). Previous studies have shown a positive correlation between virulence in the *G. mellonella* infection model and mammalian models (Jander, Rahme et al. 2000, Miyata, Casey et al. 2003). Furthermore, *G. mellonella* has been established as a

Figure 3.5.11 Twitching and swarming motility of AYE and AYE $\Delta$ adeRS grown on 1% and 0.3% agar for 24 hrs at 37°C

A. Twitching motility



B. Swarming motility

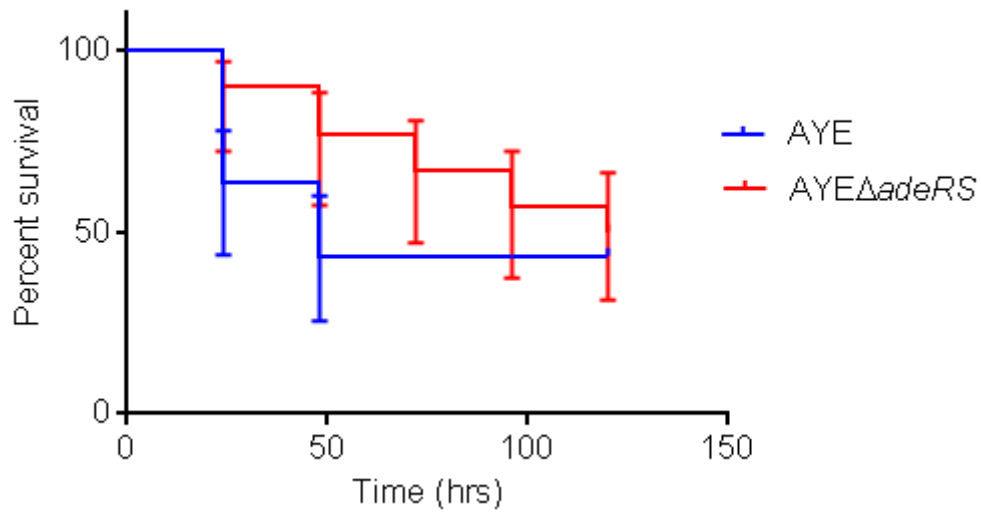


good model system to study *A. baumannii* pathogenesis as larvae can be maintained at 37°C and have both a cellular and humoral immune response (Peleg, Jara et al. 2009). In the *G. mellonella* model, when compared with the parental strain, AYE $\Delta$ *adeRS* showed a small but not statistically significant decrease in virulence at an infectious dose of 10<sup>6</sup> CFU (Figure 3.6.1).

### **3.6. Determining the transcriptome of AYE $\Delta$ *adeRS***

To identify changes in gene expression that may account for the difference in biofilm phenotype between AYE and AYE $\Delta$ *adeRS* and to understand the role of the TCS AdeRS in regulation of genes involved in antimicrobial resistance and virulence in *A. baumannii* strain AYE, RNA-Seq was carried out. This technology allows transcriptome profiling using DNA sequencing. A population of total RNA is converted to a library of cDNA fragments tagged with adaptors. Each molecule is then sequenced using high-throughput technology to obtain short sequences (reads) from one end (single-end sequencing) or both ends (pair-end sequencing). The reads are typically 30–400 bp, depending on the DNA-sequencing technology used and can be mapped to a reference genome. Gene expression levels can be deduced from the total number of reads that map to the gene (depth) (Wang, Gerstein et al. 2009). RNA was prepared in Birmingham and sent to ARK Genomics, Edinburgh for library preparation and sequencing. Three biological replicates per strain were sequenced on an Illumina HiSeq platform using single ended reads. Data were checked for quality and analysed by bioinformatics collaborator, Dr Alasdair Ivens (University of Edinburgh) and submitted to ArrayExpress (E-MTAB-4047). RNA samples were prepared and sequenced in two separate batches as a two samples sent in the first shipment produced poor quality sequencing data. Heat map plotting of gene

**Figure 3.6.1 Kaplan Meir survival curve to show virulence of AYE and AYE $\Delta$ adeRS in *G. mellonella***



Data show mean percentage survival (n=30) of *G. mellonella* after inoculation with  $10^6$  CFU bacteria. Error bars represent SEM.



expression changes in individual samples showed that samples prepared and sequenced at the same time clustered together (Figure 3.6.2). Deletion of the entire 1366 bp *adeS* gene and 126 bp of *adeR* was confirmed by the absence of reads mapping to this region of the genome in each *AYEΔadeRS* sample. *AYE* samples showed fairly low read depth (< 50) across *adeRS* with increased numbers of reads (read depth 100 – 2000) mapping across *adeABC* (Figure 3.6.3). This suggested a low level of expression of *adeRS* in the parental strain and high expression of the *adeABC* operon. *AYEΔadeRS* showed an absence of reads mapped to *adeS* and the 126 bp deleted region of *adeR* and very low read depth across *adeABC* (Figure 3.6.3). The absence of reads mapped to the deleted portion of *adeRS* demonstrated an absence of RNA transcribed from this region. Low read depth across *adeABC* suggested reduced expression of this operon compared with the parental strain. There was significantly less expression of *adeS* in *AYEΔadeRS* compared with *AYE* (Table 3.6.1, Table 3.6.2). There was no significant change in expression of *adeR*.

All gene expression changes in *AYEΔadeRS* compared with *AYE* were plotted by locus tag to easily identify highly differentially expressed genes or operons (Figure 3.6.4). The RND efflux pump operon *adeABC* showed a 128, 91 and 28-fold reduction in expression of each gene, respectively. Differential expression of operons encoding type IV pilus assembly, biogenesis and regulatory proteins such as *pilGHIJ*, *pilTU* and *pilBCD* was observed, with increased expression of up to 8-fold. These genes have previously been shown to be involved in twitching motility and natural transformation in *A. baumannii* (Antunes, Imperi et al. 2011, Harding, Tracy et al. 2013, Wilharm, Piesker et al. 2013). Type IV pili have also been associated with the ability of *A. baumannii* to form a biofilm on plastic (Tucker, Nowicki et al. 2014).

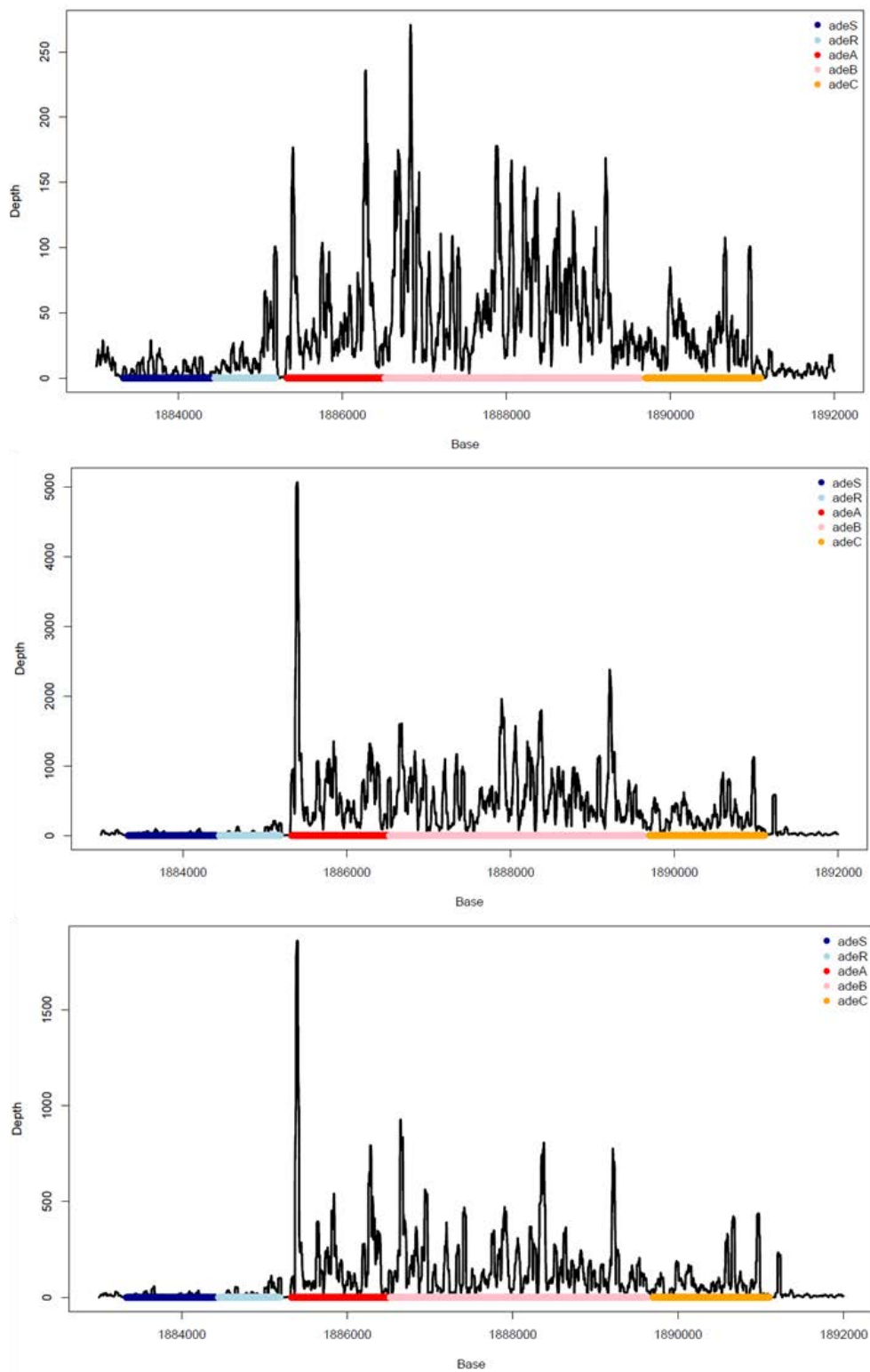
**Figure 3.6.2 Heat map plot of gene expression changes in 6 biological replicates (3 x AYE and 3 x AYE $\Delta$ adeRS) prepared and sequenced on different days**



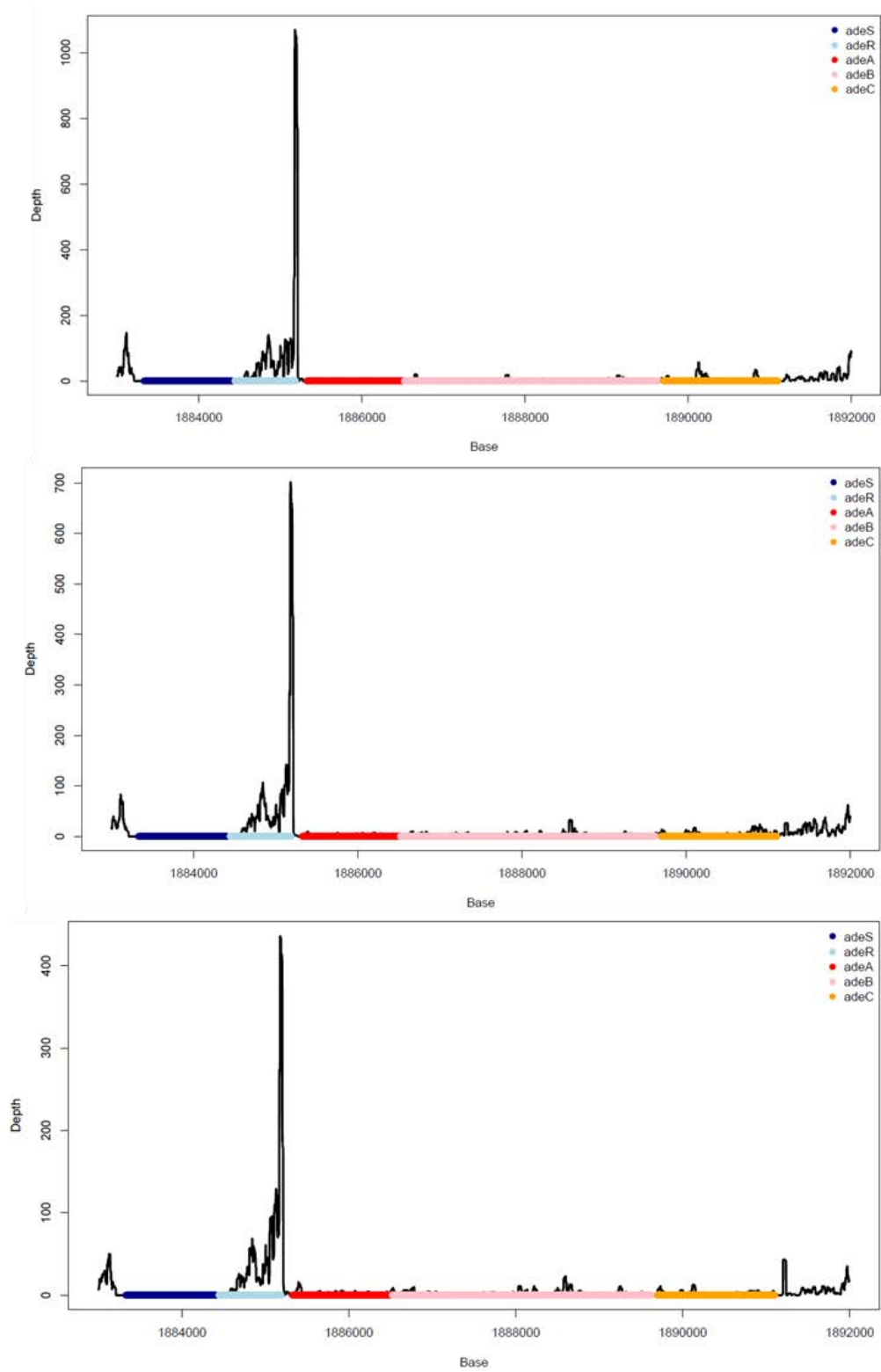
Samples AYE 1 and AYE 2 were prepared and sequenced as one set and samples AYE $\Delta$ adeRS 1-3 and AYE 3 were prepared and sequenced as another. Lines represent individual genes and the X axis represents the whole AYE chromosome.

Figure 3.6.3 Number of reads aligned to each base across the *adeRS adeABC* region in each AYE and AYE $\Delta$ *adeRS* sample

A. AYE



## B. $\Delta adeRS$



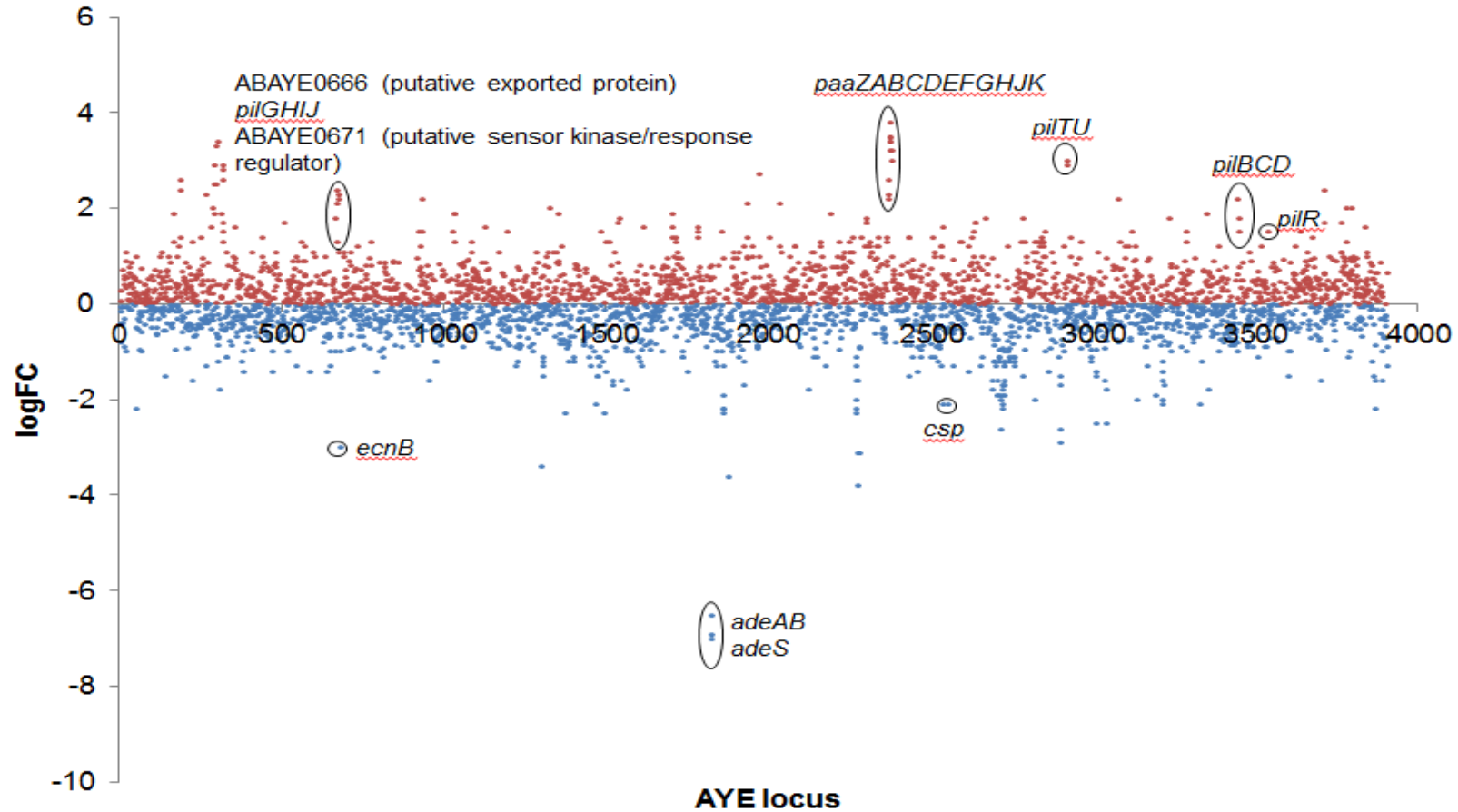
**Table 3.6.1 The top 10 genes with the most significantly changed expression in *AYEΔadeRS* compared with *AYE***

Gene ID	Start	End	Description	Common Name	Strand	Type	log2 fold change	Fold change	P.Value
ABAYE1819	1883328	1884413	two-component sensor	<i>adeS</i>	-	gene	-6.90	0.008	2.00E-07
ABAYE1822	1886521	1889631	RND protein	<i>adeB</i>	+	gene	-6.50	0.011	1.30E-05
ABAYE1821	1885325	1886524	membrane fusion protein	<i>adeA</i>	+	gene	-7.00	0.008	4.20E-05
ABAYE1823	1889696	1891105	outer membrane protein	<i>adeC</i>	+	gene	-4.80	0.036	5.60E-05
ABAYE3702	3735843	3736049	fragment of conserved hypothetical protein (partial)		-	pseudogene	-1.60	0.330	3.60E-04
ABAYE1474	1541855	1542541	putative glutathione S-transferase		+	gene	-1.30	0.406	3.60E-04
ABAYE1539	1603553	1604008	3-dehydroquinate dehydratase type II	<i>aroQ</i>	-	gene	1.80	3.482	4.40E-04
ABAYE1561	1626579	1626947	putative intracellular sulfur oxidation protein (DsrE-like)		-	gene	-1.80	0.287	4.70E-04
ABAYE2274	2318942	2319259	hypothetical protein		+	gene	-3.10	0.117	7.10E-04
ABAYE3074	3110289	3110585	hypothetical protein putative membrane protein		-	gene	2.20	4.595	8.50E-04

**Table 3.6.2 The top 10 genes with the largest fold change in expression in AYEΔadeRS compared with AYE**

Gene ID	Start	End	Description	Common Name	Strand	Type	log2 Fold change	Fold change	P.Value
ABAYE2369	2412094	2412888	enoyl-CoA hydratase phenylacetic acid degradation subunit of Phenylacetate-CoA oxygenase	<i>paaG</i>	-	gene	3.80	13.929	5.40E-02
ABAYE2374	2416037	2416351	phenylacetic acid degradation subunit of Phenylacetate-CoA oxygenase	<i>paaB</i>	-	gene	3.50	11.314	5.00E-02
ABAYE2372	2414752	2415252	phenylacetic acid degradation subunit of Phenylacetate-CoA oxygenase	<i>paaD</i>	-	gene	3.50	11.314	5.80E-02
ABAYE2373	2415269	2416024	phenylacetic acid degradation subunit of Phenylacetate-CoA oxygenase	<i>paaC</i>	-	gene	3.40	10.556	5.20E-02
ABAYE2370	2412885	2413658	enoyl-CoA hydratase phenylacetic acid degradation membrane fusion protein	<i>paaF</i>	-	gene	3.40	10.556	5.60E-02
ABAYE1821	1885325	1886524	two-component sensor	<i>adeA</i>	+	gene	-7.00	0.008	4.20E-05
ABAYE1819	1883328	1884413	RND protein	<i>adeS</i>	-	gene	-6.90	0.008	2.00E-07
ABAYE1822	1886521	1889631	ABAYE_16s_5	<i>adeB</i>	+	gene	-6.50	0.011	1.30E-05
ABAYE_16s_5	487461	488915	ABAYE_16s_5		+	rRNA	-4.90	0.033	3.00E-02
ABAYE1823	1889696	1891105	outer membrane protein	<i>adeC</i>	+	gene	-4.80	0.036	5.60E-05

Figure 3.6.4 Log2 fold change in expression of all genes of the AYE genome in AYEΔadeRS compared with AYE



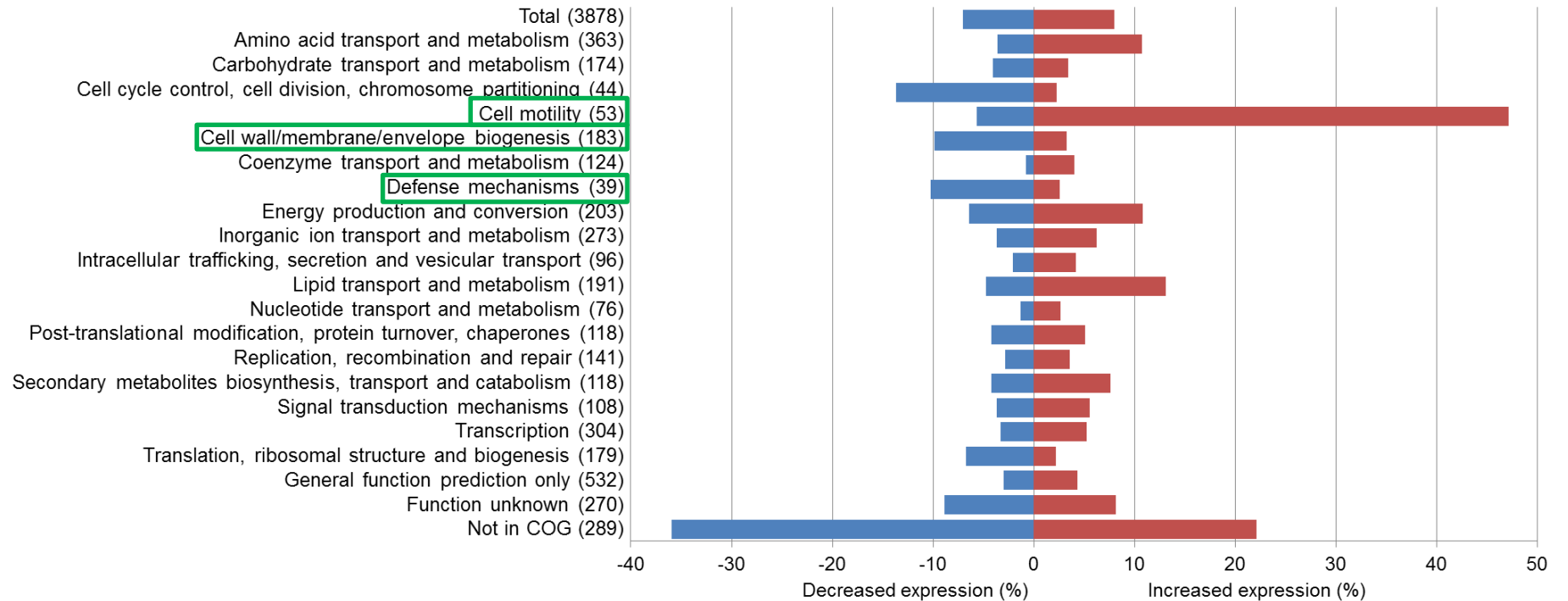
Genes with increased and decreased expression are coloured red and blue, respectively. Gene names or annotations are provided for genes within differentially expressed operons or highly differentially expressed genes with known function.

Increased expression of the *paaZABCDEFGHJK* operon was also seen. This operon encodes the PAA catabolic pathway which is important in the catabolism of several aromatic compounds. It has been shown previously that expression of this operon is regulated by the sensor kinase *GacS*, part of the *GacSA* two component system (Cerqueira, Kostoulis et al. 2014). Interestingly, deletion of *gacS* resulted in down-regulation of the *paa* operon, whereas deletion of *adeRS* in the present study gave increased expression of up to 14-fold. Deletion of *paaE* by Cerqueira *et al.* showed a role for this operon in virulence in *A. baumannii* (Cerqueira, Kostoulis et al. 2014).

A raw P value cut-off of 0.05 was used to produce a list of significantly changed genes (Table 3.6.1, Table 3.6.2). The raw P value was chosen as opposed to the more stringent adjusted P value as this gave a more comprehensive list of changed genes that may affect the phenotype and ensured that no genuinely changed genes would be excluded from the list. There were 308 genes with increased expression and 271 with decreased expression in *AYEΔadeRS* compared with *AYE* indicating a wide ranging impact that results from loss of this system. Differentially expressed genes were categorised into cluster of orthologous groups (COGs) (Tatusov, Galperin et al. 2000) and correlations with the phenotypic changes seen in *AYEΔadeRS* sought (Figure 3.6.5). Firstly, differential expression of genes known to confer antimicrobial resistance was identified. In addition to increased expression of the RND efflux pump genes *adeABC*, genes encoding four ethidium bromide resistance proteins (*ebr*) and chloramphenicol resistance protein A (*cmIA*) showed increased expression of 1.6- fold and a tetracycline resistance protein (*tetA*) had 1.3-fold increased expression. One putative MDR RND efflux pump (ABAYE3036) had 1.9 fold increased expression, whilst expression of another (ABAYE1796) was



**Figure 3.6.5 Clusters of orthologous groups (COG) and the percentage of genes with increased expression (red) and decreased expression (blue) in *AYEΔadeRS* compared with *AYE* within each group as determined by RNA-Seq**



The total number of genes per COG is shown in parentheses. Groups related to antibiotic resistance, biofilm formation and virulence are marked by a green box.

decreased by 1.5 fold. Genes encoding products with known and potential virulence functions, such as pili (Bahar, Goffer et al. 2009) and acinetobactin transport systems (Gaddy, Arivett et al. 2012), had significant ( $P < 0.05$ ) changes in expression levels in *AYEΔadeRS*. For instance, there was increased expression of genes that encode motility, such as competence genes *comB*, *comC*, *comF*, *comL*, *comM*, *comN* *comO* and *comQ* (2.5 – 9.8-fold). These genes putatively encode DNA uptake channels and deletion of *comEC* in *A. baumannii* has been shown to reduce DNA uptake, motility and virulence in *G. mellonella* (Wilharm, Piesker et al. 2013). There was also increased expression of *pilB*, *pilC*, *pilD*, *pilG*, *pilH*, *pilI*, *pilJ*, *pilT*, *pilU* and *pilZ* (1.7 – 8-fold). As previously mentioned, these type IV pili genes play a role in natural transformation, twitching motility, biofilm formation and virulence. The *pil* and *com* genes were categorised into the ‘cell motility’ group by COG annotation. This was the largest group of changed genes in *AYEΔadeRS* by RNA-Seq with 47% of all motility genes showing decreased expression. Changed biofilm genes include decreased expression of a PgaC-like gene (2-fold) that putatively encodes a protein involved in synthesis of cell-associated poly-beta-(1-6)-N-acetylglucosamine (PNAG), which is required for biofilm formation on abiotic surfaces (Choi, Slamti et al. 2009) and decreased expression of five putative biofilm associated genes; ABAYE0792, 1395, 1397, 1470, 1473 (1.7-2.5-fold). In addition, multiple putative transport protein, outer membrane protein and transcriptional regulator genes that lacked a comprehensive annotation showed differential expression.

### **3.7. Discussion**

This work was carried out using an *adeRS* deletion mutant of strain AYE and the phenotype presented has been interpreted as the result of lack of both proteins of the

two component system AdeRS. However, as such a small part of *adeR* was deleted it is possible that part of the gene is still transcribed and a truncated protein may be produced. Mapping of RNA-Seq reads to the *adeRS* operon showed that in *AYEΔadeRS* there were no reads mapped to the deleted sequences; however there was a large peak in expression at the beginning of *adeR*. It is hypothesised that this is a result of the cell sensing low levels of AdeRS and attempting to increase production; this could result in truncated AdeR with no or reduced function being produced. This may be induced by the increased levels of AdeABC or changed levels of other proteins whose expression is regulated by AdeRS in the mutant. It is possible that AdeR, the response regulator, can receive a signal from a sensor kinase other than AdeS (West and Stock 2001). If a truncated, but functional, AdeR protein is produced in *AYEΔadeRS* it may be that some AdeR activity is retained. However, this is unlikely as protein domain prediction indicated that 27 amino acid of the signal receiver domain was deleted. Western blotting would allow detection of the AdeR protein by separating proteins from *AYEΔadeRS* using gel electrophoresis and staining for AdeR using specific antibodies. However, currently no such antibodies are available. Using an alternative method, Sun *et al.* were able to demonstrate constitutive production of a truncated AdeS protein in an *A. baumannii* clinical isolate and by introducing a series of recombinant *adeRS* constructs into an *adeRS* knockout strain, showed that the truncated product interacted with AdeR and stimulated expression of AdeABC (Sun, Perng et al. 2012). Ideally, a mutant in which the entire two component system operon *adeRS* is deleted should be used. However, due to the technical difficulties in genetically manipulating *A. baumannii*, particularly MDR strains such as AYE, this study was continued with the mutant

obtained. A previous study by Marchand *et al.* showed that deletion of *adeR* produced a very similar change in drug resistance profile as seen with deletion of *adeS* in *A. baumannii* (Marchand, Damier-Piolle *et al.* 2004). However, as these genes are transcribed as an operon, it is possible that disruption of *adeR* may have a polar effect on *adeS*, which is located downstream. This phenomenon would explain the similar phenotype seen in *adeR* and *adeS* mutants.

Since the RNA-Seq experiments described here were carried out (August 2012), RNA-Seq protocols have been revised and bacterial RNA-Seq now uses paired end reads as these generate high-quality, alignable sequence data (Rumbo-Feal, Gómez *et al.* 2013). The clustering of RNA samples prepared on the same day demonstrates the variability in data generated from samples prepared on different days and sequenced on different runs and highlights the need to standardise as much of the procedure as possible in experiments of this kind. RNA extraction and library preparation of samples from the same strain should be carried out on the same day and all samples should be sequenced in a single run so as to minimise variation.

The hypothesis explored was that AdeRS regulates expression of genes, including the RND MDR efflux pump genes *adeABC*, that are required for drug resistance, biofilm formation and virulence. In *A. baumannii* BM4587, a clinical isolate from France that has been extensively characterised by the Courvalin group, AdeABC has a well-defined role in resistance to antimicrobials. Characterisation of isogenic mutants overproducing or deleted for Ade pumps showed that AdeABC had a broad substrate range, including  $\beta$ -lactams, fluoroquinolones, tetracyclines-tigecycline, macrolides-lincosamides, and chloramphenicol, and conferred clinical resistance to aminoglycosides (Magnet, Courvalin *et al.* 2001, Yoon, Courvalin *et al.* 2013, Yoon,

Nait Chabane et al. 2015). Deletion of *adeRS* in AYE resulted in decreased MICs of the same antibiotics, leading to the conclusion that the decrease in expression of *adeABC* in *AYEΔadeRS* is responsible for the change in drug resistance profile seen in this strain. This is in agreement with previous studies to inactivate *adeR* and *adeS* in clinical isolate BM4454, which also led to susceptibility to substrates of the AdeABC efflux pump (Marchand, Damier-Piolle et al. 2004). However, it should be noted that, due to the vast range of antibiotic resistance mechanisms present in *A. baumannii*, determination of MICs of pump deletion mutants of MDR isolates may not be the best way to identify the substrates of an efflux pump. Background resistance due to a complex set of resistance determinants such as  $\beta$ -lactamases and aminoglycoside-modifying enzymes means that the effect of deletion of efflux pump genes may be masked. The observed decrease in efflux activity in *AYEadeRS* supports the hypothesis that the increase in susceptibility to the antimicrobials tested in AYE lacking AdeRS is due to down regulation of AdeABC and therefore reduced efflux. The decrease in efflux activity means that substrates of the pump are not extruded as efficiently and therefore accumulate inside the cell and are lethal at lower external concentrations. The H33342 efflux assay measures accumulation of dye in the cell and has been shown to provide greater sensitivity in measuring efflux than some other methods (Coldham, Webber et al. 2010). However, not only is intracellular accumulation affected by efflux, but it is also influenced by other factors such as changes in membrane permeability caused by altered production of outer membrane porins (Coldham, Webber et al. 2010). Therefore, efflux activity can only be inferred by this assay as it is not being directly measured. For this reason a second efflux assay, using ethidium bromide, was used. In this method, cells are

'pre-loaded' with ethidium bromide and efflux of the dye is observed by measuring the decrease in fluorescence over time. This method measures efflux in a more direct manner. Data obtained with H33342 and ethidium bromide indicate lower levels of efflux in the *adeRS* mutant.

The *adeRS* mutant displayed reduced biofilm formation on mucosal tissue. Although there was no change in the number of adherent cells on the mucosal tissue with deletion of *adeRS*, there was a clear difference in the structure of the biofilm when imaged with LIVE/DEAD<sup>®</sup> staining and confocal laser scanning microscopy. This is a phenomenon that has been previously observed with *Staphylococcus aureus* (Anderson, Lin et al. 2012). This suggests that AdeRS does not affect initial attachment to the tissue but that cells lacking this TCS are unable to form a mature biofilm on mucosal tissue. This was supported by SEM imaging of biofilms formed on glass cover slips. AYE was able to form a complex biofilm with visible extracellular matrix present, whereas the *adeRS* deletion mutant was not. As described above, there were 16 genes associated with biofilm formation with differential expression in *AYEΔadeRS* compared with AYE. Although these genes have previously only been associated with biofilm formation on abiotic surfaces, it is possible that these changes, along with the down-regulation of the RND efflux pump genes *adeABC*, may be responsible for the decreased biofilm formation on PVM observed in this mutant. Similar observations have been made in *Salmonella* efflux pump mutants, which are able to adhere to surfaces but not able to produce a mature biofilm (Baugh, Ekanayaka et al. 2012). MDR efflux pumps of the RND family have also been shown to be required for virulence and biofilm formation in several other Gram negative bacterial species (Buckley, Webber et al. 2006, Nishino, Latifi et al. 2006,

Kvist, Hancock et al. 2008, Padilla, Llobet et al. 2010, Matsumura, Furukawa et al. 2011, Baugh, Ekanayaka et al. 2012, Perez, Poza et al. 2012, Liao, Schurr et al. 2013, Baugh, Phillips et al. 2014). In *Salmonella*, inactivation or deletion of MDR efflux genes led to down-regulation of known virulence factors and genes involved in biofilm formation (Webber, Bailey et al. 2009, Baugh, Ekanayaka et al. 2012). PVM is made up of stratified squamous epithelium, similar in structure to human mucosal surfaces (Anderson, Parks et al. 2013). However, as *A. baumannii* most commonly colonise respiratory surfaces and wounds, this may not provide the most relevant surface on which to study *A. baumannii* infection. The surface of the vaginal mucosa is moist due to secretions from glands of the cervix and this may affect the biofilm ability of the strains tested here. Despite this, the growth characteristics of *A. baumannii* on the PVM were similar to those observed using a 3D human skin equivalent model (de Breij, Haisma et al. 2012). Therefore, differences in the ability of the *A. baumannii* TCS mutant, *AYEΔadeRS*, to form a biofilm in the PVM model may have implications for respiratory and wound infections. Nevertheless, the mucosal biofilm model also has limitations. In order to count cells and visualise biofilms, explants must be washed and stained. Therefore, a different explant must be used each day. This means that the biofilm imaged on day two is not a direct development of the biofilm visualised on day one. Variation between explants due to size, location and tissue damage during preparation is possible. To minimise this variation, each experiment was conducted using a single animal and explants of uniform size were obtained from the porcine vagina using a standard 5 mm biopsy punch. In addition, the mucosal tissue is colonised with normal flora when excised and has to be washed with a combination of antibiotics and anti-fungals to remove

any contaminating elements. Although measures were taken to ensure that there was no effect on viability of the tissue with washing, it is possible that this may have had an adverse effect on epithelial cells. Further limitations of the PVM model are the lack of blood supply, which would allow for influx of immune cells to the site of infection, and the inability to study biofilm dispersal as the model is static in nature (Anderson, Lin et al. 2012, Anderson, Parks et al. 2013, Anderson, Scholz et al. 2013).

### **3.8. Further work**

To confirm that there is no production of the AdeS protein and determine whether the AdeR protein is produced (despite a 126 bp fragment of the gene being deleted) in AYE $\Delta$ *adeRS* Western blotting should be carried out. In order to do this, antibodies against AdeR and AdeS need to be generated. This method would show the presence or absence of the AdeR and AdeS proteins and confirm that deletion of the gene abolishes production of the TCS. It is possible that deletion of a single one of the two components of this system produces a different phenotype to the other. Inactivation of AdeS should remove the ability of the cell to sense certain extracellular signals, but not its ability to initiate a response and inactivation of AdeR should remove the ability to initiate a response but not the ability to sense extracellular signals. If another sensor kinase or response regulator were able to take the place of AdeS or AdeR, respectively, then TCS function may be retained. To give a complete picture of the role of the individual components of the AdeRS regulatory system, deletion mutants of *adeR* and *adeS* only and a double *adeRS* mutant should be made in AYE and their phenotype characterised and compared to that of the mutant described in this study. It should also be noted that these genes are



transcribed as an operon and therefore deletion of *adeR* may have a downstream effect on expression of *adeS*.

The limitations of the method used for RNA-Seq have been discussed. RNA-Seq of the new single and double mutants should be repeated using paired end reads. Steps should be taken to minimise variation between samples, for example all RNA extractions should be performed on the same day and samples should be sequenced on the same run. To improve the robustness of the data, more biological replicates should be used. A recent study by Schurch *et al* recommended that at least 6 replicates per condition are used for RNA-Seq experiments (Schurch, Schofield et al. 2015).

AdeRS is a two component system regulator. These systems allow bacteria to regulate their internal environment in response to extracellular signals. However, the nature of the signal and the mechanism of AdeRS activation are unknown (Marchand, Damier-Piolle et al. 2004). TCSs have previously been shown to respond to stress conditions such as antibiotic exposure, acid stress and starvation in other organisms (Elabed, Merghni et al. 2016, Kellogg and Kristich 2016, Liu, Liu et al. 2016). To identify the extracellular signals that AdeRS responds to, AYE and *AYEΔadeRS* should be grown in different conditions such as varying iron, osmolarity, temperature and antibiotic stress. Those conditions at which the AdeRS deletion mutant shows a growth defect compared with the parental strain may reflect the extracellular signals that are sensed by this two component system. In addition, RNA-Seq of the parental strain AYE under different iron, osmolarity, temperature and antibiotic stress conditions should be carried out to identify conditions under which

*adeABC* is differentially expressed. This may indicate conditions under which the AdeRS TCS is activated, altering expression of the AdeABC efflux pump genes.

### **3.9. Key findings**

- Deletion of AdeRS in *A. baumannii* strain AYE resulted in decreased MICs of antibiotics and dyes due to a reduction in efflux activity.
- An AdeRS deletion mutant of *A. baumannii* strain AYE displayed decreased biofilm formation and epithelial cell killing in a mucosal model.
- Deletion of AdeRS in *A. baumannii* strain AYE produced changed expression of 579 genes including several genes involved in drug resistance, biofilm formation and virulence.

## **4. The Role of the RND Efflux Pump AdeB in Antibiotic Resistance, Biofilm Formation and Virulence**

### **4.1. Background**

Increased expression of MDR efflux pump genes such as the *Acinetobacter* RND efflux pump genes *adeABC* leads to MDR and is commonly seen in clinical isolates of *A. baumannii* (Marchand, Damier-Piolle et al. 2004, Yoon, Courvalin et al. 2013). Multi-drug efflux systems have previously been associated with biofilm formation and virulence in a number of organisms using various models (Kvist, Hancock et al. 2008, Matsumura, Furukawa et al. 2011, Baugh, Ekanayaka et al. 2012, Liao, Schurr et al. 2013, Yoon, Nait Chabane et al. 2015). As described in Chapter 3 deletion of *adeRS* in AYE resulted in a decrease in MICs of several antibiotics that have been previously described as substrates of this pump and a decrease in biofilm formation (Magnet, Courvalin et al. 2001, Yoon, Nait Chabane et al. 2015). To investigate whether the decreased expression of *adeABC* observed in *AYEΔadeRS* was responsible for the phenotype seen in this strain, an AdeB efflux pump mutant was created in AYE and the phenotype characterised. To determine whether the observed phenotype was strain-specific, a second efflux pump mutant in Singaporean clinical isolate S1 was also characterised.

### **4.2. Hypothesis**

Deletion of *adeB* will result in a decrease in antibiotic resistance, biofilm formation and virulence and will alter the transcriptome in *A. baumannii*.

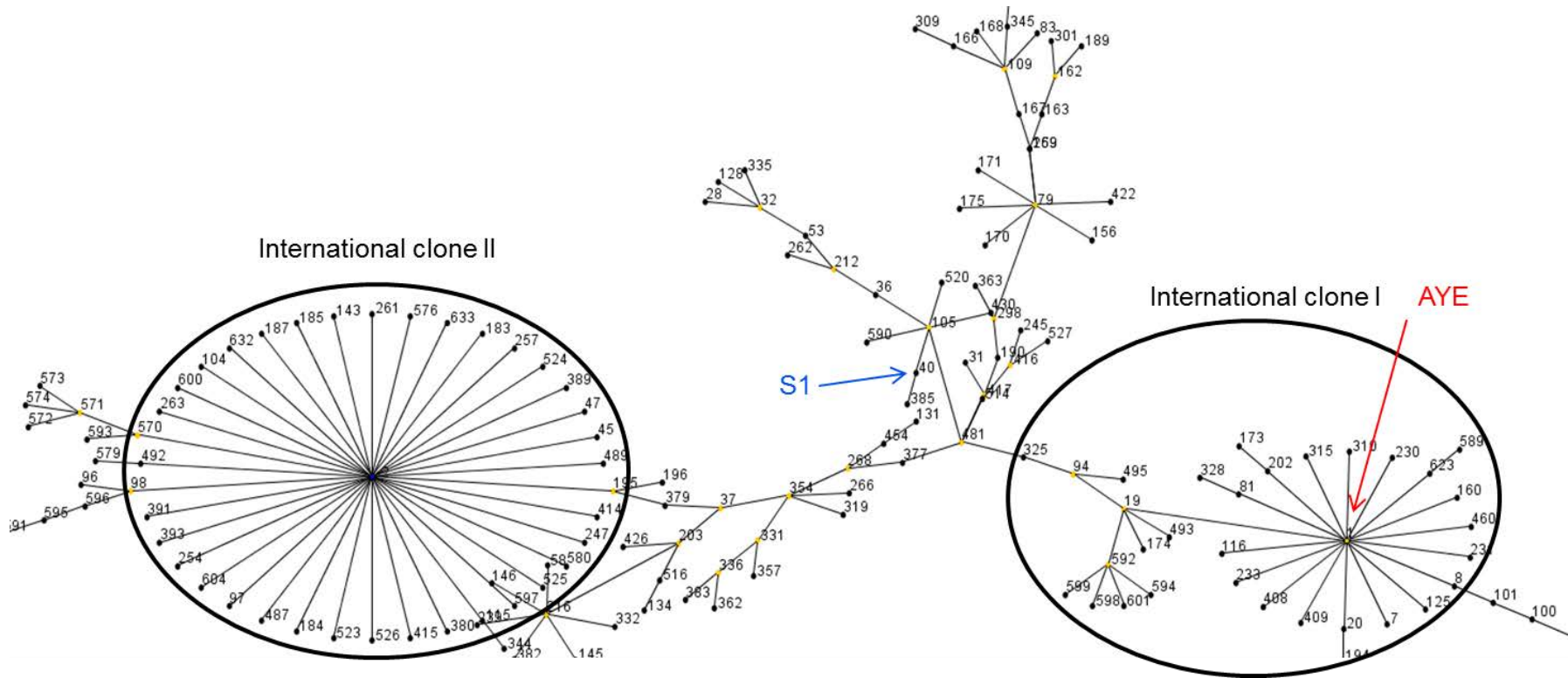
### **4.3. Aims**

The aim of this study was to identify the consequences of deletion of *adeB* in *A. baumannii* strain AYE and clinical isolate S1, respectively. The objectives were to use a novel gene deletion method to delete *adeB* in strain AYE, to characterise the antibiotic resistance, biofilm formation and virulence phenotype of deletion mutants *AYEΔadeB* and *S1ΔadeAB* and to use RNA-Seq to identify transcriptomic changes in these strains.

### **4.4. Choice of strains and verification of strains**

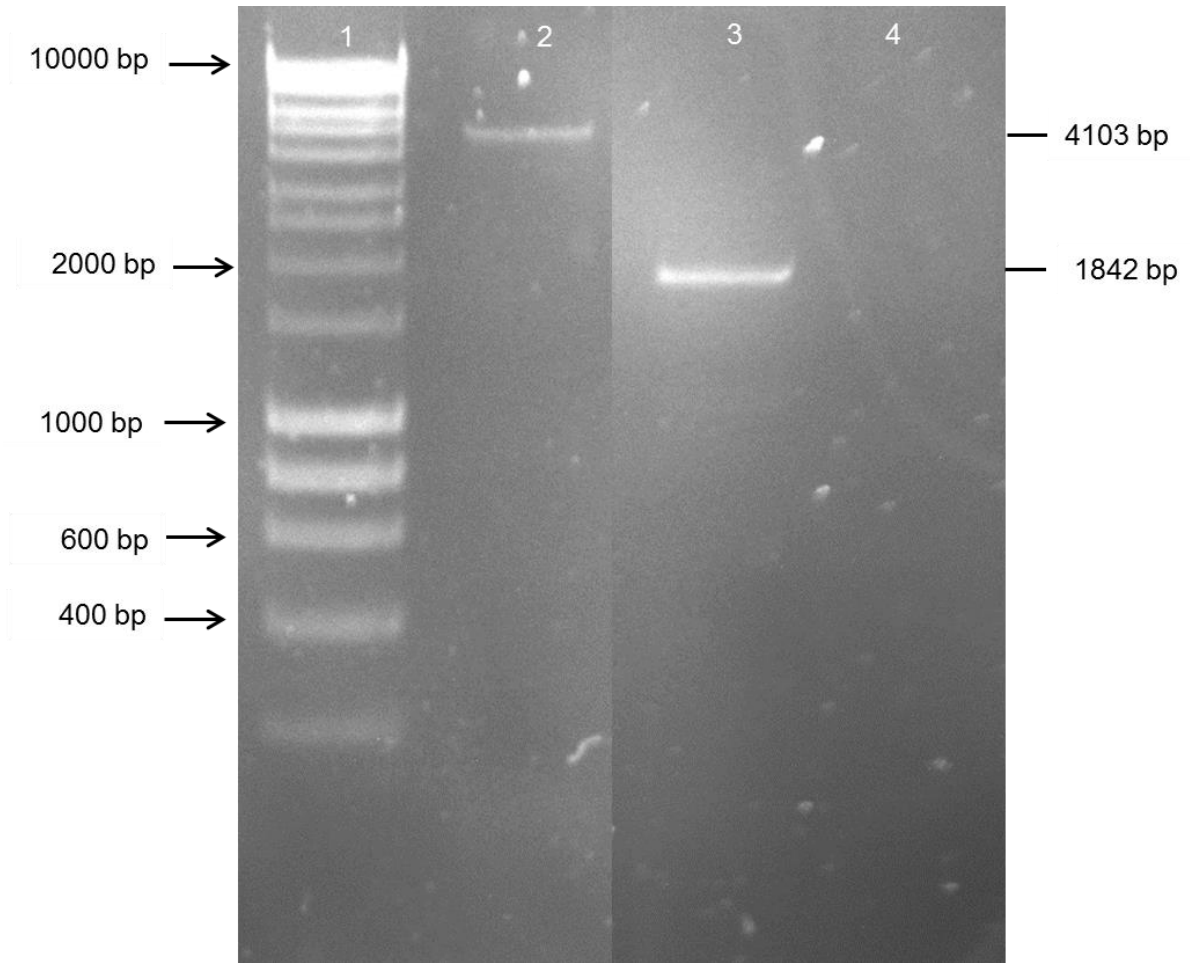
The reasons for using *A. baumannii* AYE are discussed in Chapter 3. A clinical isolate from Singapore, S1, that was more susceptible to antibiotics than strain AYE and had no mutation in *adeS* and therefore did not express a high level of *adeABC*, was also studied. Together these strains represent clones that are internationally successful (strain AYE is ST 1 of International clone I and S1 is ST40 and representative of strains causing infection in SE Asia) (Koh, Tan et al. 2012) (Figure 4.4.1). Deletion of 222 bp of *adeA* and 1914 bp of *adeB* in S1 to create the *S1ΔadeAB* mutant was carried out and verified by Professor Kim Lee Chua (National University of Singapore) using a markerless deletion method (Amin, Richmond et al. 2013). Deletion was confirmed in Birmingham by amplification of the deleted region by PCR (Figure 4.4.2). Amplification of the region in S1 produced a 4103 bp amplicon, whereas amplification in *S1ΔadeAB* produced a 1842 bp amplicon, confirming deletion of a 2261 bp fragment spanning the last 222 bp of *adeA*, the first 1914 bp of *adeB* and a 125 bp intergenic region. To predict how much of the AdeA and AdeB proteins were removed by deletion and to illustrate which part of the protein remained and may still be functional, I-TASSER protein modelling software

Figure 4.4.1 Relationships between 615 *A. baumannii* isolates based on MLST data (Pasteur scheme) as calculated by the BURST algorithm



Circles indicate major international groups. AYE is marked in red and S1 is marked in blue.

**Figure 4.4.2 Verification of *adeAB* gene deletion in S1 by PCR**



Lane	Template	Predicted fragment size (bp)	Actual fragment size (bp)
1	Hyperladder 1kb	-	-
2	S1	4103	4103
3	<i>S1ΔadeAB</i>	1842	1842
4	Negative control	0	0

Although all PCR products were electrophoresed on the same gel; the figure has been constructed from a single image to show only those strains relevant to this study.

was used. Deletion of 222 bp of *adeA* removed the last 74 amino acids of the AdeA protein (Figure 4.5.1). Deletion of 1914 bp of *adeB* removed the first 638 amino acids of the AdeB protein including the predicted AdeC binding domain and transmembrane helices (Figure 4.5.1). Deletion of *adeB* in AYE was jointly carried out in this study at University of Birmingham and Public Health England, Porton Down. All strains used in this study were confirmed as *A. baumannii* using a *gyrB* PCR as described in Chapter 3.

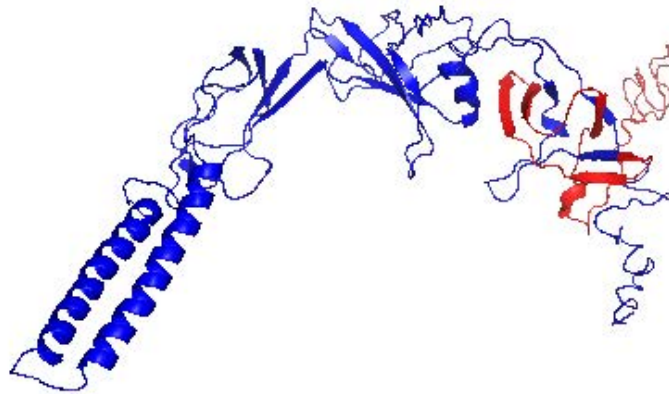
#### **4.5. Optimisation of the gene deletion method and deletion of *adeB* in AYE**

To delete the *adeB* gene in *A. baumannii* strain AYE, a modified version of a markerless deletion method was used (Amin, Richmond et al. 2013). *E. coli* S17-1 containing a modified version of the pMo130-TelR suicide vector was created by Matthew Wand (PHE) and sent to Birmingham (Figure 4.5.2). This vector contained an *A. baumannii* *groES* promoter driving a modified *sacB* gene with an *A. baumannii* *ompA* leader sequence replacing the *Burkholderia*-originated leader sequence in the original vector (Matthew Wand, unpublished data). The vector backbone also contained upstream and downstream fragments of the AYE *relA* gene, which were later removed sequentially to maintain the BamHI restriction site between the two fragments.

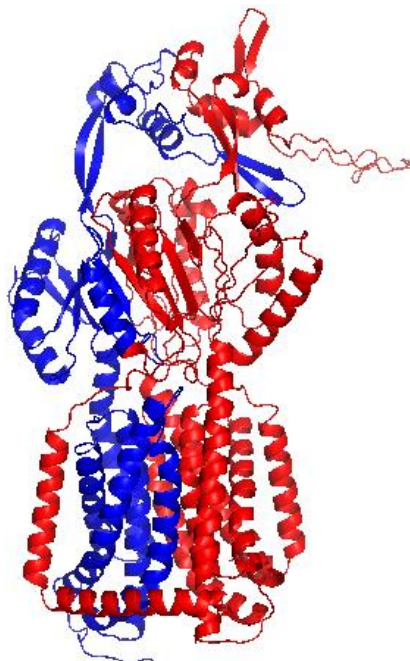
Primers were designed to amplify 855 bp and 874 bp fragments upstream (UP) and downstream (DWN) of the region of *adeB* to be deleted (Table 2.2.1). UP primers were designed with NotI and BamHI restriction sites and DWN primers were tagged with BamHI and SphI restriction sites. A 1131 bp region from position 995 to position

**Figure 4.5.1 Predicted protein structure of AdeA and AdeB in S1 $\Delta$ adeAB**

AdeA



AdeB

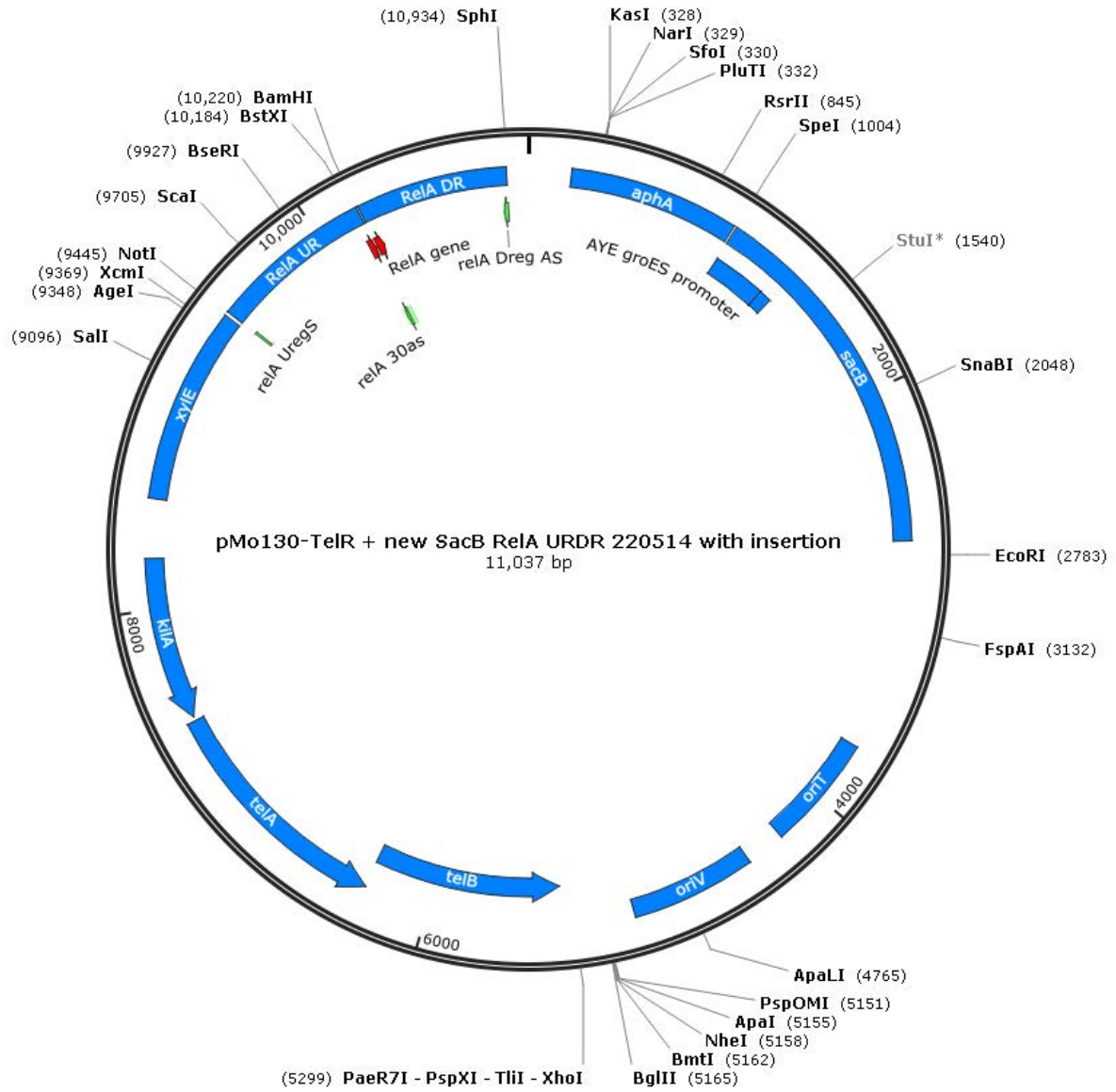


Amino acids for which the coding sequence was deleted are highlighted in red.



**Figure 4.5.2 pMo130-TelR suicide vector containing a *groES* promoter driving a modified *sacB* gene with AYE *relA* up and down fragments**

Created with SnapGene®



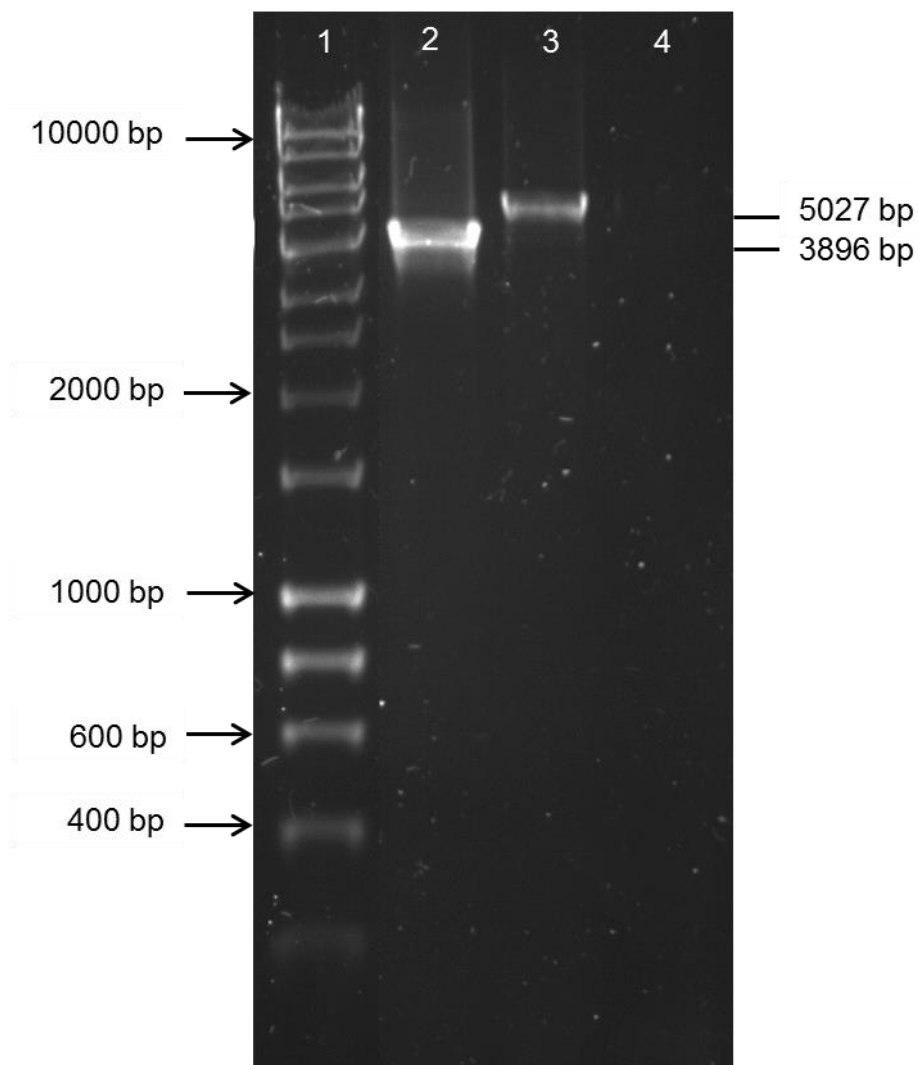
2126 was deleted in order to inactivate the gene whilst avoiding disrupting the genes upstream and downstream. However, it was noted that as *adeABC* is transcribed as an operon it was possible that transcription of *adeC* could be affected by deletion of a fragment of *adeB*. The pMo130-TelR vector was digested with NotI and BamHI restriction enzymes to excise the *relA* UP fragment and the *adeB* UP fragment was ligated into the digested plasmid. pM0130-TelR-*adeB*UP was then transformed into  $\alpha$ -Select Electrocompetent Cells and the presence of the *adeB* UP fragment was confirmed by amplification of the UP fragment by colony PCR. Following this, the vector was digested with BamHI and SphI restriction enzymes to excise the *relA* DWN fragment and the *adeB* DWN fragment was ligated into the digested plasmid. The vector was then transformed into *E. coli* S17-1, verified by PCR and conjugated into *A. baumannii* AYE. Ligation of the DWN fragment and conjugation of the plasmid into AYE was carried out by Laura Bonney at PHE. After conjugation, candidate colonies containing the pMo130-TelR-*adeB*UPDWN vector integrated into the chromosome were streaked onto LB agar and those displaying a yellow halo, indicating presence of the *xylE* gene integrated onto the plasmid, were selected and streaked onto LB agar containing 10% sucrose. XylE converts pyrocatechol to a yellow-colored 2-hydroxymuconic semialdehyde (Amin, Richmond et al. 2013). Presence of sucrose in the medium stimulated loss of the plasmid as a result of SacB activity. The *sacB* gene encodes levansucrase, which can catalyse sucrose hydrolysis followed by levan synthesis. When the *sacB* gene is expressed in Gram-negative bacteria the production of levansucrase is lethal in the presence of sucrose (Gay, Le Coq et al. 1985). This resulted in colonies containing the UP and DWN

region of the *adeB* gene with the fragment in-between deleted by double recombination.

#### **4.5.1. Verification of *adeB* deletion in AYE**

Deletion of *adeB* was verified by amplification of the deleted region by PCR and sequencing of the PCR amplicon (Figure 4.5.3). Amplification of the region in AYE produced a 5027 bp amplicon, whereas amplification in AYE $\Delta$ *adeB* produced a 3896 bp amplicon, confirming deletion of a 1131 bp fragment in the centre of the *adeB* gene (Figure 4.4.2A). Sequencing using the UP forward primer confirmed deletion of a region of *adeB* beginning at the 3' end of the UP fragment and sequencing using the DOWN reverse primer confirmed that this deletion ended at the 5' end of the DOWN fragment, as expected (Figure 4.4.2B). To predict which region of the AdeB protein was removed by this deletion, I-TASSER protein modelling software was used. Deletion of 1131 bp in the centre of the gene removed 377 amino acids which spanned the length of the predicted protein structure and included areas of the predicted AdeC binding domain and transmembrane helices (Figure 4.5.4).

**Figure 4.5.3 Verification of *adeB* gene deletion in AYE by PCR and DNA sequencing**



Lane	Template	Predicted fragment size (bp)	Actual fragment size (bp)
1	Hyperladder 1kb	-	-
2	<i>AYEΔadeB</i>	3896	3896
3	AYE	5027	5027
4	Negative control	0	0

Although all PCR products were electrophoresed on the same gel; the figure has been constructed from a single image to show only those strains relevant to this study.

## B. Alignment of the AYE *adeB* sequence with upstream sequencing data for AYEΔ*adeB*

```

AYE      AAAATGGTAAGCCTGCTACCGCGGCTGCAATTCAATTAAGCCCGGGAGCTAACGCCGTGA
AYEadeB AAAATGGTAAGCCTGCTACCGCGGCTGCAATTCAATTAAGCCCGGGAGCTAACGCCGTGA
*****

AYE      AAAC T GCCGAAGGTGTTTCGAGCAAAAATTGAAGAATTGAAGCTAAATTTACCGGAAGGCA
AYEadeB AAAC T GCCGAAGGTGTTTCGAGCAAAAATTGAAGAATTGAAGCTAAATTTACCGGAAGGCA
*****

AYE      TGGAAATTTAGTATTCCTTACGACACCGCGCGTTTGTCAAATTTCAATTGAAAAGGTAA
AYEadeB TGGAAATTTAGTATTCCTTACGACACCGCGCGTTTGGATCCTGAAGGGTTGCCACAGGTT
***** * * * *

AYE      TTCATACATTACTTGAAGCCATGGTTCTGGTTTTTCATTGTGATGTA--TCTATTTTACA
AYEadeB ACAATATTTCTT--TAAAAATTGACCGTGAAAAGCTTAGTGCACCTGGTGTTAAGTTTC
    * * * * * * * * * * * * * * * *

AYE      CAATGTCCGCTATACGCTTATTCAGCAATTGTGGCGCCTATTGCCTTACTCGGTACTTT
AYEadeB TGATGTTTCAGACATCATCTCTACATCAATGGGTTCATGTA--TATCAATGACTTCCCT
    * * * * * * * * * * * * * * * *

AYE      TACCGTGAITGGTTGCCGGCTTTTCAATTAACGTACTCACCATGTTTCGGT----ATGG
AYEadeB AA---TCAAG-----GACGTATGCAACAAGTCATTTACAAGTTGAGGCTAAATCA
    * * * * * * * * * * * * * * * * * *

```

Sequences were aligned using Clustal Omega. \* indicates a position with a single, fully conserved residue. The *adeB* gene is highlighted in yellow and the deleted region is highlighted in blue.

## B. Alignment of the AYE *adeB* sequence with downstream sequencing data for AYEΔ*adeB*

```

AYE      ATCTTTC AATTGCATACGTGATTTAGCCTCAACTTG TACAATGACTTGTGCATACGTCC
AYEadeB ATCTTTC AATTGCATACGTGATTTAGCCTCAACTTG TACAATGACTTGTGCATACGTCC
*****

AYE      TTGATTAGGGAAGTCATTGATATACATTGAACCCATTGATGTAGAGATGATGCTGAAAC
AYEadeB TTGATTAGGGAAGTCATTGATATACATTGAACCCATTGATGTAGAGATGATGCTGAAAC
*****

AYE      ATCAGAAA AACTTAACACCAAGTGC ACTAAGCTTTTCACGGTCAATTTTAAAGAAATATT
AYEadeB ATCAGAAA AACTTAACACCAAGTGC ACTAAGCTTTTCACGGTCAATTTTAAAGAAATATT
*****

AYE      GTCACCTTGTGGCAACCCTTCAATTC CAAACCATATAGAACTTTTATTCTTGGC--TGC
AYEadeB GTCACCTTGTGGCAACCCTTCAAGGATCCACGGCGTGGTGTCTGTAAGGAATACTAAATTC
***** * * * * * * * *

AYE      CAT---TGCCATAAGTTCATCTTGAGCAGC--CAATAAAGCAGG---CATACCTAAGT
AYEadeB CATGCCTTCCGGTAAATTTAGCTTCAATTTCTCAATTTTGTCTCGAACACCTTCGGCAGT
    * * * * * * * * * * * * * * * *

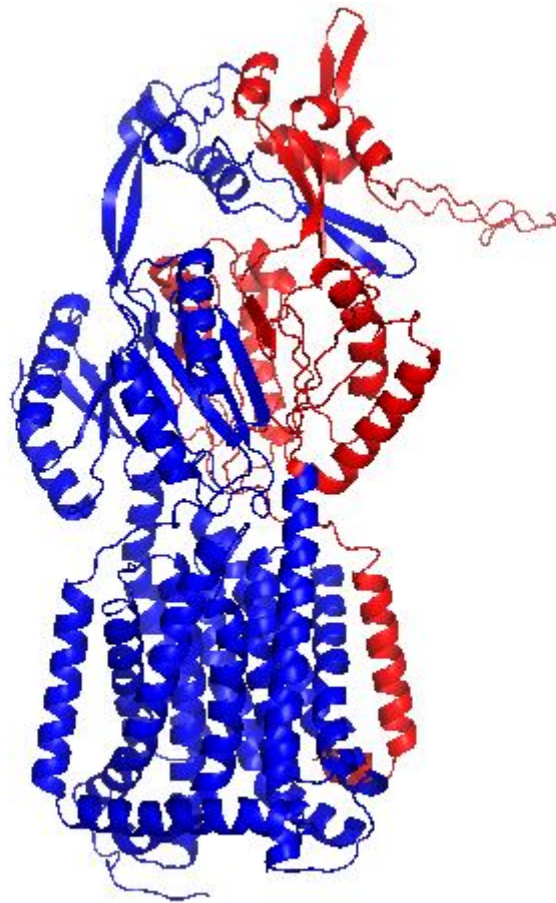
AYE      TAGCACGGTCTTGTAAACGTAGGCTGAAACCTGAAAAAGTACCTAACTCATCAATAGCGG
AYEadeB TTTACGGGTTAGCTCCCGG-GCTTAATTGAATTGCAGCCGGTAGCAGGCTTACCAT
    * * * * * * * * * * * * * *

AYE      GTGGTAAACGGCCATGGTCTCGCCTTCCG TACTGTTCCGCATAGAAGAATTAACGTCCG
AYEadeB TTTCCAAAATGGCAAAGTTATATGCTTGTGAACCTATTTCTACATGGCAACATCAGATA
    * * * * * * * * * * * * * *

```

Sequences were aligned using Clustal Omega. \* indicates a position with a single, fully conserved residue. The *adeB* gene is highlighted in yellow and the deleted region is highlighted in blue.

**Figure 4.5.4 Predicted protein structure of AdeB in *AYEΔadeB***



Amino acids for which the coding sequence was deleted are highlighted in red.

## **4.6. Determining the phenotype of an *A. baumannii* AYE mutant lacking AdeB and an S1 mutant lacking AdeAB**

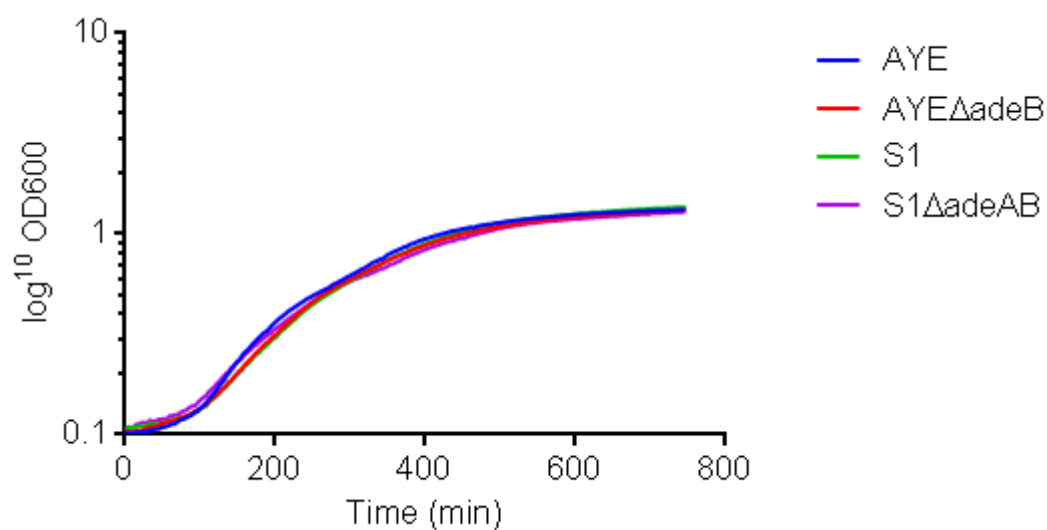
### **4.6.1. Bacterial growth kinetics of *AYEΔadeB* and *S1ΔadeAB***

To ensure that there was no growth defect in either *AYEΔadeB* or *S1ΔadeAB*, the growth kinetics of the parental and mutant strains were determined. *AYEΔadeB* showed a significant reduction in generation time compared with AYE. However, there was no difference in the final optical density at 600 nm reached by the two strains (Figure 4.6.1). There was no difference in the generation times of *S1ΔadeAB* and S1. However, the final optical density at 600 nm reached by this mutant was significantly lower than that for AYE (Figure 4.6.1).

### **4.6.2. Antimicrobial susceptibility of *AYEΔadeB* and *S1ΔadeAB***

To determine whether there was a change in the drug resistance profile of AYE or S1 with deletion of *adeB*, the MICs of commonly used antibiotics and dyes and those previously shown to be substrates of AdeABC (Yoon, Nait Chabane et al. 2015) were determined (Table 4.6.1). With deletion of *adeB* in AYE there was a decrease in the MIC of meropenem, imipenem, kanamycin, gentamicin, ciprofloxacin, tetracycline, tigecycline, chloramphenicol, the dye ethidium bromide and the efflux inhibitors CCCP (a proton gradient uncoupler) and PAβN (an inhibitor of AcrB and MexB, homologues of AdeB) with deletion of *adeB* in AYE. Other than meropenem, CCCP and PAβN, *AYEΔadeB* had altered susceptibility to the same compounds as *AYEΔadeRS* but the MIC of most antibiotics was lower after deletion of *adeB*. Deletion of *adeAB* in S1 resulted in a decrease in the MIC of PAβN only, although the

**Figure 4.6.1 Growth kinetics of AYE, AYE $\Delta$ adeB, S1 and S1 $\Delta$ adeAB in LB broth at 37°C**



Data are shown as the mean of 3 biological replicates and are representative of a single independent experiment carried out at least 3 times.

Generation times and optical density at stationary phase ( $\pm$ standard deviation)				
Strain	Mean generation time (min)	<i>P</i> value	OD600 at stationary phase	<i>P</i> value
AYE	121 $\pm$ 3.295	-	1.323 $\pm$ 0.030	-
AYE $\Delta$ adeB	107 $\pm$ 7.087	0.036	1.318 $\pm$ 0.004	0.815
S1	104 $\pm$ 6.024	-	1.365 $\pm$ 0.022	-
S1 $\Delta$ adeAB	112 $\pm$ 4.234	0.372	1.290 $\pm$ 0.012	0.006



**Table 4.6.1 MICs of antibiotics and dyes against AYE, AYE $\Delta$ adeB, S1 and S1 $\Delta$ adeAB**

		MIC ( $\mu$ g/ml)			
		AYE		S1	S1
		AYE	$\Delta$ adeB		$\Delta$ adeAB
Ampicillin	expt 1	>1024	>1024	16	16
	expt 2	>1024	>1024	16	16
	expt 3	>1024	>1024	16	16
Ceftazidime	expt 1	1024	1024	1024	1024
	expt 2	1024	1024	1024	1024
	expt 3	1024	1024	1024	1024
Imipenem	expt 1	1.5	0.75	0.125	0.125
	expt 2	1.5	0.75	0.125	0.19
	expt 3	1.5	0.75	0.125	0.125
Meropenem	expt 1	0.25	0.125	0.94	0.94
	expt 2	0.25	0.125	0.94	0.94
	expt 3	0.25	0.125	0.94	0.94
Kanamycin	expt 1	1024	256	1	1
	expt 2	512	128	1	1
	expt 3	1024	256	1	1
Gentamicin	expt 1	128	4	0.25	0.25
	expt 2	64	4	0.25	0.25
	expt 3	128	4	0.25	0.25
Norfloxacin	expt 1	128	128	2	2

	expt 2	128	128	2	2
	expt 3	128	128	2	2
Ciprofloxacin	expt 1	128	32	0.25	0.25
	expt 2	128	64	0.25	0.25
	expt 3	128	32	0.25	0.25
Colistin	expt 1	1	1	0.5	0.5
	expt 2	1	1	0.5	0.5
	expt 3	1	1	0.5	0.5
Tetracycline	expt 1	256	128	4	4
	expt 2	256	64	4	4
	expt 3	256	128	4	4
Tigecycline	expt 1	1	0.25	0.12	0.12
	expt 2	1	0.25	0.12	0.12
	expt 3	1	0.25	0.12	0.12
Chloramphenicol	expt 1	512	256	128	128
	expt 2	512	256	128	128
	expt 3	512	256	128	128
Carbonyl cyanide	expt 1	32	16	16	16
3-chlorophenyl	expt 2	32	16	16	16
hydrazone	expt 3	32	16	16	16
Phenylalanine-	expt 1	1024	512	512	128
arginine beta-	expt 2	1024	256	512	128
naphthylamide	expt 3	1024	512	256	128
Ethidium bromide	expt 1	512	128	256	256

expt 2	512	64	256	256
expt 3	512	128	256	256

---

Data are shown as the results of three individual experiments carried out on different days. Blue text indicates a decrease in MIC value compared with the parental strain

MIC of most drugs against S1 was much lower than for AYE with only ceftazidime and chloramphenicol displaying MICs of > 128 µg/ml (Table 4.6.1).

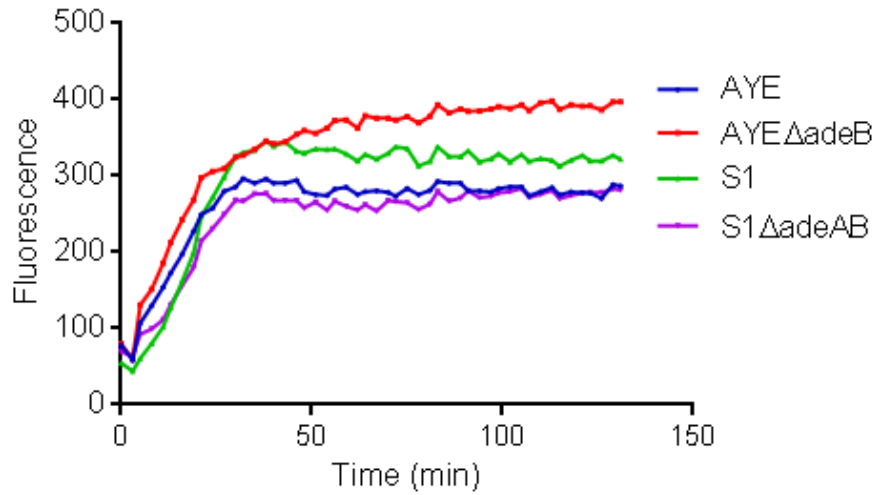
#### **4.6.3. Hoechst 33342 (bis-benzimide) accumulation by *AYEΔadeB* and *S1ΔadeAB***

As described in Chapter 3, accumulation of H33342 is a good indication of efflux activity in *A. baumannii* (Richmond, Chua et al. 2013). Accumulation of H33342 in AYE and S1 was compared with *AYEΔadeB* and *S1ΔadeAB*, respectively, to investigate whether there was a relative difference in the intracellular levels of this substrate. When compared with AYE, the steady state accumulation level of the dye H33342 in *AYEΔadeB* was 34% higher ( $P < 0.0001$ ), indicating reduced levels of efflux in this deletion mutant (Figure 4.6.2). When compared with *AYEΔadeRS* (Chapter 3), *AYEΔadeB* showed similar levels of H33342 accumulation, suggesting that the reduction in efflux activity displayed by the AdeRS deletion mutant is a result of down-regulation of the *adeABC* efflux pump genes. There was no difference in accumulation of H33342 in *S1ΔadeAB* when compared with its parental strain S1, consistent with the minimal changes in MICs (Figure 3.5.2).

#### **4.6.4. Ethidium bromide efflux by *AYEΔadeB* and *S1ΔadeAB***

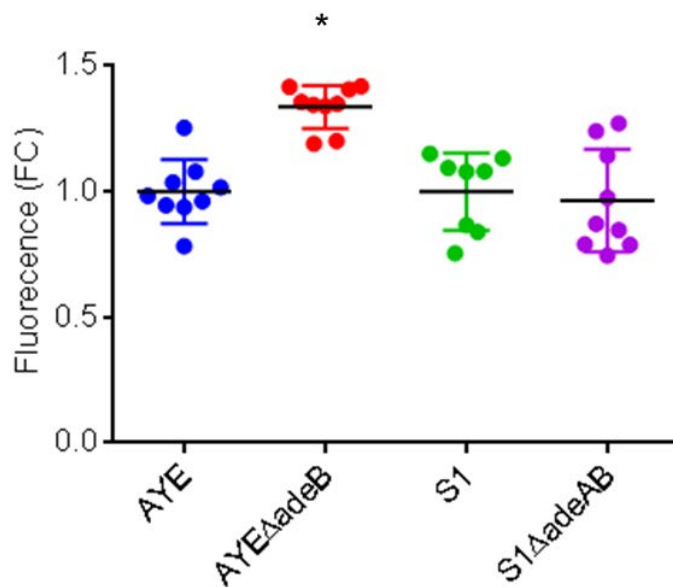
To investigate whether there was a relative difference in ethidium bromide efflux levels, efflux of this dye by AYE and S1 was compared with that by *AYEΔadeB* and *S1ΔadeAB*, respectively. The final intracellular level of ethidium bromide was 56% higher in the *AYEΔadeB* mutant ( $P > 0.0001$ ) and 36% higher in the *S1ΔadeAB* mutant ( $P > 0.05$ ) when each was compared with their respective parental strain (Figure 4.6.3B). This indicated reduced efflux of this dye in both mutants.

**Figure 4.6.2 Accumulation of H33342 by AYE, AYE $\Delta$ adeB, S1 and S1 $\Delta$ adeAB**  
**A. Accumulation of H33342 in AYE, AYE $\Delta$ adeB, S1 and S1 $\Delta$ adeAB over time**



Data are shown as fluorescence values over time and represent the mean of three biological replicates. Data are a representative example of a single independent experiment carried out at least three times.

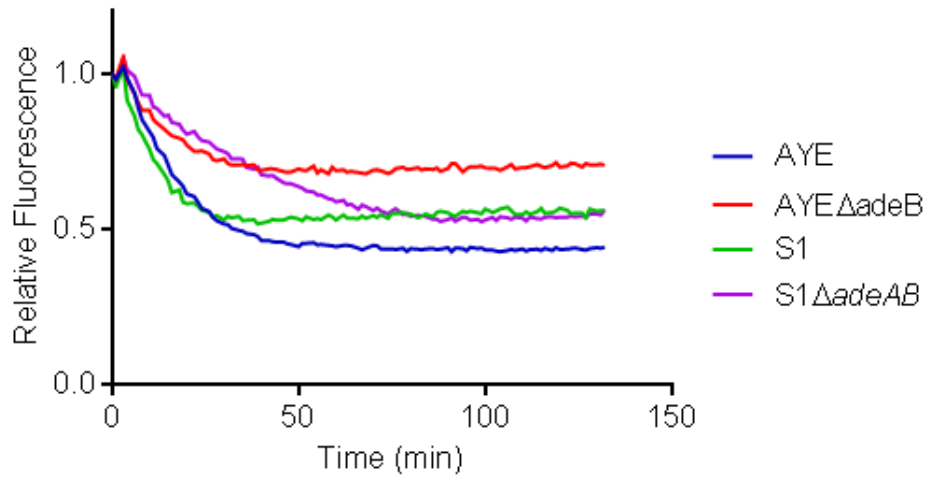
**B. Fold change in accumulation of Hoechst H33342 in AYE, AYE $\Delta$ adeB, S1 and S1 $\Delta$ adeAB**



Data are plotted as independent biological replicates to show variation within each strain. Data are presented as fold change compared to the parental strain +/- standard deviation. Student's t-tests were performed and those returning P values of less than 0.05 are indicated by \*.

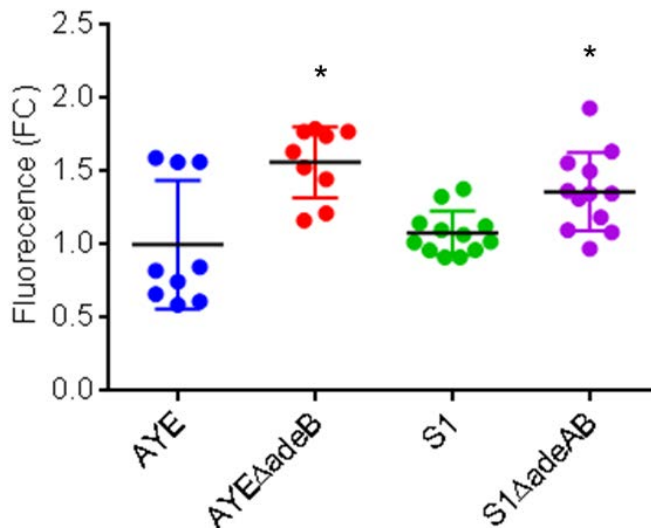
**Figure 4.6.3 Efflux of ethidium bromide by AYE, AYE $\Delta$ adeB, S1 and S1 $\Delta$ adeAB**

**A. Efflux of ethidium bromide by AYE, AYE $\Delta$ adeB, S1 and S1 $\Delta$ adeAB over time**



Data are shown as fluorescence relative to the starting fluorescence levels for each strain and represent the mean of three biological replicates. Data are a representative example of a single independent experiment carried out at least three times.

**B. Fold change in intracellular levels of ethidium bromide in AYE, AYE $\Delta$ adeB, S1 and S1 $\Delta$ adeAB**



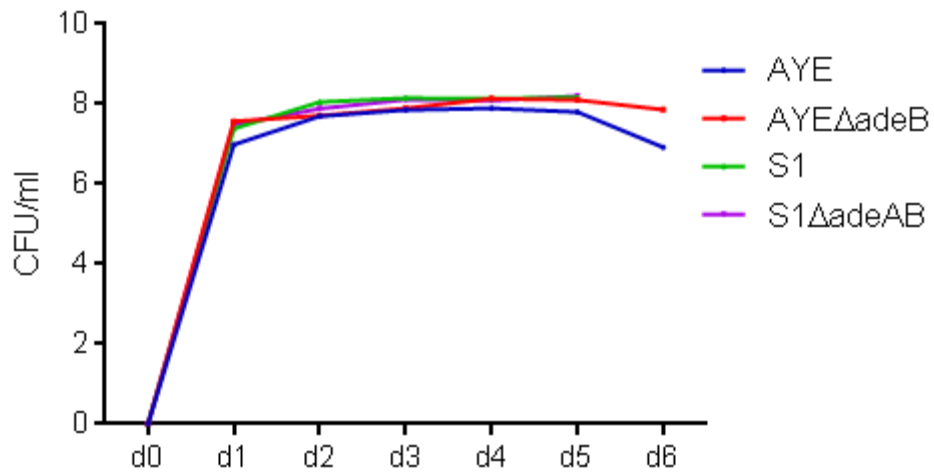
Data are plotted as independent biological replicates to show variation within each strain. Data are presented as fold change compared to the parental strain +/- standard deviation. Student's t-tests were performed and those returning P values of less than 0.05 are indicated by \*

Furthermore, the rate of efflux was greatly reduced in *S1ΔadeAB* when compared with *S1* (as seen by the initial change in relative fluorescence of the two strains; Figure 4.6.3A). These results are in contrast with the Hoechst accumulation assay, which did not detect any change in efflux levels in *S1ΔadeAB* when compared with *S1*, suggesting that the ethidium bromide efflux assay may be a more sensitive assay and is able to detect subtle changes in efflux that cannot be seen when measuring accumulation of H33342 or MICs of antibiotics. Furthermore, the reduction in efflux in *AYEΔadeB* was greater than that seen in *AYEΔadeRS*, suggesting that efflux levels are lower in the *AdeB* mutant than in the *AdeRS* mutant in this strain. This result is in line with the lower MICs of some antibiotics observed for *AYEΔadeB* when compared with *AYEΔadeRS*.

#### **4.6.5. Biofilm formation by *AYEΔadeB* and *S1ΔadeAB* in an *ex vivo* model**

To investigate whether *AdeB* is important for biofilm formation on biotic surfaces, growth of *AYE*, *AYEΔadeB*, *S1* and *S1ΔadeAB* on PVM was measured. Experiments with *AYEΔadeB* were carried out by Michele Anderson (University of Minnesota) Counts of adherent and planktonic cells were taken at 24 hr time points up to 144 hours. As seen previously with *AYE* and ATCC 19606, there was a rapid increase in the number of adherent cells on PVM up to the one day time point, followed by a slow but steady increase between one and six days Figure 4.6.4. *S1* showed similar growth to strain *AYE* in both adherent cell counts and biofilm imaging. There was no significant difference between numbers of adherent cells of parental or mutant strain for at any time point (Figure 4.6.4). However, LIVE/DEAD<sup>®</sup> staining and confocal laser scanning microscopy showed a similar difference between the infection

**Figure 4.6.4 Adherent and planktonic bacterial cells counts of AYE, AYE $\Delta$ adeB, S1 and S1 $\Delta$ adeAB grown at 37°C on PVM**



Data are shown as mean CFU/ml of 3 biological replicates and are representative of a single independent experiment carried out at least 3 times.

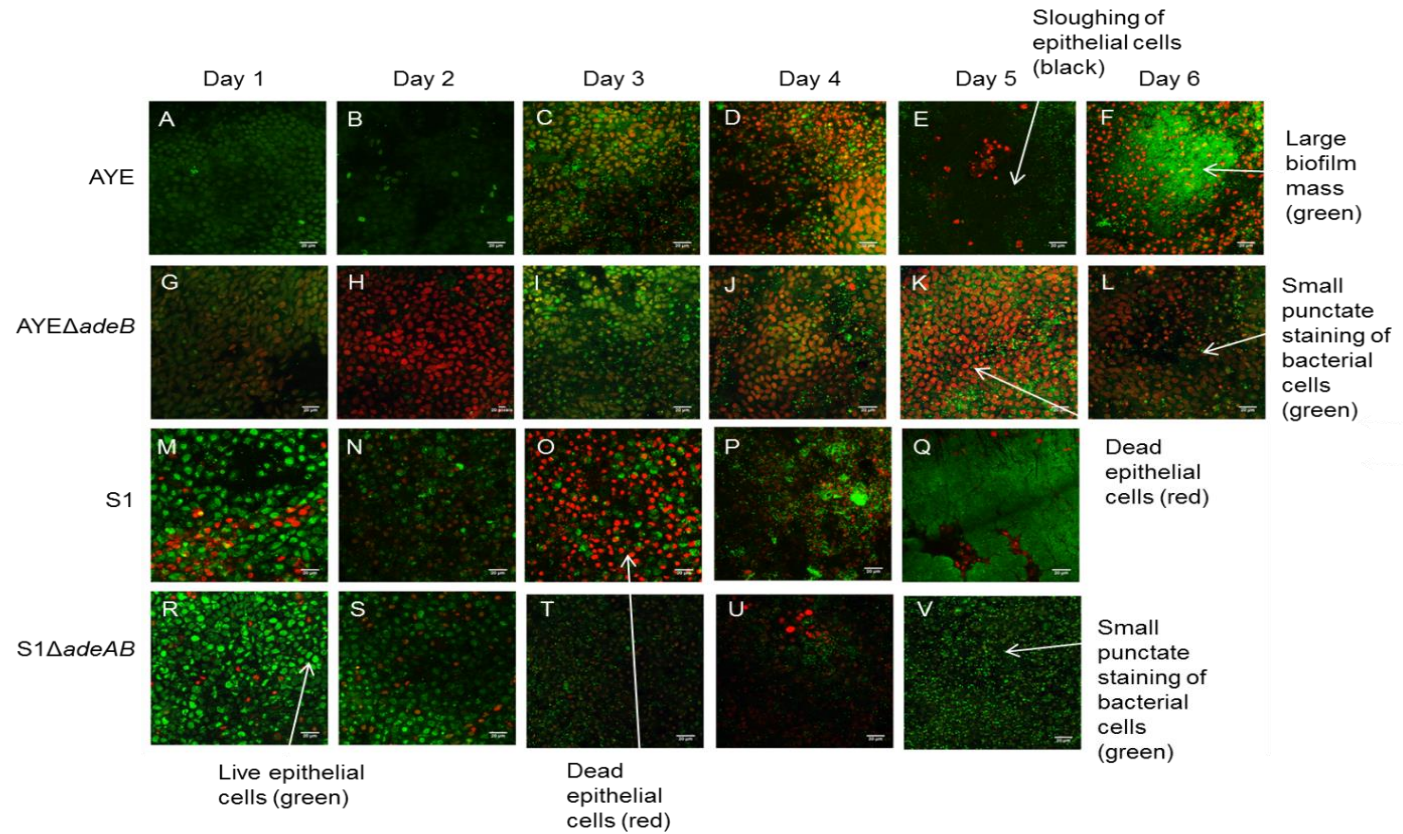


phenotype of AYE and AYE $\Delta$ *adeB* and S1 and S1 $\Delta$ *adeAB*, respectively (Figure 4.6.5). As with previous experiments, at three days post-infection AYE infected tissue displayed epithelial cell death (red) and by six days post-infection large biofilm masses and epithelial cell sloughing was visible, as described in Chapter 3. S1 was able to form a robust biofilm more rapidly than AYE and a thick biofilm mat could be seen by day five, at which point the experiment was stopped (Figure 4.6.5 panels M-Q). However, when compared with their respective parental strains, both *adeB* mutants showed a defect in biofilm formation when imaged by confocal microscopy. At days five and six, S1 and AYE, respectively, formed large biofilm masses with extensive epithelial cell sloughing (Figure 4.6.5 panels F&Q) whereas, although the mutants were able to cause epithelial cell death, only individual bacterial cells were observed to be attached to the mucosal tissue and less sloughing was evident (Figure 4.6.5 panels L&V). These data suggest that the AdeABC efflux pump plays a key role in biofilm formation on mucosal tissue and host cell cytotoxicity and that decreased production of this MDR efflux pump may be responsible for the similar phenotype seen in AYE $\Delta$ *adeRS*.

#### **4.6.6. Biofilm formation by AYE $\Delta$ *adeB* and S1 $\Delta$ *adeAB* *in vitro***

To determine whether lack of AdeB in AYE and S1 also conferred a change in biofilm formation on an abiotic surface, each parental strain and deletion mutant were grown in three different *in vitro* models to measure biofilm; a microfluidic cell, polypropylene pegs and polystyrene test tubes.

**Figure 4.6.5 Confocal laser scanning microscopy of *AYE*, *AYEΔadeB*, *S1* and *S1ΔadeAB* biofilms using LIVE/DEAD® staining and visualised at 1-6 days**



Uninfected epithelia are live (green) and intact. Red, rounded epithelial cells indicate cell death. Small, punctate, green staining indicates bacterial cells and large, green staining masses indicate bacterial biofilm. Black areas depict exposed extracellular matrix. Arrows indicate examples of live and dead epithelial cells, bacterial cells, epithelial cell sloughing and biofilm masses.

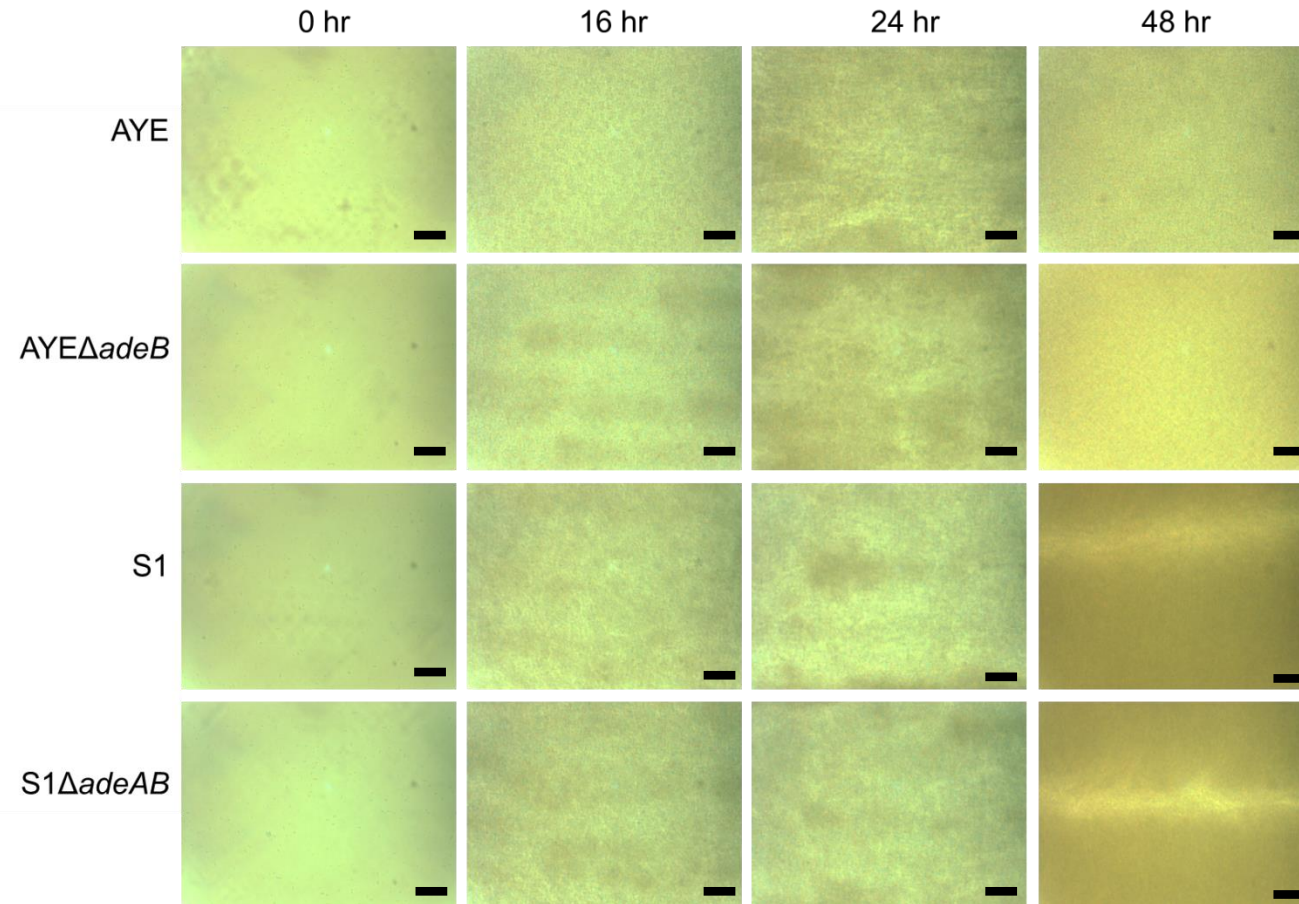
#### **4.6.6.1. Biofilm formation by *AYEΔadeB* and *S1ΔadeAB* in a microfluidic cell**

Biofilm formation by *AYE*, *AYEΔadeB*, *S1* and *S1ΔadeAB* was studied under flow conditions in order to replicate formation on a medical device implanted in the body. At 0 hrs, attachment of individual bacterial cells to the walls of the flow cell could be seen by phase microscopy (Figure 4.6.6). There was no difference between initial attachment of *AYE* and *AYEΔadeB* or *S1* and *S1ΔadeAB*. All strains formed a robust biofilm after 16 hrs and rapid growth could be seen in this time period. Thick biofilm coverage of the surface of the microfluidic cell was observed at 16, 24 and 48 hrs (Figure 4.6.6). When compared visually, there was no difference in the biofilm formed by either strain at any time point (Figure 4.6.6).

#### **4.6.6.2. Biofilm formation by *AYEΔadeB* and *S1ΔadeAB* on polypropylene pegs**

To quantify the amount of biofilm formed by *AYE*, *AYEΔadeB*, *S1* and *S1ΔadeAB* after 8 hrs incubation, biofilms were grown on polypropylene pegs and quantified by crystal violet staining. In this *in vitro* model, there was a 30% decrease in biofilm mass ( $P < 0.001$ ) at 30°C and a 19% decrease in biofilm mass ( $P < 0.01$ ) at 37°C produced by *AYEΔadeB* when compared with *AYE* (Figure 4.6.7). However, there was no change in biofilm formation by *S1ΔadeAB* at either temperature (Figure 4.6.7) suggesting that the role of AdeABC in biofilm formation is dependent on both the strain of *A. baumannii* and the biofilm model used.

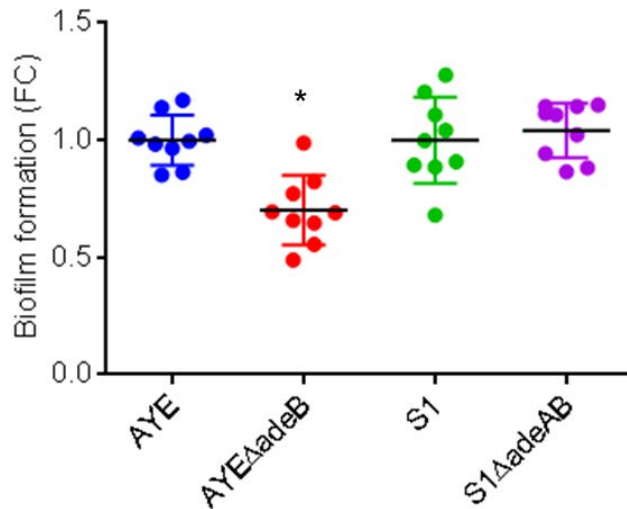
**Figure 4.6.6 Phase contrast microscopy images of AYE, AYE $\Delta$ adeB, S1 and S1 $\Delta$ adeAB biofilms formed under flow conditions of 0.3 dynes up to 48 hrs**



Images show attachment of bacterial cells to the inner surface of a microfluidic channel. Grey dots show adherence of individual cells to the surfaces whereas solid grey areas indicate bacterial growth and biofilm production. Black bar depicts a 10  $\mu$ m scale.

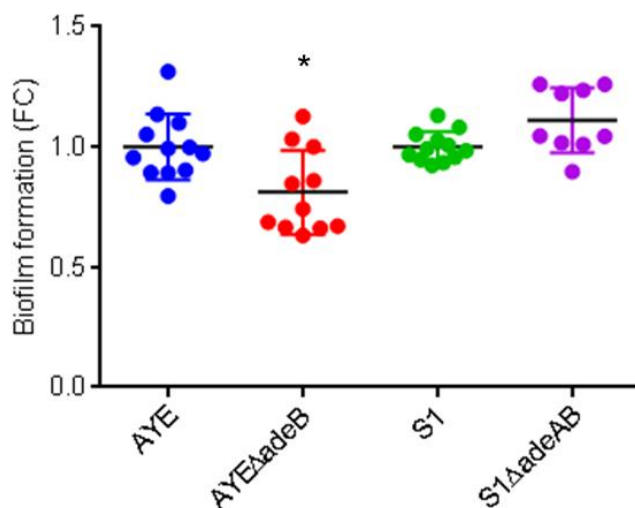
**Figure 4.6.7 Biofilm formation by *AYE*, *AYE* $\Delta$ *adeB*, *S1* and *S1* $\Delta$ *adeAB* on polypropylene pegs as determined by crystal violet staining**

**A. 30°C**



Data are plotted as independent biological replicates to show variation within each strain. Data are presented as fold change compared to the parental strain +/- standard deviation. Student's t-tests were performed and those returning P values of less than 0.05 are indicated by \*.

**B. 37°C**



Data are plotted as independent biological replicates to show variation within each strain. Data are presented as fold change compared to the parental strain +/- standard deviation. Student's t-tests were performed and those returning P values of less than 0.05 are indicated by \*.

#### **4.6.6.3. Pellicle formation by *AYEΔadeB* and *S1ΔadeAB***

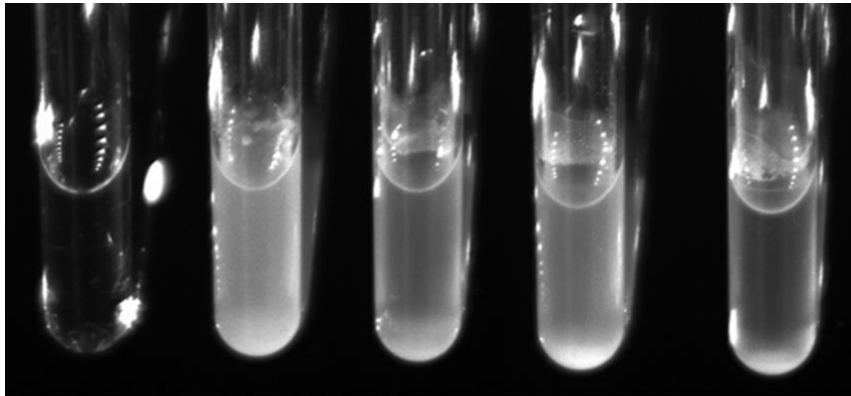
To assess the ability of *AYE*, *AYEΔadeB*, *S1* and *S1ΔadeAB* to form a pellicle at the air/liquid interface, cultures were incubated statically in polystyrene test tubes for 48 hours at 30°C and 37°C. A thick biofilm mat could be seen at the surface with all strains but there was no difference between strains in the amount of pellicle formed when examined visually (Figure 4.6.8).

#### **4.6.6.4. Biofilm formation by *AYEΔadeB* and *S1ΔadeAB* on glass cover slips**

In order to visualise biofilms formed by *adeB* deletion mutants in *AYE* and *S1* and to determine whether mutants were unable to adhere to abiotic surfaces or were adherent but unable to form a biofilm, as seen in *AYEΔadeRS* and in the mucosal model, bacterial cultures were incubated on glass slides for 24 hrs before being fixed for scanning electron microscopy (SEM). As described in Chapter 3, *AYE* formed a three dimensional biofilm with ECM visibly produced. *AYEΔadeB* showed an altered biofilm phenotype compared with *AYE*, with no clumping of cells and no ECM. Individual cells also appeared slightly more rounded and the surface of the cells was uneven (Figure 4.6.9). Furthermore, the coverage of the surface of the cover slip was far sparser after incubation with *AYEΔadeB*, as was observed with *AYEΔadeRS*. This is in agreement with results seen in the mucosal model and the *in vitro* polypropylene peg model. In contrast with *AYE*, strain *S1*, did not form a mature biofilm at the 24 hour time point. There was good biofilm coverage of the cover slip after incubation with *S1*, however, very little three dimensional clumping of cells could be seen and there was minimal evidence of ECM (Figure 4.6.9). Like *AYEΔadeB*,

**Figure 4.6.8 Pellicle formation by AYE, AYE $\Delta$ adeB, S1 and S1 $\Delta$ adeAB incubated statically at 37°C**

A. Visualised under white light



Negative AYE AYE $\Delta$ adeB S1 S1 $\Delta$ adeAB

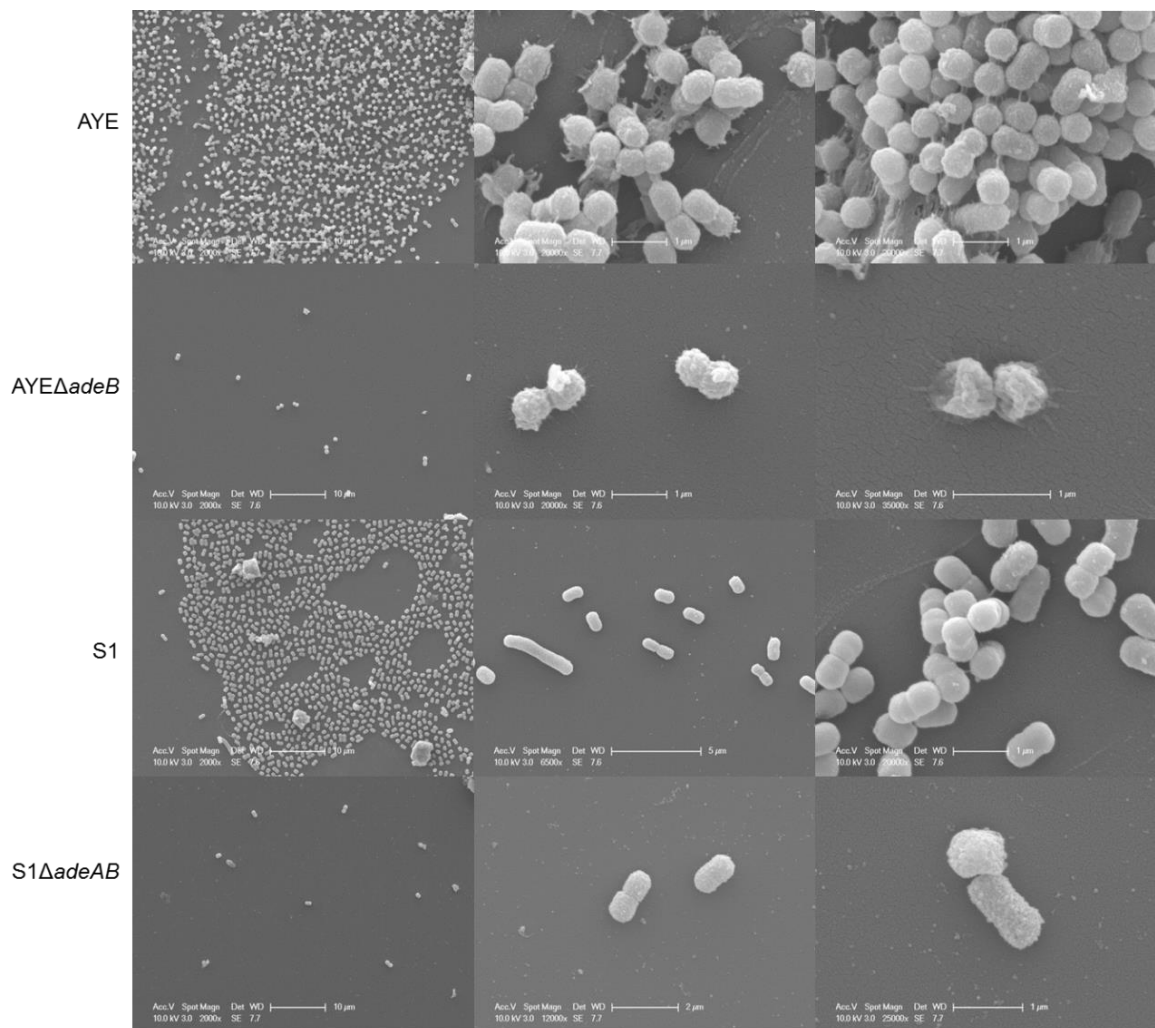
B. Visualised under natural light



Negative AYE AYE $\Delta$ adeB S1 S1 $\Delta$ adeAB



**Figure 4.6.9 Scanning electron microscopy of AYE, AYE $\Delta$ adeB, S1 and S1 $\Delta$ adeAB biofilms on glass cover slips**



Images show attachment of bacterial cells, production of ECM and formation of a biofilm on the surface of a glass cover slip.



S1 $\Delta$ *adeAB* was not able to form a biofilm and showed sparse coverage of the cover slip, although there was still some attachment to the surface (Figure 4.6.9). As discussed in Chapter 3, although this difference was not observed in the other *in vitro* models, it is possible that they are not sensitive enough to detect the change seen in this mutant by SEM.

#### **4.6.7. Motility of AYE $\Delta$ *adeB* and S1 $\Delta$ *adeAB***

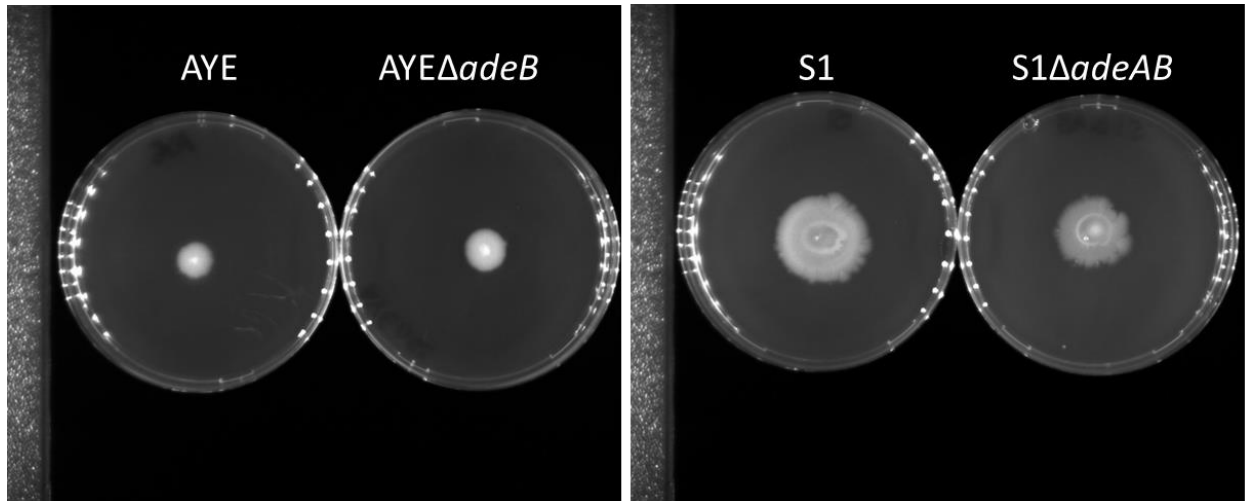
As described in Chapter 3, strain AYE displayed some twitching motility but did not show swarming motility, as with the majority of *A. baumannii* strains. S1 showed a similar phenotype with slightly more twitching motility evident and no swarming motility. AYE $\Delta$ *adeB* did not show any defect in twitching or swarming motility when compared with parental strain AYE (Figure 4.6.10). S1 $\Delta$ *adeAB* showed no difference in swarming motility but there was a small decrease in twitching motility when compared with S1 (Figure 4.6.10). This was not visible with an *adeB* mutant in AYE, but this may be due to the lower levels of motility displayed by this strain.

#### **4.6.8. Virulence of AYE $\Delta$ *adeB* and S1 $\Delta$ *adeAB* in the *Galleria mellonella* model of infection**

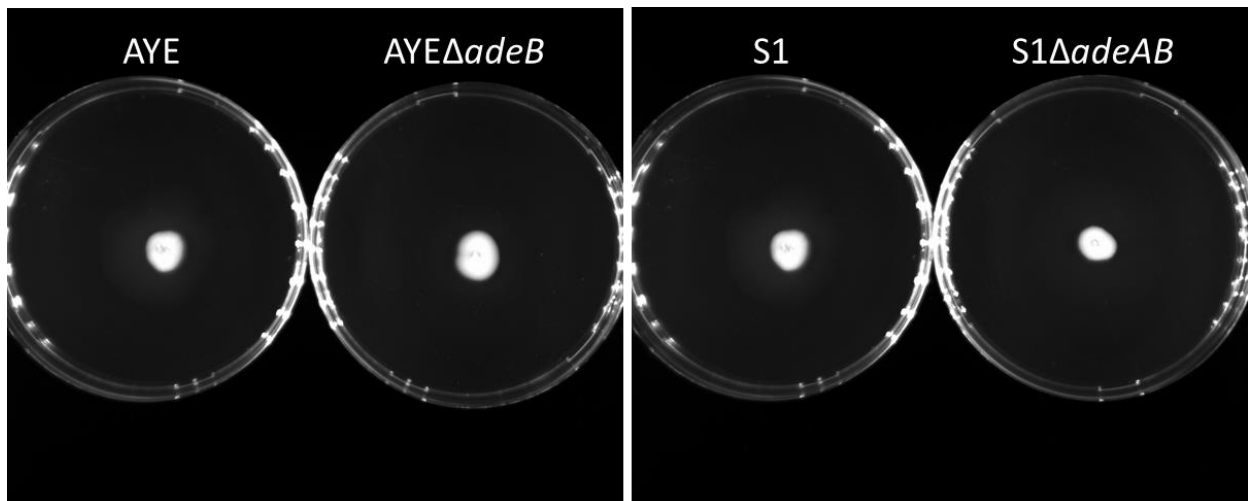
S1 $\Delta$ *adeAB* displayed attenuated virulence in the *G. mellonella* model, when compared with S1. After infection with S1, all larvae were dead by day two, whereas 60% were still alive at day five after infection with the mutant (Figure 4.6.11). AYE was less virulent in *G. mellonella* compared with S1 and there was no significant difference in the killing of larvae by AYE and AYE $\Delta$ *adeB* (Figure 4.6.11). This suggests a strain-specific role for AdeABC in virulence in *A. baumannii*. It is possible

Figure 4.6.10 Twitching and swarming motility of AYE, AYE $\Delta$ adeB, S1 and S1 $\Delta$ adeAB grown on 1% and 0.3% agar for 24 hrs at 37°C

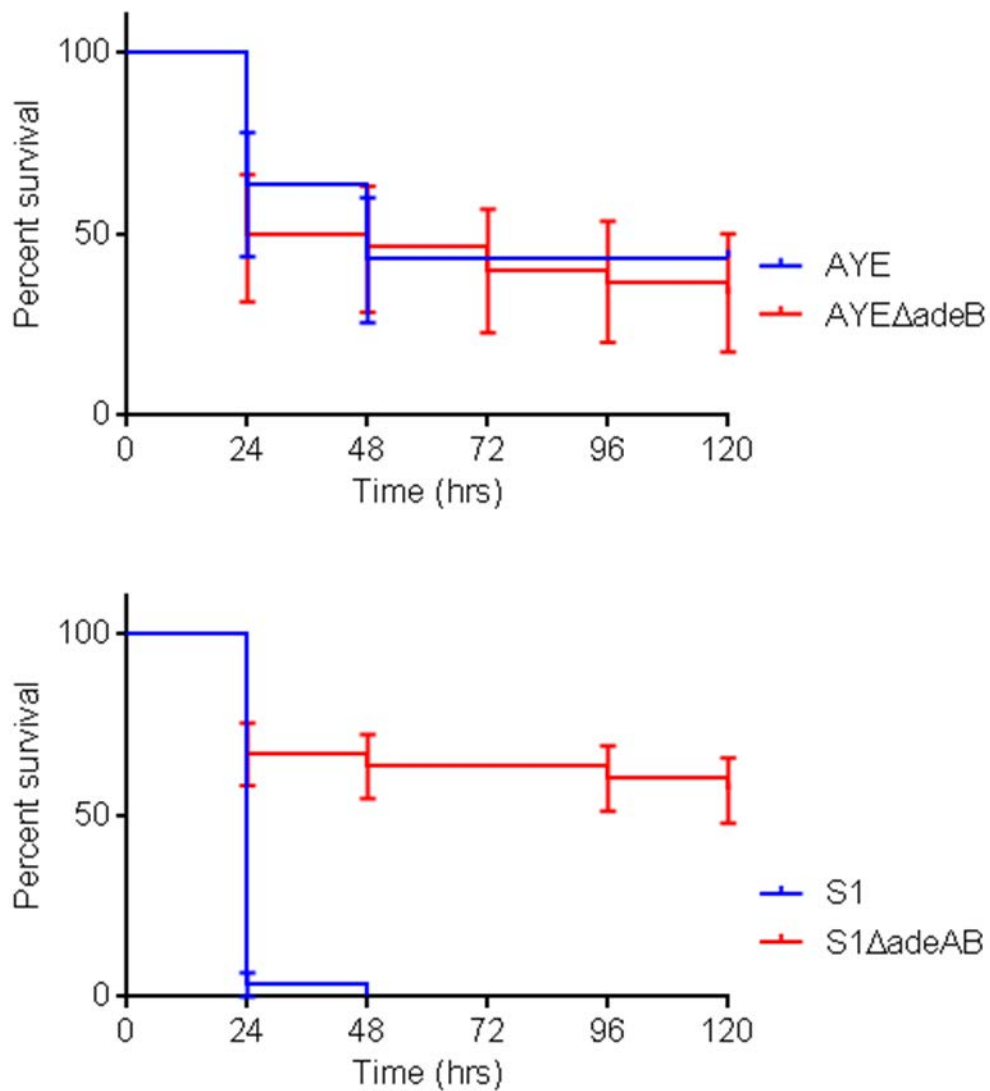
A. Twitching motility



B. Swarming motility



**Figure 4.6.11 Kaplan Meir survival curves to show virulence of AYE, AYE $\Delta$ adeB, S1 and S1 $\Delta$ adeAB in *G. mellonella***



Data show percentage survival (n=30) of *G. mellonella* after inoculation with  $10^6$  CFU bacteria. Error bars represent SEM.

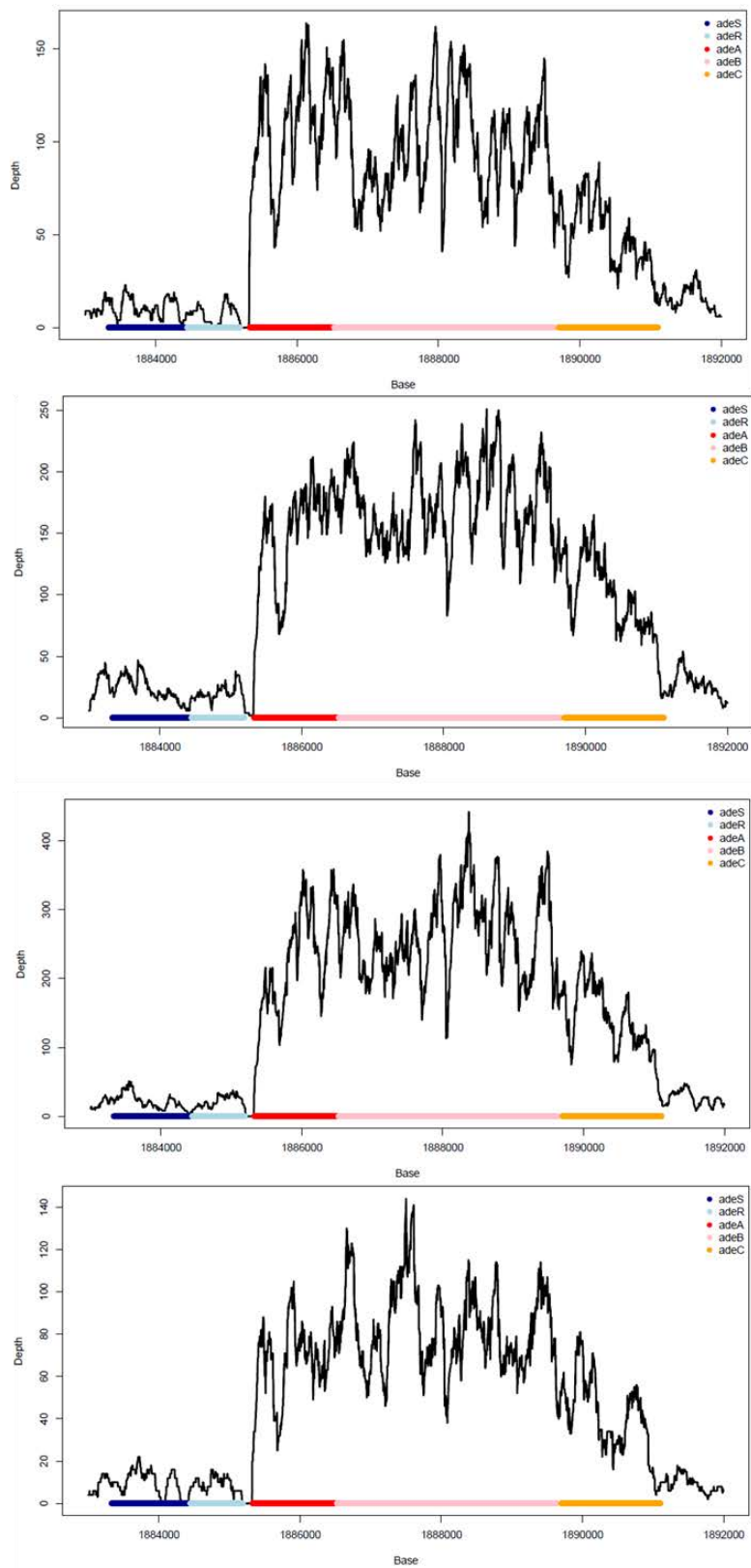
that the AdeABC efflux pump is not expressed by AYE *in vivo*, possibly explaining the reduced virulence displayed by this strain and the absence of altered virulence levels in the AYE $\Delta$ *adeB* mutant.

#### **4.7. Determining the transcriptome of AYE $\Delta$ *adeB* and S1 $\Delta$ *adeAB***

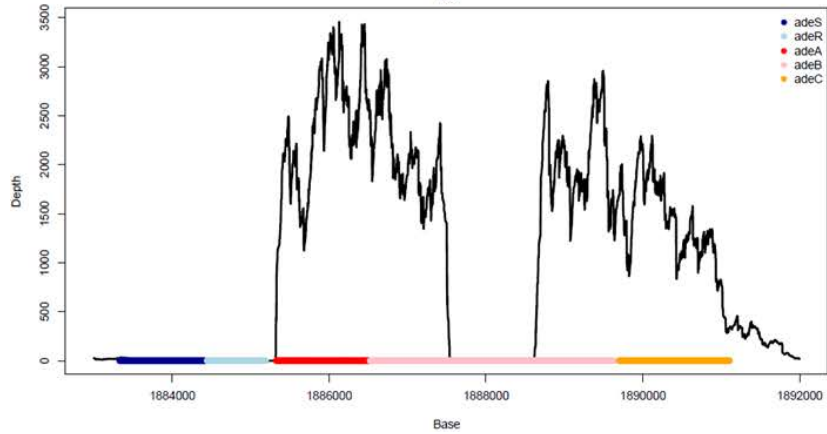
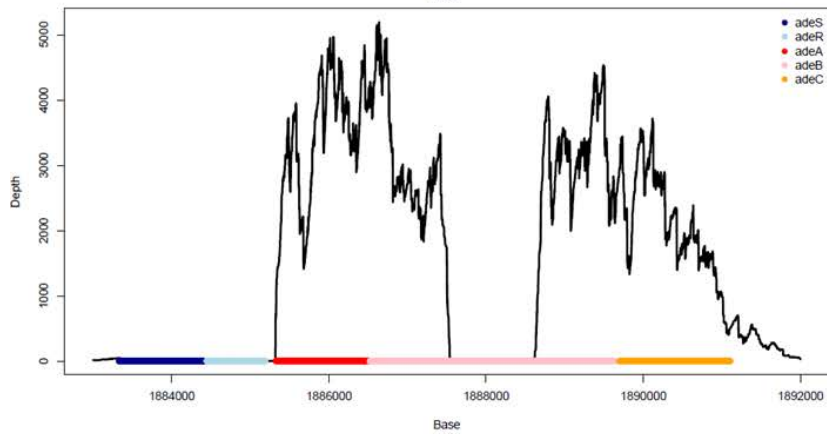
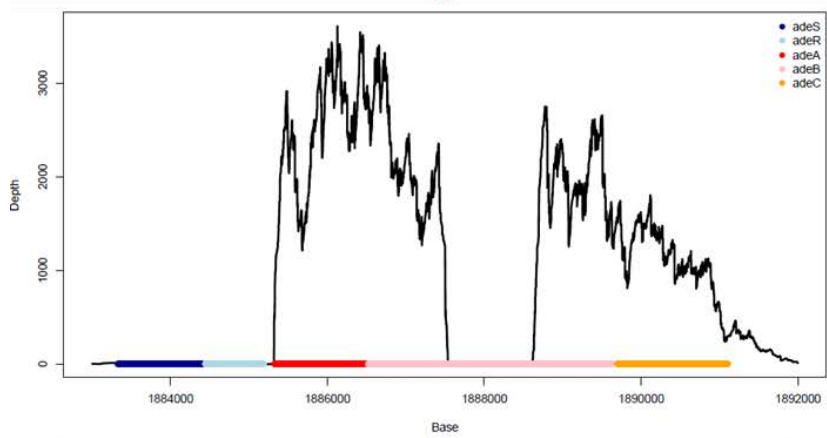
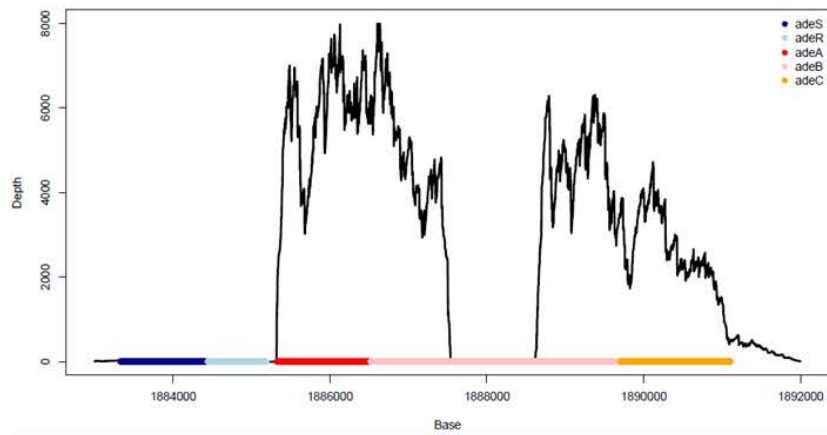
To identify changes in gene expression that may account for the change in phenotype with deletion of *adeB* in AYE and S1 and to give insight into the difference in phenotype between the two deletion mutants, RNA-Seq was carried out. Transcriptomic changes in AYE $\Delta$ *adeB* were also compared to those in AYE $\Delta$ *adeRS* to help to understand to what extent the down-regulation of *adeABC* is responsible for the phenotype of AYE $\Delta$ *adeRS*. AYE and AYE $\Delta$ *adeB* RNA was prepared and four biological replicates were sequenced in Birmingham in March 2015, whilst S1 and S1 $\Delta$ *adeAB* RNA was prepared in Birmingham in September 2015 and sent to BGI genomics, Hong Kong for library preparation and sequencing of three biological replicates. Data were checked for quality and analysed by Dr Alasdair Ivens (University of Edinburgh) and submitted to ArrayExpress (accession E-MTAB-4049, E-MTAB-4071). Deletion of a 1131 bp fragment in the centre of *adeB* in AYE $\Delta$ *adeB* and a 2261 bp fragment spanning the last 222 bp of *adeA*, the first 1914 bp of *adeB* and a 125 bp intergenic region in S1 $\Delta$ *adeAB* was confirmed by the absence of reads mapping to these regions of the genes in each sample (Figure 4.7.1). As seen in Chapter 3, parental strain AYE showed fairly low read depth (< 50) across *adeRS* with higher read depth (> 100) across *adeABC* (Figure 4.7.1). This suggested a low level of expression of *adeRS* in AYE and high expression of the *adeABC* operon.

Figure 4.7.1 Number of reads aligned to each base across the *adeRS adeABC* region in each sample

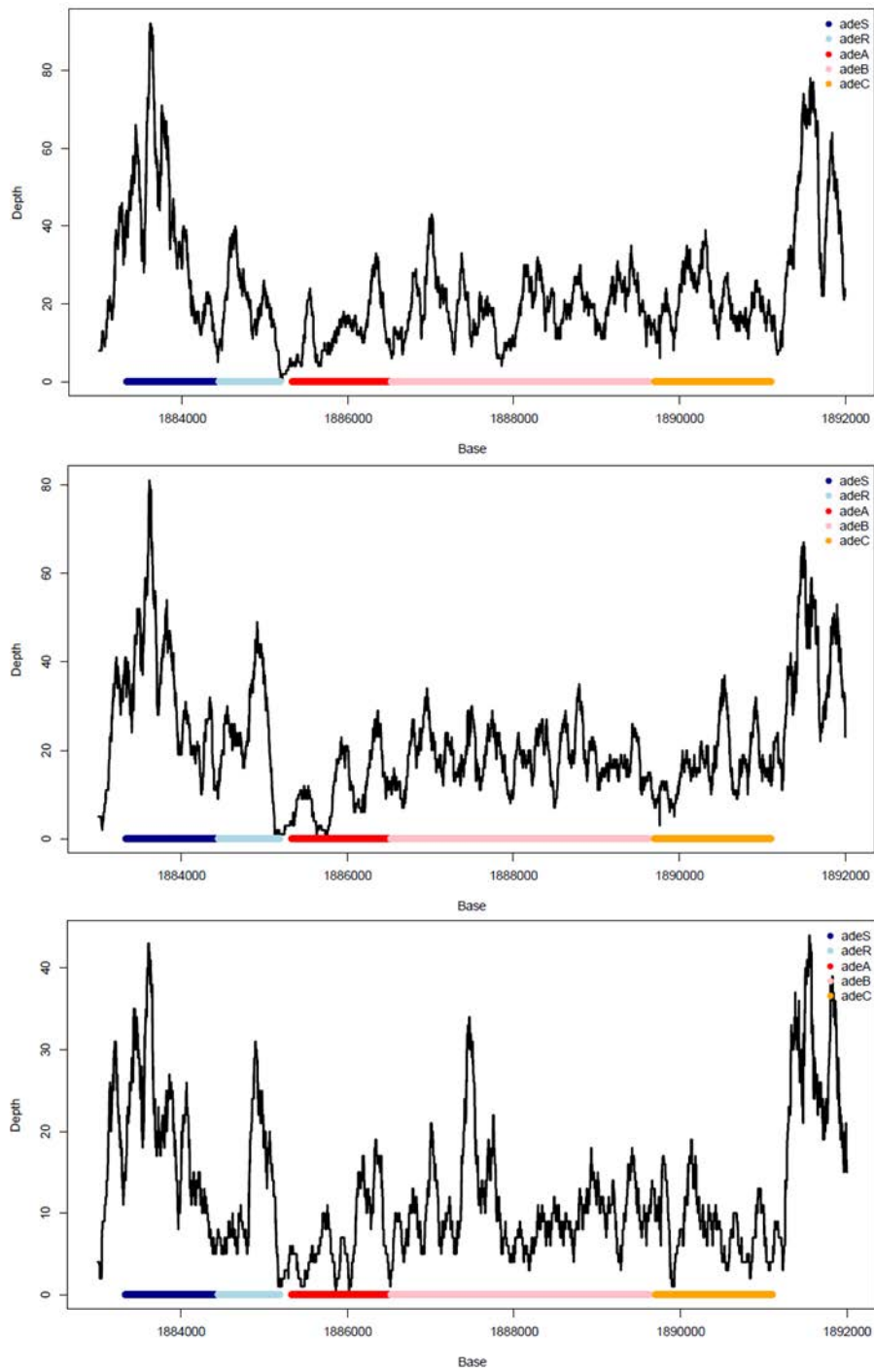
A. AYE



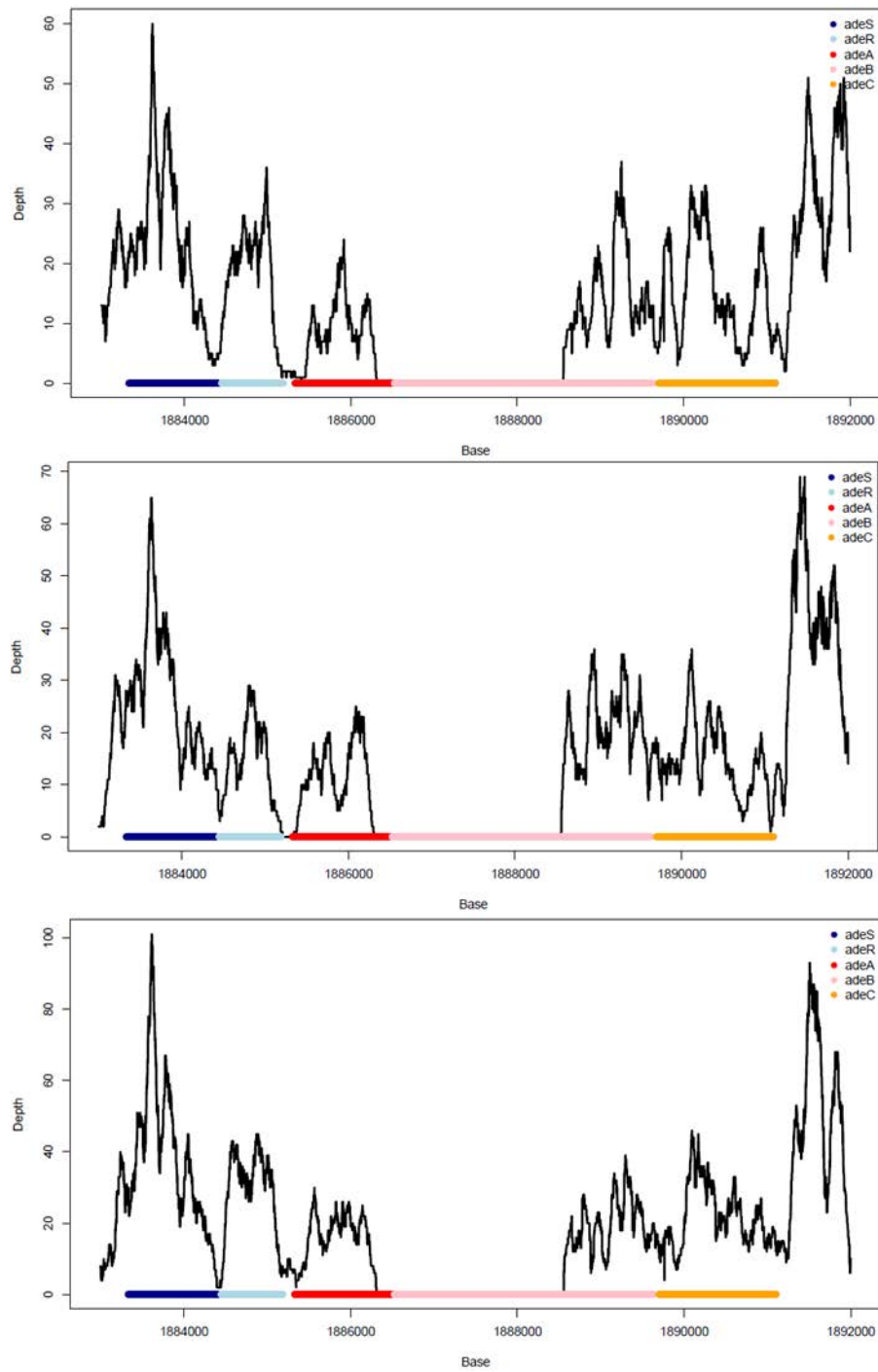
## B. $\Delta adeB$



### C. S1



## D. S1ΔadeAB

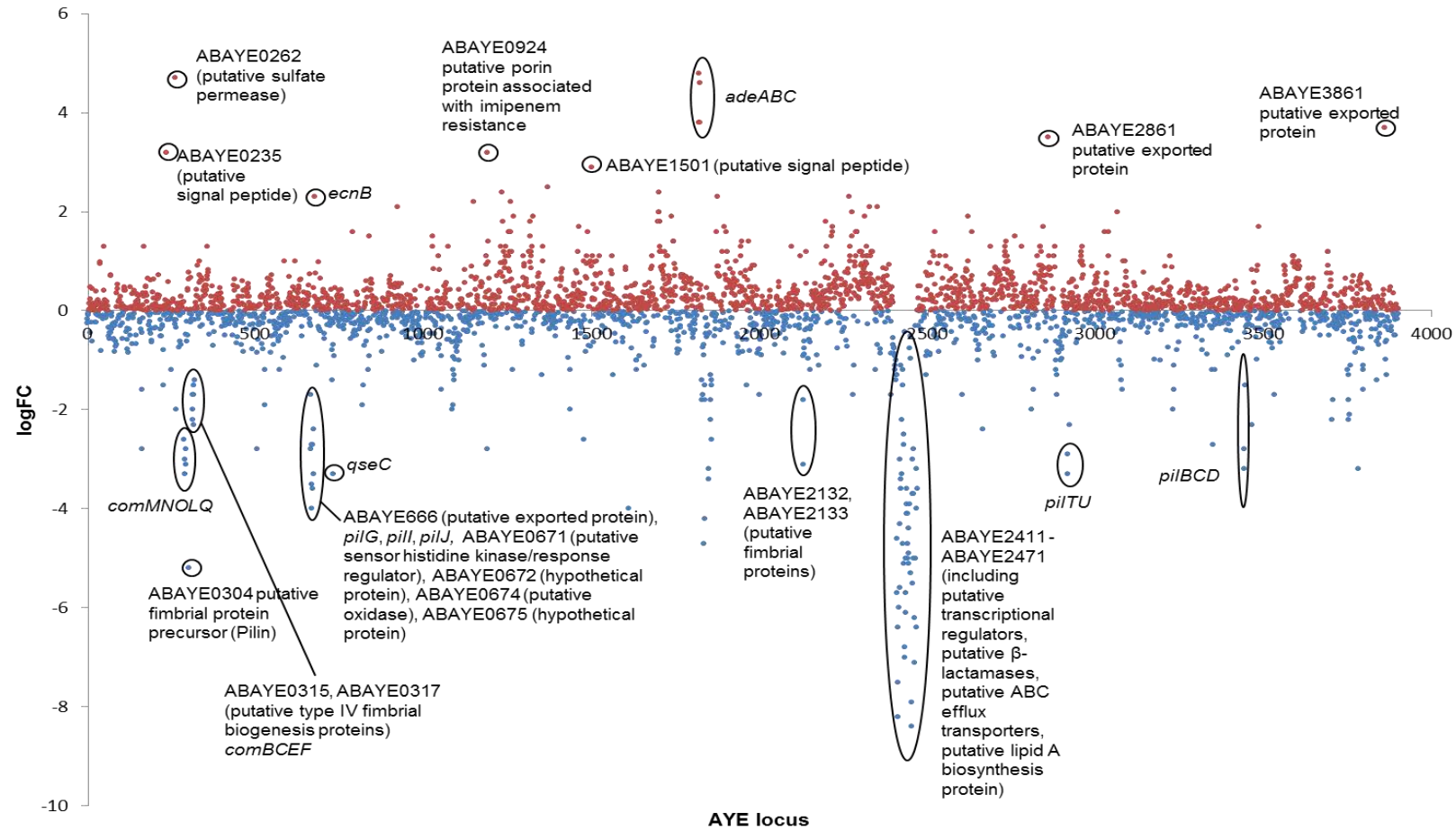




AYE $\Delta$ *adeB* samples showed an absence of reads mapping to the deleted fragment in the middle of the *adeB* gene. In excess of 4000 reads were mapped to the undeleted region of the *adeABC* operon resulting in a 28, 14 and 24-fold increase in expression of *adeA*, *adeB* and *adeC*, respectively, in AYE $\Delta$ *adeB* compared with AYE (Figure 4.7.2). Less than 100 reads mapped to the *adeRS* and *adeABC* operons in S1. Aside from the large deleted fragment spanning *adeA* and *adeB*, S1 $\Delta$ *adeAB* showed similar read depth to the parental strain, S1, across both *adeRS* and *adeABC*. There was a 2.3-fold decrease in expression of *adeB* in S1 $\Delta$ *adeAB* compared with S1. As only 222 bp of the 3' end of *adeA* was deleted, reads were still mapped to the first 978 bp of this gene; there was also no significant change in gene expression.

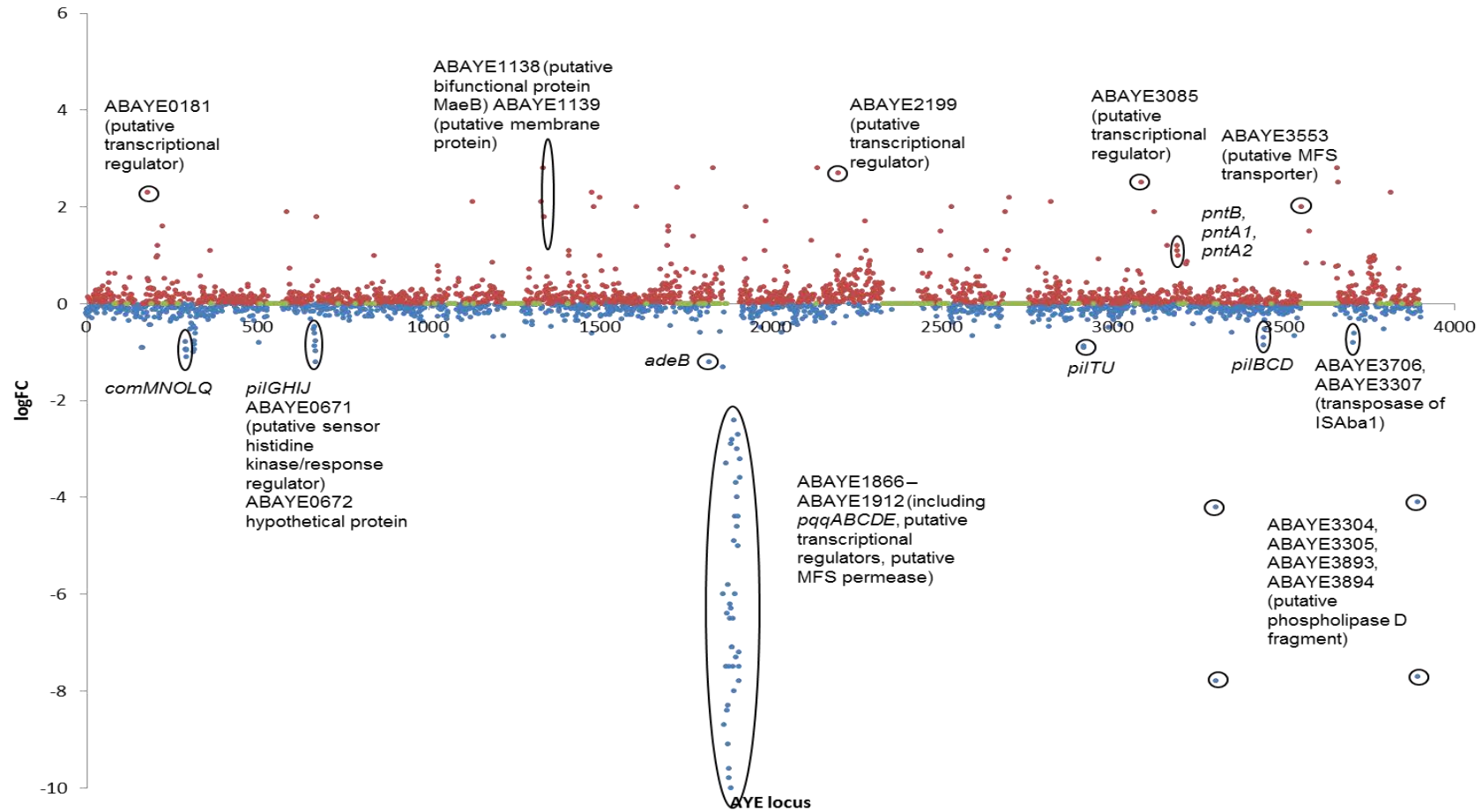
All gene expression changes in AYE $\Delta$ *adeB* compared with AYE and S1 $\Delta$ *adeAB* compared with S1 were plotted by locus tag to identify highly differentially expressed genes or operons (Figure 4.7.2, Figure 4.7.3). There was decreased expression of multiple *com* and *pil* operons in both *adeB* deletion mutants. AYE $\Delta$ *adeB* also had highly increased expression of genes encoding several putative products such as signal peptides (ABAYE0235, ABAYE1501), sulfate permeases (ABAYE0262), porin proteins (ABAYE0924) and exported proteins (ABAYE2861, ABAYE3861) and *ecnB*, a bacteriolytic lipoprotein. Decreased expression of *comBCEF*, *comMNOLQ*, *pilGIJ*, *pilTU* and *pilBCD* operons was also observed in this strain along with decreased expression of genes encoding putative fimbrial proteins (ABAYE0304), exported proteins (ABAYE2434, ASBAYE2435, ABAYE2444, ABAYE2463, ABAYE2464), transcriptional regulators (ABAYE2443, ABAYE0671),  $\beta$ -lactamases (ABAYE2456), efflux pumps (ABAYE2419) and lipid A biosynthesis proteins (ABAYE2468).

Figure 4.7.2 Log2 fold change in expression of all genes of the AYE genome in AYEΔadeB compared with AYE



Genes with increased and decreased expression are coloured red and blue, respectively. Gene names or annotations are provided for genes within differentially expressed operons or highly differentially expressed genes with known function.

**Figure 4.7.3 Log2 fold change in expression of all genes of the AYE genome in S1ΔadeAB compared with S1**



Genes with increased and decreased expression are coloured red and blue, respectively. Gene names or annotations are provided for genes within differentially expressed operons or highly differentially expressed genes with known function.

S1 $\Delta$ *adeAB* had highly increased expression of genes encoding putative products such as transcriptional regulators (ABAYE0181, ABAYE2199, ABAYE 3085), membrane proteins (ABAYE1139) and MFS transporters (ABAYE3553), and the *pnt* operon which encodes pyridine nucleotide transhydrogenase. Decreased expression of *comMNOLQ*, *pilGHIJ*, *pilTU*, *pilBCD* and *pqqABCDE* operons was also observed in S1 $\Delta$ *adeAB*. Furthermore, in this strain there was decreased expression of genes encoding putative transcriptional regulators (ABAYE1900, ABAYE1908, ABAYE1912), MFS permeases (ABAYE1907), transposases (ABAYE3706, ABAYE3707) and phospholipase D fragments (ABAYE3304, ABAYE3305, ABAYE3893, ABAYE3894, ABAYE1870, ABAYE1871). Genes with large changes in expression encoding hypothetical or putative products were often found directly upstream or downstream of the *com* or *pil* genes with changed expression. This suggests that they may be encoded as an operon.

A raw P value cut-off of 0.05 was used to produce a list of significantly changed genes (Table 4.7.1, Table 4.7.2, Table 4.7.3, Table 4.7.4). The raw P value was chosen as opposed to the more stringent adjusted P value as this gave a more comprehensive list of changed genes that may affect the phenotype and ensured that no genuinely changed genes would be excluded from the list. Compared with AYE, there were 693 genes with increased expression in AYE $\Delta$ *adeB* and 477 genes with decreased expression. Compared with S1, there were 164 genes with increased expression and 119 genes with decreased expression in S1 $\Delta$ *adeAB*. Differentially expressed genes were categorised into cluster of orthologous groups (COGs) (Tatusov, Galperin et al. 2000) and correlations with the phenotypic changes seen in each efflux pump mutant sought (Figure 4.7.4, Figure 4.7.5). Genes encoding

**Table 4.7.1 The top 10 genes with the most significantly changed expression in *AYEΔadeB* compared with *AYE***

Gene ID	Start	End	Description	Common Name	Strand	Type	log2 fold change	Fold change	P.Value
ABAYE2456	2507740	2509014	putative beta-lactamase		+	gene	-5.50	0.022	1.50E-12
ABAYE2463	2512856	2514487	putative exported protein		+	gene	-7.10	0.007	2.00E-12
ABAYE2436	2483124	2484032	hypothetical protein		-	gene	-6.10	0.015	3.00E-12
ABAYE2418	2465596	2465997	hypothetical protein		+	gene	-5.60	0.021	3.10E-12
ABAYE2460	2510646	2511596	putative hydroxyacyl-CoA dehydrogenase		-	gene	-5.00	0.031	3.40E-12
ABAYE2415	2463296	2463799	hypothetical protein		-	gene	-6.40	0.012	3.80E-12
ABAYE2444	2493411	2493728	putative exported protein		-	gene	-5.00	0.031	5.80E-12
ABAYE2416	2463816	2464349	hypothetical protein		-	gene	-6.00	0.016	9.00E-12
ABAYE2465	2515510	2516814	putative Permease (major facilitator superfamily)		-	gene	-5.00	0.031	1.80E-11
ABAYE2419	2466093	2467037	putative transport protein (ABC superfamily)		+	gene	-4.30	0.051	2.00E-11

**Table 4.7.2 The top 10 genes with the largest fold change in expression in AYEΔ*adeB* compared with AYE**

Gene ID	Start	End	Description	Common Name	Strand	Type	log2 fold change	Fold change	P.Value
ABAYE1821	1885325	1886524	membrane fusion protein	<i>adeA</i>	+	gene	4.80	27.858	1.80E-10
ABAYE0262	275986	278187	putative sulfate permease		+	gene	4.70	25.992	8.00E-08
ABAYE1823	1889696	1891105	outer membrane protein	<i>adeC</i>	+	gene	4.60	24.251	6.80E-10
ABAYE1822	1886521	1889631	RND protein	<i>adeB</i>	+	gene	3.80	13.929	3.70E-09
ABAYE1824	1891198	1892112	conserved hypothetical protein		-	gene	3.80	13.929	2.00E-09
ABAYE2454	2503999	2507145	hypothetical protein		-	gene	-8.40	0.003	7.70E-11
ABAYE2413	2461269	2461772	conserved hypothetical protein		-	gene	-8.20	0.003	1.30E-10
ABAYE2453	2501269	2503986	fragment of putative Rhs family protein		-	pseudo gene	-7.90	0.004	1.10E-09
ABAYE2414	2461822	2463318	conserved hypothetical protein		-	gene	-7.50	0.006	2.40E-08
ABAYE2463	2512856	2514487	putative exported protein		+	gene	-7.10	0.007	2.00E-12

**Table 4.7.3 The top 10 genes with the most significantly changed expression in S1ΔadeAB compared with S1**

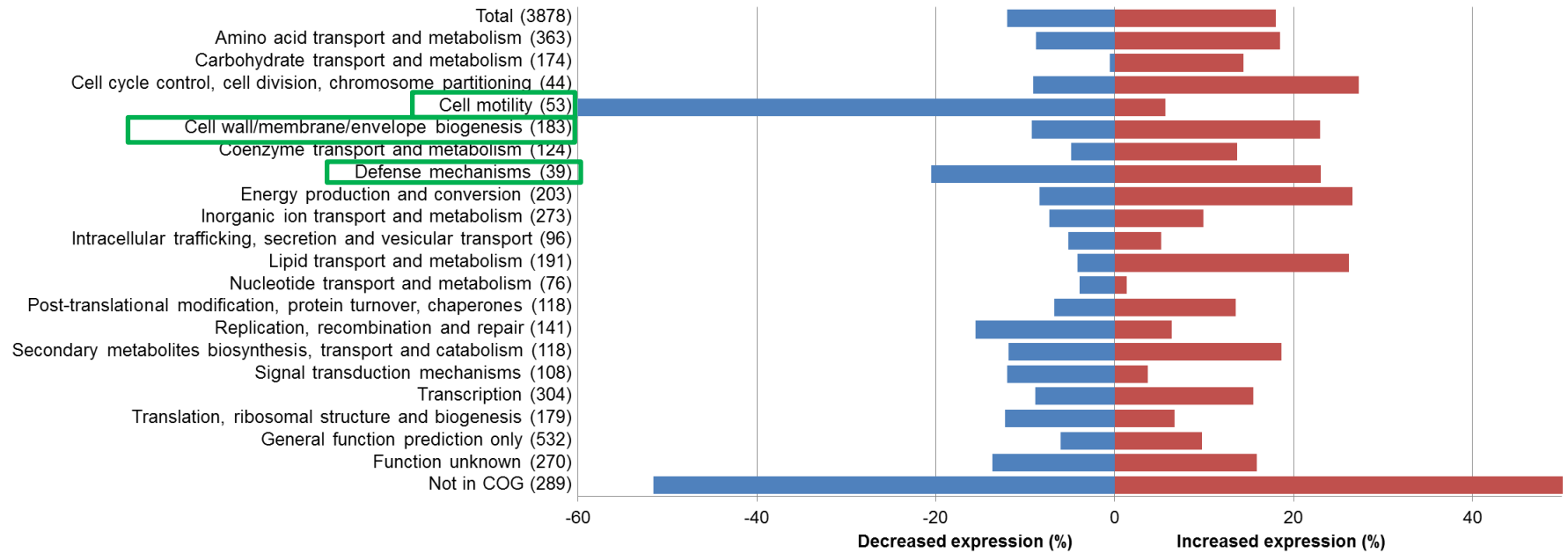
Gene ID	Start	End	Description	Common Name	Strand	Type	log2 fold change	Fold change	P.Value
ABAYE1878	1936951	1938105	coenzyme PQQ synthesis protein E	<i>pqqE</i>	-	gene	-9.10	0.002	3.40E-09
ABAYE1877	1935882	1936958	Zn-dependent dipeptidase	<i>acdP</i>	-	gene	-8.30	0.003	5.30E-09
ABAYE1880	1938383	1939141	coenzyme PQQ synthesis protein C	<i>pqqC</i>	-	gene	-9.60	0.001	1.30E-08
ABAYE1910	1963576	1964997	putative D-beta-hydroxybutyrate permease		-	gene	-7.80	0.004	2.80E-08
ABAYE1881	1939150	1940061	coenzyme PQQ synthesis protein B	<i>pqqB</i>	-	gene	-9.80	0.001	3.60E-08
ABAYE3706	3350123	3351448	putative phospholipase D protein fragment		+	pseudo gene	-7.80	0.004	3.80E-08
ABAYE1866	1929033	1929386	hypothetical protein		-	gene	-8.70	0.002	6.70E-08
ABAYE1879	1938102	1938386	coenzyme PQQ synthesis protein D	<i>pqqD</i>	-	gene	-7.50	0.006	1.20E-07
ABAYE1893	1948063	1948755	molybdate transport protein (ABC superfamily)	<i>modB</i>	-	gene	-7.50	0.006	1.50E-07
ABAYE1885	1940590	1942509	fragment of polyphosphate kinase polyphosphoric acid kinase	<i>ppk</i>	-	pseudo gene	-10.00	0.001	3.20E-07

**Table 4.7.4 The top 10 genes with the largest fold change in expression in S1Δ*adeAB* compared with S1**

Gene ID	Start	End	Description	Common Name	Strand	Type	log2 fold change	Fold change	P.Value
ABAYE1338	1398953	1399354	putative transthyretin domain		-	gene	2.80	6.964	4.00E-05
ABAYE1833	1900750	1900971	hypothetical protein		-	gene	2.80	6.964	1.90E-04
ABAYE2140	2189632	2189811	putative exported protein		+	gene	2.80	6.964	1.10E-03
ABAYE3658	3685510	3685983	Protein arsC (Arsenate reductase)	<i>arsC</i>	+	gene	2.80	6.964	1.20E-04
ABAYE2199	2247394	2247723	putative transcriptional regulator (ArsR family)		-	gene	2.70	6.498	2.40E-04
ABAYE1885	1940590	1942509	fragment of polyphosphate kinase	<i>ppk</i>	-	pseudo gene	-10.00	0.001	3.20E-07
ABAYE1881	1939150	1940061	coenzyme PQQ synthesis protein B	<i>pqqB</i>	-	gene	-9.80	0.001	3.60E-08
ABAYE1880	1938383	1939141	coenzyme PQQ synthesis protein C	<i>pqqC</i>	-	gene	-9.60	0.001	1.30E-08
ABAYE1878	1936951	1938105	coenzyme PQQ synthesis protein E	<i>pqqE</i>	-	gene	-9.10	0.002	3.40E-09
ABAYE1866	1929033	1929386	hypothetical protein		-	gene	-8.70	0.002	6.70E-08

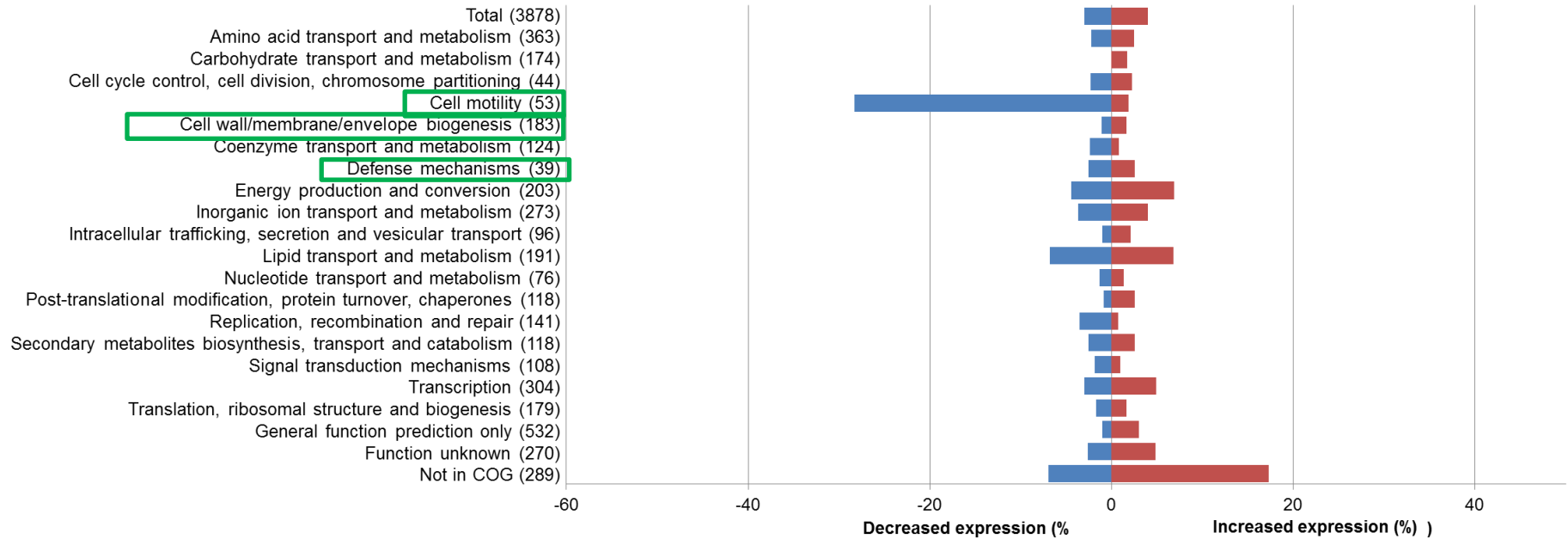


**Figure 4.7.4 Clusters of orthologous groups (COG) and the percentage of genes with increased expression (red) and decreased expression (blue) in *AYEΔadeB* compared with *AYE* within each group as determined by RNA-Seq**



The total number of genes per COG is shown in parentheses. Groups related to antibiotic resistance, biofilm formation and virulence are marked by a green box.

**Figure 4.7.5 Clusters of orthologous groups (COG) and the percentage of genes with increased expression (red) and decreased expression (blue) in S1ΔadeAB compared with S1 within each group as determined by RNA-Seq**



The total number of genes per COG is shown in parentheses. Groups related to antibiotic resistance, biofilm formation and virulence are marked by a green box.

products known to confer antibiotic resistance were identified in each mutant. In *AYEΔadeB* there was increased expression of a tetracycline efflux pump gene, *tetA* (1.4-fold); membrane fusion protein gene *AdeT* (1.4-fold), which is associated with MDR by active efflux in *A. baumannii* (Srinivasan, Rajamohan et al. 2011), a gene annotated as a putative porin associated with imipenem resistance (ABAYE0924) (4.3-fold) and two genes annotated as putative MDR efflux systems (ABAYE1777, ABAYE3036) (1.4-fold, 3-fold). There was decreased expression of genes encoding a putative tetracycline resistance protein (ABAYE2235) (1.7-fold) and the lipid phosphoethanolamine transferase *EptA* (2.5-fold), which has been associated with colistin resistance, (Adams, Nickel et al. 2009, Arroyo, Herrera et al. 2011, Beceiro, Llobet et al. 2011). There was altered expression of six genes putatively encoding β-lactamases (ABAYE0825, 1940, 2122, 2456, 3619, 3623; 2.2-50-fold) in *AYEΔadeB*. The only gene that was possibly related to drug-resistance and for which differential expression was detected, albeit a small increase, in *S1ΔadeAB* was a putative MDR efflux system (ABAYE3036) (1.1-fold). Interestingly, increased expression of this gene was seen in all three deletion mutants. In the *adeB* deletion mutants and similar to strain *AYEΔadeRS*, genes encoding products with known and potential virulence functions such as pili (Bahar, Goffer et al. 2009) and acinetobactin transport systems (Gaddy, Arivett et al. 2012), also had significant changes in expression levels. The ferric acinetobactin transport system operon *bauDCEBA*, which encodes proteins required for persistence and virulence (Mihara, Tanabe et al. 2004, Gaddy, Arivett et al. 2012), had decreased expression in *AYEΔadeB* (1.9 – 3.7-fold). In contrast to the significant increase in expression of these genes in *AYEΔadeRS* and the most striking change observed in both efflux pump mutants was in expression of cell

motility genes. The competence (*com*) genes which, as previously discussed, are associated with DNA uptake, motility and virulence, were all expressed significantly less in *AYEΔadeB* and *S1ΔadeAB* (1.7–10-fold). Likewise, there was a significant decrease in expression of the type IV pili genes, which are involved in natural transformation, twitching motility and biofilm formation. One other putative biofilm-associated gene (*ABAYE0792*) showed increased expression (3-fold) in *AYEΔadeB*. No other genes with an annotated biofilm function had altered expression in *S1ΔadeAB*. However, multiple putative transcriptional regulators (*araC*, *lysR* and *tetR* family) that lacked a comprehensive annotation had differential expression in both mutants.

#### **4.8. Discussion**

This study was carried out using two different efflux pump mutants. *AYEΔadeB* was created specifically for this study using an optimised method for creating targeted gene deletions in *A. baumannii* (Amin, Richmond et al. 2013). Primers were designed to delete a 1131 bp region in the middle of the *adeB* gene, rendering it inactive. Mapping of RNA-Seq reads showed that in this mutant there were no reads mapped to the deleted sequences. It was assumed that lack of expression of this region would result in lack of AdeB protein. However, it was not possible to confirm this by Western blotting as no antibodies were available and time did not permit raising them. Interestingly, RNA-Seq showed increased expression of *adeA* and *adeC* in the mutant. It is hypothesised that lack of AdeB triggers the cell to increase *adeABC* expression in order to produce more of the AdeABC efflux pump proteins and it is this that causes the apparent increase in the number of *adeA*, *adeB* and *adeC* reads mapped to the genome. It is also possible that the increased expression of these

genes may result in increased protein production and this could have caused some or all of the phenotypes observed in this mutant. Previous studies in *E. coli* and *S. Typhimurium* have shown that some MFPs homologous to AdeA, such as AcrA, can form a complex with multiple different RND components, such as AcrB and AcrF, and this may affect antibiotic resistance (Elkins and Nikaido 2003, Smith and Blair 2014). Altered expression of OMPs such as OmpA38, OmpA32, CarO and OmpW and has also been implicated in *A. baumannii* resistance to tetracycline, chloramphenicol, aztreonam and nalidixic acid (Yun, Choi et al. 2008, Smani, Fabrega et al. 2014). S1Δ*adeAB* was created in the laboratory of Professor Kim Lee Chua (National University of Singapore) (Amin, Richmond et al. 2013). The deletion spanned 222 bp of *adeA* and 1914 bp of *adeB*. RNA sequencing showed that the first 978 bp of *adeA* was still transcribed. Therefore is it possible that a truncated protein of 326 amino acid may be produced. However, as almost one fifth of the protein is missing it is unlikely that this protein would retain function and therefore, the phenotype presented has been interpreted as the result of lack of both proteins. This presents some difficulties with comparing this mutant with the AYE *adeB* deletion mutant; as the latter still produces a functional AdeA. However, due to the technical difficulties in genetically manipulating *A. baumannii*, this study was continued with the mutant obtained.

Individual RNA-Seq experiments described here and in Chapter 3 were carried out on separate occasions. A summary of the protocols used for each experiment can be seen in Table 4.8.1. Although the experiments were carried out according to best practice, as discussed in Chapter 3, it is now known that there can be variability in

**Table 4.8.1 Protocols used for RNA-Seq experiments**

<b>Dataset</b>	<b>Date</b>	<b>Service provider</b>	<b>Machine</b>	<b>Sequencing type</b>	<b>No. of biological replicates</b>
AYE vs <i>AYEΔadeRS</i>	Aug-12	ARK genomics	Hi-seq	Single-end	3
AYE vs <i>AYEΔadeB</i>	Mar-15	University of Birmingham	Mi-seq	Paired-end	4
S1 vs <i>S1ΔadeAB</i>	Sep-15	BGI Hong Kong	Hi-seq	Paired-end	3

data generated from samples prepared on different days and sequenced on different runs and it is important to standardise as much of the RNA-Seq procedure as possible. In order to minimise variability as much as possible when comparing between data sets, all RNA-seq data from across the three individual experiments were analysed as a single set by Dr Alasdair Ivens (University of Edinburgh), a renowned expert in bioinformatics. This allowed gene expression changes in one mutant to be compared with another. However, future work would ensure that all RNA-seq experiments are carried out at the same time, using the same protocol and technology.

The hypothesis investigated was that the AdeABC efflux pump is required for drug resistance, biofilm formation and virulence. Deletion of *adeB* in AYE resulted in decreased MICs of similar antibiotics previously shown by the Courvalin group to be substrates of the AdeABC efflux pump in *A. baumannii* BM4587 (Magnet, Courvalin et al. 2001, Yoon, Courvalin et al. 2013, Yoon, Nait Chabane et al. 2015). The observed decrease in efflux activity in *AYEΔadeB* suggests that increased drug susceptibility is a result of reduced levels of efflux in this strain. Changes in MICs were more pronounced with deletion of *adeB* than *adeRS*. This suggests that although deletion of *adeRS* results in up to 128-fold decrease in expression of *adeABC*, the efflux pump is still transcribed albeit at low level in the *adeRS* mutant. It may be that this is also responsible for the difference in the amount of biofilm formed by these strains on plastic. Whilst deletion of *adeB* in strain AYE resulted in a significant decrease in biofilm formation at both 30°C and 37°C, deletion of *adeRS* had no significant effect. It is hypothesised that low levels of expression of *adeABC* in

strain *AYEΔadeRS* are sufficient to maintain biofilm function, whereas inactivation of the pump in *AYEΔadeB* significantly reduces the ability to form a biofilm.

Deletion of *adeAB* in a different background, clinical isolate S1, resulted in no change in drug susceptibility however increased susceptibility to the efflux inhibitor, PAβN was detected. It is hypothesised that the limited impact upon susceptibility to antimicrobials after inactivation of AdeAB in S1 is a result of little change in expression of *adeABC* between S1 and its mutant. S1 does not possess the Ala94Val mutation in AdeS that is associated with overexpression of *adeABC* (Hornsey, Loman et al. 2011) and so does not express high levels of *adeABC*. This may explain the modest impact of deletion of *adeAB* in S1 upon susceptibility to antibiotics and is why S1 is more susceptible to antibiotics than strain AYE. The observed decrease in efflux in *S1ΔadeAB* was also less than that seen in *AYEΔadeB*, supporting this hypothesis. Deletion of *adeAB* in S1 also had no significant effect on biofilm formation on plastic, which also may be due to the small impact of deleting a gene expressed at low level.

Both the *adeB* mutant in AYE and the *adeAB* mutant in S1 displayed reduced biofilm formation on mucosal tissue when visualised by confocal laser scanning microscopy. Furthermore, as seen with the *adeRS* mutant in AYE, there was no change in the number of adherent cells on the mucosal tissue. S1 was able to form a biofilm more rapidly than AYE, suggesting that there may be other factors present in this strain that contribute to biofilm formation on mucosal tissue. The biofilm phenotype of the efflux pump deletion mutants was similar to that observed in the AdeRS deletion mutant (Chapter 3), suggesting that the biofilm defect in these strains is due to down regulation or deletion of the *adeB* gene. Deletion of *adeB* in AYE and *adeAB* in S1



also resulted in decreased expression of *pil* genes. These encode type IV pili, which have previously been associated with the ability of *A. baumannii* to form a biofilm on plastic (Tucker, Nowicki et al. 2014) and this may play a role in the biofilm defect observed in these mutants.

Despite a change in expression of known (and putative) genes that confer virulence in *A. baumannii*, such as the acinetobactin iron acquisition system, and pilin genes, deletion of *adeB* in strain AYE had no effect on virulence in *G. mellonella*. A similar observation was made for the AYE $\Delta$ *adeRS* mutant (Chapter 3). It is possible that AYE does not express the *adeABC* efflux genes *in vivo*. In contrast, deletion of *adeAB* in S1 greatly reduced virulence in the *G. mellonella* model. The membrane fusion protein (MFP) gene, *adeA*, is also partially deleted in strain S1, which may account for this observation. As discussed above, previous studies have shown that some MFPs can interact with multiple different RND components (Elkins and Nikaido 2003, Smith and Blair 2014). The presence of AdeA in strain AYE may allow it to interact with other proteins and so compensate for the lack of AdeB and ameliorate any impact upon virulence in this model. However, no other *A. baumannii* efflux pumps have so far been shown to play a role in virulence. This could indicate a strain-specific role for the AdeABC efflux pump in virulence. As a correlation between virulence in *G. mellonella* and in humans has previously been observed with *A. baumannii* (Peleg, Jara et al. 2009) this could indicate that for some *A. baumannii* strains, such as S1, AdeABC is required for infection in humans.

#### 4.9. Further work

To confirm that AdeB is not produced in either mutant and to determine whether AdeA is produced in *S1ΔadeAB* (despite a 222 bp fragment of the gene being deleted), Western blotting should be carried out. In order to do this, antibodies against AdeA and AdeB need to be generated as there are currently none available. This method would show the presence or absence of the AdeA and AdeB proteins and confirm whether deletion of a fragment of the gene abolishes production of the efflux pump proteins. It is possible that the different sized fragments deleted in *AYEΔadeB* and *S1ΔadeAB* affected the phenotype of these mutants. In order to standardise the experiment, the same deletion should be created in each strain to confirm that AdeB has a strain-specific role in antibiotic resistance, biofilm formation and virulence. To elucidate the role of each component of the efflux pump in each strain, *adeA* and *adeB* should be deleted alone and in combination in both AYE and S1. Nonetheless, it should be noted that the *adeABC* efflux pump genes are transcribed as an operon and therefore deletion of *adeA* is likely to have a downstream effect on expression of *adeB*. Furthermore, *adeB* should be deleted in other *A. baumannii* strains representative of those causing infection in different countries.

As mentioned previously, this study used RNA-Seq data from multiple experiments carried out at different times using different protocols. In order to minimise variation, all RNA-Seq experiments should be repeated together, ensuring that the same service provider, machine and sequencing method is used. As discussed in Chapter 3, steps should be taken to minimise variation in sample preparation and sequencing and more biological replicates should be used to give more robust data.

#### 4.10. Key findings

- Deletion of AdeB in *A. baumannii* strain AYE resulted in decreased MICs of antibiotics and dyes and was associated with a reduction in efflux activity.
- An AdeB deletion mutant of *A. baumannii* strain AYE and an AdeAB deletion mutant of S1 displayed decreased biofilm formation and epithelial cell killing in a mucosal model.
- Deletion of AdeB had a strain-specific effect on biofilm formation on plastic and virulence in *G. mellonella*.
- Deletion of AdeB in *A. baumannii* strain AYE and AdeAB in S1 produced changed expression of genes related to drug resistance, biofilm formation and virulence.

## **5. The Role of AdeRS and AdeAB in Antibiotic Resistance, Biofilm Formation and Motility in Military Isolate AB5075**

### **5.1. Background**

As described in Chapters 3 and 4, deletion of AdeRS or AdeB in MDR strain AYE resulted in decreased susceptibility to antibiotics by reduced efflux activity and decreased biofilm formation on biotic and abiotic surfaces. Deletion of AdeAB in another strain, clinical isolate S1, resulted in a different phenotype to that observed in AYE; decreased biofilm formation on a biotic surface only and decreased virulence in *Galleria mellonella*. To determine whether the strain-specific effect of deletion or down-regulation of the AdeABC efflux pump in AYE and S1 was also seen in a strain representative of contemporary isolates from infections in military casualties, the phenotype of military isolate AB5075 was characterised and compared to isogenic mutants with transposon insertions in *adeR*, *adeS*, *adeA* and *adeB* (Jacobs, Thompson et al. 2014, Gallagher, Ramage et al. 2015).

### **5.2. Hypothesis**

Inactivation of *adeR*, *adeS*, *adeA* or *adeB* by transposon insertion will affect antibiotic resistance, biofilm formation and motility in a MDR contemporary military isolate AB5075.

### **5.3. Aims**

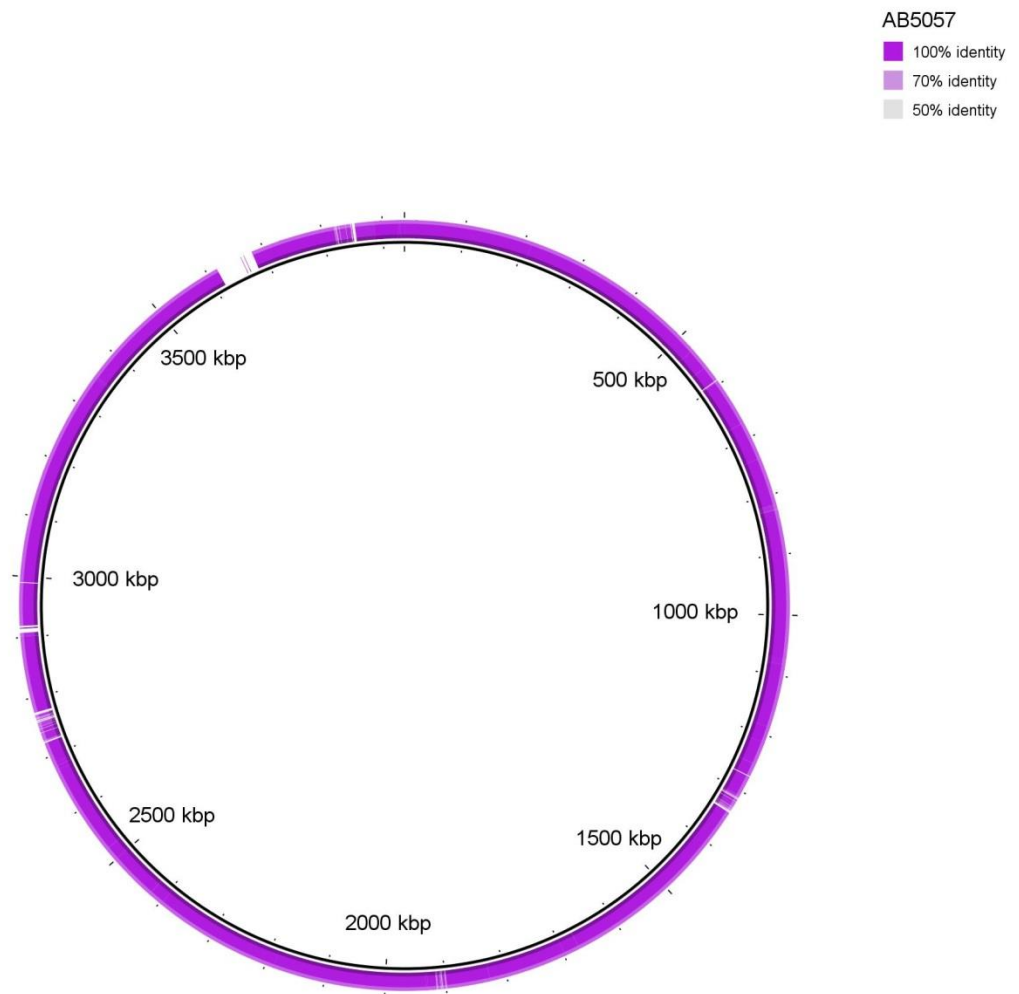
The aim of this study was to identify the consequences of transposon mutagenesis of *adeR*, *adeS*, *adeA* and *adeB* in *A. baumannii* strain AB5075. The objectives were to

characterise the antibiotic resistance, biofilm formation and motility phenotype of transposon mutants of AB5075 obtained from the University of Washington.

#### **5.4. Choice of strains and verification of strains**

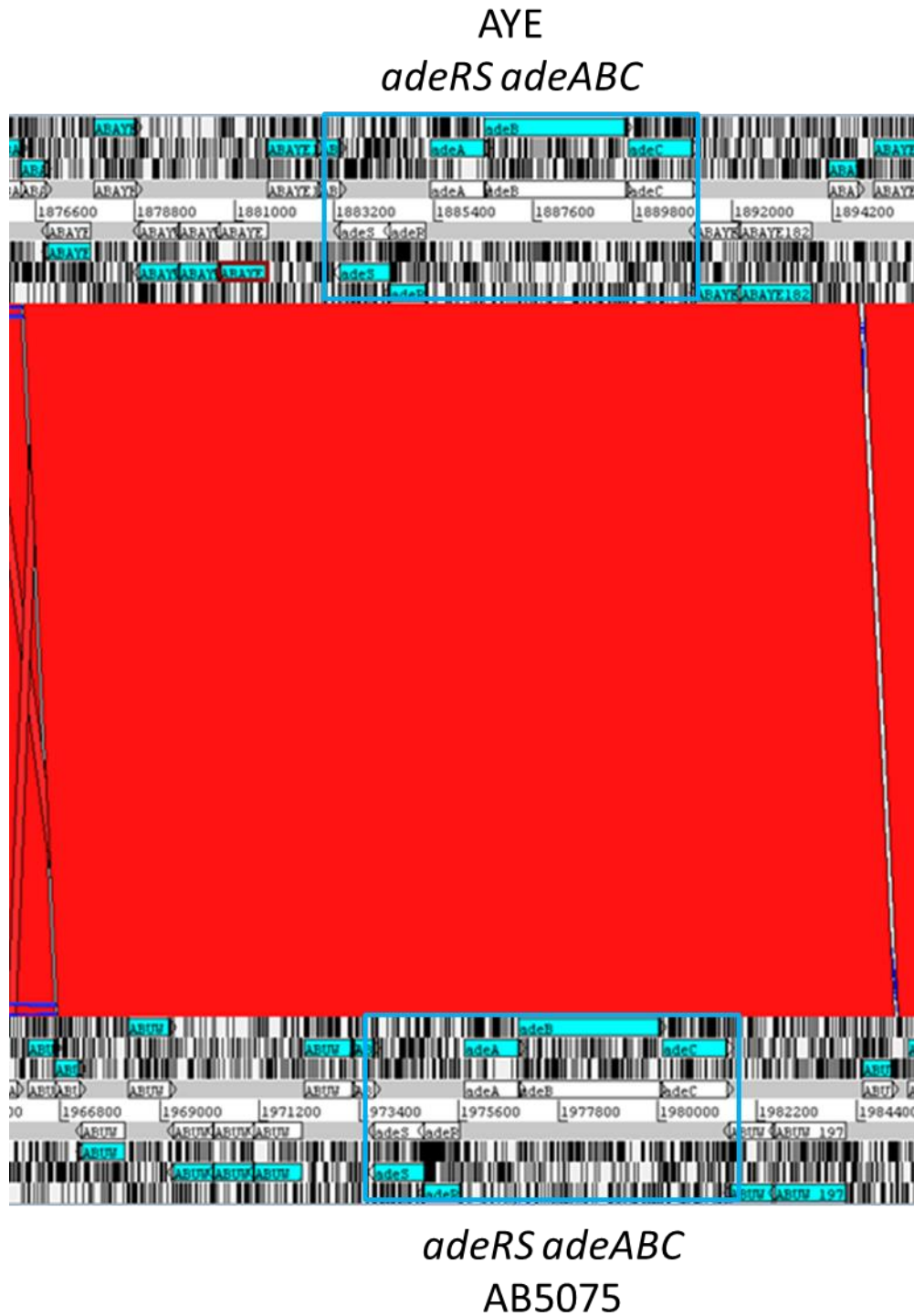
Strain AB5075 is a clinical isolate from a patient in the US military health care system and was selected by Jacobs *et al.* as a model strain that is representative of current clinical isolates. It is highly virulent in established model infections, and can be genetically manipulated without a potential sacrifice to virulence and antibiotic resistance (Jacobs, Thompson *et al.* 2014). AB5075 was isolated from a patient with osteomyelitis in 2008. Like strain AYE, AB5075 is ST1 of International clone 1. Comparison of the genomes of AYE and AB5075 using the Basic Local Alignment Search Tool (BLAST) Ring Image Generator (BRIG) (Alikhan, Petty *et al.* 2011) showed high sequence similarity between the two strains (Figure 5.4.1) and alignment of the *adeRS* and *adeABC* sequences of AYE and AB5075 using the Artemis Comparison Tool (ACT) (Carver, Rutherford *et al.* 2005) showed 100% sequence identity between the two strains, with AB5075 possessing the same Ala94Val mutation in AdeS as AYE (Figure 5.4.2). This mutation has been previously associated with upregulation of the AdeABC efflux system and increased resistance to antibiotics (Hornsey, Loman *et al.* 2011). A comprehensive ordered transposon (Tn26 and Tn101) mutant library was constructed in this strain by Gallagher *et al.*, providing an arrayed library of mutants with defined transposon insertions in most non-essential genes (Gallagher, Ramage *et al.* 2015). In order to minimise missed genotype-phenotype associations arising from non-inactivating mutations, several different mutations were constructed for each gene. Due to the long and labourious

**Figure 5.4.1 BRIG output image of BLAST comparison of the AB5075 genome (purple) against an AYE reference genome**



The black inner ring represents the AYE genome and the purple ring represents the AB5975 genome. Gaps in the purple ring indicate areas of the AYE genome that are not present in AB5075.

Figure 5.4.2 Snapshot of a BLASTN comparison of the *adeRS* and *adeABC* regions of AYE and AB5075 using ACT



The *adeRS* and *adeABC* operons are marked by the blue box. Red indicates 100% sequence identity.

process required to create genetic modifications in *A. baumannii*, Tn26 or Tn101 mutants with insertional inactivation of *adeR*, *adeS*, *adeA* and *adeB* were obtained from this transposon mutant library (Gallagher, Ramage et al. 2015). Two mutants, with insertions in different locations in each gene were obtained for each of *adeR*, *adeS*, *adeA* and *adeB* (Table 5.4.1). Transposon insertion into each gene was confirmed by PCR using primers internal to the transposon in combination with primers with homology to the gene, and with primers that spanned the insertion region, producing a larger or no amplicon for the transposon insertion mutant (Figure 5.4.1, Figure 5.4.2). Amplification of a 1284 bp product was seen using a reverse primer binding to *adeS* and a forward primer specific to the Tn26 transposon in Tn26-*adeR*1. For Tn101-*adeR*2 verification, a 694 bp product was produced from parental strain AB5075 using primers spanning the Tn101 insertion site, whereas no product was observed for the mutant. Amplification of a 589 bp product was seen using a reverse primer binding to *adeS* and a forward primer binding to the Tn26 transposon in Tn26-*adeS*1. For Tn26-*adeS*2 verification, a 979 bp product was produced from parental strain AB5075 using primers spanning the Tn101 insertion site, whereas no product was observed for the mutant. Amplification of a 724 bp and 948 bp product was seen using a forward primer binding to *adeA* and a reverse primer specific to the Tn26 transposon in Tn26-*adeA*1 and Tn26-*adeA*2, respectively. Amplification of a 2385 bp and 2373 bp product was seen using a forward primer binding to *adeA* and a reverse primer specific to the Tn26 transposon in Tn26-*adeB*1 and Tn26-*adeB*2, respectively.



**Table 5.4.1 Transposon mutants obtained from the University of Washington Transposon Mutant Library**

<b>Strain</b>	<b>Genome</b>	<b>Tn</b>				<b>Gene</b>	<b>Position within gene</b>	
<b>name</b>	<b>Transposon</b>	<b>Position</b>	<b>Direction</b>	<b>Ab Locus</b>	<b>Strand</b>	<b>Name</b>	<b>(total bp of gene)</b>	<b>Frame</b>
Tn26-								
<i>adeR1</i>	Tn26	1974926	F	ABUW_1973	-	<i>adeR</i>	671(744)	-3
Tn101-								
<i>adeR2</i>	Tn101	1975476	F	ABUW_1973	-	<i>adeR</i>	121(744)	-2
Tn26-								
<i>adeS1</i>	Tn26	1974227	F	ABUW_1972	-	<i>adeS</i>	595(1086)	-2
Tn26-								
<i>adeS2</i>	Tn26	1974689	R	ABUW_1972	-	<i>adeS</i>	133(1086)	+2
Tn26-								
<i>adeA1</i>	Tn26	1976299	F	ABUW_1974	+	<i>adeA</i>	558(1191)	+1
Tn26-								
<i>adeA2</i>	Tn26	1976523	F	ABUW_1974	+	<i>adeA</i>	782(1191)	+3

Tn26-

<i>adeB1</i>	Tn26	1977961	F	ABUW_1975	+	<i>adeB</i>	1030(3108)	+2
--------------	------	---------	---	-----------	---	-------------	------------	----

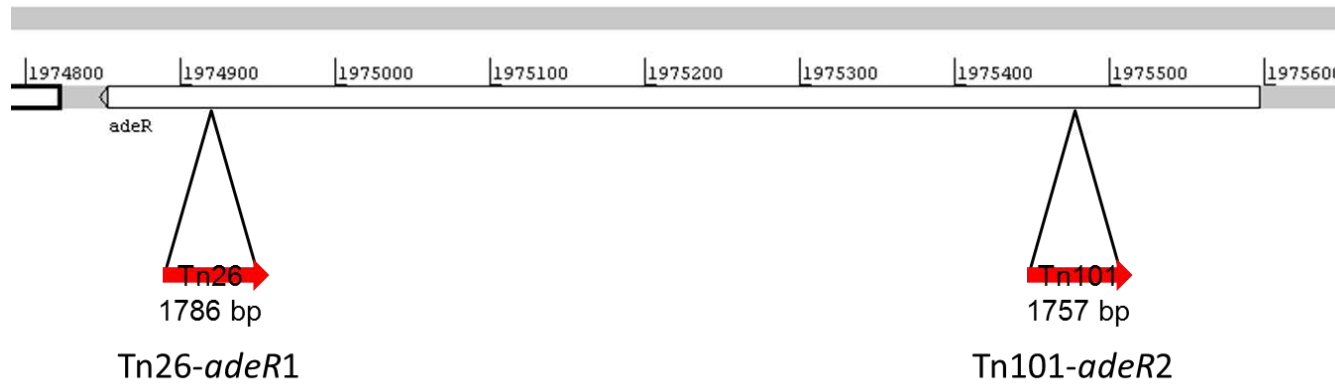
Tn26-

<i>adeB2</i>	Tn26	1979116	F	ABUW_1975	+	<i>adeB</i>	2185(3108)	+2
--------------	------	---------	---	-----------	---	-------------	------------	----

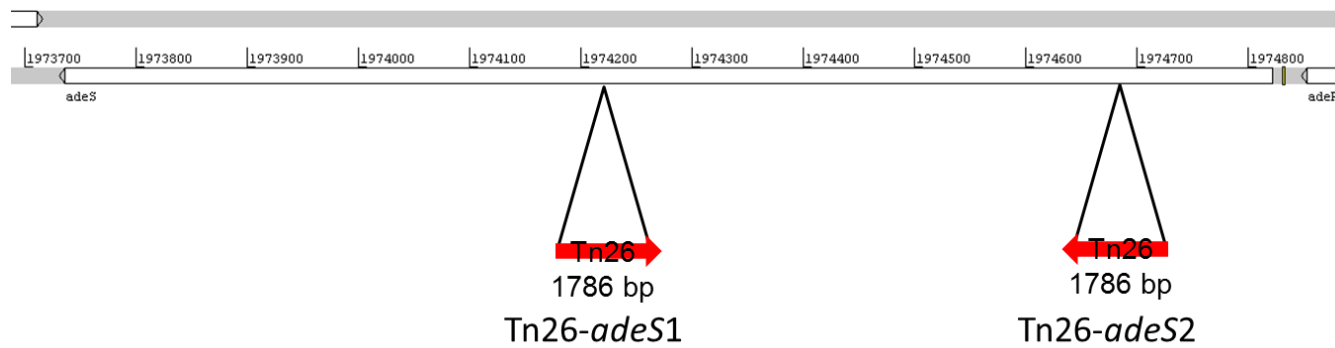
---

Figure 5.4.1 Schematic showing the location of transposon insertion in each AB5075 transposon mutant

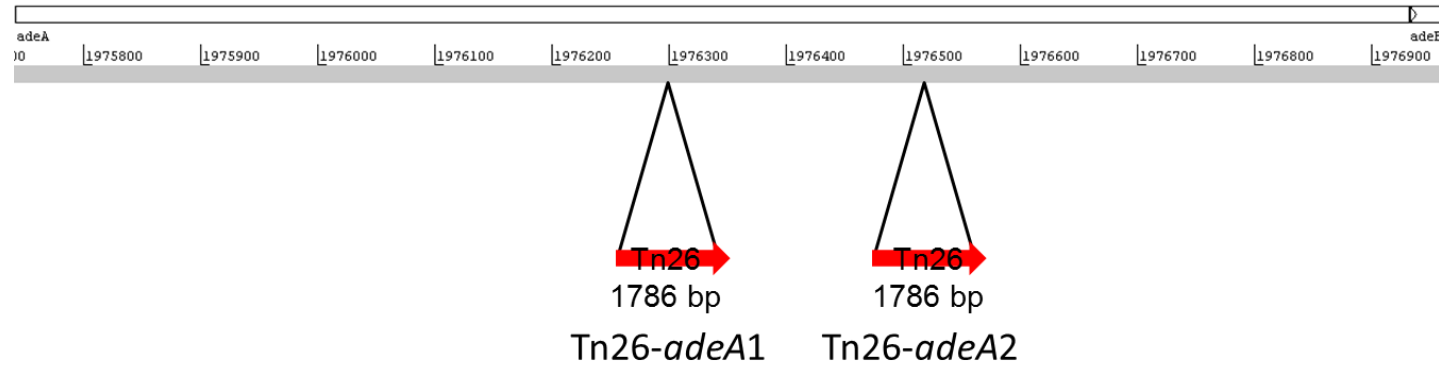
**A. Transposon insertion in *adeR***



**B. Transposon insertion in *adeS***



### C. Transposon insertion in *adeA*



### D. Transposon insertion in *adeB*

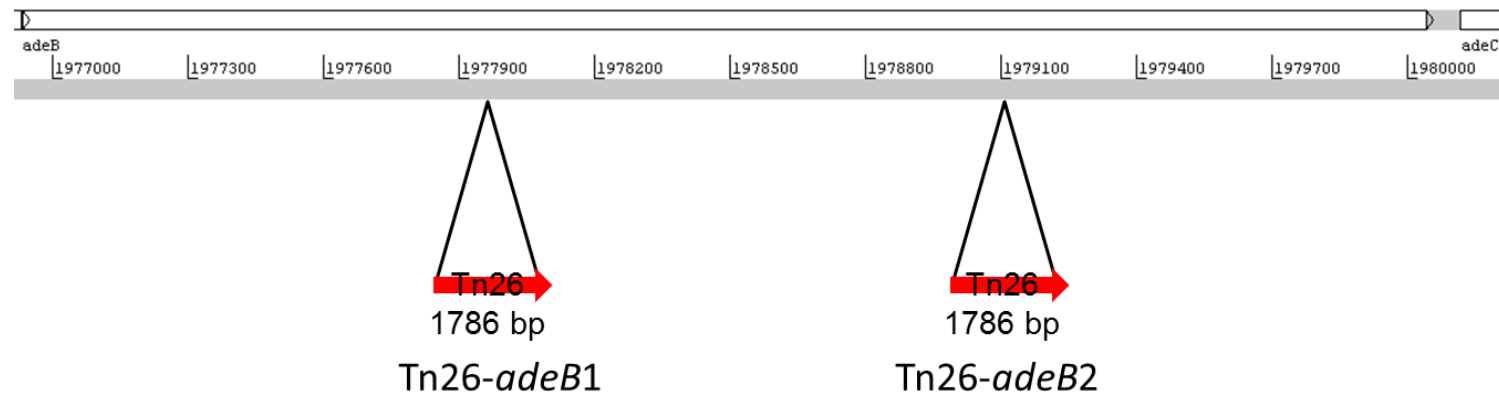
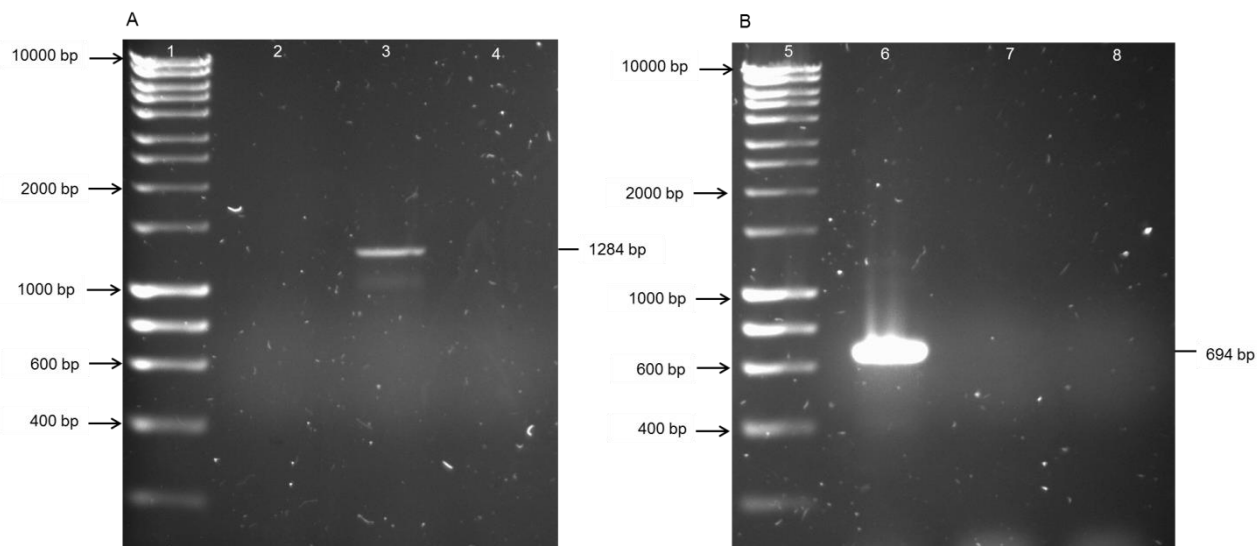


**Figure 5.4.2 Verification of transposon insertion in AB5075 transposon mutants by PCR**

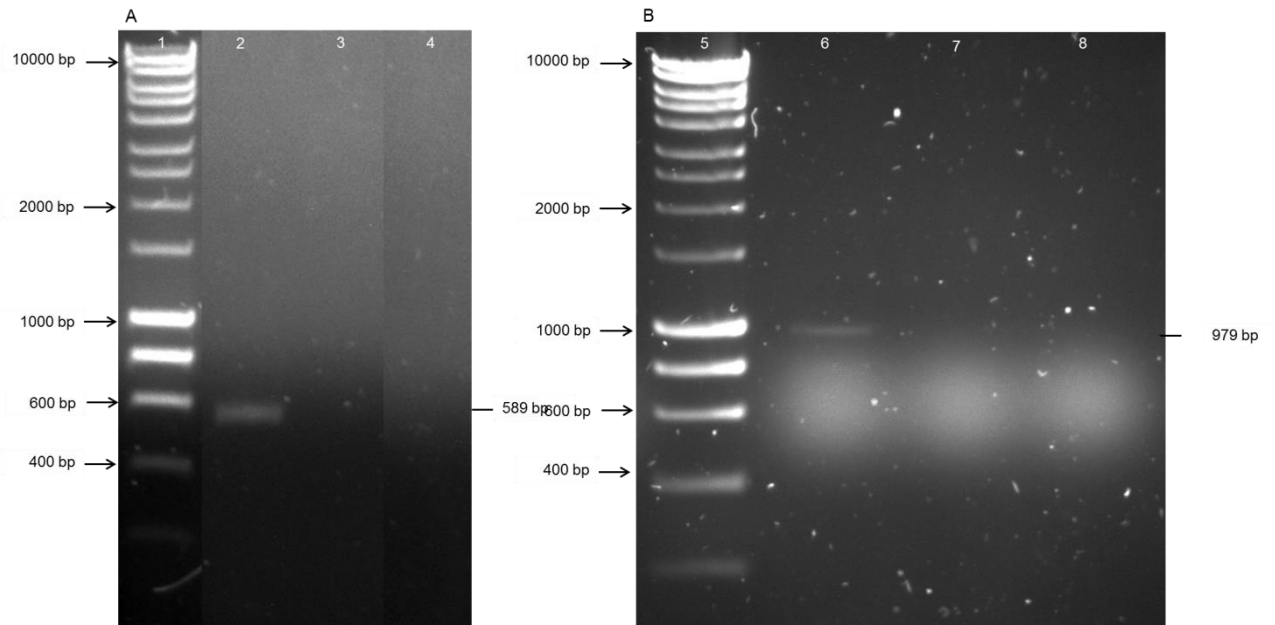
**A. Tn26-*adeR1* and Tn101-*adeR2* verification**



Panels: A, PCR amplimers produced using primer internal to the transposon and primer with homology to the gene; B, PCR amplimers produced using primers spanning the insertion region.

Lane	Template	Predicted fragment size (bp)	Actual fragment size (bp)
1	Hyperladder 1kb	-	-
2	AB5075	0	0
3	Tn26- <i>adeR1</i>	1284	1284
4	Negative control	0	0
5	Hyperladder 1kb	-	-
6	AB5075	694	694
7	Tn101- <i>adeR2</i>	2451	0
8	Negative control	0	0

## B. Tn26-*adeS1* and Tn26-*adeS2* verification

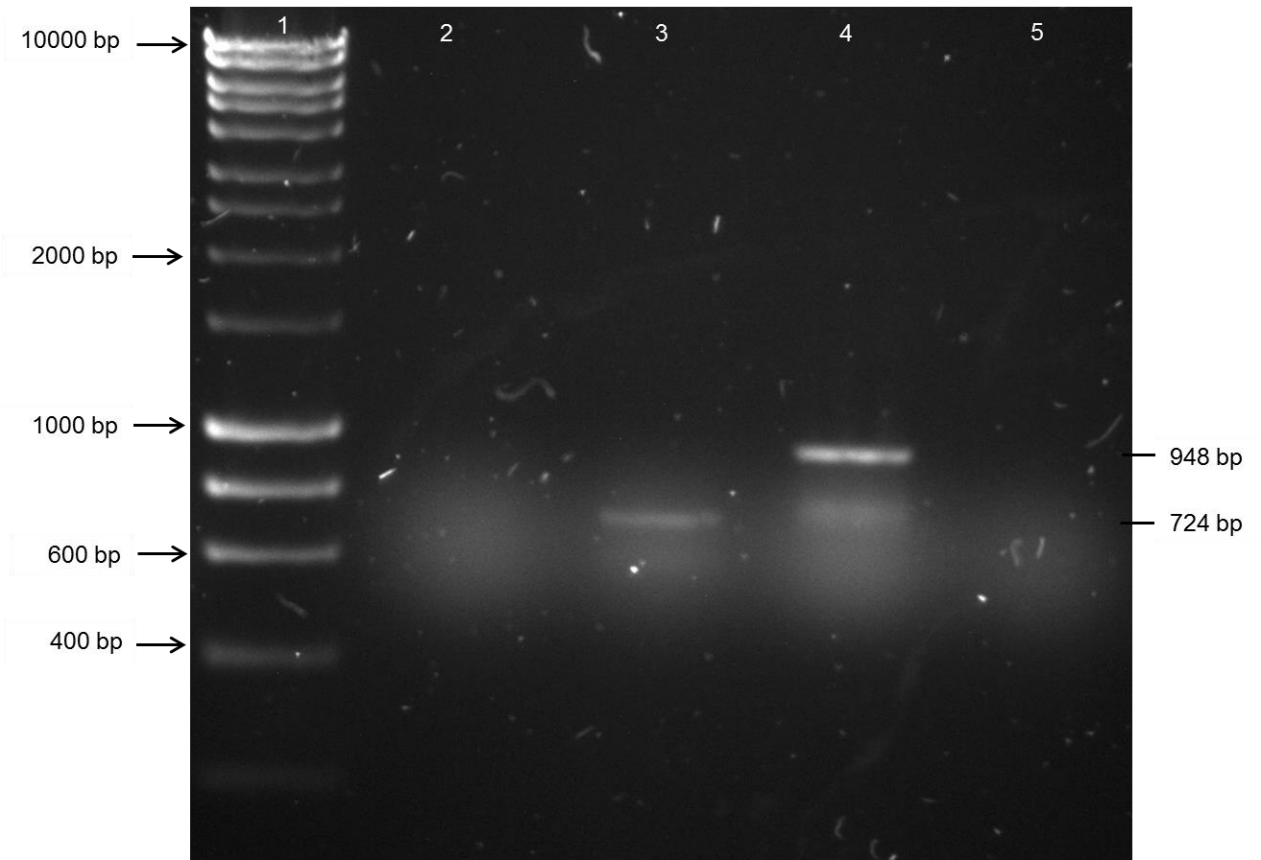


Panels: A, PCR amplimers produced using primer internal to the transposon and primer with homology to the gene; B, PCR amplimers produced using primers spanning the insertion region.

Lane	Template	Predicted fragment size (bp)	Actual fragment size (bp)
1	Hyperladder 1kb	-	-
2	Tn26- <i>adeS1</i>	589	589
3	AB5075	0	0
4	Negative control	0	0
5	Hyperladder 1kb	-	-
6	AB5075	979	979
7	Tn26- <i>adeS2</i>	2765	0
8	Negative control	0	0

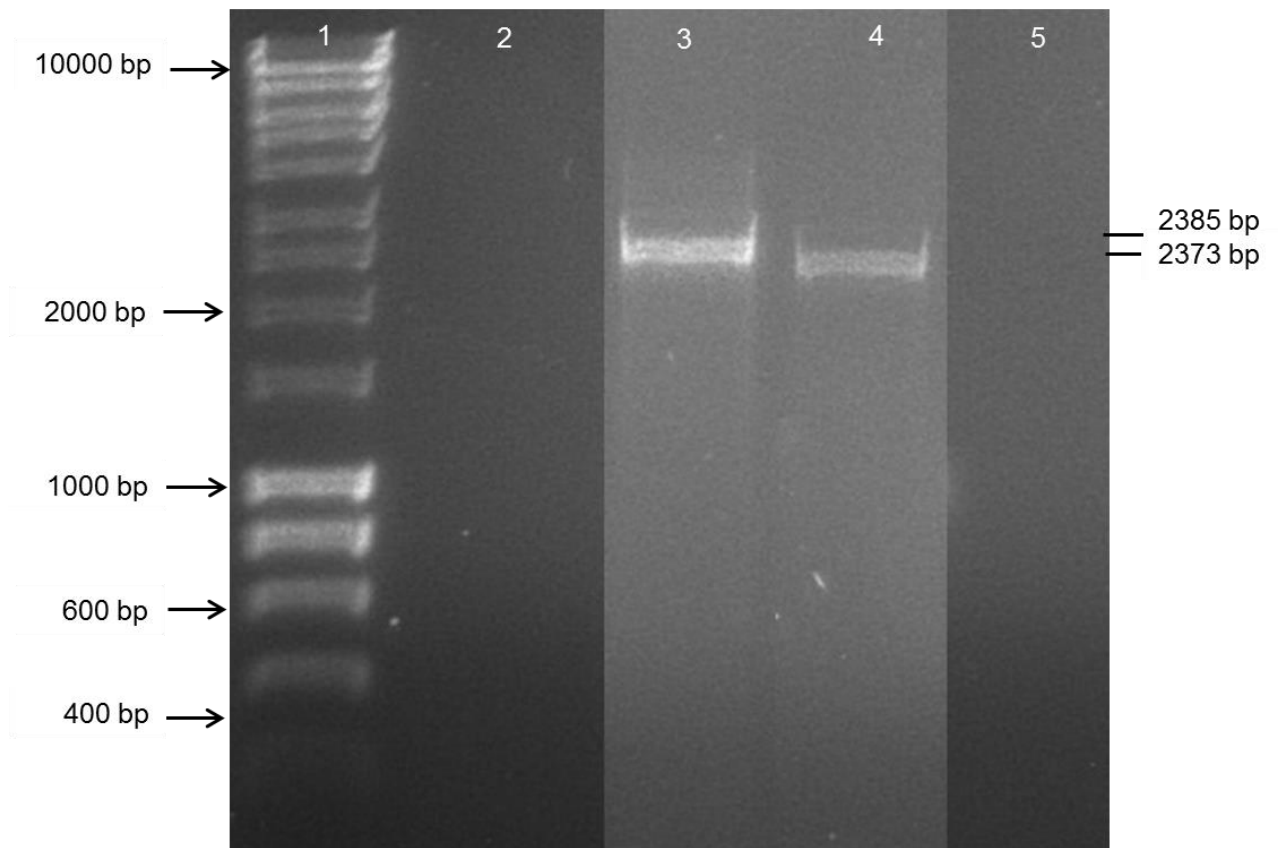
Although all PCR products were electrophoresed on the same gel; the figure has been constructed from a single image to show only those strains relevant to this study.

### C. Tn26-*adeA1* and Tn26-*adeA2* verification



Lane	Template	Predicted fragment size (bp)	Actual fragment size (bp)
1	Hyperladder 1kb	-	-
2	AB5075	0	0
3	Tn26- <i>adeA1</i>	724	724
4	Tn26- <i>adeA2</i>	948	948
5	Negative control	0	0

#### D. Tn26-*adeB1* and Tn26-*adeB2* verification



Lane	Template	Predicted fragment size (bp)	Actual fragment size (bp)
1	Hyperladder 1kb	-	-
2	AB5075	0	0
3	Tn26- <i>adeB1</i>	2385	2385
4	Tn26- <i>adeB2</i>	2373	2373
5	Negative control	0	0

Although all PCR products were electrophoresed on the same gel; the figure has been constructed from a single image to show only those strains relevant to this study.



## **5.5. Determining the phenotype of *adeR*, *adeS*, *adeA* and *adeB* transposon mutants in AB5075**

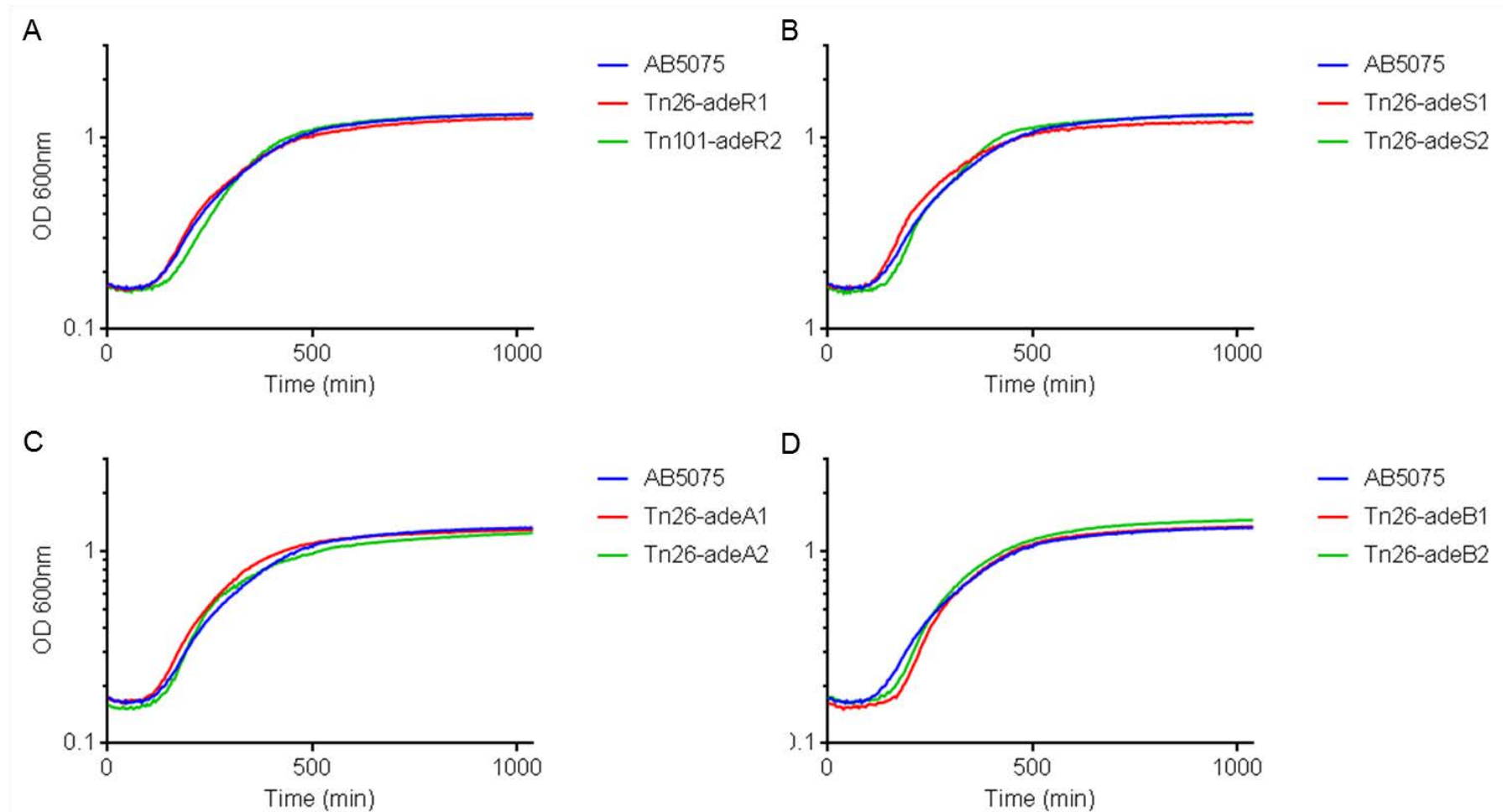
### **5.5.1. Bacterial growth kinetics of AB5075 transposon mutants**

To determine whether Tn26 or Tn101 inactivation of *adeR*, *adeS*, *adeA* or *adeB* had an effect on the growth rate of AB5075, the growth kinetics of the parental strain and Tn mutants were determined by measuring the optical density of cell cultures grown in LB broth at 37°C over time. The generation time of both *adeB* transposon mutants was significantly lower than that of the parental strain AB5075 ( $P < 0.05$ ), suggesting that deletion of *adeB* in this strain confers a small growth defect (Figure 5.5.1, Table 5.5.1). However, there was no difference in the final optical density at 600 nm reached by the *adeB* transposon mutants. A similar phenotype was observed in an *adeB* deletion mutant in AYE, with a significant decrease in generation time but no change in final optical density at 600 nm. The final optical density at 600 nm reached by Tn26-*adeR*1 and Tn26-*adeS*1 was significantly lower than that reached by the parental strain ( $P < 0.05$ ), but there was no difference in the generation times of these mutants when compared with AB5075 (Figure 5.5.1, Table 5.5.1).

### **5.5.2. Antimicrobial susceptibility of AB5075 transposon mutants**

To determine whether transposon insertion into *adeR*, *adeS*, *adeA* or *adeB* resulted in a change in susceptibility to antimicrobials, the MICs of commonly used antibiotics and dyes and those previously shown to be substrates of the AdeABC RND efflux pump in BM4587 (Yoon, Nait Chabane et al. 2015) were determined.. According to EUCAST recommended breakpoints ([http://www.eucast.org/clinical\\_breakpoints/](http://www.eucast.org/clinical_breakpoints/)) the

Figure 5.5.1 Growth kinetics of AB5075 transposon mutants in LB broth at 37°C



Panels: A, Tn-*adeR* mutants; B, Tn-*adeS* mutants; C, Tn-*adeA* mutants; D, Tn-*adeB* mutants. Data are shown as the mean of 3 biological replicates and are representative of a single independent experiment carried out at least 3 times.

**Table 5.5.1 Generation times and optical density at stationary phase of AB5075 transposon mutants in LB broth at 37°C**

Strain	Mean generation time (min)	<i>P</i> value	OD600 at stationary phase	<i>P</i> value
AB5075	103 ± 9.090	-	1.324 ± 0.009	-
Tn26- <i>adeR1</i>	101 ± 12.103	0.927	1.265 ± 0.004	0.001-
Tn101- <i>adeR2</i>	89 ± 13.622	0.379	1.317 ± 0.024	0.655
Tn26- <i>adeS1</i>	114 ± 12.982	0.425	1.199 ± 0.051	0.014
Tn26- <i>adeS2</i>	79 ± 3.976	0.104	1.313 ± 0.020	0.426
Tn26- <i>adeA1</i>	105 ± 13.383	0.847	1.292 ± 0.137	0.708
Tn26- <i>adeA2</i>	78 ± 1.703	0.092	1.244 ± 0.140	0.382
Tn26- <i>adeB1</i>	70 ± 1.846	0.042	1.344 ± 0.009	0.063
Tn26- <i>adeB2</i>	72 ± 1.398	0.049	1.155 ± 0.077	0.054

parental strain AB5075 was resistant to gentamicin, imipenem, meropenem and ciprofloxacin (Table 5.5.2). There were no EUCAST recommended breakpoint concentrations available for *Acinetobacter* spp. and seven drugs: ampicillin, ceftazidime, kanamycin, norfloxacin, tetracycline, tigecycline or chloramphenicol. There was a decrease in the MICs of kanamycin, gentamicin, tigecycline and the efflux inhibitor PA $\beta$ N for all eight transposon mutants tested (Table 5.5.2). Although some of these changes were only 2-fold, which is considered to be the margin of error for this method, these changes were consistent in three independent experiments. A decrease in the MIC of these antibiotics was also observed with deletion of *adeRS* or *adeB* in strain AYE (Table 3.5.1, Table 4.6.1). The change in the MIC of kanamycin and gentamicin was greater in transposon mutants Tn26-*adeA1* and Tn26-*adeA2* and greater still in Tn26-*adeB1* and Tn26-*adeB2*. Furthermore, a decrease in the MICs of ciprofloxacin and ethidium bromide was also observed for Tn26-*adeB1* and Tn26-*adeB2*. The Tn26 transposon contains a tetracycline resistance gene; in accordance with this there was an increase in the MIC of tetracycline in Tn26-*adeR1*, Tn26-*adeS1*, Tn26-*adeS2* and Tn26-*adeA1*, Tn26-*adeA2*, Tn26-*adeB1* and Tn26-*adeB2*. There was a small decrease in the MIC of colistin in Tn26-*adeS1*, Tn26-*adeS2* and Tn26-*adeA2* and an increase in Tn26-*adeA2*, Tn26-*adeB1* and Tn26-*adeB2*.

### **5.5.3. Hoechst 33342 (bis-benzimide) accumulation by AB5075 transposon mutants**

As described in Chapter 3, accumulation of H33342 is a good indication of efflux activity in *A. baumannii* (Richmond, Chua et al. 2013). To determine whether there

**Table 5.5.2 MICs of antibiotics and dyes against AB5075 transposon mutants**

	MIC (µg/ml)								
	<b>AB5075</b>	<b>Tn26- <i>adeR1</i></b>	<b>Tn101- <i>adeR2</i></b>	<b>Tn26- <i>adeS1</i></b>	<b>Tn26- <i>adeS2</i></b>	<b>Tn26- <i>adeA1</i></b>	<b>Tn26- <i>adeA2</i></b>	<b>Tn26- <i>adeB1</i></b>	<b>Tn26- <i>adeB2</i></b>
Ampicillin	1024	1024	1024	1024	1024	1024	1024	1024	1024
Ceftazidime	>1024	>1024	>1024	>1024	>1024	>1024	>1024	>1024	>1024
Imipenem	19	19	19	19	19	19	19	19	19
Meropenem	24	24	24	24	24	24	24	24	24
Kanamycin	1024	512	512	512	512	256	256	128	128
Gentamicin	64	8	8	4	4	4	4	2	2
Norfloxacin	128	128	128	128	128	128	128	128	128
Ciprofloxacin	128	128	128	128	128	128	128	64	64

Colistin	2	2	2	0.5	1	8	2	8	4
Tetracycline	1	16	1	16	16	16	16	16	16
Tigecycline	2	0.5	0.5	0.5	0.5	0.5	0.5	0.5	0.5
Chloramphenicol	512	512	512	512	512	512	512	512	512
PA $\beta$ N	1024	512	512	512	512	512	512	512	512
Ethidium bromide	512	512	512	512	512	512	512	256	256

---

Blue text indicates a decrease in MIC compared to that for AB5075; red text indicates an increase in MIC compared to that for AB5075.

was a relative difference in the intracellular accumulation levels of this substrate. Accumulation of H33342 in each transposon mutant was compared with that in AB5075 (Figure 5.5.2). When compared with AB5075, there was no significant difference in the steady state accumulation level of H33342 in any of the Tn26 or Tn101 mutants. These data suggest that there is no change in efflux levels of this substrate with inactivation of *adeR*, *adeS*, *adeA* or *adeB*.

#### **5.5.4. Ethidium bromide efflux by AB5075 transposon mutants**

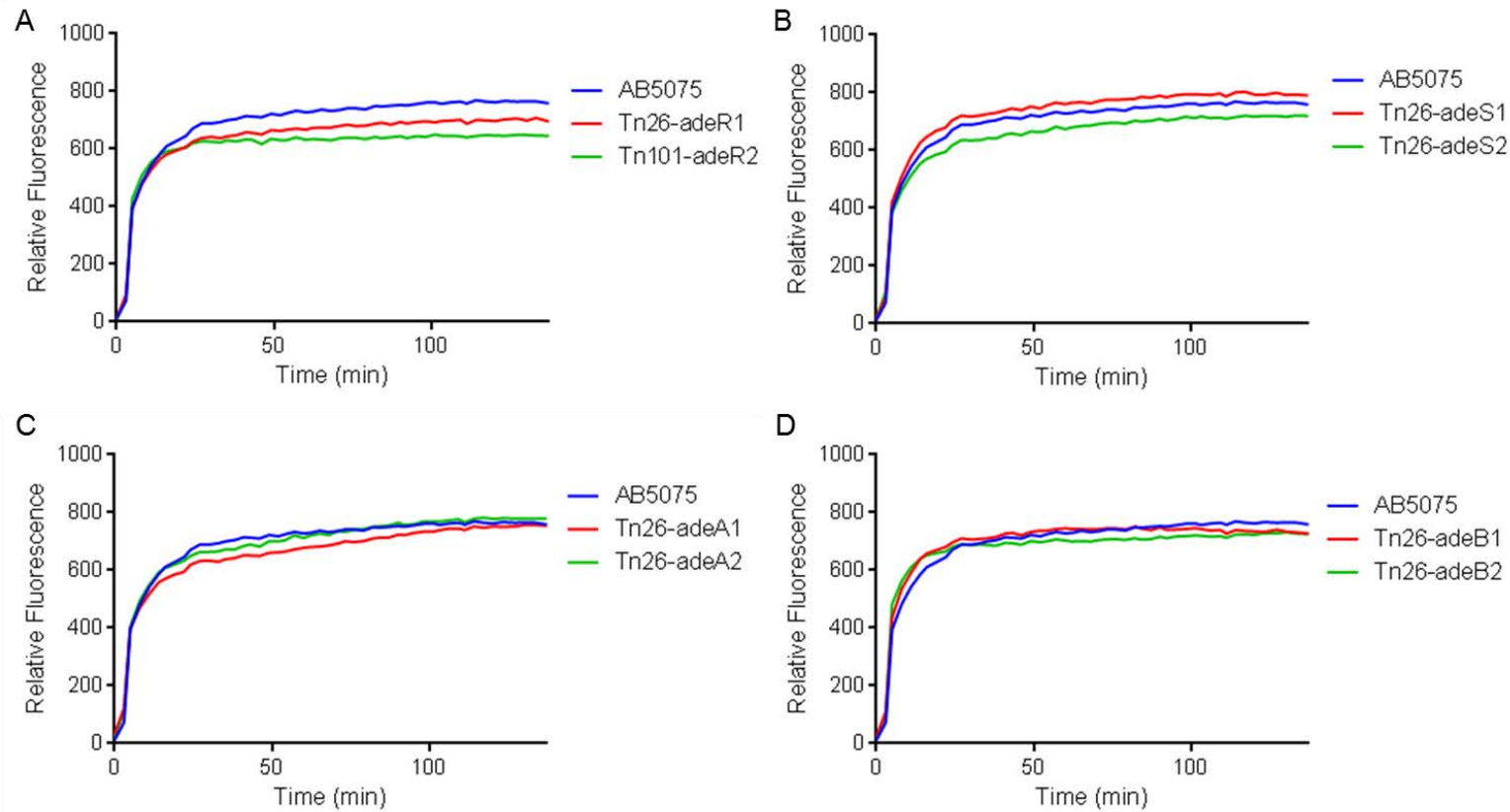
Efflux of ethidium bromide by AB5075 and its transposon mutants was measured to investigate whether there was a difference in the relative efflux levels of this substrate. Except for Tn26-*adeS2*, the relative steady state accumulation level of ethidium bromide was significantly higher in all mutants (Figure 5.5.3). The biggest change in accumulation was observed in Tn26-*adeA2*, in which the final accumulation level of ethidium bromide was 62% higher than in the parental strain AB5075.

#### **5.5.5. Biofilm formation by AB5075 transposon mutants *in vitro***

AB5075 is a clinical isolate taken from the US military health care system and is representative of current clinical isolates causing infection in hospitals (Jacobs, Thompson et al. 2014). In order to determine whether the ability to form a biofilm in abiotic surfaces is important in the clinical success of these isolates and whether AdeRS and AdeAB play a role in this process, biofilm formation in three different *in vitro* models was measured.

**Figure 5.5.2 Accumulation of H33342 by AB5075 transposon mutants**

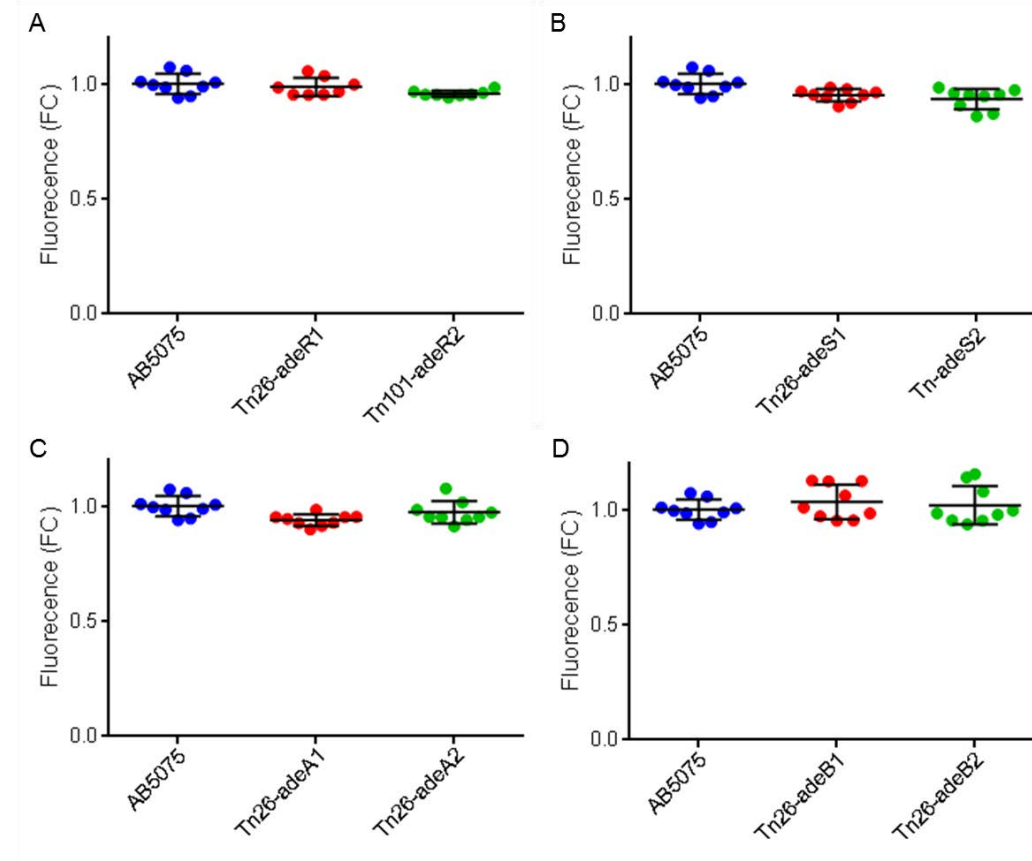
**A. Accumulation of H33342 in AB5075 transposon mutants over time**



Panels: A, Tn-*adeR* mutants; B, Tn-*adeS* mutants; C, Tn-*adeA* mutants; D, Tn-*adeB* mutants. Data are shown as fluorescence values over time and represent the mean of three biological replicates. Data are a representative example of a single independent experiment carried out at least three times.



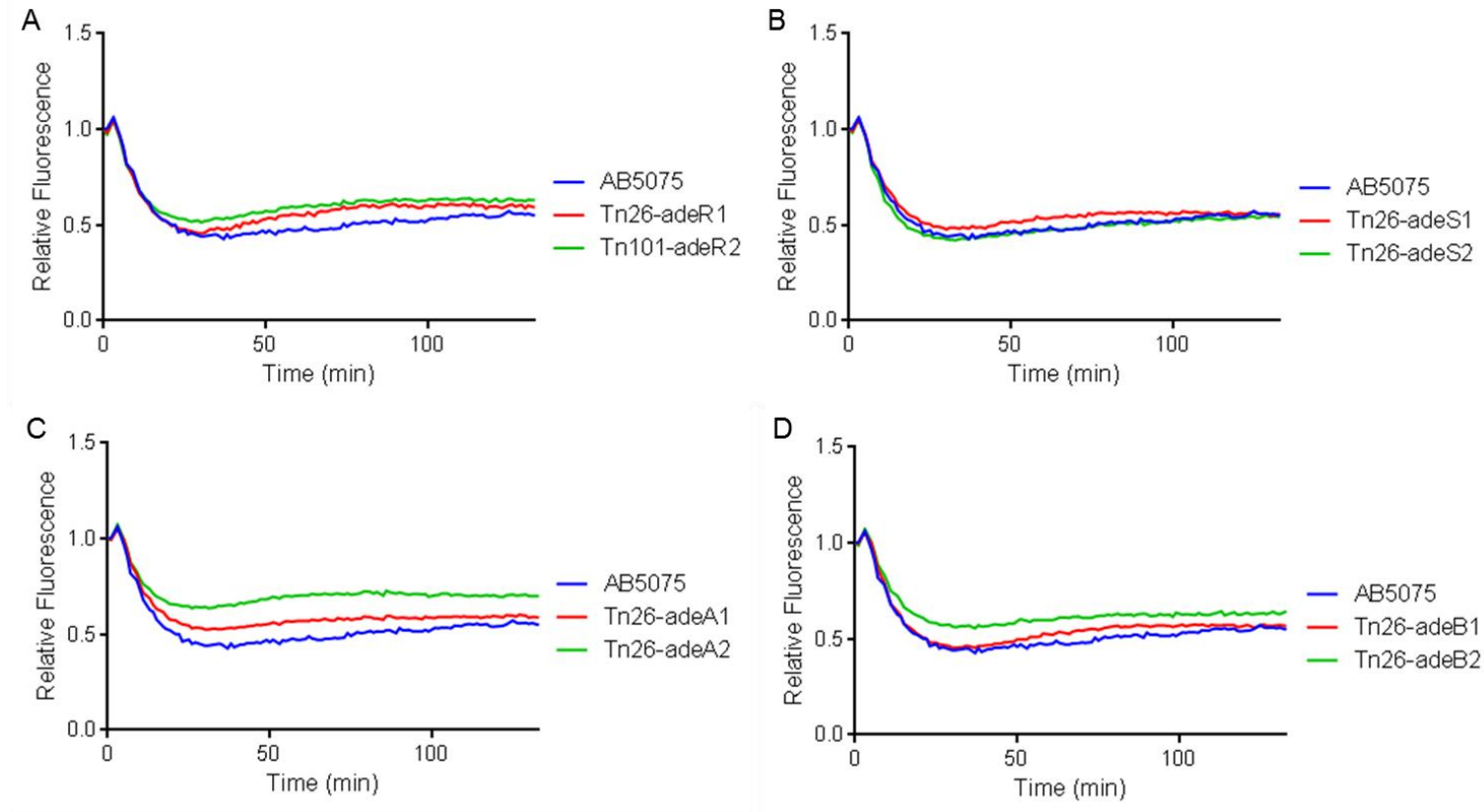
## B. Fold change in accumulation of Hoechst H33342 in AB5075 transposon mutants



Panels: A, Tn-*adeR* mutants; B, Tn-*adeS* mutants; C, Tn-*adeA* mutants; D, Tn-*adeB* mutants. Data are plotted as independent biological replicates to show variation within each strain. Data are presented as fold change compared to AB5075 at the point at which steady state accumulation was reached +/- standard deviation. Student's t-tests were performed and those returning P values of less than 0.05 are indicated by \*.

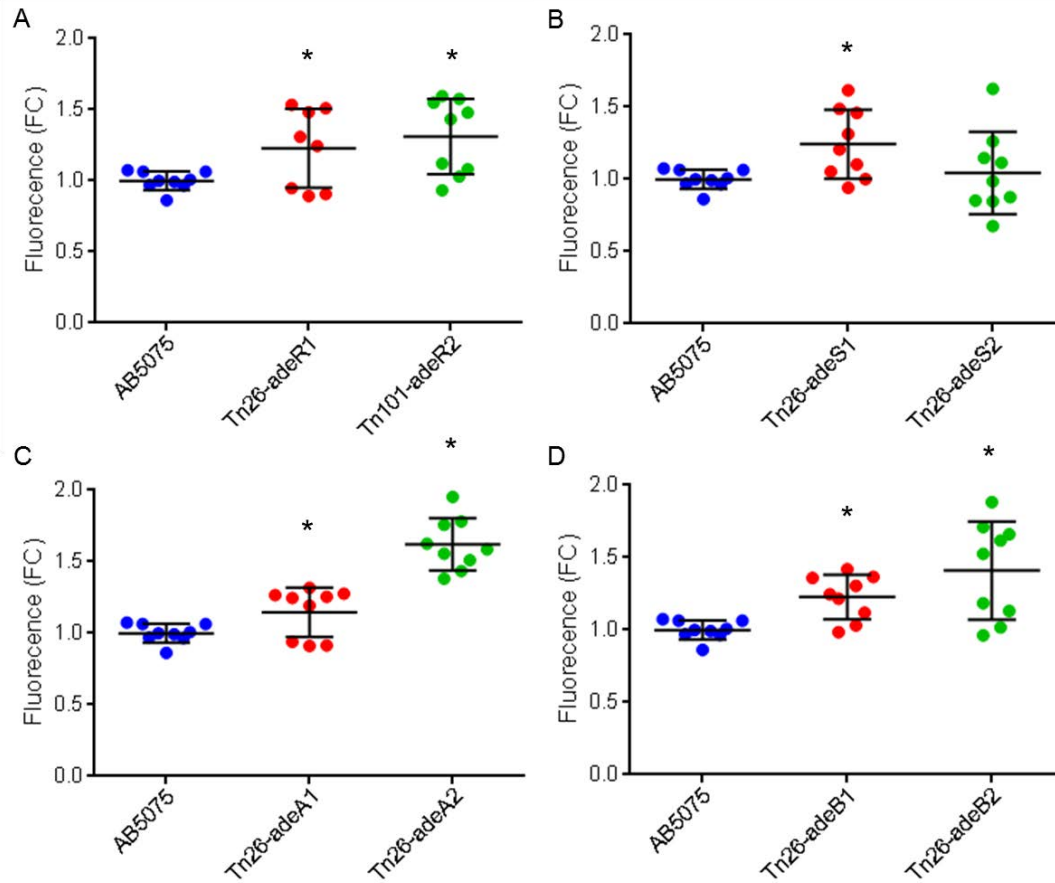
**Figure 5.5.3 Efflux of ethidium bromide by AB5075 transposon mutants**

**A. Efflux of ethidium bromide by AB5075 transposon mutants over time**



Panels: A, Tn-*adeR* mutants; B, Tn-*adeS* mutants; C, Tn-*adeA* mutants; D, Tn-*adeB* mutants . Data are shown as fluorescence relative to the starting fluorescence levels for each strain and represent the mean of three biological replicates. Data are a representative example of a single independent experiment carried out at least three times.

**B. Fold change in intracellular levels of ethidium bromide in AB5075 transposon mutants**



Panels: A, Tn-*adeR* mutants; B, Tn-*adeS* mutants; C, Tn-*adeA* mutants; D, Tn-*adeB* mutants . Data are plotted as independent biological replicates to show variation within each strain. Data are presented as fold change in final fluorescence value compared to AYE +/- standard deviation. Student's t-tests were performed and those returning P values of less than 0.05 are indicated by \*.

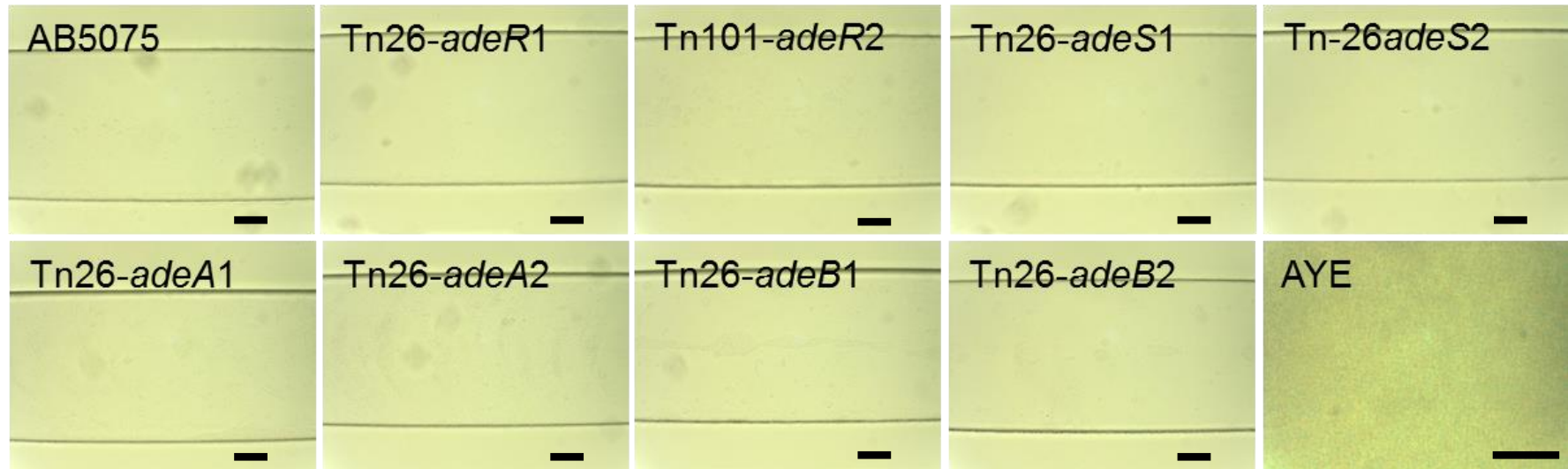
#### **5.5.5.1. Biofilm formation by AB5075 transposon mutants in a microfluidic cell**

Biofilm formation by AB5075 and its transposon mutants was studied under flow conditions in order to mimic biofilm formation on a medical device implanted in the body. AYE, which is also ST1, was included as a comparator and an example of a strain that rapidly produces a robust biofilm. As seen previously, AYE formed a robust biofilm after 16 hrs and thick biofilm coverage of the surface of the microfluidic cell was observed at 48 hrs (Figure 5.5.4). In contrast, AB5075 and the Tn26 and Tn101 mutants showed very little evidence of biofilm formation, even after 48 hrs.

#### **5.5.5.2. Biofilm formation AB5075 transposon mutants on polypropylene pegs**

To quantify the amount of biofilm formed by AB5075 and its transposon mutants, biofilms were grown on polypropylene pegs at 30°C and 37°C as described in Chapter 3. In this *in vitro* model, Tn26-*adeA2* showed a statistically significant decrease in biofilm formation. However this was only observed at 37°C (Figure 5.5.5). When compared with AYE, neither the parental strain nor the transposon mutants displayed a strong biofilm phenotype. This agrees with the results seen in the microfluidic cell. The mass of the AYE biofilm was 2.8 and 2.3 times that of AB5075 at 30° and 37°, respectively (Figure 5.5.5).

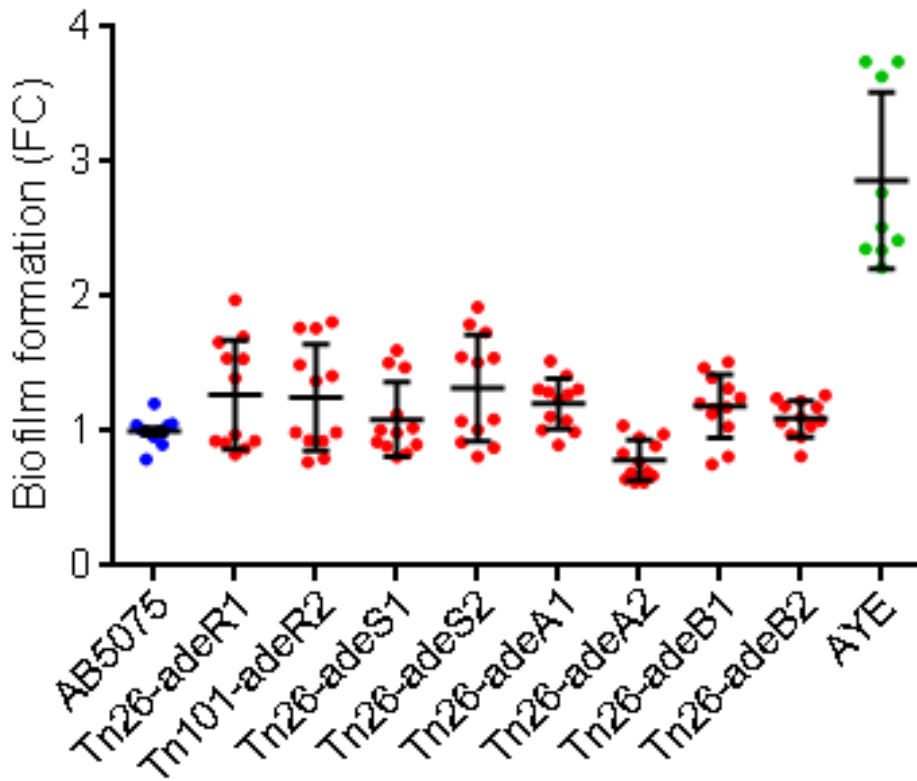
**Figure 5.5.4 Phase contrast microscopy images of AB5075 transposon mutant biofilms formed under flow conditions of 0.3 dynes at 48 hrs**



Images show attachment of bacterial cells to the inner surface of a microfluidic channel. Grey dots show adherence of individual cells to the surfaces whereas solid grey areas indicate bacterial growth and biofilm production. Black bar depicts a 20  $\mu\text{m}$  scale.

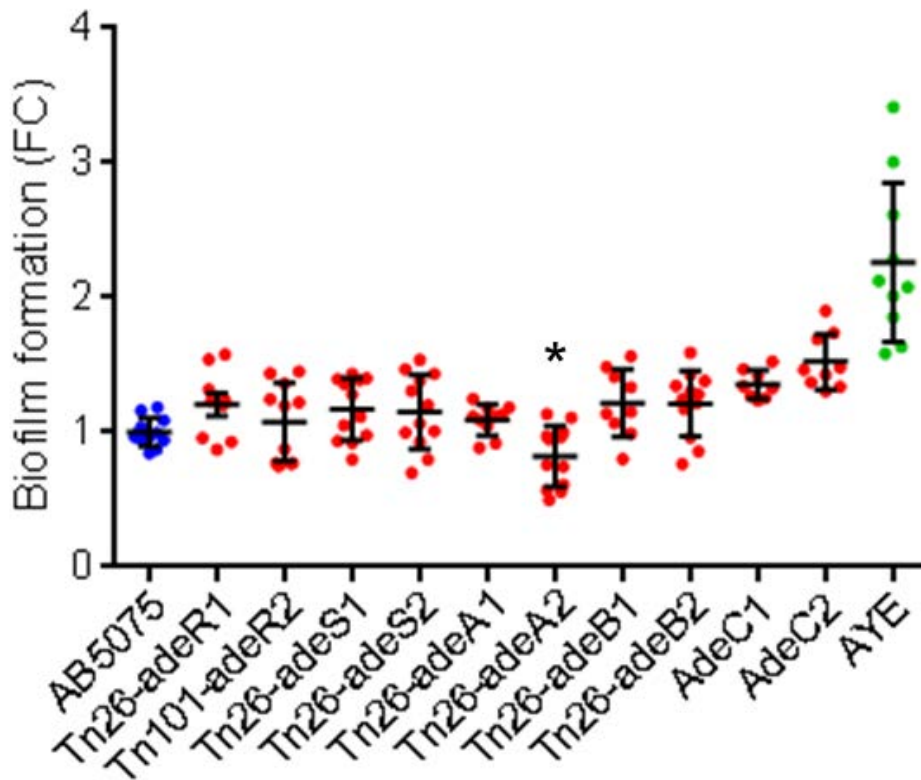
Figure 5.5.5 Biofilm formation by AB5075 transposon mutants on polypropylene pegs as determined by crystal violet staining

A. 30°C



Data are plotted as independent biological replicates to show variation within each strain. Data are presented as fold change in final fluorescence value compared to AB5075 +/- standard deviation. Student's t-tests were performed and those returning P values of less than 0.05 are indicated by \*.

B. 37C



Data are plotted as independent biological replicates to show variation within each strain. Data are presented as fold change in final fluorescence value compared to AB5075 +/- standard deviation. Student's t-tests were performed and those returning P values of less than 0.05 are indicated by \*.

### **5.5.5.3. Pellicle formation by AB5075 transposon mutants**

To examine the ability of AB5075 and its transposon mutants to form a pellicle at the air/liquid interface, cultures were incubated in test tubes for 48 hrs and pellicle formation was examined visually. A thick biofilm mat could be seen on the surface of the liquid of all cultures (Figure 5.5.6). However, there was no visual difference in the size of the pellicle formed by any of the Tn26 or Tn101 mutants.

### **5.5.6. Motility of AB5075 transposon mutants**

To determine whether inactivation of *adeR*, *adeS*, *adeA* or *adeB* had any effect on motility of AB5075, twitching and swarming motility were measured in 1% Mueller Hinton agar and 0.3% Luria-Bertani agar, respectively. AB5075 displayed some twitching motility and no swarming motility, typical of International Clone I (Figure 5.5.7); this motility phenotype was also observed with strain AYE. There was no change in twitching motility displayed by any of the Tn26 and Tn101 mutants. However, there was an increase in swarming motility in some of the mutants; AB5075 displayed coverage of 1.87% of the agar plate at 24 hrs whereas Tn101-*adeR2*, Tn26-*adeS2*, Tn26-*adeB1* and Tn*adeB2* covered 15.44%, 18.37%, 26.29% and 95.83%, respectively. This increase in motility was not seen in any of the AYE or S1 deletion mutants characterised in Chapters 3 and 4. However, a significant change in the expression of motility genes was observed in AYE $\Delta$ *adeRS*, AYE $\Delta$ *adeAB* and S1 $\Delta$ *adeAB* and it may be a similar change in expression of genes such as the *pil* and *com* operons that produces the increase in motility seen in these Tn26 and Tn101 mutants.



Figure 5.5.6 Pellicle formation by AB5075 transposon mutants incubated statically at 37°C and visualised under white light

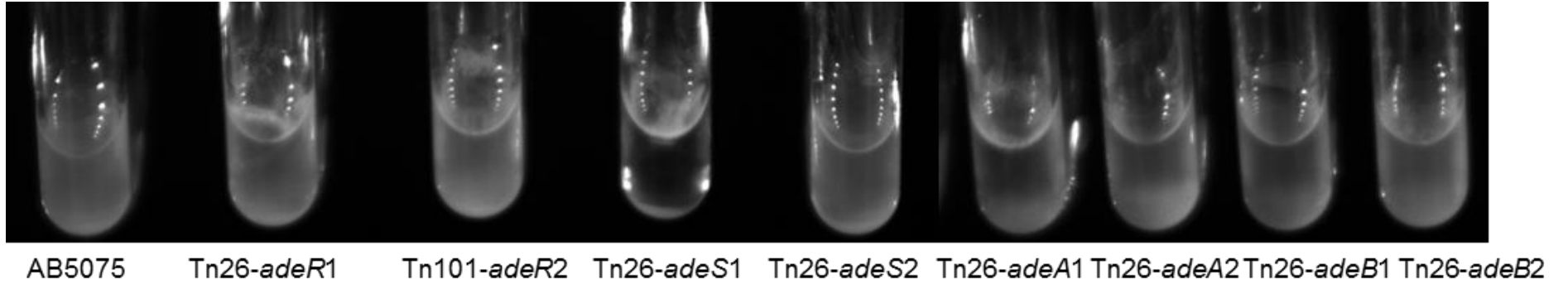
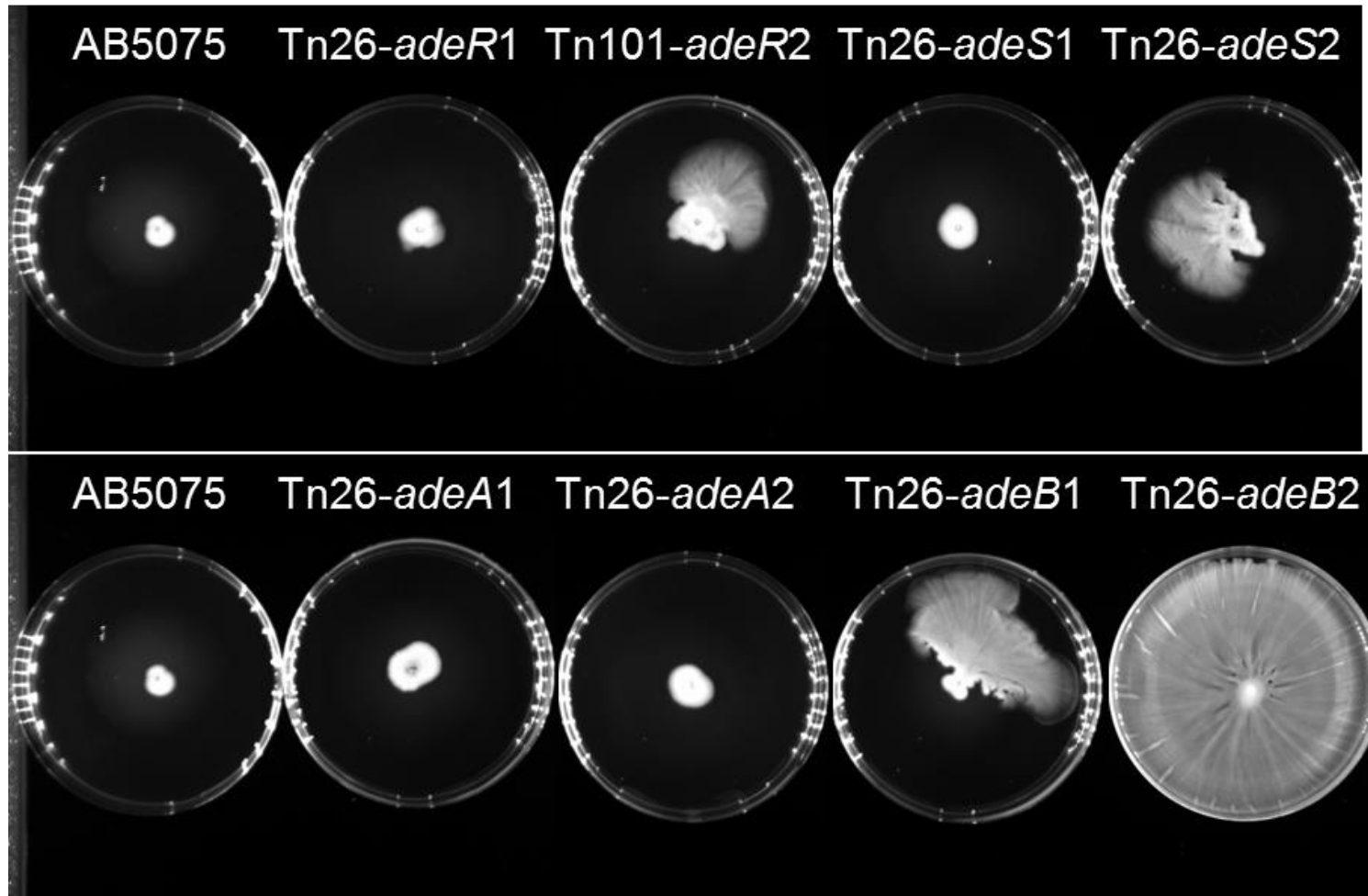


Figure 5.5.7 Swarming motility of AB5075 Tn mutants grown on 0.3% agar for 24 hrs at 37°C



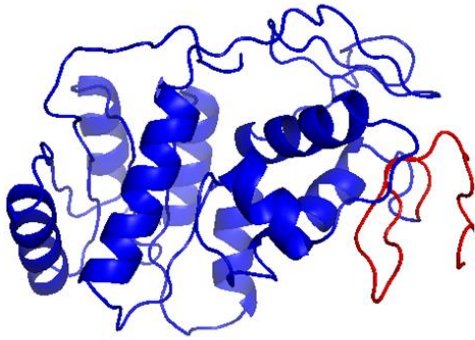
## 5.6. Protein modelling of AB5075 transposon mutants

To predict how much of the AdeR, AdeS, AdeA and AdeB proteins are removed by transposon insertion into the gene and to illustrate which part of the protein remains and may still be functional, I-TASSER protein modelling software was used to generate a predicted protein model based on sequence homology to known protein structures (Yang, Yan et al. 2015). Protein structures were viewed in PyMOL (<http://www.pymol.org>) and amino acids that were coded for downstream of the transposon insertion site were coloured in red. It was predicted that the STOP codons within the transposon sequence would prevent translation of the protein downstream of the insertion site and so these parts of the protein would not be produced.

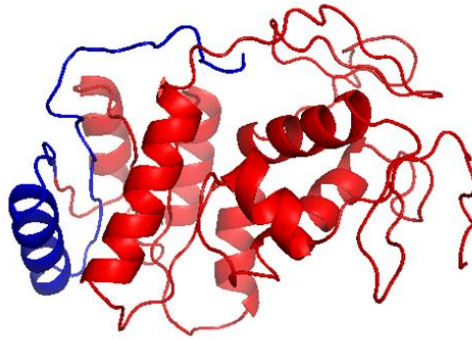
Insertion of the transposon in Tn26-*adeR1* occurred at position 671 in the gene, resulting in the last 25 amino acids being deleted (Figure 5.6.1). As the coding region for the first 223 amino acids was still intact and this includes the effector domain and the majority of the signal receiver domain, this could result in an assembled protein, retaining some AdeR function. However, the MIC changes observed for Tn26-*adeR1* were the same as those observed for Tn101-*adeR2*, which only has the coding region for the first 40 amino acids intact (Figure 5.6.1). AdeR in Tn101-*adeR2* is very unlikely to retain any function as only the first 28 amino acids of the effector domain and none of the signal receiver domain is present. These data suggest that AdeR is inactivated in both of these mutants. In Tn26-*adeS1* and Tn26-*adeS2*, translation of a substantial part of the protein, including the histidine kinase domain and the transmembrane domain, was removed by transposon insertion

Figure 5.6.1 Predicted protein structures of AdeR, AdeS, AdeA and AdeB generated by I-TASSER

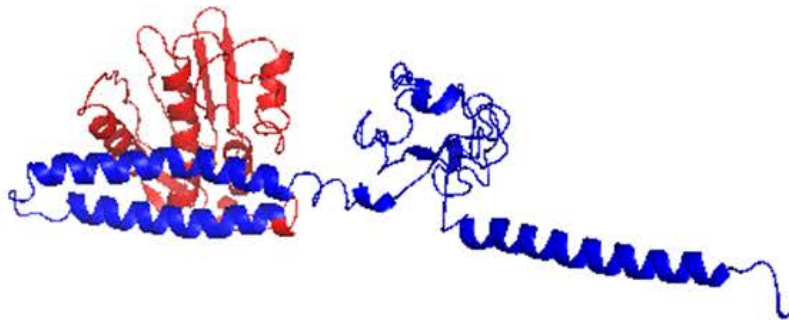
Tn26-*adeR1*



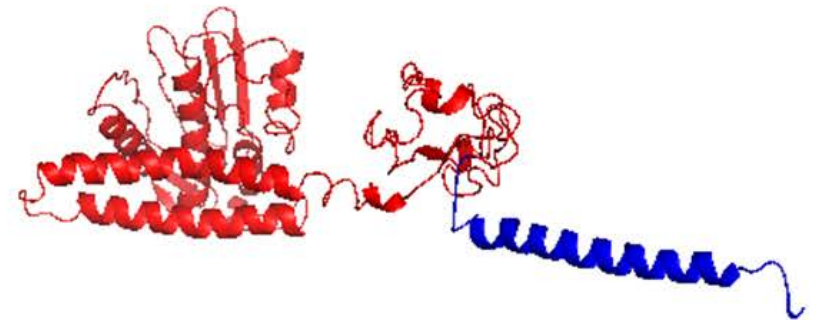
Tn101-*adeR2*



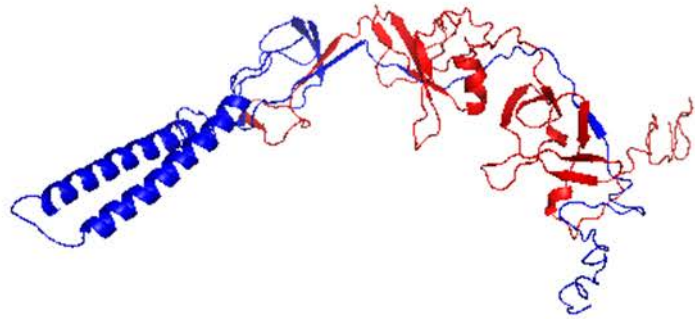
Tn26-*adeS1*



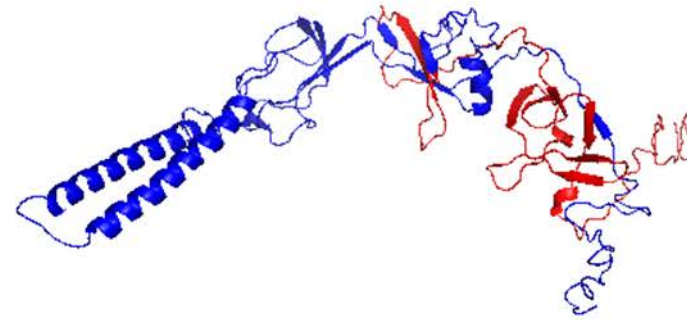
Tn26-*adeS2*



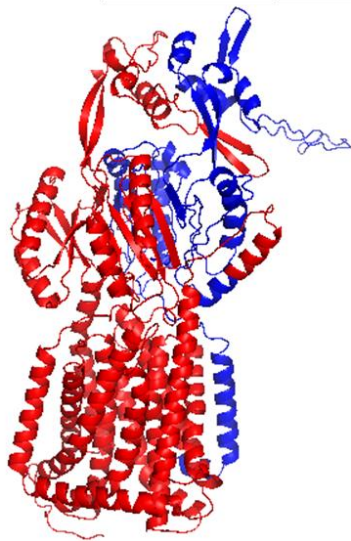
Tn26-*adeA1*



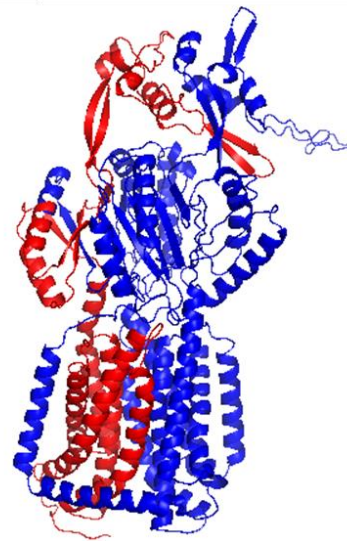
Tn26-*adeA2*



Tn26-*adeB1*



Tn26-*adeB2*



Amino acids upstream and downstream of the transposon insertion site are coloured in blue and red, respectively.

(163 and 317 amino acids, respectively), suggesting that AdeS is likely to be non-functional in both of these mutants (Figure 5.6.1). In Tn26-*adeA1* and Tn26-*adeA2*, translation of 211 and 136 amino acids, respectively, was removed by transposon insertion (Figure 5.6.1), which is likely to result in a non-functional protein. In Tn26-*adeB1* and Tn26-*adeB2*, translation of 693 and 308 amino acids, respectively, was removed by transposon insertion (Figure 5.6.1). In both Tn26-*adeB* mutants, the deletion spanned the length of the predicted protein structure and included areas of the predicted AdeC binding domain and transmembrane helices. Therefore, these mutants were considered to have inactive proteins and a non-functional AdeABC MDR efflux pump.

## **5.7. Discussion**

The mutants used in this study were obtained from the University of Washington (Gallagher, Ramage et al. 2015). This allowed multiple deletion mutants in a contemporary military wound isolate to be studied. Both the Tn26 and Tn101 transposons produced multiple STOP codons irrespective of the location of the frame insertion. However, it was not possible to confirm lack of protein production by Western blotting as no antibodies were available for AdeR, AdeS, AdeA or AdeB. Therefore protein modelling was used to determine whether a possible truncated protein could be produced containing the region(s) required for activity. It is possible that a truncated protein could be produced in each of the mutants. However, as demonstrated by protein modelling, it is unlikely that these proteins would be translated or retain functionality.

The hypothesis was that AdeRS and AdeAB play a similar role in strain AB5075 as in AYE and S1 and that inactivation of the genes encoding this TCS and efflux pump would affect antibiotic resistance, biofilm formation and motility in a similar manner as described in Chapters 3 and 4. AYE is representative of International clone I (Fournier, Vallenet et al. 2006) and was isolated in 2001 from a patient in France (Poirel, Menuteau et al. 2003). S1 is representative of strains causing infection in SE Asia; it was isolated in 2006 in Singapore (Koh, Tan et al. 2012). It is possible that AYE and S1 are not representative of the clinical isolates infecting patients in USA and UK hospitals. AB5075 is a clinical isolate from an osteomyelitis infection in a patient in the US military hospital system in 2008 and was selected as a model strain that is highly virulent and representative of current clinical isolates (Jacobs, Thompson et al. 2014). In this study, transposon mutants of AB5075 were used to demonstrate the role of AdeRS and AdeAB in antibiotic resistance, biofilm formation and motility in a contemporary clinical isolate.

All of the Tn26 and Tn101 mutants displayed lower MICs of antibiotics previously shown to be substrates of the AdeABC efflux pump (Yoon, Nait Chabane et al. 2015). As seen with *adeRS* and *adeB* deletion mutants in AYE, changes in MIC were more pronounced with inactivation of genes encoding components of the AdeABC efflux pump than those encoding the TCS AdeRS. This supports the hypothesis that although inactivation of *adeR* or *adeS* results in a decrease in expression of *adeABC*, the efflux pump is still transcribed at a low level in these mutants. The decrease in efflux of ethidium bromide in all Tn26 and Tn101 mutants supports the hypothesis that the increase in susceptibility to the antimicrobials tested was due to down-regulation or inactivation of AdeABC and therefore reduced efflux. This was also

observed in *adeRS* and *adeB* deletion mutants of AYE. These results are in contrast with the Hoechst accumulation assay, which did not detect any change in efflux levels in the Tn26 or Tn101 mutants. This phenomenon was also observed with an efflux pump mutant in clinical isolate S1, suggesting that the ethidium bromide efflux assay is a more sensitive assay and ethidium bromide may be a more appropriate substrate for measuring efflux by AdeABC. A difference in the MIC of colistin was detected for some of the Tn26 mutants. There is no evidence to show that efflux pumps are involved in resistance to colistin in *A. baumannii* and so it is hypothesised that this is due to changed expression of other genes as a result of inactivation of *adeS*, *adeA* or *adeB*. For example, analysis of the transcriptome of an *adeB* deletion mutant in AYE showed decreased expression of the lipid phosphoethanolamine transferase gene *eptA*, which has been previously associated with colistin resistance, (Adams, Nickel et al. 2009, Arroyo, Herrera et al. 2011, Beceiro, Llobet et al. 2011).

Unlike strain AYE, AB5075 did not produce a strong biofilm *in vitro*. It is hypothesised that this low starting level of biofilm formation in the parental strain of the mutants is responsible for the lack of change in biofilm formation in the transposon mutants. Unfortunately, it was not possible to measure biofilm formation of these strains on in the PVM model due to time and logistical constraints (it required secondment to the USA). It is possible that like strain S1, which did not appear to form a strong biofilm on glass cover slips but did form microcolonies in the PVM model, AB5075 may still be able to form a biofilm on a mucosal surface despite a low biofilm phenotype on abiotic surfaces. Similarly, it was not possible to measure virulence in these strains; however, previous work has shown that AB5075 is highly virulent in murine pulmonary and *G. mellonella* models of infection (Jacobs, Thompson et al. 2014). It



is hypothesised that as in strain S1, which was also highly virulent in *G. mellonella*, inactivation or down-regulation of the efflux pump AdeABC by transposon insertion in either *adeR*, *adeS*, *adeA* or *adeB* would produce a significant virulence defect in this strain.

Interestingly, transposon inactivation of *adeR*, *adeS* and *adeB* produced a motility phenotype that was not seen in deletion mutants of these genes in AYE or S1. Increased swarming motility was observed in Tn101-*adeR2* and Tn26-*adeS2* but not in Tn26-*adeR1* or Tn26-*adeS1*. These data suggest that the location of the transposon insertion is important in determining the motility phenotype. Transposon mutants Tn101-*adeR2* and Tn26-*adeS2* have a much larger part of the protein deleted, which may impact motility more significantly than in Tn26-*adeR1* and Tn26-*adeS1*. Tn26-*adeR1* retains the entire effector domain, whereas Tn26-*adeR2* does not. This domain is hypothesised to trigger a cellular response upon phosphorylation. Tn26-*adeS1* retains a histidine kinase ATP-ase, which is deleted in Tn26-*adeS2*. This domain is predicted to be an ATP binding site. It is possible that the presence of these domains allows Tn26-*adeR1* and Tn26-*adeS1* to retain some AdeR and AdeS activity and therefore an altered motility phenotype is not observed in these strains. Previous work has shown no effect on motility with overexpression of efflux pumps in *A. baumannii* but has highlighted reduced expression of the diaminobutyrate-2-oxoglutarate aminotransferase involved in biosynthesis of diaminopropane (a polyamine required for *A. baumannii* surface-associated motility) in an efflux pump overexpresser (Skiebe, de Berardinis et al. 2012, Yoon, Nait Chabane et al. 2015). It is possible that transposon mutants that do not produce AdeR, AdeS or AdeB may

have increased production of diaminobutyrate-2-oxoglutarate aminotransferase, resulting in increased motility on wet agar.

## **5.8. Further work**

As discussed in Chapters 3 and 4, it is possible that individual components of the AdeRS and the AdeABC systems may interact with components of other systems, allowing some function of these systems to be retained. In order to gain a greater understanding of the role of each system in antimicrobial resistance, biofilm and virulence, both single and double mutants should be created in strain AB5075. Furthermore, it would be interesting to include AdeC in this study, creating both a single and a triple mutant in combination with *adeA* and *adeB* to elucidate the role of this OMP in the phenotype.

To further understand the role of AdeRS and AdeAB in biofilm formation and virulence, the phenotype of the transposon mutants should be tested in other models. This study has shown that biofilm formation can vary significantly depending on the model used and therefore it is important to measure biofilm formation in multiple *in vitro* and *ex vivo* models as described in Chapter 3. AB5075 was selected by Jacobs *et. al.* as a strain that is representative of clinical isolates due to its high levels of virulence in a murine pulmonary and *G. mellonella* model (Jacobs, Thompson et al. 2014). It is therefore an ideal strain in which to study the role of the AdeRS TCS and the AdeABC efflux pump in virulence. Further work should focus on measuring virulence of the AB5075 transposon mutants in multiple models such as the murine pulmonary and *G. mellonella* models.

## 5.9. Key findings

- Inactivation of *adeR*, *adeS*, *adeA* and *adeB* by transposon insertion in AB5075 resulted in a decrease in the MICs of some antibiotics.
- *adeR*, *adeS*, *adeA* and *adeB* transposon mutants in AB5075 displayed decreased levels of efflux of ethidium bromide.
- *adeR*, *adeS* and *adeB* transposon mutants displayed increased swarming motility.

## 6. Overall Discussion and Conclusions

*Acinetobacter baumannii* is a nosocomial pathogen and is a significant problem in hospitals worldwide. This organism is often multi-drug resistant, can persist in the environment and forms a biofilm on environmental surfaces and wounds. Overproduction of efflux pumps that export toxic compounds can lead to multi-drug resistance.

A summary of the results presented in this thesis can be seen in Table 5.9.1. The primary aim of this study was to characterise the phenotype of a mutant lacking the two component system AdeRS in the MDR strain AYE. A mutant lacking AdeRS displayed increased susceptibility to antibiotics and decreased levels of efflux of ethidium bromide. Furthermore, RNA-seq data showed a 128, 91 and 28-fold decrease in expression of *adeA*, *adeB* and *adeC*, respectively, in the AdeRS deletion mutant when compared with the parental strain AYE. A reduction in efflux explains the increased susceptibility to antibiotics as when these toxic compounds are extruded at a reduced rate they accumulate in the bacterial cell and so are lethal at lower external concentrations. These data add to those from previous studies that show that AdeRS is a regulator of the RND efflux pump AdeABC, which extrudes several classes of antibiotics including aminoglycosides,  $\beta$ -lactams, fluoroquinolones, tetracyclines, tigecycline and chloramphenicol (Marchand, Damier-Piolle et al. 2004, Yoon, Nait Chabane et al. 2015).

A porcine vaginal mucosal (PVM) model was adapted in this study to measure *A. baumannii* biofilm formation on a mucosal surface that represents a natural infection of the epithelium (Anderson, Parks et al. 2013). In this model, inactivation of AdeRS

**Table 5.9.1 Summary of mutant phenotypes compared with their respective parental strains**

	<b>Antibiotic resistance</b>	<b>Motility</b>	<b>Biofilm formation on plastic</b>	<b>Biofilm formation on PVM</b>	<b>Biofilm formation on glass</b>	<b>Virulence</b>
<b><i>AYEΔadeRS</i></b>	↓	=	=	↓	↓	=
<b><i>AYEΔadeB</i></b>	↓	=	↓	↓	↓	=
<b><i>S1ΔadeAB</i></b>	=	=	=	↓	↓	↓
<b><i>AB5075 Tn26-adeR1</i></b>	↓	=	=	ND	ND	ND
<b><i>AB5075 Tn101-adeR2</i></b>	↓	↑	=	ND	ND	ND
<b><i>AB5075 Tn26-adeS1</i></b>	↓	=	=	ND	ND	ND

<b>AB5075 Tn26- <i>adeS2</i></b>	↓	↑	=	ND	ND	ND
<b>AB5075 Tn26- <i>adeA1</i></b>	↓	=	=	ND	ND	ND
<b>AB5075 Tn26- <i>adeA2</i></b>	↓	=	=	ND	ND	ND
<b>AB5075 Tn26- <i>adeB1</i></b>	↓	↑	=	ND	ND	ND
<b>AB5075 Tn26- <i>adeB2</i></b>	↓	↑	=	ND	ND	ND

↑, increased compared with the parental strain; ↓, decreased compared with the parental strain; ND, experiment not done for this strain

in AYE also resulted in a decrease in biofilm formation. Multi-drug efflux systems have been previously associated with biofilm formation in several other species (Kvist, Hancock et al. 2008, Matsumura, Furukawa et al. 2011, Baugh, Ekanayaka et al. 2012, Liao, Schurr et al. 2013, Yoon, Nait Chabane et al. 2015). However, previous work with *A. baumannii* used an abiotic model of biofilm formation in which biofilms are grown on plastic surfaces and quantified using crystal violet staining (Yoon, Nait Chabane et al. 2015). In the present study, using a similar colorimetric quantification model to Yoon *et al.* no change in biofilm formation was observed with deletion of *adeRS*. However, a reduction in biofilm formation was observed when biofilms on glass cover slips and mucosal tissue were visualised by microscopy. Strain AYE formed a robust, complex biofilm with evidence of an extracellular matrix whereas only individual cells of *AYEΔadeRS* were attached to the surface. Quantification of the number of adherent cells of *AYEΔadeRS* on the mucosal tissue showed no difference to the number of wild type AYE, suggesting that cells are able to attach but lack the ability to form a mature biofilm. A similar observation was made for *S. aureus* and *S. Typhimurium* (Anderson, Lin et al. 2012, Baugh, Ekanayaka et al. 2012). This may explain why no difference was observed with alternative biofilm quantification methods as these do not differentiate between attached cells and those in a complex biofilm. This highlights the need to measure biofilm formation in different models. It has also been shown by others that the factors required for attachment and biofilm formation may differ depending on the surface (Anderson, Moreau-Marquis et al. 2008, Otto 2008, de Breij, Gaddy et al. 2009, Anderson, Lin et al. 2012).

The next aim of this research was to determine whether the phenotype of the *AYEΔadeRS* mutant was due to decreased expression of the efflux pump genes *adeABC* in strain AYE. Inactivation of *adeB* produced decreased susceptibility to the same antibiotics, a similar decrease in efflux activity and reduced biofilm formation on PVM as seen for the *AYEΔadeRS* mutant. These data support the hypothesis that the phenotype observed in *AYEΔadeRS* is a result of decreased expression of the AdeABC efflux pump genes in this mutant. The MICs of some antibiotics were lower against *AYEΔadeB* than those against *AYEΔadeRS*. It is hypothesised that the greater reduction in efflux in the AdeB mutant, resulted in increased accumulation of antibiotic in the cell. This suggests that AdeABC may be a better target for inhibitors and drug discovery research than AdeRS.

Inactivation of AdeRS and AdeAB by transposon insertion in military clinical isolate AB5075 also resulted in increased susceptibility to substrates of AdeABC and decreased efflux activity. Like strain AYE, AB5075 is ST1 and MDR and so it was expected that inactivation of AdeRS and AdeAB in this clinical isolate would result in a similar phenotype to that in AYE. However, unlike in strain AYE, inactivation of AdeRS and AdeB also resulted in an increase in motility in AB5075. Analysis of the genome of AB5075 showed no difference in the genomic context of AdeRS, AdeABC or known motility genes so it is hypothesised that this phenotype is due to expression changes in motility genes that were not present in AYE due to strain variation. Altered motility in *A. baumannii* has previously been observed as a result of inactivation or changed expression of *pil*, *com*, *dat* and *ddc* genes but not efflux pump genes (Antunes, Imperi et al. 2011, Skiebe, de Berardinis et al. 2012, Harding, Tracy et al. 2013, Wilharm, Piesker et al. 2013, Yoon, Nait Chabane et al. 2015).



Inactivation of AdeAB in clinical isolate S1, which is ST40, did not produce any change in susceptibility to antibiotics. S1 has no mutation in *adeRS* and so does not overexpress the efflux pump AdeABC. It has been shown by the Courvalin group that AdeABC is tightly regulated and only confers MDR when overexpressed (Magnet, Courvalin et al. 2001, Yoon, Courvalin et al. 2013, Yoon, Nait Chabane et al. 2015). Therefore, it is hypothesised that deletion of the pump genes in S1 had no effect on the MICs of antibiotics because they are only expressed at low levels to begin with. However, S1 $\Delta$ *adeAB* showed reduced biofilm formation in the PVM model and on glass cover slips, further supporting the hypothesis that AdeABC plays an important role in biofilm formation. PVM is made up of stratified squamous epithelium, similar in structure to human mucosal surfaces (Anderson, Parks et al. 2013) and the growth characteristics of *A. baumannii* on the PVM were similar to those observed using a 3D human skin equivalent model (de Breij, Haisma et al. 2012). Therefore, differences in the ability of *A. baumannii* mutants to form a biofilm in the PVM model may have implications for the formation of biofilms in respiratory and wound infections. These data suggest that inhibition of MDR efflux pumps may be a useful strategy to help prevent or treat colonisation in patients by *A. baumannii*.

Furthermore, deletion of AdeAB in S1 significantly reduced virulence in a *Galleria mellonella* model, suggesting that the AdeABC efflux pump is required for killing of *G. mellonella* in this strain. This effect was not seen with deletion of AdeB in strain AYE, indicating that AdeABC has a strain-specific role in *A. baumannii* and may perform different functions in different strains. A correlation between pathogenicity in *G. mellonella* and in humans has previously been observed with *A. baumannii* (Peleg, Jara et al. 2009). Therefore, these data suggest that for some *A. baumannii* strains,

such as S1, AdeABC may be required for infection in humans. The finding that the major MDR RND efflux pump in *A. baumannii* can also play a fundamental role in its ability to infect its host further underscores a role for MDR efflux pumps in the biology of pathogenic bacteria. However, data presented here suggest that broad conclusions about the role of specific genes and proteins in this species should not be drawn from the study of single strains and that multiple *A. baumannii* strains should be used in future studies.

## **6.1. Future work arising from this study**

There are several hypotheses arising from the work described in this thesis:

### **Hypothesis 1**

Disruption of AdeRS or AdeABC in different strains of *A. baumannii* will have a strain-specific effect on antibiotic resistance, biofilm formation, virulence and motility.

### **Suggested work**

Create deletion mutants of individual genes *adeR*, *adeS*, *adeA*, *adeB* and *adeC* in each of the strains studied here; AYE, S1 and AB5075. This will allow the effect of inactivation of each component of the AdeRS two component system and the AdeABC RND efflux pump to be established. This will also allow the phenotype of deletion mutants in different strains to be directly compared.

### **Hypothesis 2**

Disruption of AdeRS or AdeABC in different *A. baumannii* strains will alter the expression of genes involved in antibiotic resistance, biofilm formation, virulence and motility.

### **Suggested work**

Western blotting should be used to confirm that deletion of each gene removes expression of the protein product for that gene and does not affect expression of other proteins encoded downstream. RNA-Seq experiments should be carried out with each deletion mutant to determine changes in the transcriptome compared with the parental strain. Changes in the transcriptome of deletion mutants created in different strain backgrounds should also be compared with a particular focus on genes known to encode proteins required for motility, virulence and biofilm formation as this study has identified differences in these phenotypic functions. Reverse transcription PCR would then be used to confirm expression changes in genes of interest.

### **Hypothesis 3**

Deletion or decreased expression of AdeABC in *A. baumannii* will affect biofilm formation in animal models.

### **Suggested work**

Biofilm formation by each deletion mutant should be measured in alternative models, such as the murine wound model described by Thompson *et al.* (Thompson, Black et al. 2014). *A. baumannii* wound infections are common in military casualties and biofilms are an important virulence factor in wound infection (Davis, Moran et al. 2005, Hujer, Hujer et al. 2006, Sebeny, Riddle et al. 2008, O'Shea 2012, Percival, Hill et al. 2012). The murine wound model allows an inoculum of a clinically relevant MDR *A. baumannii* strain to proliferate and form a biofilm within a wound, which can then be assessed using multiple quantitative and qualitative techniques (Thompson,

Black et al. 2014). Furthermore RNA-seq technology should be used to determine transcriptomic changes in cells whilst in a biofilm compared with planktonic cells, providing insight into the genes that may play a role in biofilm formation on wound surfaces.

#### **Hypothesis 4**

Deletion or decreased expression of AdeABC in *A. baumannii* will affect virulence in animal models.

#### **Suggested work**

Mouse models of infection should be used to evaluate the virulence of the deletion mutants. *A. baumannii* most commonly causes ventilator-associated pneumonia, which can be modelled through instillation of a bacterial suspension into the trachea or intranasally (van Faassen, KuoLee et al. 2007, Wang, Ozer et al. 2014, Yoon, Balloy et al. 2016), whilst systemic infection can be modelled using intraperitoneal injection (Breslow, Meissler et al. 2011, Roux, Danilchanka et al. 2015, Yoon, Balloy et al. 2016). Using these models, Yoon *et al.* recently showed that overproduction of the AdeABC efflux pump in *A. baumannii* BM4587 resulted in decreased competitiveness in an intraperitoneal mouse model (Yoon, Balloy et al. 2016). However, the AdeABC-overexpressing mutant was more virulent in mice inoculated intranasally, demonstrating the importance of measuring virulence in different models. It has been suggested that the intranasal model of infection is the most clinically relevant model as it mimics the most frequent type of human *A. baumannii* infection (Yoon, Balloy et al. 2016). Use of these animal models may provide a more

accurate and clinically relevant measure of the role of AdeRS and AdeABC in *A. baumannii* infection.

## **Publications associated with this study**

1. **Richmond, G. E.**, L. P. Evans, M. J. Anderson, M. E. Wand, L. C. Bonney, A. Ivens, K. L. Chua, M. A. Webber, J. M. Sutton, M. L. Peterson and L. J. Piddock (2016). "The *Acinetobacter baumannii* Two-Component System AdeRS Regulates Genes Required for Multidrug Efflux, Biofilm Formation, and Virulence in a Strain-Specific Manner." *MBio* 7(2).
2. **Richmond, G. E.**, K. L. Chua and L. J. Piddock (2013). "Efflux in *Acinetobacter baumannii* can be determined by measuring accumulation of H33342 (bis-benzimide)." *J Antimicrob Chemother.*
3. Amin, I. M., **G. E. Richmond**, P. Sen, T. H. Koh, L. J. Piddock and K. L. Chua (2013). "A method for generating marker-less gene deletions in multidrug-resistant *Acinetobacter baumannii*." *BMC Microbiol* 13: 158.

## **International conference presentations associated with this study**

1. "Efflux Pumps are Required for Biofilm Formation and Virulence in *Acinetobacter baumannii*" **G. E. Richmond**, M. J. Anderson, M. E. Wand, M. A. Webber, J. M. Sutton, M. L. Peterson, L. J. V. Piddock

10th International Symposium on the Biology of *Acinetobacter*. 2015. Athens, Greece

2. "Inhibition of Efflux in *Acinetobacter baumannii* Prevents Biofilm Formation" **Grace E Richmond**, Mark Webber, Laura J V Piddock

54<sup>th</sup> Interscience Conference on Antimicrobial Agents and Chemotherapy. 2014. Washington, USA.

3. "AdeABC is Required for Biofilm Formation and Virulence in *Acinetobacter baumannii*" **Grace E Richmond**, Matthew E Wand, J M Sutton, Kim Lee Chua, Laura J V Piddock

114th General Meeting of the American Society for Microbiology. 2013. Denver, USA.

## References

- Adams, M. D., G. C. Nickel, S. Bajaksouzian, H. Lavender, A. R. Murthy, M. R. Jacobs and R. A. Bonomo (2009). "Resistance to colistin in *Acinetobacter baumannii* associated with mutations in the PmrAB two-component system." Antimicrob Agents Chemother **53**(9): 3628-3634.
- Afzal-Shah, M., N. Woodford and D. M. Livermore (2001). "Characterization of OXA-25, OXA-26, and OXA-27, molecular class D beta-lactamases associated with carbapenem resistance in clinical isolates of *Acinetobacter baumannii*." Antimicrob Agents Chemother **45**(2): 583-588.
- Al-Mousa, H. H., A. A. Omar, V. D. Rosenthal, M. F. Salama, N. Y. Aly, M. El-Dossoky Noweir, F. M. Rebello, D. M. Narciso, A. F. Sayed, A. Kurian, S. M. George, A. M. Mohamed, R. J. Ramapurath and S. T. Varghese (2016). "Device-associated infection rates, bacterial resistance, length of stay, and mortality in Kuwait: International Nosocomial Infection Consortium findings." Am J Infect Control **44**(4): 444-449.
- Alikhan, N. F., N. K. Petty, N. L. Ben Zakour and S. A. Beatson (2011). "BLAST Ring Image Generator (BRIG): simple prokaryote genome comparisons." BMC Genomics **12**: 402.
- Álvarez-Pérez, S., B. Lievens, H. Jacquemyn and C. M. Herrera (2013). "*Acinetobacter nectaris* sp. nov. and *Acinetobacter boissieri* sp. nov., isolated from floral nectar of wild Mediterranean insect-pollinated plants." International Journal of Systematic and Evolutionary Microbiology **63**(Pt 4): 1532-1539.



Amin, I. M., G. E. Richmond, P. Sen, T. H. Koh, L. J. Piddock and K. L. Chua (2013). "A method for generating marker-less gene deletions in multidrug-resistant *Acinetobacter baumannii*." BMC Microbiol **13**: 158.

Anandham, R., H.-Y. Weon, S.-J. Kim, Y.-S. Kim, B.-Y. Kim and S.-W. Kwon (2010). "*Acinetobacter brisouii* sp. nov., isolated from a wetland in Korea." The Journal of Microbiology **48**(1): 36-39.

Anderson, G. G., S. Moreau-Marquis, B. A. Stanton and G. A. O'Toole (2008). "In Vitro Analysis of Tobramycin-Treated *Pseudomonas aeruginosa* Biofilms on Cystic Fibrosis-Derived Airway Epithelial Cells." Infect Immun **76**(4): 1423-1433.

Anderson, M. J., Y. C. Lin, A. N. Gillman, P. J. Parks, P. M. Schlievert and M. L. Peterson (2012). "Alpha-toxin promotes *Staphylococcus aureus* mucosal biofilm formation." Frontiers in cellular and infection microbiology **2**: 64.

Anderson, M. J., Y. C. Lin, A. N. Gillman, P. J. Parks, P. M. Schlievert and M. L. Peterson (2012). "Alpha-toxin promotes *Staphylococcus aureus* mucosal biofilm formation." Front Cell Infect Microbiol **2**: 64.

Anderson, M. J., P. J. Parks and M. L. Peterson (2013). "A mucosal model to study microbial biofilm development and anti-biofilm therapeutics." Journal of microbiological methods **92**(2): 201-208.

Anderson, M. J., M. T. Scholz, P. J. Parks and M. L. Peterson (2013). "Ex vivo porcine vaginal mucosal model of infection for determining effectiveness and toxicity of antiseptics." Journal of applied microbiology **115**(3): 679-688.

Andrews, J. M. (2001). "Determination of minimum inhibitory concentrations." J Antimicrob Chemother **48 Suppl 1**: 5-16.

Anstey, N. M., B. J. Currie and K. M. Withnall (1992). "Community-acquired *Acinetobacter* pneumonia in the Northern Territory of Australia." Clin Infect Dis **14**(1): 83-91.

Anthony, K. B., N. O. Fishman, D. R. Linkin, L. B. Gasink, P. H. Edelstein and E. Lautenbach (2008). "Clinical and Microbiological Outcomes of Serious Infections with Multidrug-Resistant Gram-Negative Organisms Treated with Tigecycline." Clinical Infectious Diseases **46**(4): 567-570.

Antunes, L. C., F. Imperi, A. Carattoli and P. Visca (2011). "Deciphering the multifactorial nature of *Acinetobacter baumannii* pathogenicity." PLoS One **6**(8): e22674.

Antunes, L. C. S., P. Visca and K. J. Towner (2014). "*Acinetobacter baumannii*: evolution of a global pathogen." Pathogens and Disease **71**(3): 292-301.

Arroyo, L. A., C. M. Herrera, L. Fernandez, J. V. Hankins, M. S. Trent and R. E. Hancock (2011). "The *pmrCAB* operon mediates polymyxin resistance in *Acinetobacter baumannii* ATCC 17978 and clinical isolates through phosphoethanolamine modification of lipid A." Antimicrob Agents Chemother **55**(8): 3743-3751.

Badave, G. K. and D. Kulkarni (2015). "Biofilm Producing Multidrug Resistant *Acinetobacter baumannii*: An Emerging Challenge." Journal of Clinical and Diagnostic Research : JCDR **9**(1): DC08-DC10.

Bahar, O., T. Goffer and S. Burdman (2009). "Type IV Pili are required for virulence, twitching motility, and biofilm formation of *acidovorax avenae* subsp. *Citrulli*." Mol Plant Microbe Interact **22**(8): 909-920.

Baugh, S., A. S. Ekanayaka, L. J. Piddock and M. A. Webber (2012). "Loss of or inhibition of all multidrug resistance efflux pumps of *Salmonella enterica* serovar Typhimurium results in impaired ability to form a biofilm." J Antimicrob Chemother **67**(10): 2409-2417.

Baugh, S., C. R. Phillips, A. S. Ekanayaka, L. J. V. Piddock and M. A. Webber (2014). "Inhibition of multidrug efflux as a strategy to prevent biofilm formation." Journal of Antimicrobial Chemotherapy **69**(3): 673-681.

Baumann, P. (1968). "Isolation of *Acinetobacter* from soil and water." J Bacteriol **96**(1): 39-42.

Beachey, E. H. (1981). "Bacterial adherence: adhesin-receptor interactions mediating the attachment of bacteria to mucosal surface." J Infect Dis **143**(3): 325-345.

Beceiro, A., E. Llobet, J. Aranda, J. A. Bengoechea, M. Doumith, M. Hornsey, H. Dhanji, H. Chart, G. Bou, D. M. Livermore and N. Woodford (2011). "Phosphoethanolamine modification of lipid A in colistin-resistant variants of *Acinetobacter baumannii* mediated by the *pmrAB* two-component regulatory system." Antimicrob Agents Chemother **55**(7): 3370-3379.

Beijerinck, M. (1911). "Pigmenten als oxydatieproducten gevormd door bacterien." Vers. Konin. Akad. Wet. Ams. **19**: 1092-1103.

Bentancor, L. V., J. M. O'Malley, C. Bozkurt-Guzel, G. B. Pier and T. Maira-Litran (2012). "Poly-N-acetyl-beta-(1-6)-glucosamine is a target for protective immunity against *Acinetobacter baumannii* infections." Infect Immun **80**(2): 651-656.

Bentancor, L. V., A. Routray, C. Bozkurt-Guzel, A. Camacho-Peiro, G. B. Pier and T. Maira-Litran (2012). "Evaluation of the trimeric autotransporter Ata as a vaccine candidate against *Acinetobacter baumannii* infections." Infect Immun **80**(10): 3381-3388.

Berlau, J., H. Aucken, H. Malnick and T. Pitt (1999). "Distribution of *Acinetobacter* species on skin of healthy humans." Eur J Clin Microbiol Infect Dis **18**(3): 179-183.

Bernards, A. T., J. van der Toorn, C. P. van Boven and L. Dijkshoorn (1996). "Evaluation of the ability of a commercial system to identify *Acinetobacter* genomic species." Eur J Clin Microbiol Infect Dis **15**(4): 303-308.

Bonnin, R. A., L. Poirel and P. Nordmann (2014). "New Delhi metallo-beta-lactamase-producing *Acinetobacter baumannii*: a novel paradigm for spreading antibiotic resistance genes." Future Microbiol **9**(1): 33-41.

Boo, T. W., F. Walsh and B. Crowley (2006). "First report of OXA-23 carbapenemase in clinical isolates of *Acinetobacter* species in the Irish Republic." J Antimicrob Chemother **58**(5): 1101-1102.

Bou, G., G. Cerveró, M. A. Domínguez, C. Quereda and J. Martínez-Beltrán (2000). "Characterization of a Nosocomial Outbreak Caused by a Multiresistant *Acinetobacter baumannii* Strain with a Carbapenem-Hydrolyzing Enzyme: High-Level

Carbapenem Resistance in *A. baumannii* Is Not Due Solely to the Presence of  $\beta$ -Lactamases." Journal of Clinical Microbiology **38**(9): 3299-3305.

Bou, G. and J. Martinez-Beltran (2000). "Cloning, nucleotide sequencing, and analysis of the gene encoding an AmpC beta-lactamase in *Acinetobacter baumannii*." Antimicrob Agents Chemother **44**(2): 428-432.

Bouvet, P. J. and P. A. Grimont (1987). "Identification and biotyping of clinical isolates of *Acinetobacter*." Ann Inst Pasteur Microbiol **138**(5): 569-578.

Bouvet, P. J. M. and P. A. D. Grimont (1986). "Taxonomy of the Genus *Acinetobacter* with the Recognition of *Acinetobacter baumannii* sp. nov., *Acinetobacter haemolyticus* sp. nov., *Acinetobacter johnsonii* sp. nov., and *Acinetobacter junii* sp. nov. and Emended Descriptions of *Acinetobacter calcoaceticus* and *Acinetobacter lwoffii*." International Journal of Systematic Bacteriology **36**(2): 228-240.

Breslow, J. M., J. J. Meissler, Jr., R. R. Hartzell, P. B. Spence, A. Truant, J. Gaughan and T. K. Eisenstein (2011). "Innate immune responses to systemic *Acinetobacter baumannii* infection in mice: neutrophils, but not interleukin-17, mediate host resistance." Infect Immun **79**(8): 3317-3327.

Brisou, J. and A. R. Prevot (1954). "Etudes de systematique bacterienne. X. Revision des especes reunies dans le genere *Achromobacter*." Ann. Inst. Pasteur **86**: 722-728.

Brossard, K. A. and A. A. Campagnari (2012). "The *Acinetobacter baumannii* biofilm-associated protein plays a role in adherence to human epithelial cells." Infect Immun **80**(1): 228-233.

Buckley, A. M., M. A. Webber, S. Cooles, L. P. Randall, R. M. La Ragione, M. J. Woodward and L. J. Piddock (2006). "The AcrAB-TolC efflux system of *Salmonella enterica* serovar Typhimurium plays a role in pathogenesis." Cell Microbiol **8**(5): 847-856.

Camarena, L., V. Bruno, G. Euskirchen, S. Poggio and M. Snyder (2010). "Molecular mechanisms of ethanol-induced pathogenesis revealed by RNA-sequencing." PLoS Pathog **6**(4): e1000834.

Carbonne, A., T. Naas, K. Blanckaert, C. Couzigou, C. Cattoen, J. L. Chagnon, P. Nordmann and P. Astagneau (2005). "Investigation of a nosocomial outbreak of extended-spectrum beta-lactamase VEB-1-producing isolates of *Acinetobacter baumannii* in a hospital setting." J Hosp Infect **60**(1): 14-18.

Carr, E. L., P. Kämpfer, B. K. C. Patel, V. Gürtler and R. J. Seviour (2003). "Seven novel species of *Acinetobacter* isolated from activated sludge." International Journal of Systematic and Evolutionary Microbiology **53**(4): 953-963.

Carver, T. J., K. M. Rutherford, M. Berriman, M. A. Rajandream, B. G. Barrell and J. Parkhill (2005). "ACT: the Artemis Comparison Tool." Bioinformatics **21**(16): 3422-3423.

Catalano, M., L. S. Quelle, P. E. JERIC, A. Di Martino and S. M. Maimone (1999). "Survival of *Acinetobacter baumannii* on bed rails during an outbreak and during sporadic cases." J Hosp Infect **42**(1): 27-35.

Ceri, H., M. E. Olson, C. Stremick, R. R. Read, D. Morck and A. Buret (1999). "The Calgary Biofilm Device: new technology for rapid determination of antibiotic susceptibilities of bacterial biofilms." J Clin Microbiol **37**(6): 1771-1776.

Cerqueira, G. M., X. Kostoulas, C. Khoo, I. Aibinu, Y. Qu, A. Traven and A. Y. Peleg (2014). "A Global Virulence Regulator in *Acinetobacter baumannii* and its Control of the Phenylacetic Acid Catabolic Pathway." Journal of Infectious Diseases.

Chaladchalam, S., P. Diraphat, F. Utrarachkij, O. Suthienkul, R. Samakoses and K. Siripanichgon (2008). "Bed rails and endotracheal tube connectors as possible sources for spreading *Acinetobacter baumannii* in ventilator-associated pneumonia patients." The Southeast Asian journal of tropical medicine and public health **39**(4): 676-685.

Chang, H. C., Y. F. Wei, L. Dijkshoorn, M. Vaneechoutte, C. T. Tang and T. C. Chang (2005). "Species-level identification of isolates of the *Acinetobacter calcoaceticus*-*Acinetobacter baumannii* complex by sequence analysis of the 16S-23S rRNA gene spacer region." J Clin Microbiol **43**(4): 1632-1639.

Chau, S.-L., Y.-W. Chu and E. T. S. Houang (2004). "Novel Resistance-Nodulation-Cell Division Efflux System AdeDE in *Acinetobacter* Genomic DNA Group 3." Antimicrobial Agents and Chemotherapy **48**(10): 4054-4055.

Chen, M. Z., P. R. Hsueh, L. N. Lee, C. J. Yu, P. C. Yang and K. T. Luh (2001). "Severe community-acquired pneumonia due to *Acinetobacter baumannii*." Chest **120**(4): 1072-1077.

Cheng, H.-Y., Y.-F. Chen and H.-L. Peng (2010). "Molecular characterization of the PhoPQ-PmrD-PmrAB mediated pathway regulating polymyxin B resistance in *Klebsiella pneumoniae* CG43." Journal of Biomedical Science **17**(1): 60.

Cho, Y. J., D. C. Moon, J. S. Jin, C. H. Choi, Y. C. Lee and J. C. Lee (2009). "Genetic basis of resistance to aminoglycosides in *Acinetobacter* spp. and spread of *armA* in *Acinetobacter baumannii* sequence group 1 in Korean hospitals." Diagnostic Microbiology and Infectious Disease **64**(2): 185-190.

Choi, A. H., L. Slamti, F. Y. Avci, G. B. Pier and T. Maira-Litran (2009). "The *pgaABCD* locus of *Acinetobacter baumannii* encodes the production of poly-beta-1-6-N-acetylglucosamine, which is critical for biofilm formation." J Bacteriol **191**(19): 5953-5963.

Choi, C. H., E. Y. Lee, Y. C. Lee, T. I. Park, H. J. Kim, S. H. Hyun, S. A. Kim, S. K. Lee and J. C. Lee (2005). "Outer membrane protein 38 of *Acinetobacter baumannii* localizes to the mitochondria and induces apoptosis of epithelial cells." Cell Microbiol **7**(8): 1127-1138.

Choi, C. H., J. S. Lee, Y. C. Lee, T. I. Park and J. C. Lee (2008). "*Acinetobacter baumannii* invades epithelial cells and outer membrane protein A mediates interactions with epithelial cells." BMC Microbiol **8**: 216.

Choi, J. Y., G. Ko, W. Jheong, G. Huys, H. Seifert, L. Dijkshoorn and K. S. Ko (2013). "*Acinetobacter kookii* sp. nov., isolated from soil." International Journal of Systematic and Evolutionary Microbiology **63**(Pt 12): 4402-4406.



Chu, Y. W., S. L. Chau and E. T. S. Houang (2006). "Presence of active efflux systems AdeABC, AdeDE and AdeXYZ in different *Acinetobacter* genomic DNA groups." Journal of Medical Microbiology **55**(4): 477-478.

Chu, Y. W., C. M. Leung, E. T. Houang, K. C. Ng, C. B. Leung, H. Y. Leung and A. F. Cheng (1999). "Skin carriage of *Acinetobacters* in Hong Kong." J Clin Microbiol **37**(9): 2962-2967.

Chuang, Y. C., W. H. Sheng, S. Y. Li, Y. C. Lin, J. T. Wang, Y. C. Chen and S. C. Chang (2011). "Influence of genospecies of *Acinetobacter baumannii* complex on clinical outcomes of patients with acinetobacter bacteremia." Clin Infect Dis **52**(3): 352-360.

Cisneros, J. M., M. J. Reyes, J. Pachon, B. Becerril, F. J. Caballero, J. L. Garcia-Garmendia, C. Ortiz and A. R. Cobacho (1996). "Bacteremia due to *Acinetobacter baumannii*: epidemiology, clinical findings, and prognostic features." Clin Infect Dis **22**(6): 1026-1032.

Coelho, J., N. Woodford, M. Afzal-Shah and D. Livermore (2006). "Occurrence of OXA-58-like carbapenemases in *Acinetobacter* spp. collected over 10 years in three continents." Antimicrob Agents Chemother **50**(2): 756-758.

Coelho, J. M., J. F. Turton, M. E. Kaufmann, J. Glover, N. Woodford, M. Warner, M.-F. Palepou, R. Pike, T. L. Pitt, B. C. Patel and D. M. Livermore (2006). "Occurrence of Carbapenem-Resistant *Acinetobacter baumannii* Clones at Multiple Hospitals in London and Southeast England." Journal of Clinical Microbiology **44**(10): 3623-3627.

Coldham, N. G., M. Webber, M. J. Woodward and L. J. Piddock (2010). "A 96-well plate fluorescence assay for assessment of cellular permeability and active efflux in *Salmonella enterica* serovar Typhimurium and *Escherichia coli*." J Antimicrob Chemother **65**(8): 1655-1663.

Corbella, X., J. Ariza, C. Ardanuy, M. Vuelta, F. Tubau, M. Sora, M. Pujol and F. Gudiol (1998). "Efficacy of sulbactam alone and in combination with ampicillin in nosocomial infections caused by multiresistant *Acinetobacter baumannii*." J Antimicrob Chemother **42**(6): 793-802.

Corvec, S., L. Poirel, T. Naas, H. Drugeon and P. Nordmann (2007). "Genetics and expression of the carbapenem-hydrolyzing oxacillinase gene blaOXA-23 in *Acinetobacter baumannii*." Antimicrob Agents Chemother **51**(4): 1530-1533.

Costerton, J. W., P. S. Stewart and E. P. Greenberg (1999). "Bacterial biofilms: a common cause of persistent infections." Science **284**(5418): 1318-1322.

Coyne, S., P. Courvalin and B. Perichon (2011). "Efflux-mediated antibiotic resistance in *Acinetobacter* spp." Antimicrob Agents Chemother **55**(3): 947-953.

Coyne, S., G. Guigon, P. Courvalin and B. Périchon (2010). "Screening and Quantification of the Expression of Antibiotic Resistance Genes in *Acinetobacter baumannii* with a Microarray." Antimicrobial Agents and Chemotherapy **54**(1): 333-340.

Coyne, S., N. Rosenfeld, T. Lambert, P. Courvalin and B. Perichon (2010). "Overexpression of resistance-nodulation-cell division pump AdeFGH confers

multidrug resistance in *Acinetobacter baumannii*." Antimicrob Agents Chemother **54**(10): 4389-4393.

Da Silva, G. J., S. Quinteira, E. Bertolo, J. C. Sousa, L. Gallego, A. Duarte and L. Peixe (2004). "Long-term dissemination of an OXA-40 carbapenemase-producing *Acinetobacter baumannii* clone in the Iberian Peninsula." J Antimicrob Chemother **54**(1): 255-258.

Dai, T., C. K. Murray, M. S. Vrahas, D. G. Baer, G. P. Tegos and M. R. Hamblin (2012). "Ultraviolet C light for *Acinetobacter baumannii* wound infections in mice: potential use for battlefield wound decontamination?" J Trauma Acute Care Surg **73**(3): 661-667.

Damier-Piolle, L., S. Magnet, S. Bremont, T. Lambert and P. Courvalin (2008). "AdelJK, a resistance-nodulation-cell division pump effluxing multiple antibiotics in *Acinetobacter baumannii*." Antimicrob Agents Chemother **52**(2): 557-562.

Davis, K. A., K. A. Moran, C. K. McAllister and P. J. Gray (2005). "Multidrug-resistant *Acinetobacter* extremity infections in soldiers." Emerg Infect Dis **11**(8): 1218-1224.

de Breij, A., J. Gaddy, J. van der Meer, R. Koning, A. Koster, P. van den Broek, L. Actis, P. Nibbering and L. Dijkshoorn (2009). "CsuA/BABCDE-dependent pili are not involved in the adherence of *Acinetobacter baumannii* ATCC19606T to human airway epithelial cells and their inflammatory response." Research in Microbiology **160**(3): 213-218.

de Breij, A., E. M. Haisma, M. Rietveld, A. El Ghalbzouri, P. J. van den Broek, L. Dijkshoorn and P. H. Nibbering (2012). "Three-Dimensional Human Skin Equivalent

as a Tool To Study *Acinetobacter baumannii* Colonization." Antimicrobial Agents and Chemotherapy **56**(5): 2459-2464.

Dexter, C., G. L. Murray, I. T. Paulsen and A. Y. Peleg (2015). "Community-acquired *Acinetobacter baumannii*: clinical characteristics, epidemiology and pathogenesis." Expert Review of Anti-infective Therapy **13**(5): 567-573.

Dijkshoorn, L., H. Aucken, P. Gerner-Smidt, P. Janssen, M. E. Kaufmann, J. Garaizar, J. Ursing and T. L. Pitt (1996). "Comparison of outbreak and nonoutbreak *Acinetobacter baumannii* strains by genotypic and phenotypic methods." Journal of Clinical Microbiology **34**(6): 1519-1525.

Dijkshoorn, L., A. Nemec and H. Seifert (2007). "An increasing threat in hospitals: multidrug-resistant *Acinetobacter baumannii*." Nature reviews. Microbiology **5**(12): 939-951.

Dolzani, L., E. Tonin, C. Lagatolla, L. Prandin and C. Monti-Bragadin (1995). "Identification of *Acinetobacter* isolates in the *A. calcoaceticus*-*A. baumannii* complex by restriction analysis of the 16S-23S rRNA intergenic-spacer sequences." J Clin Microbiol **33**(5): 1108-1113.

Donald, H. M., W. Scaife, S. G. Amyes and H. K. Young (2000). "Sequence analysis of ARI-1, a novel OXA beta-lactamase, responsible for imipenem resistance in *Acinetobacter baumannii* 6B92." Antimicrob Agents Chemother **44**(1): 196-199.

Durante-Mangoni, E., M. Del Franco, R. Andini, M. Bernardo, M. Giannouli and R. Zarrilli "Emergence of colistin resistance without loss of fitness and virulence after

prolonged colistin administration in a patient with extensively drug-resistant *Acinetobacter baumannii*." Diagnostic Microbiology and Infectious Disease(0).

Duszynska, W., V. D. Rosenthal, B. Dragan, P. Wegrzyn, A. Mazur, P. Wojtyra, A. Tomala and A. Kubler (2015). "Ventilator-associated pneumonia monitoring according to the INICC project at one centre." Anaesthesiol Intensive Ther **47**(1): 34-39.

Ehrenstein, B., A. T. Bernards, L. Dijkshoorn, P. Gerner-Smidt, K. J. Towner, P. J. Bouvet, F. D. Daschner and H. Grundmann (1996). "*Acinetobacter* species identification by using tRNA spacer fingerprinting." J Clin Microbiol **34**(10): 2414-2420.

Eijkelkamp, B. A., U. H. Stroehler, K. A. Hassan, M. S. Papadimitriou, I. T. Paulsen and M. H. Brown (2011). "Adherence and motility characteristics of clinical *Acinetobacter baumannii* isolates." FEMS Microbiol Lett **323**(1): 44-51.

Elabed, H., A. Merghni, R. Hamza, A. Bakhrouf and K. Gaddour (2016). "Molecular analysis of the adaptive response in *Salmonella* Typhimurium after starvation in salty conditions." J Infect Dev Ctries **10**(1): 74-81.

Elkins, C. A. and H. Nikaido (2003). "Chimeric Analysis of AcrA Function Reveals the Importance of Its C-Terminal Domain in Its Interaction with the AcrB Multidrug Efflux Pump." Journal of Bacteriology **185**(18): 5349-5356.

Endimiani, A., F. Luzzaro, R. Migliavacca, E. Mantengoli, A. M. Hujer, K. M. Hujer, L. Pagani, R. A. Bonomo, G. M. Rossolini and A. Toniolo (2007). "Spread in an Italian

hospital of a clonal *Acinetobacter baumannii* strain producing the TEM-92 extended-spectrum beta-lactamase." Antimicrob Agents Chemother **51**(6): 2211-2214.

Enoch, D. A., C. Summers, N. M. Brown, L. Moore, M. I. Gillham, R. M. Burnstein, R. Thaxter, L. M. Enoch, B. Matta and O. Sule (2008). "Investigation and management of an outbreak of multidrug-carbapenem-resistant *Acinetobacter baumannii* in Cambridge, UK." Journal of Hospital Infection **70**(2): 109-118.

Evans, B. A., S. Brown, A. Hamouda, J. Findlay and S. G. Amyes (2007). "Eleven novel OXA-51-like enzymes from clinical isolates of *Acinetobacter baumannii*." Clin Microbiol Infect **13**(11): 1137-1138.

Evans, L. P. (2012). Investigating Two Component Regulatory Systems for the Determination of Adaptive Responses in *Acinetobacter baumannii*. MPhil, University of Birmingham.

Falagas, M. E., K. N. Fragoulis, S. K. Kasiakou, G. J. Sermaidis and A. Michalopoulos (2005). "Nephrotoxicity of intravenous colistin: a prospective evaluation." International Journal of Antimicrobial Agents **26**(6): 504-507.

Falagas, M. E., P. I. Rafailidis, E. Ioannidou, V. G. Alexiou, D. K. Matthaiou, D. E. Karageorgopoulos, A. Kapaskelis, D. Nikita and A. Michalopoulos (2010). "Colistin therapy for microbiologically documented multidrug-resistant Gram-negative bacterial infections: a retrospective cohort study of 258 patients." International Journal of Antimicrobial Agents **35**(2): 194-199.

Falagas, M. E., P. I. Rafailidis, S. K. Kasiakou, P. Hatzopoulou and A. Michalopoulos (2006). "Effectiveness and nephrotoxicity of colistin monotherapy vs. colistin-

meropenem combination therapy for multidrug-resistant Gram-negative bacterial infections." Clinical Microbiology and Infection **12**(12): 1227-1230.

Fattahian, Y., I. Rasooli, S. L. Mousavi Gargari, M. R. Rahbar, S. Darvish Alipour Astaneh and J. Amani (2011). "Protection against *Acinetobacter baumannii* infection via its functional deprivation of biofilm associated protein (Bap)." Microb Pathog **51**(6): 402-406.

Feng, G.-D., S.-Z. Yang, Y.-H. Wang, M.-R. Deng and H.-H. Zhu (2014). "*Acinetobacter guangdongensis* sp. nov., isolated from abandoned lead-zinc ore." International Journal of Systematic and Evolutionary Microbiology **64**(Pt 10): 3417-3421.

Fishbain, J. and A. Y. Peleg (2010). "Treatment of *Acinetobacter* infections." Clin Infect Dis **51**(1): 79-84.

Forster, D. H. and F. D. Daschner (1998). "*Acinetobacter* species as nosocomial pathogens." Eur J Clin Microbiol Infect Dis **17**(2): 73-77.

Fournier, P. E., D. Vallenet, V. Barbe, S. Audic, H. Ogata, L. Poirel, H. Richet, C. Robert, S. Mangenot, C. Abergel, P. Nordmann, J. Weissenbach, D. Raoult and J. M. Claverie (2006). "Comparative genomics of multidrug resistance in *Acinetobacter baumannii*." PLoS Genet **2**(1): e7.

Fu, Y., J. Zhou, H. Zhou, Q. Yang, Z. Wei, Y. Yu and L. Li (2010). "Wide dissemination of OXA-23-producing carbapenem-resistant *Acinetobacter baumannii* clonal complex 22 in multiple cities of China." Journal of Antimicrobial Chemotherapy **65**(4): 644-650.

Gaddy, J. A. and L. A. Actis (2009). "Regulation of *Acinetobacter baumannii* biofilm formation." Future microbiology **4**(3): 273-278.

Gaddy, J. A., B. A. Arivett, M. J. McConnell, R. Lopez-Rojas, J. Pachon and L. A. Actis (2012). "Role of acinetobactin-mediated iron acquisition functions in the interaction of *Acinetobacter baumannii* strain ATCC 19606T with human lung epithelial cells, *Galleria mellonella* caterpillars, and mice." Infect Immun **80**(3): 1015-1024.

Gaddy, J. A., A. P. Tomaras and L. A. Actis (2009). "The *Acinetobacter baumannii* 19606 OmpA protein plays a role in biofilm formation on abiotic surfaces and in the interaction of this pathogen with eukaryotic cells." Infect Immun **77**(8): 3150-3160.

Gallagher, L. A., E. Ramage, E. J. Weiss, M. Radey, H. S. Hayden, K. G. Held, H. K. Huse, D. V. Zurawski, M. J. Brittnacher and C. Manoil (2015). "Resources for Genetic and Genomic Analysis of Emerging Pathogen *Acinetobacter baumannii*." Journal of Bacteriology **197**(12): 2027-2035.

Gallego, L. and K. Towner (2001). "Carriage of class 1 integrons and antibiotic resistance in clinical isolates of *Acinetobacter baumannii* from Northern Spain." Journal of Medical Microbiology **50**(1): 71-77.

Garcia-Garmendia, J.-L., C. Ortiz-Leyba, J. Garnacho-Montero, F.-J. Jimenez-Jimenez, C. Parez-Paredes, A. E. Barrero-Almodovar and M. G. Miner (2001). "Risk Factors for *Acinetobacter baumannii* Nosocomial Bacteremia in Critically Ill Patients: A Cohort Study." Clinical Infectious Diseases **33**(7): 939-946.



Garcia-Quintanilla, M., M. R. Pulido, J. Pachon and M. J. McConnell (2014). "Immunization with lipopolysaccharide-deficient whole cells provides protective immunity in an experimental mouse model of *Acinetobacter baumannii* infection." PLoS One **9**(12): e114410.

Garrison, M. W., R. Mutters and M. J. Dowzicky (2009). "In vitro activity of tigecycline and comparator agents against a global collection of Gram-negative and Gram-positive organisms: tigecycline Evaluation and Surveillance Trial 2004 to 2007." Diagn Microbiol Infect Dis **65**(3): 288-299.

Gay, P., D. Le Coq, M. Steinmetz, T. Berkelman and C. I. Kado (1985). "Positive selection procedure for entrapment of insertion sequence elements in gram-negative bacteria." J Bacteriol **164**(2): 918-921.

Gerner-Smidt, P. (1992). "Ribotyping of the *Acinetobacter calcoaceticus*-*Acinetobacter baumannii* complex." J Clin Microbiol **30**(10): 2680-2685.

Gerner-Smidt, P., I. Tjernberg and J. Ursing (1991). "Reliability of phenotypic tests for identification of *Acinetobacter* species." J Clin Microbiol **29**(2): 277-282.

Goel, M. K., P. Khanna and J. Kishore (2010). "Understanding survival analysis: Kaplan-Meier estimate." International Journal of Ayurveda Research **1**(4): 274-278.

Gordon, N. C., K. Png and D. W. Wareham (2010). "Potent synergy and sustained bactericidal activity of a vancomycin-colistin combination versus multidrug-resistant strains of *Acinetobacter baumannii*." Antimicrob Agents Chemother **54**(12): 5316-5322.

Gordon, N. C. and D. W. Wareham (2009). "A review of clinical and microbiological outcomes following treatment of infections involving multidrug-resistant *Acinetobacter baumannii* with tigecycline." Journal of Antimicrobial Chemotherapy **63**(4): 775-780.

Greene, C., G. Vadlamudi, D. Newton, B. Foxman and C. Xi (2016). "The influence of biofilm formation and multidrug resistance on environmental survival of clinical and environmental isolates of *Acinetobacter baumannii*." Am J Infect Control.

Haimovich, B. and J. C. Tanaka (1995). "Magainin-induced cytotoxicity in eukaryotic cells: kinetics, dose-response and channel characteristics." Biochim Biophys Acta **1240**(2): 149-158.

Halachev, M. R., J. Z. Chan, C. I. Constantinidou, N. Cumley, C. Bradley, M. Smith-Banks, B. Oppenheim and M. J. Pallen (2014). "Genomic epidemiology of a protracted hospital outbreak caused by multidrug-resistant *Acinetobacter baumannii* in Birmingham, England." Genome Med **6**(11): 70.

Hall-Stoodley, L., J. W. Costerton and P. Stoodley (2004). "Bacterial biofilms: from the natural environment to infectious diseases." Nature reviews. Microbiology **2**(2): 95-108.

Hamouda, A. and S. G. Amyes (2004). "Novel *gyrA* and *parC* point mutations in two strains of *Acinetobacter baumannii* resistant to ciprofloxacin." J Antimicrob Chemother **54**(3): 695-696.

Harding, C. M., E. N. Tracy, M. D. Carruthers, P. N. Rather, L. A. Actis and R. S. Munson (2013). "*Acinetobacter baumannii* Strain M2 Produces Type IV Pili Which

Play a Role in Natural Transformation and Twitching Motility but Not Surface-Associated Motility." mBio **4**(4).

Hassan, K. A., S. M. Jackson, A. Penesyan, S. G. Patching, S. G. Tetu, B. A. Eijkelkamp, M. H. Brown, P. J. F. Henderson and I. T. Paulsen (2013). "Transcriptomic and biochemical analyses identify a family of chlorhexidine efflux proteins." Proceedings of the National Academy of Sciences **110**(50): 20254-20259.

Hassan, K. A., Q. Liu, P. J. F. Henderson and I. T. Paulsen (2015). "Homologs of the *Acinetobacter baumannii* Acel Transporter Represent a New Family of Bacterial Multidrug Efflux Systems." mBio **6**(1).

He, X., F. Lu, F. Yuan, D. Jiang, P. Zhao, J. Zhu, H. Cheng, J. Cao and G. Lu (2015). "Biofilm formation caused by clinical *Acinetobacter baumannii* isolates is associated with over-expression of the AdeFGH efflux pump." Antimicrobial Agents and Chemotherapy.

Henrichsen, J. (1975). "The influence of changes in the environment on twitching motility." Acta Pathol Microbiol Scand B **83**(3): 179-186.

Henwood, C. J., T. Gatward, M. Warner, D. James, M. W. Stockdale, R. P. Spence, K. J. Towner, D. M. Livermore and N. Woodford (2002). "Antibiotic resistance among clinical isolates of *Acinetobacter* in the UK, and in vitro evaluation of tigecycline (GAR-936)." J Antimicrob Chemother **49**(3): 479-487.

Héritier, C., L. Poirel, T. Lambert and P. Nordmann (2005). "Contribution of Acquired Carbapenem-Hydrolyzing Oxacillinases to Carbapenem Resistance in *Acinetobacter baumannii*." Antimicrobial Agents and Chemotherapy **49**(8): 3198-3202.

Higgins, P. G., M. Lehmann, H. Wisplinghoff and H. Seifert (2010). "gyrB multiplex PCR to differentiate between *Acinetobacter calcoaceticus* and *Acinetobacter* genomic species 3." J Clin Microbiol **48**(12): 4592-4594.

Higgins, P. G., H. Wisplinghoff, O. Krut and H. Seifert (2007). "A PCR-based method to differentiate between *Acinetobacter baumannii* and *Acinetobacter* genomic species 13TU." Clin Microbiol Infect **13**(12): 1199-1201.

Higgins, P. G., H. Wisplinghoff, D. Stefanik and H. Seifert (2004). "In vitro activities of the beta-lactamase inhibitors clavulanic acid, sulbactam, and tazobactam alone or in combination with beta-lactams against epidemiologically characterized multidrug-resistant *Acinetobacter baumannii* strains." Antimicrob Agents Chemother **48**(5): 1586-1592.

Hobley, L., C. Harkins, C. E. MacPhee and N. R. Stanley-Wall (2015). "Giving structure to the biofilm matrix: an overview of individual strategies and emerging common themes." FEMS Microbiol Rev **39**(5): 649-669.

Hoch, J. A. (2000). "Two-component and phosphorelay signal transduction." Current Opinion in Microbiology **3**(2): 165-170.

Høiby, N., T. Bjarnsholt, M. Givskov, S. Molin and O. Ciofu (2010). "Antibiotic resistance of bacterial biofilms." International Journal of Antimicrobial Agents **35**(4): 322-332.

Holloway, K. P., N. G. Roupael, J. B. Wells, M. D. King and H. M. Blumberg (2006). "Polymyxin B and Doxycycline Use in Patients with Multidrug-Resistant *Acinetobacter*

*baumannii* Infections in the Intensive Care Unit." The Annals of Pharmacotherapy **40**(11): 1939-1945.

Hornsey, M., N. Loman, D. W. Wareham, M. J. Ellington, M. J. Pallen, J. F. Turton, A. Underwood, T. Gaulton, C. P. Thomas, M. Doumith, D. M. Livermore and N. Woodford (2011). "Whole-genome comparison of two *Acinetobacter baumannii* isolates from a single patient, where resistance developed during tigecycline therapy." J Antimicrob Chemother **66**(7): 1499-1503.

Hou, P. F., X. Y. Chen, G. F. Yan, Y. P. Wang and C. M. Ying (2012). "Study of the correlation of imipenem resistance with efflux pumps AdeABC, AdeIJK, AdeDE and AbeM in clinical isolates of *Acinetobacter baumannii*." Chemotherapy **58**(2): 152-158.

Hraiech, S., A. Roch, H. Lepidi, T. Atieh, G. Audoly, J.-M. Rolain, D. Raoult, J.-M. Brunel, L. Papazian and F. Brégeon (2013). "Impaired Virulence and Fitness of a Colistin-Resistant Clinical Isolate of *Acinetobacter baumannii* in a Rat Model of Pneumonia." Antimicrobial Agents and Chemotherapy **57**(10): 5120-5121.

Hu, H., K. Johani, I. B. Gosbell, A. S. W. Jacombs, A. Almatroudi, G. S. Whiteley, A. K. Deva, S. Jensen and K. Vickery (2015). "Intensive care unit environmental surfaces are contaminated by multidrug-resistant bacteria in biofilms: combined results of conventional culture, pyrosequencing, scanning electron microscopy, and confocal laser microscopy." Journal of Hospital Infection **91**(1): 35-44.

Huang, L., L. Sun, G. Xu and T. Xia (2008). "Differential susceptibility to carbapenems due to the AdeABC efflux pump among nosocomial outbreak isolates of *Acinetobacter baumannii* in a Chinese hospital." Diagnostic Microbiology and Infectious Disease **62**(3): 326-332.

Huang, Z. M., P. H. Mao, Y. Chen, L. Wu and J. Wu (2004). "Study on the molecular epidemiology of SHV type beta-lactamase-encoding genes of multiple-drug-resistant *Acinetobacter baumannii*." Zhonghua Liu Xing Bing Xue Za Zhi **25**(5): 425-427.

Hujer, K. M., A. M. Hujer, E. A. Hulten, S. Bajaksouzian, J. M. Adams, C. J. Donskey, D. J. Ecker, C. Massire, M. W. Eshoo, R. Sampath, J. M. Thomson, P. N. Rather, D. W. Craft, J. T. Fishbain, A. J. Ewell, M. R. Jacobs, D. L. Paterson and R. A. Bonomo (2006). "Analysis of Antibiotic Resistance Genes in Multidrug-Resistant *Acinetobacter* sp. Isolates from Military and Civilian Patients Treated at the Walter Reed Army Medical Center." Antimicrob Agents Chemother **50**(12): 4114-4123.

Hwa, W. E., G. Subramaniam, M. B. Mansor, O. S. Yan, D. Anbazhagan and S. S. Devi (2010). "Iron regulated outer membrane proteins (IROMPs) as potential targets against carbapenem-resistant *Acinetobacter* spp. isolated from a Medical Centre in Malaysia." Indian J Med Res **131**: 578-583.

Ikonomidis, A., S. Pournaras, A. N. Maniatis, N. J. Legakis and A. Tsakris (2006). "Discordance of meropenem versus imipenem activity against *Acinetobacter baumannii*." International Journal of Antimicrobial Agents **28**(4): 376-377.

Jacobs, A. C., I. Hood, K. L. Boyd, P. D. Olson, J. M. Morrison, S. Carson, K. Sayood, P. C. Iwen, E. P. Skaar and P. M. Dunman (2010). "Inactivation of phospholipase D diminishes *Acinetobacter baumannii* pathogenesis." Infect Immun **78**(5): 1952-1962.

Jacobs, A. C., M. G. Thompson, C. C. Black, J. L. Kessler, L. P. Clark, C. N. McQueary, H. Y. Gancz, B. W. Corey, J. K. Moon, Y. Si, M. T. Owen, J. D. Hallock, Y. I. Kwak, A. Summers, C. Z. Li, D. A. Rasko, W. F. Penwell, C. L. Honnold, M. C.

Wise, P. E. Waterman, E. P. Lesho, R. L. Stewart, L. A. Actis, T. J. Palys, D. W. Craft and D. V. Zurawski (2014). "AB5075, a Highly Virulent Isolate of *Acinetobacter baumannii*, as a Model Strain for the Evaluation of Pathogenesis and Antimicrobial Treatments." mBio **5**(3).

Jander, G., L. G. Rahme and F. M. Ausubel (2000). "Positive correlation between virulence of *Pseudomonas aeruginosa* mutants in mice and insects." J Bacteriol **182**(13): 3843-3845.

Janssen, P., K. Maquelin, R. Coopman, I. Tjernberg, P. Bouvet, K. Kersters and L. Dijkshoorn (1997). "Discrimination of *Acinetobacter* genomic species by AFLP fingerprinting." Int J Syst Bacteriol **47**(4): 1179-1187.

Jawad, A., J. Heritage, A. M. Snelling, D. M. Gascoyne-Binzi and P. M. Hawkey (1996). "Influence of relative humidity and suspending menstrua on survival of *Acinetobacter* spp. on dry surfaces." J Clin Microbiol **34**(12): 2881-2887.

Jawad, A., H. Seifert, A. M. Snelling, J. Heritage and P. M. Hawkey (1998). "Survival of *Acinetobacter baumannii* on dry surfaces: comparison of outbreak and sporadic isolates." J Clin Microbiol **36**(7): 1938-1941.

Jawad, A., A. M. Snelling, J. Heritage and P. M. Hawkey (1998). "Exceptional desiccation tolerance of *Acinetobacter radioresistens*." J Hosp Infect **39**(3): 235-240.

Jensen, R. B., S. C. Wang and L. Shapiro (2002). "Dynamic localization of proteins and DNA during a bacterial cell cycle." Nat Rev Mol Cell Biol **3**(3): 167-176.

Jernaes, M. W. and H. B. Steen (1994). "Staining of *Escherichia coli* for flow cytometry: Influx and efflux of ethidium bromide." Cytometry **17**(4): 302-309.

Johnson, E. N., T. C. Burns, R. A. Hayda, D. R. Hospenthal and C. K. Murray (2007). "Infectious complications of open type III tibial fractures among combat casualties." Clin Infect Dis **45**(4): 409-415.

Johnson, E. N., V. C. Marconi and C. K. Murray (2009). "Hospital-acquired device-associated infections at a deployed military hospital in Iraq." J Trauma **66**(4 Suppl): S157-163.

Jung, J. Y., M. S. Park, S. E. Kim, B. H. Park, J. Y. Son, E. Y. Kim, J. E. Lim, S. K. Lee, S. H. Lee, K. J. Lee, Y. A. Kang, S. K. Kim, J. Chang and Y. S. Kim (2010). "Risk factors for multi-drug resistant *Acinetobacter baumannii* bacteremia in patients with colonization in the intensive care unit." BMC Infect Dis **10**: 228.

Kallel, H., M. Bahloul, L. Hergafi, M. Akrouf, W. Ketata, H. Chelly, C. B. Hamida, N. Rekik, A. Hammami and M. Bouaziz (2006). "Colistin as a salvage therapy for nosocomial infections caused by multidrug-resistant bacteria in the ICU." International Journal of Antimicrobial Agents **28**(4): 366-369.

Karageorgopoulos, D. E. and M. E. Falagas (2008). "Current control and treatment of multidrug-resistant *Acinetobacter baumannii* infections." Lancet Infect Dis **8**(12): 751-762.

Kellogg, S. L. and C. J. Kristich (2016). "Functional Dissection of the CroRS Two-Component System Required for Resistance to Cell Wall Stressors in *Enterococcus faecalis*." J Bacteriol **198**(8): 1326-1336.



Kempf, M. and J.-M. Rolain (2012). "Emergence of resistance to carbapenems in *Acinetobacter baumannii* in Europe: clinical impact and therapeutic options." International Journal of Antimicrobial Agents **39**(2): 105-114.

Kersey, P. J., J. E. Allen, M. Christensen, P. Davis, L. J. Falin, C. Grabmueller, D. S. T. Hughes, J. Humphrey, A. Kerhornou, J. Khobova, N. Langridge, M. D. McDowall, U. Maheswari, G. Maslen, M. Nuhn, C. K. Ong, M. Paulini, H. Pedro, I. Toneva, M. A. Tuli, B. Walts, G. Williams, D. Wilson, K. Youens-Clark, M. K. Monaco, J. Stein, X. Wei, D. Ware, D. M. Bolser, K. L. Howe, E. Kulesha, D. Lawson and D. M. Staines (2014). "Ensembl Genomes 2013: scaling up access to genome-wide data." Nucleic Acids Research **42**(D1): D546-D552.

Kim, B. N., A. Y. Peleg, T. P. Lodise, J. Lipman, J. Li, R. Nation and D. L. Paterson (2009). "Management of meningitis due to antibiotic-resistant *Acinetobacter* species." Lancet Infect Dis **9**(4): 245-255.

Kim, D., K. Baik, M. Kim, S. Park, S. Kim, M. Rhee, Y. Kwak and C. Seong (2008). "*Acinetobacter soli* sp. nov., isolated from forest soil." The Journal of Microbiology **46**(4): 396-401.

Kim, P., N.-R. Shin, J. Kim, J.-H. Yun, D.-W. Hyun and J.-W. Bae (2014). "*Acinetobacter apis* sp. nov., isolated from the intestinal tract of a honey bee, *Apis mellifera*." Journal of Microbiology **52**(8): 639-645.

Kim, S. W., C. H. Choi, D. C. Moon, J. S. Jin, J. H. Lee, J. H. Shin, J. M. Kim, Y. C. Lee, S. Y. Seol, D. T. Cho and J. C. Lee (2009). "Serum resistance of *Acinetobacter baumannii* through the binding of factor H to outer membrane proteins." FEMS Microbiol Lett **301**(2): 224-231.

Kim, W. Y., J. Y. Moon, J. W. Huh, S. H. Choi, C. M. Lim, Y. Koh, Y. P. Chong and S. B. Hong (2016). "Comparable Efficacy of Tigecycline versus Colistin Therapy for Multidrug-Resistant and Extensively Drug-Resistant *Acinetobacter baumannii* Pneumonia in Critically Ill Patients." PLoS One **11**(3): e0150642.

Kim, Y., I. K. Bae, H. Lee, S. H. Jeong, D. Yong and K. Lee (2014). "In vivo emergence of colistin resistance in *Acinetobacter baumannii* clinical isolates of sequence type 357 during colistin treatment." Diagnostic Microbiology and Infectious Disease **79**(3): 362-366.

King, L. B., M. K. Pangburn and L. S. McDaniel (2013). "Serine protease PKF of *Acinetobacter baumannii* results in serum resistance and suppression of biofilm formation." J Infect Dis **207**(7): 1128-1134.

Kirkgoz, E. and Y. Zer (2014). "Clonal comparison of *Acinetobacter* strains isolated from intensive care patients and the intensive care unit environment." Turk J Med Sci **44**(4): 643-648.

Ko, K. S., J. Y. Suh, K. T. Kwon, S.-I. Jung, K.-H. Park, C. I. Kang, D. R. Chung, K. R. Peck and J.-H. Song (2007). "High rates of resistance to colistin and polymyxin B in subgroups of *Acinetobacter baumannii* isolates from Korea." Journal of Antimicrobial Chemotherapy **60**(5): 1163-1167.

Koh, T. H., T. T. Tan, C. T. Khoo, S. Y. NG, T. Y. Tan, L.-Y. Hsu, E. E. Ooi, T. J. K. Van der Reijdent and L. Dijkshoorn (2012). "*Acinetobacter calcoaceticus*-*Acinetobacter baumannii* complex species in clinical specimens in Singapore." Epidemiology & Infection **140**(03): 535-538.

Koh, T. H., T. T. Tan, C. T. Khoo, S. Y. Ng, T. Y. Tan, L. Y. Hsu, E. E. Ooi, T. J. Van Der Reijden and L. Dijkshoorn (2012). "*Acinetobacter calcoaceticus*–*Acinetobacter baumannii* complex species in clinical specimens in Singapore." Epidemiology & Infection **140**(03): 535-538.

Krizova, L., J. McGinnis, M. Maixnerova, M. Nemeč, L. Poirel, L. Mingle, O. Sedo, W. Wolfgang and A. Nemeč (2015). "*Acinetobacter variabilis* sp. nov. (formerly DNA group 15 sensu Tjernberg & Ursing), isolated from humans and animals." International Journal of Systematic and Evolutionary Microbiology **65**(Pt 4): 1395.

Kuo, L. C., C. C. Lai, C. H. Liao, C. K. Hsu, Y. L. Chang, C. Y. Chang and P. R. Hsueh (2007). "Multidrug-resistant *Acinetobacter baumannii* bacteraemia: clinical features, antimicrobial therapy and outcome." Clinical Microbiology and Infection **13**(2): 196-198.

Kvist, M., V. Hancock and P. Klemm (2008). "Inactivation of efflux pumps abolishes bacterial biofilm formation." Appl Environ Microbiol **74**(23): 7376-7382.

La Scola, B., V. A. Gundi, A. Khamis and D. Raoult (2006). "Sequencing of the *rpoB* gene and flanking spacers for molecular identification of *Acinetobacter* species." J Clin Microbiol **44**(3): 827-832.

Lambert, P. A. (2005). "Bacterial resistance to antibiotics: Modified target sites." Advanced Drug Delivery Reviews **57**(10): 1471-1485.

Lee, H., F.-F. Hsu, J. Turk and E. A. Groisman (2004). "The PmrA-Regulated *pmrC* Gene Mediates Phosphoethanolamine Modification of Lipid A and Polymyxin Resistance in *Salmonella enterica*." Journal of Bacteriology **186**(13): 4124-4133.

Lee, J. C., J. Y. Oh, K. S. Kim, Y. W. Jeong, J. C. Park and J. W. Cho (2001). "Apoptotic cell death induced by *Acinetobacter baumannii* in epithelial cells through caspase-3 activation." APMIS **109**(10): 679-684.

Lee, Y.-T., C.-P. Fung, F.-D. Wang, C.-P. Chen, T.-L. Chen and W.-L. Cho (2011). "Outbreak of imipenem-resistant *Acinetobacter calcoaceticus*–*Acinetobacter baumannii* complex harboring different carbapenemase gene-associated genetic structures in an intensive care unit." Journal of Microbiology, Immunology and Infection(0).

Lesho, E., G. Wortmann, K. Moran and D. Craft (2005). "Fatal *Acinetobacter baumannii* Infection with Discordant Carbapenem Susceptibility." Clinical Infectious Diseases **41**(5): 758-759.

Lesho, E., E.-J. Yoon, P. McGann, E. Snesrud, Y. Kwak, M. Milillo, F. Onmus-Leone, L. Preston, K. St. Clair, M. Nikolich, H. Viscount, G. Wortmann, M. Zapor, C. Grillot-Courvalin, P. Courvalin, R. Clifford and P. E. Waterman (2013). "Emergence of Colistin-Resistance in Extremely Drug-Resistant *Acinetobacter baumannii* Containing a Novel pmrCAB Operon During Colistin Therapy of Wound Infections." Journal of Infectious Diseases **208**(7): 1142-1151.

Lessel, E. F. (1971). "International Committee on Nomenclature of Bacteria: Subcommittee on the Taxonomy of *Moraxella* and Allied Bacteria." International Journal of Systematic Bacteriology **21**(2): 213-214.

Levin, A. S. (2002). "Multiresistant *Acinetobacter* infections: a role for sulbactam combinations in overcoming an emerging worldwide problem." Clinical Microbiology and Infection **8**(3): 144-153.

Levin, A. S., C. E. Levy, A. E. I. Manrique, E. A. S. Medeiros and S. F. Costa (2003). "Severe nosocomial infections with imipenem-resistant *Acinetobacter baumannii* treated with ampicillin/sulbactam." International Journal of Antimicrobial Agents **21**(1): 58-62.

Lewis, T., N. J. Loman, L. Bingle, P. Jumaa, G. M. Weinstock, D. Mortiboy and M. J. Pallen (2010). "High-throughput whole-genome sequencing to dissect the epidemiology of *Acinetobacter baumannii* isolates from a hospital outbreak." Journal of Hospital Infection **75**(1): 37-41.

Li, W., D. Zhang, X. Huang and W. Qin (2014). "*Acinetobacter harbinensis* sp. nov., isolated from river water." International Journal of Systematic and Evolutionary Microbiology **64**(Pt 5): 1507-1513.

Li, X., A. K. Gorle, T. D. Ainsworth, K. Heimann, C. E. Woodward, J. Grant Collins and F. Richard Keene (2015). "RNA and DNA binding of inert oligonuclear rutheniumII complexes in live eukaryotic cells." Dalton Transactions **44**(8): 3594-3603.

Li, Y., W. He, T. Wang, C.-g. Piao, L.-m. Guo, J.-p. Chang, M.-w. Guo and S.-j. Xie (2014). "*Acinetobacter qingfengensis* sp. nov., isolated from canker bark of *Populus × euramericana*." International Journal of Systematic and Evolutionary Microbiology **64**(Pt 3): 1043-1050.

Li, Y., C.-g. Piao, Y.-c. Ma, W. He, H.-m. Wang, J.-p. Chang, L.-m. Guo, X.-z. Wang, S.-j. Xie and M.-w. Guo (2013). "*Acinetobacter puyangensis* sp. nov., isolated from the healthy and diseased part of *Populus × euramericana* canker bark." International Journal of Systematic and Evolutionary Microbiology **63**(Pt 8): 2963-2969.

Liao, J., M. J. Schurr and K. Sauer (2013). "The MerR-like regulator BrlR confers biofilm tolerance by activating multidrug-efflux pumps in *Pseudomonas aeruginosa* biofilms." Journal of Bacteriology.

Lin, L., B.-D. Ling and X.-Z. Li (2009). "Distribution of the multidrug efflux pump genes, *adeABC*, *adeDE* and *adeIJK*, and class 1 integron genes in multiple-antimicrobial-resistant clinical isolates of *Acinetobacter baumannii*–*Acinetobacter calcoaceticus* complex." International Journal of Antimicrobial Agents **33**(1): 27-32.

Lin, M.-F., Y.-Y. Lin, H.-W. Yeh and C.-Y. Lan (2014). "Role of the BaeSR two-component system in the regulation of *Acinetobacter baumannii* *adeAB* genes and its correlation with tigecycline susceptibility." BMC Microbiology **14**(1): 119.

Liou, M. L., P. C. Soo, S. R. Ling, H. Y. Kuo, C. Y. Tang and K. C. Chang (2013). "The sensor kinase BfmS mediates virulence in *Acinetobacter baumannii*." J Microbiol Immunol Infect.

Liu, D., Z. S. Liu, P. Hu, L. Cai, B. Q. Fu, Y. S. Li, S. Y. Lu, N. N. Liu, X. L. Ma, D. Chi, J. Chang, Y. M. Shui, Z. H. Li, W. Ahmad, Y. Zhou and H. L. Ren (2016). "Characterization of surface antigen protein 1 (SurA1) from *Acinetobacter baumannii* and its role in virulence and fitness." Vet Microbiol **186**: 126-138.

Liu, Q., X. Liu, F. Yan, Y. He, J. Wei, Y. Zhang, L. Liu and Y. Sun (2016). "Comparative transcriptome analysis of *Brucella melitensis* in an acidic environment: Identification of the two-component response regulator involved in the acid resistance and virulence of *Brucella*." Microb Pathog **91**: 92-98.

Liu, Y.-Y., Y. Wang, T. R. Walsh, L.-X. Yi, R. Zhang, J. Spencer, Y. Doi, G. Tian, B. Dong, X. Huang, L.-F. Yu, D. Gu, H. Ren, X. Chen, L. Lv, D. He, H. Zhou, Z. Liang, J.-H. Liu and J. Shen (2016). "Emergence of plasmid-mediated colistin resistance mechanism MCR-1 in animals and human beings in China: a microbiological and molecular biological study." The Lancet Infectious Diseases **16**(2): 161-168.

Loehfelm, T. W., N. R. Luke and A. A. Campagnari (2008). "Identification and characterization of an *Acinetobacter baumannii* biofilm-associated protein." J Bacteriol **190**(3): 1036-1044.

Lood, R., B. Y. Winer, A. J. Pelzek, R. Diez-Martinez, M. Thandar, C. W. Euler, R. Schuch and V. A. Fischetti (2015). "Novel phage lysin capable of killing the multidrug-resistant gram-negative bacterium *Acinetobacter baumannii* in a mouse bacteremia model." Antimicrob Agents Chemother **59**(4): 1983-1991.

López-Rojas, R., M. E. Jiménez-Mejías, J. A. Lepe and J. Pachón (2011). "*Acinetobacter baumannii* Resistant to Colistin Alters Its Antibiotic Resistance Profile: A Case Report From Spain." Journal of Infectious Diseases **204**(7): 1147-1148.

Luo, G., L. Lin, A. S. Ibrahim, B. Baquir, P. Pantapalangkoor, R. A. Bonomo, Y. Doi, M. D. Adams, T. A. Russo and B. Spellberg (2012). "Active and Passive Immunization Protects against Lethal, Extreme Drug Resistant *Acinetobacter baumannii* Infection." PLoS ONE **7**(1): e29446.

Magnet, S., P. Courvalin and T. Lambert (2001). "Resistance-nodulation-cell division-type efflux pump involved in aminoglycoside resistance in *Acinetobacter baumannii* strain BM4454." Antimicrob Agents Chemother **45**(12): 3375-3380.

Mah, T.-F. C. and G. A. O'Toole (2001). "Mechanisms of biofilm resistance to antimicrobial agents." Trends in Microbiology **9**(1): 34-39.

Mak, J. K., M.-J. Kim, J. Pham, J. Tapsall and P. A. White (2009). "Antibiotic resistance determinants in nosocomial strains of multidrug-resistant *Acinetobacter baumannii*." Journal of Antimicrobial Chemotherapy **63**(1): 47-54.

Malhotra, J., S. Anand, S. Jindal, R. Rajagopal and R. Lal (2012). "*Acinetobacter indicus* sp. nov., isolated from a hexachlorocyclohexane dump site." International Journal of Systematic and Evolutionary Microbiology **62**(Pt 12): 2883-2890.

Marchand, I., L. Damier-Piolle, P. Courvalin and T. Lambert (2004). "Expression of the RND-type efflux pump AdeABC in *Acinetobacter baumannii* is regulated by the AdeRS two-component system." Antimicrob Agents Chemother **48**(9): 3298-3304.

Marti, S., F. Fernandez-Cuenca, A. Pascual, A. Ribera, J. Rodriguez-Bano, G. Bou, J. Miguel Cisneros, J. Pachon, L. Martinez-Martinez, J. Vila and H. Grupo de Estudio de Infeccion (2006). "Prevalence of the *tetA* and *tetB* genes as mechanisms of resistance to tetracycline and minocycline in *Acinetobacter baumannii* clinical isolates." Enferm Infecc Microbiol Clin **24**(2): 77-80.

Matsumura, K., S. Furukawa, H. Ogihara and Y. Morinaga (2011). "Roles of Multidrug Efflux Pumps on the Biofilm Formation of *Escherichia coli* K-12." Biocontrol Science **16**(2): 69-72.

Matthaiou, D. K., A. Michalopoulos, P. I. Rafailidis, D. E. Karageorgopoulos, V. Papaioannou, G. Ntani, G. Samonis and M. E. Falagas (2008). "Risk factors



associated with the isolation of colistin-resistant gram-negative bacteria: a matched case-control study." Crit Care Med **36**(3): 807-811.

Mihara, K., T. Tanabe, Y. Yamakawa, T. Funahashi, H. Nakao, S. Narimatsu and S. Yamamoto (2004). "Identification and transcriptional organization of a gene cluster involved in biosynthesis and transport of acinetobactin, a siderophore produced by *Acinetobacter baumannii* ATCC 19606T." Microbiology **150**(Pt 8): 2587-2597.

Mitrophanov, A. Y. and E. A. Groisman (2008). "Signal integration in bacterial two-component regulatory systems." Genes Dev **22**(19): 2601-2611.

Miyata, S., M. Casey, D. W. Frank, F. M. Ausubel and E. Drenkard (2003). "Use of the *Galleria mellonella* caterpillar as a model host to study the role of the type III secretion system in *Pseudomonas aeruginosa* pathogenesis." Infect Immun **71**(5): 2404-2413.

Moffatt, J. H., M. Harper, P. Harrison, J. D. F. Hale, E. Vinogradov, T. Seemann, R. Henry, B. Crane, F. St. Michael, A. D. Cox, B. Adler, R. L. Nation, J. Li and J. D. Boyce (2010). "Colistin Resistance in *Acinetobacter baumannii* Is Mediated by Complete Loss of Lipopolysaccharide Production." Antimicrobial Agents and Chemotherapy **54**(12): 4971-4977.

Montaña, S., E. Vilacoba, G. M. Traglia, M. Almuzara, M. Pennini, A. Fernández, A. Sucari, D. Centrón and M. S. Ramírez (2015). "Genetic Variability of AdeRS Two-Component System Associated with Tigecycline Resistance in XDR-*Acinetobacter baumannii* Isolates." Current Microbiology: 1-7.

Moreira Silva, G., L. Morais, L. Marques and V. Senra (2011). "Pneumonia adquirida na comunidade numa crianca saudavel por *Acinetobacter*." Revista Portuguesa de Pneumologia **Epub ahead of print**.

Moskowitz, S. M., R. K. Ernst and S. I. Miller (2004). "PmrAB, a Two-Component Regulatory System of *Pseudomonas aeruginosa* That Modulates Resistance to Cationic Antimicrobial Peptides and Addition of Aminoarabinose to Lipid A." Journal of Bacteriology **186**(2): 575-579.

Motaouakkil, S., B. Charra, A. Hachimi, H. Nejmi, A. Benslama, N. Elmdaghri, H. Belabbes and M. Benbachir (2006). "Colistin and rifampicin in the treatment of nosocomial infections from multiresistant *Acinetobacter baumannii*." Journal of Infection **53**(4): 274-278.

Murray, C. K., S. A. Roop, D. R. Hospenthal, D. P. Dooley, K. Wenner, J. Hammock, N. Taufen and E. Gourdine (2006). "Bacteriology of War Wounds at the Time of Injury." Military Medicine **171**(9): 826-829.

Murray, C. K., H. C. Yun, M. E. Griffith, D. R. Hospenthal and M. J. Tong (2006). "*Acinetobacter infection*: what was the true impact during the Vietnam conflict?" Clin Infect Dis **43**(3): 383-384.

Naas, T., P. Bogaerts, C. Bauraing, Y. Degheldre, Y. Glupczynski and P. Nordmann (2006). "Emergence of PER and VEB extended-spectrum  $\beta$ -lactamases in *Acinetobacter baumannii* in Belgium." Journal of Antimicrobial Chemotherapy **58**(1): 178-182.

Nagano, N., Y. Nagano, C. Cordevant, N. Shibata and Y. Arakawa (2004). "Nosocomial transmission of CTX-M-2 beta-lactamase-producing *Acinetobacter baumannii* in a neurosurgery ward." J Clin Microbiol **42**(9): 3978-3984.

Nait Chabane, Y., S. Marti, C. Rihouey, S. Alexandre, J. Hardouin, O. Lesouhaitier, J. Vila, J. B. Kaplan, T. Jouenne and E. Dé (2014). "Characterisation of Pellicles Formed by *Acinetobacter baumannii* at the Air-Liquid Interface." PLoS ONE **9**(10): e111660.

Nemec, A., T. De Baere, I. Tjernberg, M. Vaneechoutte, T. J. van der Reijden and L. Dijkshoorn (2001). "*Acinetobacter ursingii* sp. nov. and *Acinetobacter schindleri* sp. nov., isolated from human clinical specimens." International Journal of Systematic and Evolutionary Microbiology **51**(5): 1891-1899.

Nemec, A., L. Dijkshoorn, I. Cleenwerck, T. De Baere, D. Janssens, T. J. K. van der Reijden, P. Ježek and M. Vaneechoutte (2003). "*Acinetobacter parvus* sp. nov., a small-colony-forming species isolated from human clinical specimens." International Journal of Systematic and Evolutionary Microbiology **53**(5): 1563-1567.

Nemec, A., L. Krizova, M. Maixnerova, T. J. K. van der Reijden, P. Deschaght, V. Passet, M. Vaneechoutte, S. Brisse and L. Dijkshoorn (2011). "Genotypic and phenotypic characterization of the *Acinetobacter calcoaceticus* - *Acinetobacter baumannii* complex with the proposal of *Acinetobacter pittii* sp. nov. (formerly *Acinetobacter* genomic species 3) and *Acinetobacter nosocomialis* sp. nov. (formerly *Acinetobacter* genomic species 13TU)." Research in Microbiology **162**(4): 393-404.

Nemec, A., M. Musílek, M. Maixnerová, T. De Baere, T. J. K. van der Reijden, M. Vaneechoutte and L. Dijkshoorn (2009). "*Acinetobacter beijerinckii* sp. nov. and

*Acinetobacter gyllenbergii* sp. nov., haemolytic organisms isolated from humans." International Journal of Systematic and Evolutionary Microbiology **59**(1): 118-124.

Nemec, A., M. Musílek, O. Šedo, T. De Baere, M. Maixnerová, T. J. K. van der Reijden, Z. Zdráhal, M. Vaneechoutte and L. Dijkshoorn (2010). "*Acinetobacter bereziniae* sp. nov. and *Acinetobacter guillouiae* sp. nov., to accommodate *Acinetobacter* genomic species 10 and 11, respectively." International Journal of Systematic and Evolutionary Microbiology **60**(4): 896-903.

Neonakis, I. K., D. A. Spandidos and E. Petinaki (2011). "Confronting multidrug-resistant *Acinetobacter baumannii*: a review." Int J Antimicrob Agents **37**(2): 102-109.

Neonakis, I. K., D. A. Spandidos and E. Petinaki (2014). "Is minocycline a solution for multidrug-resistant *Acinetobacter baumannii*?" Future Microbiol **9**(3): 299-305.

Nishimura, Y., H. Kanzaki and H. Iizuka (1988). "Taxonomic studies of *Acinetobacter* species based on the electrophoretic analysis of enzymes." J Basic Microbiol **28**(6): 363-370.

Nishino, K., T. Latifi and E. A. Groisman (2006). "Virulence and drug resistance roles of multidrug efflux systems of *Salmonella enterica* serovar Typhimurium." Molecular microbiology **59**(1): 126-141.

Niu, C., K. M. Clemmer, R. A. Bonomo and P. N. Rather (2008). "Isolation and characterization of an autoinducer synthase from *Acinetobacter baumannii*." J Bacteriol **190**(9): 3386-3392.

Nowak, J., T. Schneiders, H. Seifert and P. G. Higgins (2016). "The Asp20-to-Asn Substitution in the Response Regulator AdeR Leads to Enhanced Efflux Activity of AdeB in *Acinetobacter baumannii*." Antimicrob Agents Chemother **60**(2): 1085-1090.

O'Shea, M. K. (2012). "*Acinetobacter* in modern warfare." International Journal of Antimicrobial Agents **39**(5): 363-375.

Oliveira, M. S., G. V. B. Prado, S. F. Costa, R. S. Grinbaum and A. S. Levin (2008). "Ampicillin/sulbactam compared with polymyxins for the treatment of infections caused by carbapenem-resistant *Acinetobacter* spp." Journal of Antimicrobial Chemotherapy **61**(6): 1369-1375.

Oncul, O., O. Keskin, H. V. Acar, Y. Kucukardali, R. Evrenkaya, E. M. Atasoyu, C. Top, S. Nalbant, S. Ozkan, G. Emekdas, S. Cavuslu, M. H. Us, A. Pahsa and M. Gokben (2002). "Hospital-acquired infections following the 1999 Marmara earthquake." J Hosp Infect **51**(1): 47-51.

Otto, M. (2008). "*Staphylococcal* biofilms." Curr Top Microbiol Immunol **322**: 207-228.

Padilla, E., E. Llobet, A. Domenech-Sanchez, L. Martinez-Martinez, J. A. Bengoechea and S. Alberti (2010). "*Klebsiella pneumoniae* AcrAB efflux pump contributes to antimicrobial resistance and virulence." Antimicrob Agents Chemother **54**(1): 177-183.

Park, Y. K., J. Y. Choi, D. Shin and K. S. Ko (2011). "Correlation between overexpression and amino acid substitution of the PmrAB locus and colistin resistance in *Acinetobacter baumannii*." Int J Antimicrob Agents **37**(6): 525-530.

Park, Y. K., G. H. Lee, J. Y. Baek, D. R. Chung, K. R. Peck, J. H. Song and K. S. Ko (2010). "A single clone of *Acinetobacter baumannii*, ST22, is responsible for high antimicrobial resistance rates of *Acinetobacter* spp. isolates that cause bacteremia and urinary tract infections in Korea." Microb Drug Resist **16**(2): 143-149.

Peleg, A. Y. (2007). "Optimizing therapy for *Acinetobacter baumannii*." Semin Respir Crit Care Med **28**(6): 662-671.

Peleg, A. Y., J. Adams and D. L. Paterson (2007). "Tigecycline Efflux as a Mechanism for Nonsusceptibility in *Acinetobacter baumannii*." Antimicrob Agents Chemother **51**(6): 2065-2069.

Peleg, A. Y., S. Jara, D. Monga, G. M. Eliopoulos, R. C. Moellering and E. Mylonakis (2009). "*Galleria mellonella* as a Model System To Study *Acinetobacter baumannii* Pathogenesis and Therapeutics." Antimicrobial Agents and Chemotherapy **53**(6): 2605-2609.

Peleg, A. Y., H. Seifert and D. L. Paterson (2008). "*Acinetobacter baumannii*: emergence of a successful pathogen." Clin Microbiol Rev **21**(3): 538-582.

Penwell, W. F., A. B. Shapiro, R. A. Giacobbe, R.-F. Gu, N. Gao, J. Thresher, R. E. McLaughlin, M. D. Huband, B. L. M. DeJonge, D. E. Ehmann and A. A. Miller (2015). "Molecular Mechanisms of Sulbactam Antibacterial Activity and Resistance Determinants in *Acinetobacter baumannii*." Antimicrobial Agents and Chemotherapy **59**(3): 1680-1689.

Percival, S. L., K. E. Hill, D. W. Williams, S. J. Hooper, D. W. Thomas and J. W. Costerton (2012). "A review of the scientific evidence for biofilms in wounds." Wound Repair and Regeneration **20**(5): 647-657.

Perez, A., M. Poza, A. Fernandez, C. Fernandez Mdel, S. Mallo, M. Merino, S. Rumbo-Feal, M. P. Cabral and G. Bou (2012). "Involvement of the AcrAB-TolC efflux pump in the resistance, fitness, and virulence of *Enterobacter cloacae*." Antimicrob Agents Chemother **56**(4): 2084-2090.

Petersen, K., S. C. Cannegieter, T. J. van der Reijden, B. van Strijen, D. M. You, B. S. Babel, A. I. Philip and L. Dijkshoorn (2011). "Diversity and clinical impact of *Acinetobacter baumannii* colonization and infection at a military medical center." J Clin Microbiol **49**(1): 159-166.

Petersen, K., M. S. Riddle, J. R. Danko, D. L. Blazes, R. Hayden, S. A. Tasker and J. R. Dunne (2007). "Trauma-related infections in battlefield casualties from Iraq." Ann Surg **245**(5): 803-811.

Piddock, L. J. (2006). "Multidrug-resistance efflux pumps - not just for resistance." Nature reviews. Microbiology **4**(8): 629-636.

Piddock, L. J. V. (2006). "Clinically Relevant Chromosomally Encoded Multidrug Resistance Efflux Pumps in Bacteria." Clinical Microbiology Reviews **19**(2): 382-402.

Poirel, L., O. Menuteau, N. Agoli, C. Cattoen and P. Nordmann (2003). "Outbreak of extended-spectrum beta-lactamase VEB-1-producing isolates of *Acinetobacter baumannii* in a French hospital." J Clin Microbiol **41**(8): 3542-3547.

Poirel, L. and P. Nordmann (2006). "Carbapenem resistance in *Acinetobacter baumannii*: mechanisms and epidemiology." Clin Microbiol Infect **12**(9): 826-836.

Poulakou, G., F. V. Kontopidou, E. Paramythiotou, M. Kompoti, M. Katsiari, E. Mainas, C. Nicolaou, D. Yphantis, A. Antoniadou, E. Trikka-Graphakos, Z. Roussou, P. Clouva, N. Maguina, K. Kanellakopoulou, A. Armaganidis and H. Giamarellou (2009). "Tigecycline in the treatment of infections from multi-drug resistant gram-negative pathogens." Journal of Infection **58**(4): 273-284.

Pournaras, S., A. Markogiannakis, A. Ikonomidis, L. Kondyli, K. Bethimouti, A. N. Maniatis, N. J. Legakis and A. Tsakris (2006). "Outbreak of multiple clones of imipenem-resistant *Acinetobacter baumannii* isolates expressing OXA-58 carbapenemase in an intensive care unit." Journal of Antimicrobial Chemotherapy **57**(3): 557-561.

Pournaras, S., A. Poulou, K. Dafopoulou, Y. N. Chabane, I. Kristo, D. Makris, J. Hardouin, P. Cosette, A. Tsakris and E. Dé (2014). "Growth Retardation, Reduced Invasiveness, and Impaired Colistin-Mediated Cell Death Associated with Colistin Resistance Development in *Acinetobacter baumannii*." Antimicrobial Agents and Chemotherapy **58**(2): 828-832.

Poutanen, S. M., M. Louie and A. E. Simor (1997). "Risk factors, clinical features and outcome of *Acinetobacter* bacteremia in adults." Eur J Clin Microbiol Infect Dis **16**(10): 737-740.

Rajamohan, G., V. B. Srinivasan and W. A. Gebreyes (2009). "Biocide-tolerant multidrug-resistant *Acinetobacter baumannii* clinical strains are associated with higher biofilm formation." J Hosp Infect **73**(3): 287-289.



Rajamohan, G., V. B. Srinivasan and W. A. Gebreyes (2010). "Molecular and functional characterization of a novel efflux pump, AmvA, mediating antimicrobial and disinfectant resistance in *Acinetobacter baumannii*." Journal of Antimicrobial Chemotherapy **65**(9): 1919-1925.

Ravasi, P., A. S. Limansky, R. E. Rodriguez, A. M. Viale and M. A. Mussi (2011). "ISAb<sub>a</sub>825, a Functional Insertion Sequence Modulating Genomic Plasticity and blaOXA-58 Expression in *Acinetobacter baumannii*." Antimicrobial Agents and Chemotherapy **55**(2): 917-920.

Reid, G. E., S. A. Grim, C. A. Aldeza, W. M. Janda and N. M. Clark (2007). "Rapid Development of *Acinetobacter baumannii* Resistance to Tigecycline." Pharmacotherapy **27**(8): 1198-1201.

Reinert, R. R., D. E. Low, F. Rossi, X. Zhang, C. Wattal and M. J. Dowzicky (2007). "Antimicrobial susceptibility among organisms from the Asia/Pacific Rim, Europe and Latin and North America collected as part of TEST and the in vitro activity of tigecycline." Journal of Antimicrobial Chemotherapy **60**(5): 1018-1029.

Repizo, G. D., S. Gagne, M. L. Foucault-Grunenwald, V. Borges, X. Charpentier, A. S. Limansky, J. P. Gomes, A. M. Viale and S. P. Salcedo (2015). "Differential Role of the T6SS in *Acinetobacter baumannii* Virulence." PLoS One **10**(9): e0138265.

Richmond, G. E., K. L. Chua and L. J. Piddock (2013). "Efflux in *Acinetobacter baumannii* can be determined by measuring accumulation of H33342 (bis-benzamide)." J Antimicrob Chemother.

Roca, I., P. Espinal, S. Martí and J. Vila (2011). "First Identification and Characterization of an AdeABC-Like Efflux Pump in *Acinetobacter* Genomespecies 13TU." Antimicrobial Agents and Chemotherapy **55**(3): 1285-1286.

Roca, I., P. Espinal, X. Vila-Farres and J. Vila (2012). "The *Acinetobacter baumannii* Oxymoron: Commensal Hospital Dweller Turned Pan-Drug-Resistant Menace." Frontiers in microbiology **3**: 148.

Roca, I., S. Martí, P. Espinal, P. Martínez, I. Gibert and J. Vila (2009). "CraA, a Major Facilitator Superfamily Efflux Pump Associated with Chloramphenicol Resistance in *Acinetobacter baumannii*." Antimicrobial Agents and Chemotherapy **53**(9): 4013-4014.

Rodríguez-Baño, J., S. Martí, S. Soto, F. Fernández-Cuenca, J. M. Cisneros, J. Pachón, A. Pascual, L. Martínez-Martínez, C. McQueary, L. A. Actis and J. Vila (2008). "Biofilm formation in *Acinetobacter baumannii*: associated features and clinical implications." Clinical Microbiology and Infection **14**(3): 276-278.

Rosenfeld, N., C. Bouchier, P. Courvalin and B. Perichon (2012). "Expression of the resistance-nodulation-cell division pump AdeIJK in *Acinetobacter baumannii* is regulated by AdeN, a TetR-type regulator." Antimicrob Agents Chemother **56**(5): 2504-2510.

Rossau, R., A. Van Landschoot, M. Gillis and J. De Ley (1991). "Taxonomy of *Moraxellaceae* fam. nov., a New Bacterial Family To Accommodate the Genera *Moraxella*, *Acinetobacter*, and *Psychrobacter* and Related Organisms." International Journal of Systematic Bacteriology **41**(2): 310-319.

Roux, D., O. Danilchanka, T. Guillard, V. Cattoir, H. Aschard, Y. Fu, F. Angoulvant, J. Messika, J. D. Ricard, J. J. Mekalanos, S. Lory, G. B. Pier and D. Skurnik (2015). "Fitness cost of antibiotic susceptibility during bacterial infection." Sci Transl Med **7**(297): 297ra114.

Ruiz, M., S. Marti, F. Fernandez-Cuenca, A. Pascual and J. Vila (2007). "Prevalence of IS(Aba1) in epidemiologically unrelated *Acinetobacter baumannii* clinical isolates." FEMS Microbiol Lett **274**(1): 63-66.

Rumbo-Feal, S., M. J. Gómez, C. Gayoso, L. Álvarez-Fraga, M. P. Cabral, A. M. Aransay, N. Rodríguez-Ezpeleta, A. Fullaondo, J. Valle, M. Tomás, G. Bou and M. Poza (2013). "Whole Transcriptome Analysis of *Acinetobacter baumannii* Assessed by RNA-Sequencing Reveals Different mRNA Expression Profiles in Biofilm Compared to Planktonic Cells." PLoS ONE **8**(8): e72968.

Rumbo, C., M. Tomás, E. Fernández Moreira, N. C. Soares, M. Carvajal, E. Santillana, A. Beceiro, A. Romero and G. Bou (2014). "The *Acinetobacter baumannii* Omp33-36 Porin Is a Virulence Factor That Induces Apoptosis and Modulates Autophagy in Human Cells." Infection and Immunity **82**(11): 4666-4680.

Russo, T. A., N. R. Luke, J. M. Beanan, R. Olson, S. L. Sauberan, U. MacDonald, L. W. Schultz, T. C. Umland and A. A. Campagnari (2010). "The K1 capsular polysaccharide of *Acinetobacter baumannii* strain 307-0294 is a major virulence factor." Infect Immun **78**(9): 3993-4000.

Russo, T. A., U. MacDonald, J. M. Beanan, R. Olson, I. J. MacDonald, S. L. Sauberan, N. R. Luke, L. W. Schultz and T. C. Umland (2009). "Penicillin-binding

protein 7/8 contributes to the survival of *Acinetobacter baumannii* in vitro and in vivo." J Infect Dis **199**(4): 513-521.

Ruzin, A., D. Keeney and P. A. Bradford (2007). "AdeABC multidrug efflux pump is associated with decreased susceptibility to tigecycline in *Acinetobacter calcoaceticus*-*Acinetobacter baumannii* complex." J Antimicrob Chemother **59**(5): 1001-1004.

Saballs, M., M. Pujol, F. Tubau, C. Peña, A. Montero, M. A. Domínguez, F. Gudiol and J. Ariza (2006). "Rifampicin/imipenem combination in the treatment of carbapenem-resistant *Acinetobacter baumannii* infections." Journal of Antimicrobial Chemotherapy **58**(3): 697-700.

Sahl, J. W., J. D. Gillece, J. M. Schupp, V. G. Waddell, E. M. Driebe, D. M. Engelthaler and P. Keim (2013). "Evolution of a pathogen: a comparative genomics analysis identifies a genetic pathway to pathogenesis in *Acinetobacter*." PLoS One **8**(1): e54287.

Sahu, P. K., P. S. Iyer, A. M. Oak, K. R. Pardesi and B. A. Chopade (2012). "Characterization of eDNA from the clinical strain *Acinetobacter baumannii* AIIMS 7 and its role in biofilm formation." ScientificWorldJournal **2012**: 973436.

Sanchez, C. J., Jr., K. Mende, M. L. Beckius, K. S. Akers, D. R. Romano, J. C. Wenke and C. K. Murray (2013). "Biofilm formation by clinical isolates and the implications in chronic infections." BMC infectious diseases **13**: 47.

Sato, K. and T. Nakae (1991). "Outer membrane permeability of *Acinetobacter calcoaceticus* and its implication in antibiotic resistance." Journal of Antimicrobial Chemotherapy **28**(1): 35-45.

Schafer, J. J., D. A. Goff, K. B. Stevenson and J. E. Mangino (2007). "Early Experience with Tigecycline for Ventilator-Associated Pneumonia and Bacteremia Caused by Multidrug-Resistant *Acinetobacter baumannii*." Pharmacotherapy **27**(7): 980-987.

Schneider, C. A., W. S. Rasband and K. W. Eliceiri (2012). "NIH Image to ImageJ: 25 years of image analysis." Nat Methods **9**(7): 671-675.

Schurch, N. J., P. Schofield, M. Gierliński, C. Cole, A. Sherstnev, V. Singh, N. Wrobel, K. Gharbi, G. G. Simpson and T. Owen-Hughes (2015). "Evaluation of tools for differential gene expression analysis by RNA-seq on a 48 biological replicate experiment." arXiv preprint arXiv:1505.02017.

Scott, P., G. Deye, A. Srinivasan, C. Murray, K. Moran, E. Hulten, J. Fishbain, D. Craft, S. Riddell, L. Lindler, J. Mancuso, E. Milstrey, C. T. Bautista, J. Patel, A. Ewell, T. Hamilton, C. Gaddy, M. Tenney, G. Christopher, K. Petersen, T. Endy and B. Petruccelli (2007). "An outbreak of multidrug-resistant *Acinetobacter baumannii-calcoaceticus* complex infection in the US military health care system associated with military operations in Iraq." Clin Infect Dis **44**(12): 1577-1584.

Sebeny, P. J., M. S. Riddle and K. Petersen (2008). "*Acinetobacter baumannii* skin and soft-tissue infection associated with war trauma." Clin Infect Dis **47**(4): 444-449.

Seifert, H., L. Dijkshoorn, P. Gerner-Smidt, N. Pelzer, I. Tjernberg and M. Vaneechoutte (1997). "Distribution of *Acinetobacter* species on human skin: comparison of phenotypic and genotypic identification methods." J Clin Microbiol **35**(11): 2819-2825.

Seifert, H., A. Strate and G. Pulverer (1995). "Nosocomial bacteremia due to *Acinetobacter baumannii*. Clinical features, epidemiology, and predictors of mortality." Medicine (Baltimore) **74**(6): 340-349.

Sheng, W. H., J. T. Wang, S. Y. Li, Y. C. Lin, A. Cheng, Y. C. Chen and S. C. Chang (2011). "Comparative in vitro antimicrobial susceptibilities and synergistic activities of antimicrobial combinations against carbapenem-resistant *Acinetobacter* species: *Acinetobacter baumannii* versus *Acinetobacter* genospecies 3 and 13TU." Diagn Microbiol Infect Dis **70**(3): 380-386.

Siau, H., K. Y. Yuen, P. L. Ho, S. S. Wong and P. C. Woo (1999). "*Acinetobacter* bacteremia in Hong Kong: prospective study and review." Clin Infect Dis **28**(1): 26-30.

Skiebe, E., V. de Berardinis, P. Morczinek, T. Kerrinnes, F. Faber, D. Lepka, B. Hammer, O. Zimmermann, S. Ziesing, T. A. Wichelhaus, K. P. Hunfeld, S. Borgmann, S. Grobner, P. G. Higgins, H. Seifert, H. J. Busse, W. Witte, Y. Pfeifer and G. Wilharm (2012). "Surface-associated motility, a common trait of clinical isolates of *Acinetobacter baumannii*, depends on 1,3-diaminopropane." Int J Med Microbiol **302**(3): 117-128.

Smani, Y., J. Dominguez-Herrera and J. Pachón (2013). "Association of the outer membrane protein Omp33 with fitness and virulence of *Acinetobacter baumannii*." Journal of Infectious Diseases.

Smani, Y., A. Fabrega, I. Roca, V. Sanchez-Encinales, J. Vila and J. Pachon (2014). "Role of OmpA in the multidrug resistance phenotype of *Acinetobacter baumannii*." Antimicrob Agents Chemother **58**(3): 1806-1808.

Smet, A., P. Cools, L. Krizova, M. Maixnerova, O. Sedo, F. Haesebrouck, M. Kempf, A. Nemeč and M. Vaneechoutte (2014). "*Acinetobacter gandensis* sp. nov. isolated from horse and cattle." International Journal of Systematic and Evolutionary Microbiology **64**(Pt 12): 4007-4015.

Smith, H. E. and J. M. A. Blair (2014). "Redundancy in the periplasmic adaptor proteins AcrA and AcrE provides resilience and an ability to export substrates of multidrug efflux." Journal of Antimicrobial Chemotherapy **69**(4): 982-987.

Squier, C. A., M. J. Mantz, P. M. Schlievert and C. C. Davis (2008). "Porcine vagina *Ex Vivo* as a model for studying permeability and pathogenesis in mucosa." Journal of Pharmaceutical Sciences **97**(1): 9-21.

Srinivasan, V. B., G. Rajamohan and W. A. Gebreyes (2009). "Role of AbeS, a Novel Efflux Pump of the SMR Family of Transporters, in Resistance to Antimicrobial Agents in *Acinetobacter baumannii*." Antimicrobial Agents and Chemotherapy **53**(12): 5312-5316.

Srinivasan, V. B., G. Rajamohan, P. Pancholi, M. Marcon and W. A. Gebreyes (2011). "Molecular cloning and functional characterization of two novel membrane

fusion proteins in conferring antimicrobial resistance in *Acinetobacter baumannii*." J Antimicrob Chemother **66**(3): 499-504.

Stansly, P. G., R. G. Shepherd and H. J. White (1947). "Polymyxin: a new chemotherapeutic agent." Bull Johns Hopkins Hosp **81**(1): 43-54.

Stewart, P. S. and J. William Costerton (2001). "Antibiotic resistance of bacteria in biofilms." The Lancet **358**(9276): 135-138.

Su, X.-Z., J. Chen, T. Mizushima, T. Kuroda and T. Tsuchiya (2005). "AbeM, an H<sup>+</sup>-Coupled *Acinetobacter baumannii* Multidrug Efflux Pump Belonging to the MATE Family of Transporters." Antimicrobial Agents and Chemotherapy **49**(10): 4362-4364.

Sun, J.-R., M.-C. Chan, T.-Y. Chang, W.-Y. Wang and T.-S. Chiueh (2010). "Overexpression of the *adeB* Gene in Clinical Isolates of Tigecycline-Nonsusceptible *Acinetobacter baumannii* without Insertion Mutations in *adeRS*." Antimicrobial Agents and Chemotherapy **54**(11): 4934-4938.

Sun, J.-R., C.-L. Perng, M.-C. Chan, Y. Morita, J.-C. Lin, C.-M. Su, W.-Y. Wang, T.-Y. Chang and T.-S. Chiueh (2012). "A Truncated AdeS Kinase Protein Generated by *ISAbal* Insertion Correlates with Tigecycline Resistance in *Acinetobacter baumannii*." PLoS ONE **7**(11): e49534.

Sun, J. R., W. Y. Jeng, C. L. Perng, Y. S. Yang, P. C. Soo, Y. S. Chiang and T. S. Chiueh (2016). "Single amino acid substitution Gly186Val in AdeS restores tigecycline susceptibility of *Acinetobacter baumannii*." J Antimicrob Chemother **71**(6): 1488-1492.



Talaga, K., P. Krzysciak and M. Bulanda (2016). "Susceptibility to tigecycline of *Acinetobacter baumannii* strains isolated from intensive care unit patients." Anaesthesiol Intensive Ther.

Tatusov, R. L., M. Y. Galperin, D. A. Natale and E. V. Koonin (2000). "The COG database: a tool for genome-scale analysis of protein functions and evolution." Nucleic Acids Research **28**(1): 33-36.

Thompson, M. G., C. C. Black, R. L. Pavlicek, C. L. Honnold, M. C. Wise, Y. A. Alamneh, J. K. Moon, J. L. Kessler, Y. Si, R. Williams, S. Yildirim, B. C. Kirkup, R. K. Green, E. R. Hall, T. J. Palys and D. V. Zurawski (2014). "Validation of a Novel Murine Wound Model of *Acinetobacter baumannii* Infection." Antimicrob Agents Chemother **58**(3): 1332-1342.

Tomaras, A. P., C. W. Dorsey, R. E. Edelman and L. A. Actis (2003). "Attachment to and biofilm formation on abiotic surfaces by *Acinetobacter baumannii*: involvement of a novel chaperone-usher pili assembly system." Microbiology **149**(Pt 12): 3473-3484.

Tomaras, A. P., M. J. Flagler, C. W. Dorsey, J. A. Gaddy and L. A. Actis (2008). "Characterization of a two-component regulatory system from *Acinetobacter baumannii* that controls biofilm formation and cellular morphology." Microbiology **154**(Pt 11): 3398-3409.

Tomás, M. d. M., A. Beceiro, A. Pérez, D. Velasco, R. Moure, R. Villanueva, J. Martínez-Beltrán and G. Bou (2005). "Cloning and Functional Analysis of the Gene Encoding the 33- to 36-Kilodalton Outer Membrane Protein Associated with Carbapenem Resistance in *Acinetobacter baumannii*." Antimicrobial Agents and Chemotherapy **49**(12): 5172-5175.

Towner, K. J. (2009). "*Acinetobacter*: an old friend, but a new enemy." J Hosp Infect **73**(4): 355-363.

Towner, K. J., K. Levi and M. Vlassiadi (2008). "Genetic diversity of carbapenem-resistant isolates of *Acinetobacter baumannii* in Europe." Clin Microbiol Infect **14**(2): 161-167.

Tsai, Y. J., Y. C. Lin, W. B. Wu, P. H. Chiu, B. J. Lin and S. P. Hao (2013). "Biofilm formations in nasopharyngeal tissues of patients with nasopharyngeal osteoradionecrosis." Otolaryngol Head Neck Surg **148**(4): 633-636.

Tucker, A. T., E. M. Nowicki, J. M. Boll, G. A. Knauf, N. C. Burdis, M. S. Trent and B. W. Davies (2014). "Defining Gene-Phenotype Relationships in *Acinetobacter baumannii* through One-Step Chromosomal Gene Inactivation." mBio **5**(4).

Turton, J. F., M. E. Ward, N. Woodford, M. E. Kaufmann, R. Pike, D. M. Livermore and T. L. Pitt (2006). "The role of ISAba1 in expression of OXA carbapenemase genes in *Acinetobacter baumannii*." FEMS Microbiol Lett **258**(1): 72-77.

Turton, J. F., N. Woodford, J. Glover, S. Yarde, M. E. Kaufmann and T. L. Pitt (2006). "Identification of *Acinetobacter baumannii* by detection of the blaOXA-51-like carbapenemase gene intrinsic to this species." J Clin Microbiol **44**(8): 2974-2976.

Unemo, M. and W. M. Shafer (2011). "Antibiotic resistance in *Neisseria gonorrhoeae*: origin, evolution, and lessons learned for the future." Ann N Y Acad Sci **1230**: E19-28.

Urban, C., E. Go, N. Mariano and J. J. Rahal (1995). "Interaction of sulbactam, clavulanic acid and tazobactam with penicillin-binding proteins of imipenem-resistant

and -susceptible *Acinetobacter baumannii*." FEMS Microbiology Letters **125**(2-3): 193-197.

van den Broek, P. J., J. Arends, A. T. Bernardts, E. De Brauwer, E. M. Mascini, T. J. van der Reijden, L. Spanjaard, E. A. Thewessen, A. van der Zee, J. H. van Zeijl and L. Dijkshoorn (2006). "Epidemiology of multiple *Acinetobacter* outbreaks in The Netherlands during the period 1999-2001." Clin Microbiol Infect **12**(9): 837-843.

van Dessel, H., L. Dijkshoorn, T. van der Reijden, N. Bakker, A. Paauw, P. van den Broek, J. Verhoef and S. Brisse (2004). "Identification of a new geographically widespread multiresistant *Acinetobacter baumannii* clone from European hospitals." Research in Microbiology **155**(2): 105-112.

van Faassen, H., R. KuoLee, G. Harris, X. Zhao, J. W. Conlan and W. Chen (2007). "Neutrophils play an important role in host resistance to respiratory infection with *Acinetobacter baumannii* in mice." Infect Immun **75**(12): 5597-5608.

Vanechoutte, M., L. Dijkshoorn, I. Tjernberg, A. Elaichouni, P. de Vos, G. Claeys and G. Verschraegen (1995). "Identification of *Acinetobacter* genomic species by amplified ribosomal DNA restriction analysis." J Clin Microbiol **33**(1): 11-15.

Vanechoutte, M., A. Nemec, M. Musílek, T. J. K. van der Reijden, M. van den Barselaar, I. Tjernberg, W. Calame, R. Fani, T. De Baere and L. Dijkshoorn (2009). "Description of *Acinetobacter venetianus* ex Di Cello et al. 1997 sp. nov." International Journal of Systematic and Evolutionary Microbiology **59**(6): 1376-1381.

Vasilev, K., G. Reshedko, R. Orasan, M. Sanchez, J. Teras, T. Babinchak, G. Dukart, A. Cooper, N. Dartois, H. Gandjini, R. Orrico and E. Ellis-Grosse (2008). "A Phase 3,

open-label, non-comparative study of tigecycline in the treatment of patients with selected serious infections due to resistant Gram-negative organisms including *Enterobacter* species, *Acinetobacter baumannii* and *Klebsiella pneumoniae*." J Antimicrob Chemother **62 Suppl 1**: i29-40.

Vaz-Moreira, I., A. Novo, E. Hantsis-Zacharov, A. R. Lopes, M. Gomila, O. C. Nunes, C. M. Manaia and M. Halpern (2011). "*Acinetobacter rudis* sp. nov., isolated from raw milk and raw wastewater." International Journal of Systematic and Evolutionary Microbiology **61**(12): 2837-2843.

Vila, J., S. Martí and J. Sánchez-Céspedes (2007). "Porins, efflux pumps and multidrug resistance in *Acinetobacter baumannii*." Journal of Antimicrobial Chemotherapy **59**(6): 1210-1215.

Visca, P., H. Seifert and K. J. Towner (2011). "*Acinetobacter* infection – an emerging threat to human health." IUBMB Life **63**(12): 1048-1054.

Wand, M. E., L. J. Bock, L. C. Bonney and J. M. Sutton (2015). "Retention of virulence following adaptation to colistin in *Acinetobacter baumannii* reflects the mechanism of resistance." Journal of Antimicrobial Chemotherapy.

Wand, M. E., L. J. Bock, J. F. Turton, P. G. Nugent and J. M. Sutton (2012). "*Acinetobacter baumannii* virulence is enhanced in *Galleria mellonella* following biofilm adaptation." J Med Microbiol **61**(Pt 4): 470-477.

Wang, N., E. A. Ozer, M. J. Mandel and A. R. Hauser (2014). "Genome-wide identification of *Acinetobacter baumannii* genes necessary for persistence in the lung." MBio **5**(3): e01163-01114.

Wang, Z., M. Gerstein and M. Snyder (2009). "RNA-Seq: a revolutionary tool for transcriptomics." Nat Rev Genet **10**(1): 57-63.

Wareham, D. W., N. C. Gordon and M. Hornsey (2011). "In vitro activity of teicoplanin combined with colistin versus multidrug-resistant strains of *Acinetobacter baumannii*." J Antimicrob Chemother **66**(5): 1047-1051.

Webber, M. A., A. M. Bailey, J. M. A. Blair, E. Morgan, M. P. Stevens, J. C. D. Hinton, A. Ivens, J. Wain and L. J. V. Piddock (2009). "The Global Consequence of Disruption of the AcrAB-TolC Efflux Pump in *Salmonella enterica* Includes Reduced Expression of SPI-1 and Other Attributes Required To Infect the Host." Journal of Bacteriology **191**(13): 4276-4285.

Wendt, C., B. Dietze, E. Dietz and H. Ruden (1997). "Survival of *Acinetobacter baumannii* on dry surfaces." J Clin Microbiol **35**(6): 1394-1397.

West, A. H. and A. M. Stock (2001). "Histidine kinases and response regulator proteins in two-component signaling systems." Trends Biochem Sci **26**(6): 369-376.

Wilharm, G., J. Piesker, M. Laue and E. Skiebe (2013). "DNA Uptake by the Nosocomial Pathogen *Acinetobacter baumannii* Occurs during Movement along Wet Surfaces." Journal of Bacteriology **195**(18): 4146-4153.

Wright, M. S., D. H. Haft, D. M. Harkins, F. Perez, K. M. Hujer, S. Bajaksouzian, M. F. Benard, M. R. Jacobs, R. A. Bonomo and M. D. Adams (2014). "New Insights into Dissemination and Variation of the Health Care-Associated Pathogen *Acinetobacter baumannii* from Genomic Analysis." mBio **5**(1).

Wright, M. S., A. Iovleva, M. R. Jacobs, R. A. Bonomo and M. D. Adams (2016). "Genome dynamics of multidrug-resistant *Acinetobacter baumannii* during infection and treatment." Genome Med **8**(1): 26.

Yang, J., R. Yan, A. Roy, D. Xu, J. Poisson and Y. Zhang (2015). "The I-TASSER Suite: protein structure and function prediction." Nat Meth **12**(1): 7-8.

Yang, S. C., W. J. Chang, Y. H. Chang, Y. S. Tsai, T. P. Yang, C. W. Juan and M. Y. Shiau (2010). "Prevalence of antibiotics resistance and OXA carbapenemases genes in multidrug-resistant *Acinetobacter baumannii* isolates in central Taiwan." European Journal of Clinical Microbiology & Infectious Diseases **29**(5): 601-604.

Ye, D., J. Shan, Y. Huang, J. Li, C. Li, X. Liu, W. He, Y. Li and P. Mao (2015). "A gloves-associated outbreak of imipenem-resistant *Acinetobacter baumannii* in an intensive care unit in Guangdong, China." BMC Infect Dis **15**: 179.

Yoon, E.-J., Y. Nait Chabane, S. Goussard, E. Snesrud, P. Courvalin, E. Dé and C. Grillot-Courvalin (2015). "Contribution of Resistance-Nodulation-Cell Division Efflux Systems to Antibiotic Resistance and Biofilm Formation in *Acinetobacter baumannii*." mBio **6**(2).

Yoon, E. J., V. Balloy, L. Fiette, M. Chignard, P. Courvalin and C. Grillot-Courvalin (2016). "Contribution of the Ade Resistance-Nodulation-Cell Division-Type Efflux Pumps to Fitness and Pathogenesis of *Acinetobacter baumannii*." MBio **7**(3).

Yoon, E. J., P. Courvalin and C. Grillot-Courvalin (2013). "RND-type efflux pumps in multidrug-resistant clinical isolates of *Acinetobacter baumannii*: major role for

AdeABC overexpression and AdeRS mutations." Antimicrob Agents Chemother **57**(7): 2989-2995.

Yun, S. H., C. W. Choi, S. H. Park, J. C. Lee, S. H. Leem, J. S. Choi, S. Kim and S. I. Kim (2008). "Proteomic analysis of outer membrane proteins from *Acinetobacter baumannii* DU202 in tetracycline stress condition." Journal of microbiology **46**(6): 720-727.

Zhou, Z., A. A. Ribeiro, S. Lin, R. J. Cotter, S. I. Miller and C. R. H. Raetz (2001). "Lipid A Modifications in Polymyxin-resistant *Salmonella typhimurium*: PmrA-dependent 4-amino-4-deoxy-L-arabinose, and phosphoethanolamine incorporation." Journal of Biological Chemistry **276**(46): 43111-43121.

Zhu, J., C. Wang, J. Wu, R. Jiang, Z. Mi and Z. Huang (2009). "A novel aminoglycoside-modifying enzyme gene *aac(6')*-Ib in a pandrug-resistant *Acinetobacter baumannii* strain." Journal of Hospital Infection **73**(2): 184-185.